Right Ventricular Inflammation Following Lung Resection Surgery

Dr Emma Murphy

MBCHB MRCP FRCA

Submitted in the fulfilment of the requirements for the Degree of Doctor of Medicine

School of Medicine, Veterinary and Life Sciences
University of Glasgow

February 2023

Dedication

To family and close friends for their support.

And to Archie.

Abstract

Lung cancer is the third commonest cancer in the United Kingdom and the most common cancer overall in Scotland. Whilst the best chance of a cure is surgical resection, patients undergoing lung resection surgery are generally considered to be ‘high-risk’ surgical candidates and are at risk of major post-operative cardiac and respiratory complications following surgery. The literature has widely described a deterioration in right ventricular function following lung resection surgery; however, the mechanism of this dysfunction remains unclear.

The first section of this thesis describes the complex geometry, structure and physiology of the right ventricle and reviews the available methods to assess the structure and function of the right ventricle, providing context for further investigations described later in this thesis (Chapter 1). An overview of the literature describing the right ventricular response to lung resection is described in Chapter 2.

There is a complex interplay of aetiologies potentially responsible for the right ventricular dysfunction seen following lung resection including increases in afterload and altered contractility. Animal models of pulmonary embolism, which are functionally analogous to lung resection surgery and one lung ventilation with transient clamping of the lobar branches of the pulmonary artery, have widely described a right ventricular inflammatory injury leading to the hypothesis that a myocardial inflammatory injury may be a contributing factor in right ventricular dysfunction after lung resection. A review of the literature examining right ventricular inflammation after pulmonary embolism and animal models of acute afterload are described in Chapter 3. The literature demonstrates a consistent inflammatory response within the right ventricle which is associated with right ventricular dysfunction. Chapter 4 describes the methods available to measure myocardial inflammation with particular focus on cardiovascular magnetic resonance imaging given it is the gold standard imaging technique for assessment of the right ventricle.

The following chapters describe the results of a prospective, observational cohort study, examining the role of right ventricular inflammation after lung

resection using cardiovascular resonance imaging conducted by the author. The feasibility and reproducibility of T1 mapping (a marker of inflammation or oedema) and Extracellular Volume quantification (a marker of fibrosis or oedema) following lung resection are described in the first investigation in this thesis (Chapter 7). The excellent intra- and inter-observer reproducibility confirms T1 mapping is a suitable method for assessing the myocardial response to lung resection. The main finding of this work describes an increase in myocardial T1 and Extracellular Volume in the right ventricular insertion points and septum with no change in the left ventricle in the immediate peri-operative period following lung resection (Chapter 8). It is hypothesised that an increase in acute afterload results in an increase in right ventricular wall tension and paradoxical movement of the interventricular septum leading to an increase in mechanical stress in the ventricular insertion points. This triggers a discrete intrinsic myocardial inflammatory response (demonstrated with increases in myocardial T1) altering myocardial contractility which contributes to right ventricular dysfunction. On an exploratory basis, increases in T1 were associated with poorer RV function, poorer pre- and predicted post-operative lung function and poor patient reported post-operative outcomes.

Biomarkers of myocardial dysfunction (B-type natriuretic peptide and N-terminal B-type natriuretic peptide) and systemic inflammation (C-reactive protein) were measured contemporaneously with the imaging study (Chapter 9). This investigation demonstrates a rise in all three biomarkers in the peri-operative period with an early peak rise in BNP at twelve hours compared with seventy-two hours for NT-proBNP. This suggests BNP has superiority in the peri-operative period as an early indicator of patients who have sustained injury potentially allowing identification, monitoring, and therapy with the aim to intervene early in those at higher risk of peri-operative complications and poorer long term outcomes following lung resection.

This thesis provides further insight into the mechanisms of right ventricular dysfunction following lung resection. It provides validated methods for future work in this patient population, suggests an association between a myocardial inflammatory insult and post-operative right ventricular function and highlights a potentially novel diagnostic pathway allowing targeted intervention ameliorating disabling postoperative functional limitation.

Table of Contents

List of Tables

List of Figures

Grants, Publications and Presentations

Grants, publications and presentations obtained / written by the author directly pertaining to work carried out in the preparation of this thesis.

Grants

Scottish Society of Anaesthesia Research Grant 2018. Relative kinetics of BNP and NT-proBNP following lung resection surgery. £1000

Publications

Peer Reviewed Publications:

Murphy, E, Church C, Dalzell JR, Sinclair, A, McCall P, Shelley B. Right ventricular failure in ICU – ESICM Academy. Available at https://academy.esicm.org/enrol.index.php?id=255.

Murphy E, Shelley B. Clinical Presentation and Management of Right Ventricular Dysfunction. BJA Education 2019;19(6):183-190.

Murphy E, Shelley B. The right ventricle – structural and functional importance for anaesthesia and intensive care. BJA Education 2018; 18(8):239-245.

Abstract Publications:

Murphy E, Glass, A, McCall P, Shelley B. Myocardial inflammation after lung resection. Br J Anaesth 2021;126(2);E80-81

Murphy E, Glass, A, McCall P, Shelley B. Relative kinetics of B-type natriuretic peptide and N-terminal pro B-type natriuretic peptide after lung resection. Br J Anaesth 2019; 123(4):e503-504.

Murphy E, Glass A, McCall P, Kinsella J, Shelley B. CMR-derived strain-rate: A novel technique for assessing RV diastolic function after lung resection. Journal of Cardiothoracic and Vascular Anaesthesia 2018;32:S52-53.

Murphy E, Glass A, McCall P, Kinsella J, Shelley B. Cardiac-magnetic-resonance-derived strain rate: a novel technique for assessing right ventricular diastolic function post-lung resection. Br J Anaesth 2018; 121(2); e17-32.

Presentations:

Oral Presentations:

Myocardial inflammation after lung resection. American Society of Cardiovascular Anesthesiologists Annual Thoracic Anesthesia Symposium 2021 – Virtual – April 2021.

Myocardial inflammation after thoracic surgery. RCoA/NIAA Anaesthesia Research and British Journal of Anaesthesia Research Forum - Virtual 2020.

Myocardial inflammation after lung resection. European Association of Cardiothoracic Anaesthetists (EACTA) Virtual – November 2020.

Relative kinetics of B-type natriuretic peptide and N-terminal pro B-type natriuretic peptide after lung resection. British Journal of Anaesthesia Research Forum - London 2019.

CMR-derived strain-rate: A novel technique for assessing RV diastolic function after lung resection. European Association of Cardiothoracic Anaesthetists (EACTA) – Manchester 2018.

Cardiac-magnetic-resonance-derived strain rate: a novel technique for assessing right ventricular diastolic function post-lung resection. British Journal of Anaesthesia Research Forum - London, 2018.

Prizes

Hughes Medal for Best Presentation at the British Journal of Anaesthesia Research Forum – London 2018. Cardiac-magnetic-resonance-derived strain rate: a novel technique for assessing right ventricular diastolic function post-lung resection.

Acknowledgement

I would like to thank and acknowledge the support from the following people, who without their help this thesis would not be possible:

To my supervisor, Professor Ben Shelley, Honorary Professor and Consultant in Cardiothoracic Anaesthesia and Intensive Care, who took a chance by giving me a ‘stop-gap’ job all those years ago and started me off on my research journey. His enthusiasm, guidance, patience and impeccably high standards have helped me enormously throughout the years.

To my supervisor, Dr Philip McCall, Consultant in Cardiothoracic Anaesthesia and Intensive Care, for his ongoing support and encouragement.

To the MRI department at the Golden Jubilee National Hospital; in particular Vanessa Orchard and her team of radiologists for their flexibility in arranging CMR imaging for all the patients despite their own busy workload. Without their support this study would not be possible. To Des Alcorn, Consultant Radiologist, for his support in ensuring the safety of CMR imaging in the post-operative period.

To the research team at the Golden Jubilee National Hospital; Elaine Matthews, Elizabeth Boyd, and Julie Buckley who helped with the day to day running of this study.

To Dr Geeshath Jayasekera for co-reporting CMR studies in his own time.

To Mr Mo Asif, Consultant Cardiothoracic Surgeon at the Golden Jubilee National Hospital, for allowing patients under his care to participate.

To the nursing staff in the High Dependency Unit and Ward 3 West for supporting the study.

To the Association for Cardiothoracic Anaesthesia and Critical Care, the Association of Anaesthetists of Great Britain and Ireland, and the Scottish Society of Anaesthetists for funding this project.

Finally to the patients who willing took part in this study, their willingness to undertake research during a difficult and challenging time in their lives made this study possible.

Author's declaration

I declare that, except where reference is made to the contribution of others, this thesis is a result of my own work, written entirely by myself and has not been submitted for any other degree at the University of Glasgow or any other institution.

Dr Emma Murphy

Word Count: 58,508

Definitions/Abbreviations

1.5T – 1.5 Tesla
2D – Two dimensional
2mnth – Two-months post-operatively
3D – Three dimensional
3T – 3 Tesla
6MWT – Six-minute walk test

AF - Atrial fibrillation
ARDS - Acute respiratory distress syndrome
AHA - American Heart Association
ANGIE - Accelerated and navigator-gated look-locker imaging
ANOVA - Analysis of variance
ASA - American Society of Anaesthesiologists
ASD – Atrial septal defect
ASE – American Society of Echocardiography

BMI – Body Mass Index
BNP - B-type natriuretic peptide
BSA – Body surface area
BSE - British Society for Echocardiography
BTS - British Thoracic Society

CCS - Canadian Cardiovascular Society
CD - Cluster of differentiation
CI – Confidence interval
CINC - Cytokine induced neutrophil chemoattractant
CK-MB - Creatine kinase myocardial B fraction
CMR – Cardiovascular magnetic resonance
CO – Cardiac output
COPD - Chronic obstructive pulmonary disease
COV - Coefficient of variation
COX – Cyclooxygenase
CRP - C-reactive protein
CS - Circumferential strain
CT – Computed topography
CV – Chamber view

DDRV - Diastolic linear dimension of the right ventricle
DLCO - Carbon monoxide diffusion factor
DNA - Deoxyribonucleic acid
DVT - Deep vein thrombosis

ECG – Electrocardiographic
ECV – Extracellular volume
EDP – End-diastolic pressure
EDV – End-diastolic volume
Ees - End-systolic elastance
Ees: Ea - End-systolic elastance: pulmonary artery elastance
EF – Ejection fraction
EGE - Early gadolinium enhancement

EI – Eccentricity index
EMB – Endomyocardial biopsy
EQ5D – European quality of life 5 domain score
ESA - European Society of Anaesthesiology
ESC – European Society of Cardiologists
ESV - End-systolic volume
ETco$_2$ - End-tidal carbon dioxide

FAC – Fractional area change
FEV$_1$ - Forced expiratory volume in one second
FEV$_1$% - Forced expiratory volume in one second as a percentage of predicted
Fi0$_2$ - Fraction of inspired oxygen
FRC - Functional Residual Capacity
FVC – Forced vital capacity
FWLS - Free wall longitudinal strain

GHS - Global health score
GJNH - Golden Jubilee National Hospital
GLS - Global longitudinal strain
GRE – Gradient echo

H$^+$ - Hydrogen ions
HDU - High dependency unit
HLA - Horizontal long axis
HPV - Hypoxic Pulmonary Vasoconstriction
HR – Heart rate
HsTnT - High-sensitivity cardiac troponin-T

ICC - Intraclass correlation coefficient
ICU - Intensive care unit
IQR – Interquartile range
IQS - Image Quality Score
IV – Intravenous
IVC - Inferior vena cava
IVS – Intraventricular septum

LGE - Late gadolinium enhancement
LOI – Line of interest
LS - Longitudinal strain
LV – Left ventricle

MESA – Multi-Ethnic Study of Atherosclerosis
MI – Myocardial infarction
MINS - Myocardial injury after non-cardiac surgery
MiRs – MicroRNAs
MMP - Matrix metalloproteinase
MOLLI - Modified look locker technique
MPAP – Mean Pulmonary Artery Pressure
MPO – Myeloperoxidase
MRC-DS - Medical Research Council dyspnoea scale
MRI – Magnetic Resonance Imaging

***n*-** number
NICE - National Institute of Clinical Excellence
NP – Natriuretic peptides
NSAID - Non-steroidal anti-inflammatory
NSCLC - Non-small cell lung cancer
NT-proBNP - N-terminal pro-BNP
NYHA - New York Heart Association

OLV - One lung ventilation

PA – Pulmonary artery
PAAT – Pulmonary artery acceleration time
PAC – Pulmonary artery catheter
PAP – Pulmonary artery pressure
PARADIGM-HF - Prospective Comparison of ARNI with ACEI to Determine Impact on Global Mortality and Morbidity in Heart Failure
PASP – Pulmonary artery systolic pressure
PCR - Polymerase chain reaction
PCWP – Pulmonary capillary wedge pressure
PE – Pulmonary embolism
PEEP - Positive end expiratory pressure
PET - Positron emission tomography
PH – Pulmonary hypertension
PMCE - Perioperative major cardiovascular events
PMI - Peri-operative myocardial injury
PMN - Polymorphonuclear neutrophil antibodies
POD – Post-operative day
PPC - Post-operative pulmonary complications
ppo - Predicted post-operative
Pre-op – Pre-operative
PRSW - Preload recruitable stroke work
PVR – Pulmonary vascular resistance
PVRI - Pulmonary vascular resistance index

QoL - Quality of life

RA – Right atrium
RAP – Right arterial pressure
RCA – Right coronary artery
RCRI - Revised Cardiac Risk Index
RF – Radiofrequency
RHC – Right heart catheter
ROI - Regions of interest
RS - Radial strain
RV - Right ventricle
RVIP - Right ventricular insertion point
RVOT - Right ventricular outflow tract
RVEDD - Right ventricular end-diastolic diameter
RVEDV – Right ventricular end-diastolic volume
RVEDVI – Right ventricular end-diastolic volume index
RVEF – Right ventricular ejection fraction

RVESV – Right ventricular end-systolic volume
RVESVI - Right ventricular end-systolic volume index
RVMPI – Right ventricle myocardial performance index
RVSP - Right ventricular systolic pressure

SA – Short axis
$Sa0_2$ - Percentage arterial oxygen saturation
SASHA - Saturation recovery single-shot acquisition
SD – Standard deviation
SDRV - Systolic displacement of the lateral wall of the right ventricle
SHMOLLI – Shortened modified look locker technique
SNR - Signal to noise ratio
SOP - Standard operating procedure
SSFP- Steady-state free procession
STE – Speckle tracking echocardiography
SV – Stroke volume
SVR – Systemic vascular resistance

T- Tesla
TAPSE - Tricuspid annual plane systolic excursion
TDI - Tissue Doppler Imaging
ThRCRI - Thoracic Revised Cardiac Risk Index
TLCO – Transfer diffusion capacity for carbon monoxide
TNF - Tissue necrosis factor
TOE – Transoesophageal echocardiography
TR - Tricuspid regurgitation
TRJ – Tricuspid regurgitant jet
TTE – Transthoracic echocardiography
TV - Tricuspid valve

UK – United Kingdom

VATS - Video-assisted thoracoscopy
VIP – Ventricular Insertion Point
VISION - Vascular Events in Noncardiac Surgery Patients Cohort Evaluation (study)

WHO-PS - World Health Organisation Performance Status

Chapter 1 – Introduction

1.1 The Right Ventricle

1.1.1 General Introduction

In 1616, Sir William Harvey was the first physician to acknowledge in text the right ventricle (RV) and its interactions with the pulmonary circulation,

"And I ask, as the lungs are so close at hand, and in continual motion, and the vessel that supplies them is of such dimensions, what is the use or meaning of this pulse of the right ventricle? And why was nature reduced to the necessity of adding another ventricle for the sole purpose of nourishing the lungs?"

William Harvey (1628)[1]

yet up until the mid-20th century little emphasis had been placed on the RV. Prior to the 1950s, the main focus was on the left ventricle (LV), with the RV being thought of as little more than a passive structure with the sole purpose of providing a conduit between the systemic and pulmonary circulations. By the 1950s, cardiac surgeons began to understand the importance of the RV as they attempted to develop techniques for palliation of right-heart hypoplasia. The role and importance of RV function is now identified and recognised in a variety of disease states including; pulmonary hypertension (PH), myocardial infarction (MI), heart failure, obesity and obstructive sleep apnoea, pulmonary embolism (PE), valvular and congenital heart disease[2-9].

1.1.2 Normal Right Ventricle Anatomy

The RV is the most anterior chamber in the normal heart residing immediately behind the sternum. It has a complex geometry where the RV appears to wrap around the LV; in doing so it appears crescent-shaped in cross-section and triangular in side-profile, in comparison to the more ellipsoidal LV[2]. The body of the RV receives blood from the right atrium (RA), whilst the outflow tract transfers the blood to the pulmonary artery (PA). These two areas are separated by a ridge, the crista supraventricularis, which extends in to the ventricular

cavity[10]. The RV is traditionally described as having 3 components, the inlet, the trabeculated apical myocardium, and the infundibulum or conus[11].

When viewed internally, the RV has been described as an open "V" with 3 distinguished and prominent muscular bands: the moderator, parietal and septomarginal[10]. The parietal band combines with the infundibular septum to form the crista supraventricularis[12]. The septomarginal band extends to join the moderator band, which is attached to the anterior papillary muscle[12].

The RV musculature is composed of superficial and deep layers with the superficial fibres arranged circumferentially parallel to the atrioventricular groove before turning obliquely towards the cardiac apex and joining the superficial fibres of the LV[13]. The deep fibres are longitudinally aligned to the base[11].

1.1.3 Right Ventricular Blood Supply

The RV blood supply is dependent on the dominance of the coronary artery system for each individual. Eighty-percent of the population are known to have a RV supplied by the right coronary artery (RCA)[2 11 14]. Typically, the left anterior descending artery supplies the anterior wall of the RV and the anteroseptal region, the lateral wall is supplied by the marginal branches of the RCA and the posterior wall and inferoseptal regions by the posterior descending artery[14]. The infundibulum is supplied by the conal artery[14]. Venous drainage occurs from the anterior cardiac veins and drains directly into the ventricular chamber from the Thesbian veins that run a perpendicular course to the endocardial surface[14].

1.1.4 Normal Right Ventricular Perfusion

In health, perfusion of the RV occurs during both systole and diastole providing myocardial oxygen delivery throughout the cardiac cycle. In the diseased state, such as in patients with PH, increased intra-cavity pressure during systole means the distribution of blood to the RV during the cardiac cycle is more like that of the LV, predominantly occurring during diastole.[11]

1.1.5 Normal Right Ventricular Physiology

The RV is thin-walled, with approximately one-sixth of the muscle mass of the LV[15]. Although, the RV ejects the same cardiac output (CO) as the LV, it does it under different physiological conditions. Under normal conditions, ejection is maintained despite lesser muscle mass as the RV is coupled with the pulmonary circulation which has a lower vascular resistance and greater distensibility in comparison with the systemic circulation. As such both pulmonary artery pressure and vascular resistance are approximately a fifth of that the systemic circulation and RV stroke work is only around a quarter that of the LV[11]. The ability of the lung to recruit partially collapsed or unused vessels as CO increases, for example during exercise, serves to maintain coupling and accounts for the minimal changes demonstrated in pulmonary arterial pressure and reduction in pulmonary vascular resistance (PVR) seen on exercise.

Ejection of blood from the RV occurs as a result of inward movement of the RV free wall, contraction of the longitudinal fibres which draws the tricuspid annulus towards the apex and traction on the free wall at the points of attachment secondary to LV contraction; moving blood in a 'peristaltic' manner towards the RV outflow tract[16]. Compare this to the LV where blood is ejected due to a concentric contraction of the LV free wall and septum, combined with a twisting movement of the heart[2]. The performance of the RV is affected by a variety of interacting factors including preload, afterload, contractility, ventricular interdependence, and heart rate (HR)[11].

1.1.5.1 Preload

Preload is defined as the initial stretching of the cardiac fibre prior to end-diastole and is in turn influenced by a variety of factors including atrial contractility, ventricular compliance, venous return, wall tension and HR. According to the Frank-Starling mechanism, an increase in RV preload will improve myocardial contraction[11]. Classically, the RV is described as being 'tolerant' of pre-load; low muscular mass means the comparatively compliant RV is able to dilate, up to a point, in the face of excessive volume (Figure 1). With ongoing distention however, the LV may become compressed and global

ventricular impairment may occur due to ventricular interdependence[11]. RV filling time is shorter and filling velocities are lower than the LV[11].

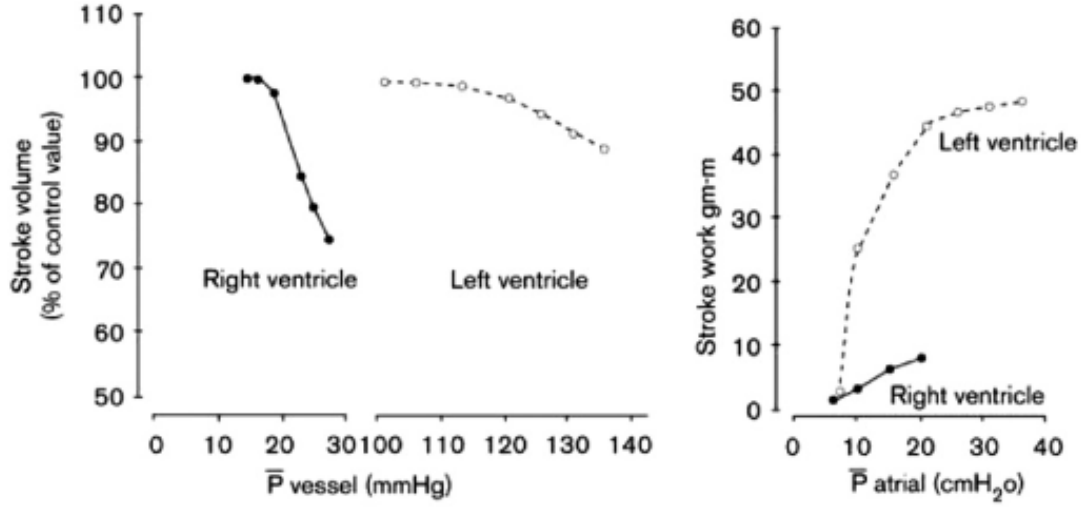

Figure 1 Differences between left and right ventricular response to preload and afterload. Increasing afterload (left image) and increasing preload (right image). RV stroke volume decreases rapidly when mean vascular pressure reaches 20mmHg in the pulmonary artery, unlike the LV which remains comparatively constant as atrial pressure increases. LV stroke work increases rapidly as left atrial pressure is raised from 10cm H_2O, while the increase in RV stroke work in response is smaller in comparison. Image from Ventetuolo et al.[17]

1.1.5.2 Contractility

Contractility describes the ability of cardiac muscle to shorten and generate force, and in its truest form it would be unaltered by preload or afterload. RV contraction occurs by three distinct mechanisms: 1) inward movement of the RV free wall, 2) longitudinal fibre contraction which shortens the long axis and pulls the tricuspid annulus towards the apex and 3) LV contraction resulting in traction of the RV free wall at the insertion points[11]. RV contractility is regulated by autonomic inputs, Frank-Starling mechanisms and HR.

1.1.5.3 Afterload

Right ventricular afterload is the load the RV has to overcome during the ejection phase of the cardiac cycle. In its most complete sense, afterload is influenced by pulmonary vascular resistance (PVR), arterial compliance, arterial resistance, and wave reflection, all taking place within the pulmonary vascular bed[18]. The RV is less well equipped to deal with acute changes in afterload due

to a reduction in cardiac muscle mass compared with the LV; as such the RV is considered to be 'intolerant' of afterload (Figure 1). PVR is used as the simplest surrogate of afterload, given that it accounts for the largest proportion of ventricular afterload; however, this does not accurately represent the complex interactions of afterload as described above (Equation 1). Pulmonary artery pressure (PAP) is a surrogate of afterload; however, it is a less reliable index as the mean PAP is a product of pulmonary blood flow and the interactions between PA compliance, contractility and PVR.

$$PVR = \frac{(MPAP - PCWP) \times 80}{CO}$$

Equation 1 Equation for derivation of pulmonary vascular resistance.
PVR – pulmonary vascular resistance, MPAP - mean pulmonary artery pressure (mmHg). PCWP - pulmonary capillary wedge pressure (mmHg). CO - cardiac output (L/min). 80 - conversion term to equalise the units. Measured in dynes-sec cm^{-5}.

1.1.5.4 Pressure-Volume Loops

Pressure-volume loops display the complex interactions of preload, afterload and contractility. Suga et al first described the LV end-systolic pressure-volume relationship as that of a linear relationship with the slope being referred to as ventricular elastance[19]. Left ventricle end-systolic elastance is load independent and often considered the most reliable measure of LV contractility.

The LV pressure-volume loop has a rectangular shape, with parallel sides due to well defined isovolumetric contraction and relaxation phases, and sharp 'corners' where the beginning and end of both systole and diastole can be easily identified (Figure 2). In comparison, RV isovolumetric contraction time is shorter than that of the LV as during early systole, the pulmonary valve opens when RV pressure exceeds that of the low-pressure PA (Figure 2). The point of end-systole is less well defined in the RV leading the RV pressure-volume loop to appear almost triangular in shape. This occurs as ejection of blood from the RV can continue despite falling RV pressure due to the momentum of blood in the low-

pressure system; as a result the isovolumetric ventricular relaxation phase is shortened or absent in the RV[2].

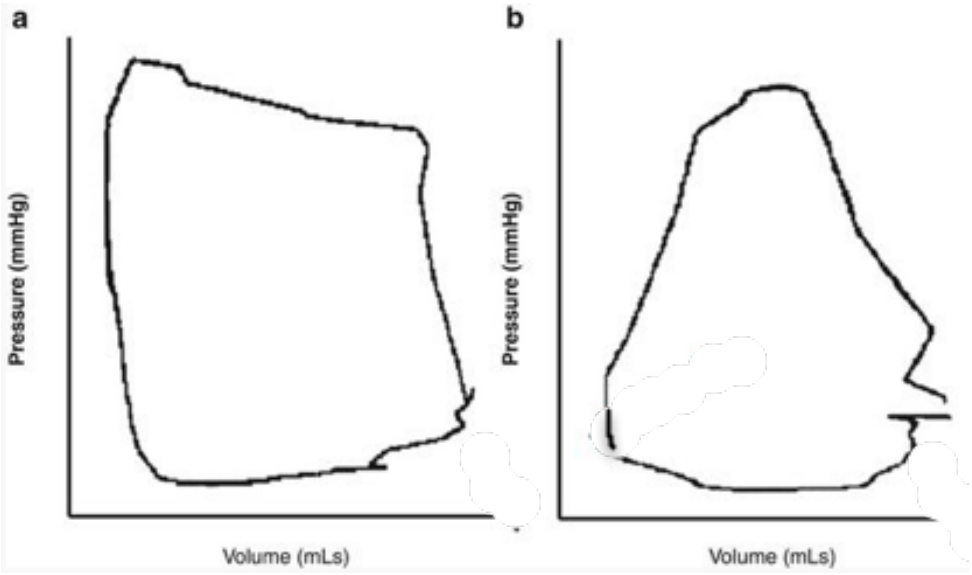

Figure 2 A comparison of pressure-volume loops.
Typical pressure-volume loops for a single cardiac cycle of the left ventricle (a) and the right ventricle (b). Note the differences in shape between both ventricles. From Sayer et al, adapted from Redington et al[20 21].

1.1.5.5 Ventricular Interdependence

Ventricular interdependence describes the phenomenon whereby the function, volume or pressure in one ventricle can directly influence that of the other[22]. Both the LV and the RV are interdependent as they are contained within the relatively non-distensible pericardial sac with a shared ventricular septum. Whilst these interactions are present continuously, it is in times of dysfunction that interdependence becomes most evident (Figure 3)[23]. When RV pressure or volume overload occurs, the RV can affect LV performance and result in a decreased LV preload and contractility. In normal hearts, LV end-diastolic pressure (EDP) usually exceeds RV-EDP. In times of RV overload, RV-EDP may exceed LV-EDP forcing the ventricular septum towards the LV during diastole. This distorts the normal LV shape reducing LV diastolic compliance and impairing LV filling[24].

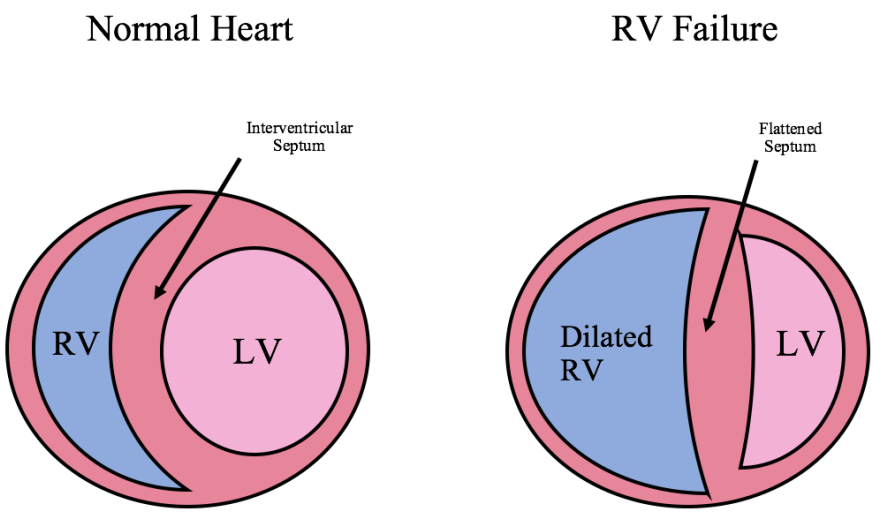

Figure 3 Graphical representation of ventricular interdependence.
In the normal heart, the RV is crescent shaped compared with the rounded LV. When RV dilatation and failure occur, the interventricular septum will shift towards the LV altering the shape of the LV. Taken from Murphy and Shelley[16].

1.1.5.6 The Right Ventricle and Pulmonary Circulation Interactions

British surgeon and anatomist, Dr John Hunter, eloquently described the RV and its interactions with the pulmonary circulation:

"When I was injecting the lungs of a man, the injection did not run freely; I then inflated them and found the injection immediately ran with freedom."

Dr John Hunter[25]

RV function relies on the interaction between the ventricle and the pulmonary circulation. The relationship between the cardiovascular and pulmonary unit is well illustrated by the concept of right ventricle-pulmonary artery (RV-PA) coupling: matching of contractility and afterload is important in maintaining ventricular function. When the right heart function is coupled with the pulmonary circulation, contractility and afterload are relatively matched[18]. Effective RV-PA coupling maintains CO while maximising the efficiency of the RV[26]. In pathological processes, both contractility and afterload may be affected; coupling is maintained if the increase in afterload is matched by an increase in contractility[18]. However, as a disease process progresses, with further increases in afterload, the RV begins to fail as a pump and contractility falls, leading to reduced CO, uncoupling and reduced efficiency of the RV.

The mechanical work of breathing impacts the RV. During spontaneous breathing, inspiration leads to a decrease in intra-pleural pressure which increases venous return and preload and is the cause of the cyclic changes in RV stroke volume seen during the normal respiratory cycle[27]. The opposite occurs during mechanical ventilation as mean airway pressures increase there is a corresponding decrease in RV stroke volume and preload and an increase in RV afterload[27]. This becomes more relevant when RV function is already impaired, such as seen in pulmonary hypertension, RV MI and acute PE[27].

1.1.5.7 Comparison of the Left and Right Ventricles

-+

	Right Ventricle	Left Ventricle
Shape	Crescent	Ellipsoidal
Structure	2 layers of fibres	3 layers of fibres
Free Wall Thickness	2-5mm	8-10mm
Circulation	Low-pressure, low-resistance	High-pressure, high-resistance
Stroke Volume (SV)	70-90ml	70-90ml
Ejection Fraction (EF)	65%	70-80%
Ventricular Pressure (diastole)	0-8mmHg	4-12mmHg
Ventricular Pressure (systole)	15-30mmHg	90-140mmHg
Afterload	PVR <250 dynes-sec/cm^{-5}	SVR 800-1200 dynes-sec/cm^{-5}
Adaptation to disease	Tolerant of preload	Tolerant of afterload

Table 1 Comparison of anatomical and physiological aspects of the normal left and right ventricle.
Taken from Murphy and Shelley[16]

1.2 Assessing the Right Ventricle

Assessing both structure and function of the RV is essential in clinical conditions affecting the right side of the heart. There are a variety of functional and imaging techniques available, each with their strengths and limitations. Assessment of the RV is challenging due to 1) its complex 3-dimensional geometry, 2) its retrosternal position, 3) its extensively trabeculated myocardium allowing for only limited definition of the endocardial borders and finally 4) the load dependence of the RV.

1.2.1 Conductance catheterisation

Measurement of RV pressure-volume loops is the gold standard method for assessment of RV function, and this can be performed invasively, using the conductance catheter. This involves the insertion of a catheter into the RV to allow real-time simultaneous measurement of cardiac chamber pressure and volume[28]. Measurement of these volumes is based on the electrical impedance of the volume of blood contained within the ventricular chamber at a given time; the ventricular wall is a poor conductor of electricity unlike blood which is a good conductor. When the ventricle is full, as occurs at end-diastole, the conductance is higher than end systole[28]. These catheters also contain a high-fidelity sensor which allows the measurement of RV pressure and subsequent generation of RV pressure-volume loops[28]. Although conductance catheters provide accurate RV assessment in a variety of clinical conditions; their use is limited by the complex measurement process, the need for specialised equipment and expertise and insertion of such a catheter is an invasive procedure with its own risks.

1.2.2 Pulmonary artery catheter

The pulmonary artery catheter (PAC) or right heart catheter (RHC) allows direct assessment of haemodynamic parameters, and is integral in the evaluation of patients with PH[18]. The PAC allows measurement of right atrial pressure (RAP), RV pressure, PAP, and pulmonary arterial wedge pressure. By calculating CO, PVR and systemic vascular resistance (SVR) can be derived. RAP is considered a surrogate of preload, PVR a measure of afterload and stroke volume (SV) as an indication of contractility. Ideally these measurements should be combined with cardiac imaging to provide a more accurate account of right heart function[18].

Volumetric PACs use a rapid-response thermistor and an electrocardiographic (ECG) electrode to plot a thermo-dilution curve corresponding to the pulsatile ejection of blood from the RV[29]. The RV ejection fraction (RVEF) can be computed by the temperature change between two successive beats[29]. RV end-systolic volume (RVESV) and end-diastolic volume (RVEDV) can be calculated from SV.

PAC insertion may result in a wide range of complications from the more minor including inadvertent arterial puncture, haemothorax, pneumothorax, thoracic duct injury, pseudo-aneurysm formation, to the serious including valve rupture, PA rupture, cardiac arrhythmias, and RV perforation[30].

1.2.3 Echocardiography

Both trans-thoracic echocardiography (TTE) and trans-oesophageal echocardiography (TOE) can be used for the assessment of RV function, with the latter more commonly utilised in the intra-operative setting or for complex valvular conditions. TTE imaging is often the first imaging modality of choice as it is readily available, safe, well validated, cost-effective and allows for bedside assessment of RV size, function and velocity-derived PA pressures[31].

LV volume calculations traditionally adopt the Simpson's rule where the user manually traces around the LV cavity endocardium at end-diastole and end-systole. Software then divides the cavities into approximately twenty parallel discs, calculates the volume of each disc (by assuming each disc is circular in cross-section) and automatically combines these disc volumes to provide an estimated LV cavity volume in end-diastole and end-systole[32]. Due to the complex geometry of the RV, summation disc type volume calculations are not easy to perform and are ultimately inaccurate in the RV[33 34]. Instead reliance on qualitative assessment of the RV still exists with TTE assessment.

The American Society of Echocardiography (ASE) have developed guidelines for the echocardiographic assessment of the right heart in adults, which are endorsed by the European Society of Cardiology (ESC) and Canadian Society for Echocardiography[35]. The British Society for Echocardiography (BSE) have also outlined a minimum dataset for echocardiography evaluation in the adult patient[36]. The ASE recommends both qualitative and quantitative assessment of the right heart including measurements of size, RV systolic function (using at least one of; fractional area change (FAC), tricuspid annual plane systolic excursion (TAPSE), RV myocardial performance index (RV-MPI) or S' wave velocity and right sided pressures[35 37].

1.2.3.1 Right Ventricle Size

For qualitative assessment of RV size, it is often compared to the LV and is normally around two-thirds the size of the LV. Measurements of the diameter at the base, mid-level and length should be taken and compared with those of the LV.

1.2.3.2 Right Systolic Function

Right ventricular systolic function can be estimated using a variety of parameters the most common of which are FAC and TAPSE. FAC is obtained from a four-chamber view by tracing the RV endocardium in systole and diastole and is expressed as a percentage change in the RV area between end-diastole and end-systole[35].

TAPSE is measured in a standard apical four-chamber view as a method to measure the distance of systolic excursion of the RV annular segment along its longitudinal plane. It assumes that displacement of the basal and adjacent segments is representative of the function of the entire right ventricle[35]. This assumption is invalid in the presence of RV pathology or RV regional wall motion abnormalities. TAPSE has the advantage of being a simple measure that is easily reproducible. TAPSE however is influenced by direction of motion, is load dependent and assumes that the displacement of a single segment of RV are representative of the function of a complex three dimensional (3D) structure[35].

RVMIP, obtained using tissue Doppler techniques, is an estimate of both RV systolic and diastolic function, defined as the ratio of isovolumetric time to ejection time[38]. It is easily reproduced and allows for calculation of RV function; however, it is less reliable when the RA pressures are elevated and disruption of the R-R interval is present in arrythymias[38].

1.2.3.2 Assessment of Pulmonary Artery Systolic Pressure

Pulmonary artery systolic pressure (PASP) can be estimated using Doppler wave analysis across the tricuspid valve. The pressure gradient across the valve can be determined from the velocity of the tricuspid regurgitant jet (TRJ) which is then

converted to pressure using the Bernoulli's principle {pressure (p) = 4 x volume (v)}[35].

1.2.3.4 Three-dimensional Echocardiography

3D echocardiography (3DE) allows for better anatomical definition of the RV in comparison with 2D imaging, which is advantageous considering the complex geometry of the RV as previously discussed[39]. It allows all three structural components of the RV (inlet, apex and infundibulum) to be adequately visualised. A more accurate measure of RVEF can be obtained as a representation of global systolic performance as no geometrical assumptions are made unlike in the two-dimensional (2D) equivalent[39]. The technique has been well validated against CMR measurements of RVEF[40]. 3DE image acquisition can be performed at the time of the 2D imaging; however a different transducer and software are required. The technique however is dependent on the adequacy of the RV image quality (which often falls short of the quality required) and a regular patient heart rate and rhythm are required[38].

1.2.3.5 Strain

Strain imaging techniques are being utilised more due to the subjective nature of visual assessment of wall motion in conventional echocardiography[41]. Strain is a dimensionless quantity of myocardial deformation and may be defined as the change in myocardial fibre length during stress at end-systole compared to its original length in its relaxed state at end systole[42]. Both strain (displacement) and strain-rate (deformation) are suited to assessment of systolic function, however, they are not a measure of contractility as deformation is load dependant[41]. Strain and strain-rate can differentiate between passive and active myocardial tissue movement unlike measurements such as TAPSE.

Tissue Doppler Imaging (TDI) is an echocardiography technique that was originally used for measuring myocardial strain. In TDI, the doppler principle of measuring the velocity of blood flow using high-frequency, low amplitude signals from moving red blood cells is utilised but using myocardial tissue motion rather than that of blood cells[43]. TDI allows for quantitative assessment of cardiac function and is used to assess both velocity and displacement. TDI uses the

strain-rate and velocity relationship, to construct strain curves and colour-coded images[41]. TDI has been used to assess RV function; however the complex geometry and anatomy of the RV has made accurate assessment of systolic function using this technique challenging.

Speckle tracking echocardiography (STE) is a newer echocardiography technique that measures myocardial deformation using “speckles”. These speckles are ultrasonic patterns of both constrictive and destructive interference within the myocardium which are followed over time using software to calculate strain[44]. Three measures of strain are typically described: longitudinal (shortening from the base to the apex), circumferential (circumferential shortening of the myocardium) and radial (myocardial thickening)[44]. STE as a measure of RV function in clinical practice and in a range of clinical conditions continues to develop[45].

1.2.4 Computed Topography

Computed topography (CT) imaging provides multi-planar imaging of the RV with well-defined endocardial borders and high spatial resolution[38]. It provides images throughout the cardiac cycle using retrospective ECG gating allowing for quantification of RV volume and function. It has advantages of other imaging techniques in that it allows for assessment of the pulmonary vasculature, lung parenchyma and can therefore provide information about pathophysiology of RV dysfunction[38]. Disadvantages include; radiation exposure, the requirement for nephrotoxic contrast and limited availability in some centres. CT imaging is unable to assess right-sided valvular and haemodynamic parameters[38].

1.2.5 Cardiovascular Magnetic Resonance

Cardiovascular magnetic resonance (CMR) is the non-invasive gold standard technique for assessing RV structure and function in a host of different clinical conditions[46-48]. It is a non-invasive, non-ionising technique that has the ability to produce high-resolution images that are unaffected by body habitus and does not require intravenous (IV) contrast.

1.2.5.1 Basic Physics of Magnetic Resonance Imaging

Magnetic resonance imaging (MRI) is based on the phenomenon of the resonance of atomic nuclei in response to radiofrequency (RF) pulses. MRI is composed of three electromagnetic components; a set of main magnetic coils, three gradient coils and an radiofrequency transmitter coil[49]. These coils individually generate a different type of magnetic field which produce magnetic resonance signals when applied to the patient producing a series of MR images.

MRI signals are generated from the water or fat of the patient's own tissues by excitation of the hydrogen ions (H^+) present in cells. The H^+ atom consists of a proton nucleus orbited by an electron and is therefore known as a proton. When a magnetic field is applied, the protons align and spin around an axis, this spinning is called precession[49]. The degree of proton excitation is dependent on the duration and amplitude of the RF pulse applied. Following proton excitation, energy is dissipated, and protons relax returning to their equilibrium state. Two discrete relaxation processes exist, T1 or longitudinal relaxation, and T2 or transverse relaxation. T2 has a faster rate of recovery than T1. These relaxation processes are utilised in T1 and T2-weighted imaging sequences.

A phased array coil is placed on the patient's chest prior to CMR imaging. This coil is composed of several component coils that maximise the MR signal strength whilst minimising interference from tissue and noise. Image acquisition is normally timed in relation to the ECG signal with the period between the two R waves described as the R-R interval (Figure 4). Data acquisition only occurs during specified time frames within the cardiac cycle which reduces motion artefact from the cardiac cycle and allows the capture of phase dependant features of the image[50].

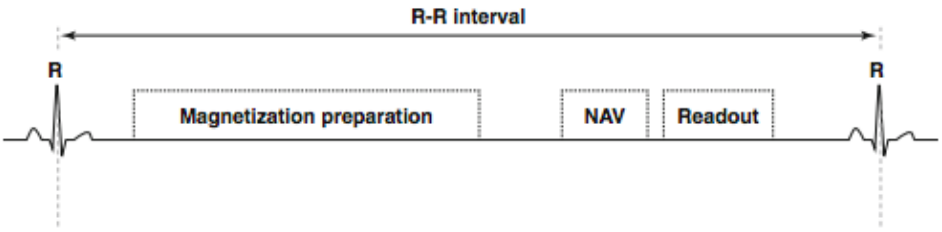

Figure 4 General structure of a CMR pulse sequence.
Between the two R waves the key elements of the pulse sequence are shown. Magnetization preparation is a means of sensitizing the protons to generate a desired image contrast. NAV – respiratory navigation aims to reduce the respiratory motion artefact and readout is the image produced at the end of the sequence[50].

1.2.5.2 Cardiovascular Magnetic Resonance Imaging Sequencing

CMR has a wide range of pulse sequences for imaging that allow definition of cardiac structure, characterisation of different tissues, and measurement of cardiovascular function[51]. Cine imaging is the main technique for imaging regional and global myocardial contractility, function and great vessel blood flow. Cine images can be described as 'movies' that show the heart in motion as it moves throughout the cardiac cycle[52]. The cardiac cycle is divided into multiple segments or frames using segmented acquisition. Each image is typically composed of information from several heart beats with each R-R interval typically divided into 10 to 20 different segments[52].

Dark blood imaging sequences, acquired using spin echo or inversion recovery techniques, are used to define heart morphology. With these techniques, protons in static or slow-moving structures i.e. the myocardium, provide high signal whereas rapidly flowing blood within vessels and the heart move in and out of the imaging slice resulting in a signal void, hence the name "dark blood"[51]. Spin echo requires a relatively long acquisition time with each image requiring an individual breath hold. It allows for the acquisition of high-resolution anatomical images of the heart, mediastinum, aorta and great vessels.

Bright blood imaging is used for acquiring high resolution cine images of RV systolic and diastolic function[51]. Typically used sequences are gradient echo (GRE) and steady-state free procession (SSFP). In these images, the blood pool will appear bright in comparison to the adjacent myocardium, which only

contains intermediate signal intensity. GRE is described as “the workhorse of cardiac imaging” due to its speed and versatility[51]. It is typically used to assess ventricular and valvular structures, measurements of flow, myocardial perfusion and angiography. SSFP is a modification of the GRE technique that produces images with excellent contrast between the blood pool and the myocardium and allows for relatively quick image acquisition[53].

1.2.5.3 Myocardial Structure and Function

CMR is accurate for measuring ejection fraction (EF) and ventricular volumes in 3D as it does not rely on geometric assumptions[51]. In order to measure volume and mass, consecutive breath-hold short axis cross-sections of the heart are obtained with the summation of discs method applied to determine total myocardial mass and volume[51 52].

1.2.5.4 Tissue Characterisation

CMR can provide non-invasive tissue characterisation that other imaging modalities cannot. CMR can provide detailed myocardial tissue characterisation with or without the use of exogenous contrast agents using a variety of relaxation parameters and weighting sequences[54]. Gadolinium (Gd) is the commonly used contrast agent in CMR. After injection of Gd into a peripheral vein, it exits from blood vessels into the interstitial space. In normal, healthy myocardium, the interstitium is a relatively small space and Gd only remains within the space for a short period of time. Diseased myocardium can alter the time Gd remains within the myocardium.

Late Gadolinium Enhancement (LGE) is a CMR technique that acquires images around ten minutes after the injection of Gd. LGE may occur as a result of conditions that increase the interstitial space due to fibrosis, such as chronic MI and cardiomyopathy.

T1 mapping is a newer CMR mapping technique. Myocardial tissue has a ‘normal’ T1 value which can be quantified with CMR imaging with generation of T1 colour-coded maps where each pixel represents the T1 in each voxel (rather than a signal intensity in arbitrary units)[55]. T1 mapping may also be performed before and after the injection of contrast to measure extracellular volume

(ECV). ECV is the relative expansion of the extracellular matrix (Equation 2)[55]. T1 values and ECV are affected by a wide variety of cardiac pathologies including MI, cardiomyopathies, valvular disease, cardiac amyloidosis, and myocarditis.

T2, like T1, can be used to distinguish between normal and abnormal myocardial tissue[56]. Quantitative T2 mapping of the myocardium allows for accurate assessment of myocardial oedema and can provide information about focal, regional or diffuse myocardial disease. T1 and T2 mapping and LGE will be discussed in greater detail in Chapter 4.

$$ECV = (1 - haematocrit)\frac{\frac{1}{post\ contrast\ T1\ myo} - \frac{1}{native\ T1\ myo}}{\frac{1}{post\ contrast\ T1\ blood} - \frac{1}{native\ T1\ blood}}$$

Equation 2 Calculation of extracellular volume.
ECV is calculated using T1 values pre-and post-contrast in both blood and myocardium. The patient's haematocrit is also required.

1.2.5.5 Magnetic Resonance Spectroscopy

Magnetic resonance spectroscopy (MRS) is an imaging technique that utilises MRI to provide non-invasive assessment of cardiac metabolism. The technique utilizes magnetic resonance signals from nuclei, such as phosphorus-31, to provide information regarding the biochemical composition and metabolic state of cardiac muscle[57 58]. Information may be gathered regarding myocardial high-energy phosphates and phospholipids including concentrations of phosphocreatine, adenosine triphosphate and phosphodiesters[57 58]. MRS use has been studied in a range of cardiovascular diseases including heart failure, cardiomyopathy, ischaemic heart disease and valvular heart disease. It offers the advantage of being non-invasive, non-ionising and does not require the use of IV contrast, however, use has been primarily limited to research applications due to low temporal and spatial resolution of the technique and limited availability and expertise.

1.2.5.6 Limitations of Cardiac Magnetic Resonance Imaging

CMR use is limited due to the cost and availability in some centres. Incompatibilities with certain ferrous implants such as implantable cardiac devices, cardiac pacemakers and aneurysm clips can prevent use. It may not always be tolerated by patients' due to issues with claustrophobia, long scan times, body habitus and the requirement for multiple breath holds to prevent respiratory motion artefact. The movement of the heart and lungs throughout the cardiac respiratory cycle presents motion artefact challenges for CMR imaging. The use of breath-holding can reduce the interference of respiratory artefact whilst motion during the cardiac cycle can be improved with the use of ECG-gated imaging[59].

1.2.5.7 Summary of Cardiac Magnetic Resonance Imaging

CMR is a non-invasive, non-ionising imaging technique which is now the gold standard imaging technique of the RV. It allows for accurate, high resolution images allowing for both volume and function evaluation, providing superior assessment in comparison to TTE. Its use is limited in some patients due to long scan times and the incompatibility of ferrous objects.

1.2.6 Biomarker Assessment of Right Ventricular Function

Biomarkers are used in a wide variety of cardiac diseases for diagnosis and monitoring including; cardiac failure, pulmonary hypertension and ischaemic heart disease. No specific biomarker exists to assess RV function, rather a range of biomarkers are used in conjunction with clinical history and imaging.

1.2.6.1 Natriuretic peptides

B-type natriuretic peptide (BNP) and N-terminal pro-BNP (NT pro-BNP) are natriuretic peptides (NPs) predominantly released from the atria in response to myocardial stretch and strain. NPs are characterised by a 17 amino acid ring structure and disulphide bond between two cysteine residues (Figure 5)[60]. BNP is synthesised as a prohormone in the cardiomyocytes and once released into the circulation, proBNP is cleaved into BNP and NT-proBNP in equal proportions. The

interaction of BNP and natriuretic peptide receptor type A mediates the biological effects via intracellular cGMP increase. The physiological effects of BNP include; diuresis, inhibition of the renin-angiotensin-aldosterone system (RAAS), and peripheral vasodilatation[61].

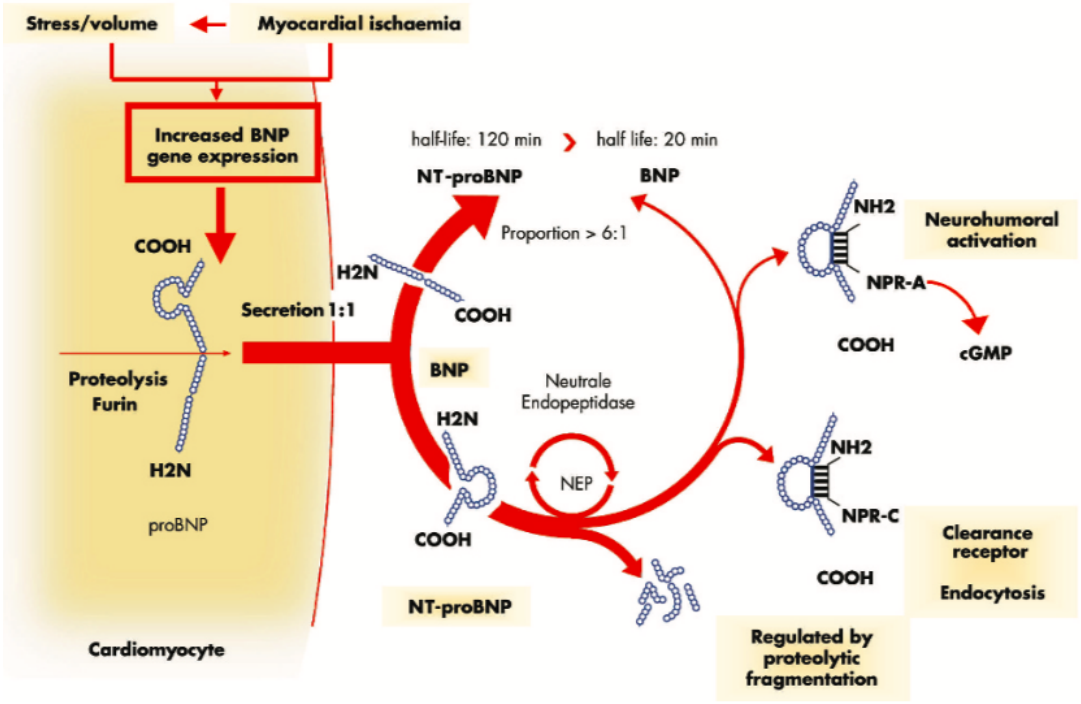

Figure 5 Illustration of BNP and NT-proBNP synthesis and release.
Taken from Weber and Hamm[61].

BNP is cleared from plasma by binding to the NP receptor type C and proteolysis by endopeptidases[61]. NT-proBNP is primarily cleared by renal excretion. BNP has a half-life of approximately twenty minutes with a longer half of one hundred and twenty minutes for NT-proBNP. In clinical practice, NT-proBNP circulating blood levels are six times higher than BNP due to the longer half-life. Both BNP and NT-proBNP are affected by age and sex with higher levels in female and older individuals[62]. Impaired renal function also increases both BNP and NT-proBNP with higher values in NT-proBNP[61].

The single, most validated and established use of NPs is in the diagnosis of congestive cardiac failure, with NP measurement recommended in the National Institute of Clinical Excellence (NICE) guidelines for diagnosis of newly suspected

heart failure[63]. Elevated levels of NPs are associated with poor long-term prognosis in patients with congestive cardiac failure[64]. Elevated NPs can aid identification of patients with PE who are at high-risk of short-term death and adverse events[65]. A meta-analysis demonstrated raised levels of BNP and NT-proBNP were associated with PE and RV dysfunction[65].

In non-cardiac surgery, pre-operative BNP levels have been shown to be predictive of both short- and long-term mortality and cardiopulmonary complications with increased levels of BNP predicting higher rates of complications[66-69]. Two meta-analyses have demonstrated that pre-operative BNP (including NT-proBNP) is an independent predictor of short-term cardiovascular complications after non-cardiac surgery[70 71]. BNP has been included in both the European Society of Anaesthesiology (ESA) and American Heart Association (AHA) guidelines for assessing peri-operative cardiac risk in patients undergoing non-cardiac surgery[72 73].

Our research group have demonstrated an increase in BNP following lung resection with a significant elevation on post-operative day one (POD1) and POD2[74]. Peri-operative BNP measurements have also demonstrated association with post-operative patient reported dyspnoea and a functional capacity (Figure 6)[74].

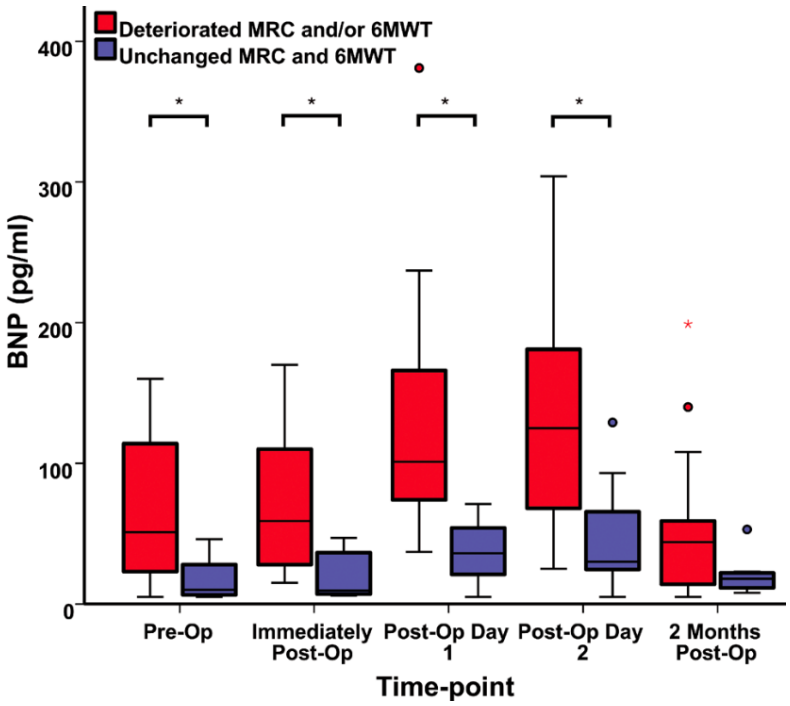

Figure 6 Comparison of BNP levels between patients with deteriorated and unchanged functional capacity following lung resection.
Change over time in patients showing functional deterioration (p <0.01, Friedman's test). Change over time in patients showing no functional deterioration. (p = 0.03, Friedman's test). Comparisons between groups using the Mann-Whitney U-tests. *p-value <0.01. BNP - B-type natriuretic peptide, MRC – medical research council. 6MWT – 6-minute walk time. Pre-op – pre-operative. Post-op – post-operative. Taken from Young et al[74].

1.2.6.2 Troponin

Cardiac troponins are released as a result of injury and ischaemia of cardiac myocytes. The troponin complex is a component of both cardiac and skeletal muscle thin filaments, consisting of three subunits, I, T and C. Troponins are known to be elevated in an extensive range of clinical cardiac and non-cardiac conditions including; MI, heart failure, stroke, cardiac arrhythmias, sepsis, and renal failure[75]. A troponin rise is commonly encountered in PE with raised troponin associated with increased frequency of RV dysfunction and poorer patient outcomes[76-78].

In non-cardiac surgery, high sensitivity troponins are used to facilitate risk stratification of those patients at risk of post-operative cardiac complications. Meta-analyses have shown both pre-operative and post-operative troponins are independent predictors of post-operative mortality[79 80]. One meta-analysis demonstrated a raised pre-operative troponin above the 99th centile was

associated with three times higher risk of major post-operative cardiovascular complications[79]. Our research group has shown a small but significant rise in post-operative TnT in those patient's undergoing lung resection[81].

1.3 Conclusion

The RV is thin-walled with a complex geometry and structure coupled to a low-pressure pulmonary system. Like the LV, its function is dependent on preload, contractility and afterload. Unlike the LV, the RV is sensitive to increases in afterload. The RV is often understudied when compared with the LV; however, the role of RV function in health and disease is increasingly recognised. With the use of newer imaging techniques, evaluating the RV is becoming less challenging.

A variety of techniques can be used to assess and evaluate RV function, but no single best technique is available in current practice. Invasive techniques, such as the conductance catheter, allow load independent assessment of function, however it is a complex technique, is only available in a handful of centres and is not used for routine clinical assessment. The PA catheter provides assessment of flow and pressure but is unable to provide reliable measurement of RV volumes. TTE is the most commonly used technique in clinical practice as it is easy to use, widely available and non-invasive. CMR is the most reproducible imagine technique for assessing both function and volume of the RV and as such is the non-invasive reference method for RV evaluation.

Chapter 2 The Right Ventricle Response to Lung Resection.

2.1 Lung Cancer

Lung cancer is the third commonest cancer in the United Kingdom, accounting for 47,388 new cancer diagnoses in 2016 (latest available data from Cancer Research UK)[82]. It remains the most common cancer overall in Scotland with 5331 cases diagnosed in 2017[83]. Only 5% of patients with lung cancer survived for 10 years or more in 2010-2011[82]. Scotland, along with the North of England, have the highest proportion of lung cancer patients per region (Figure 7)[84 85].

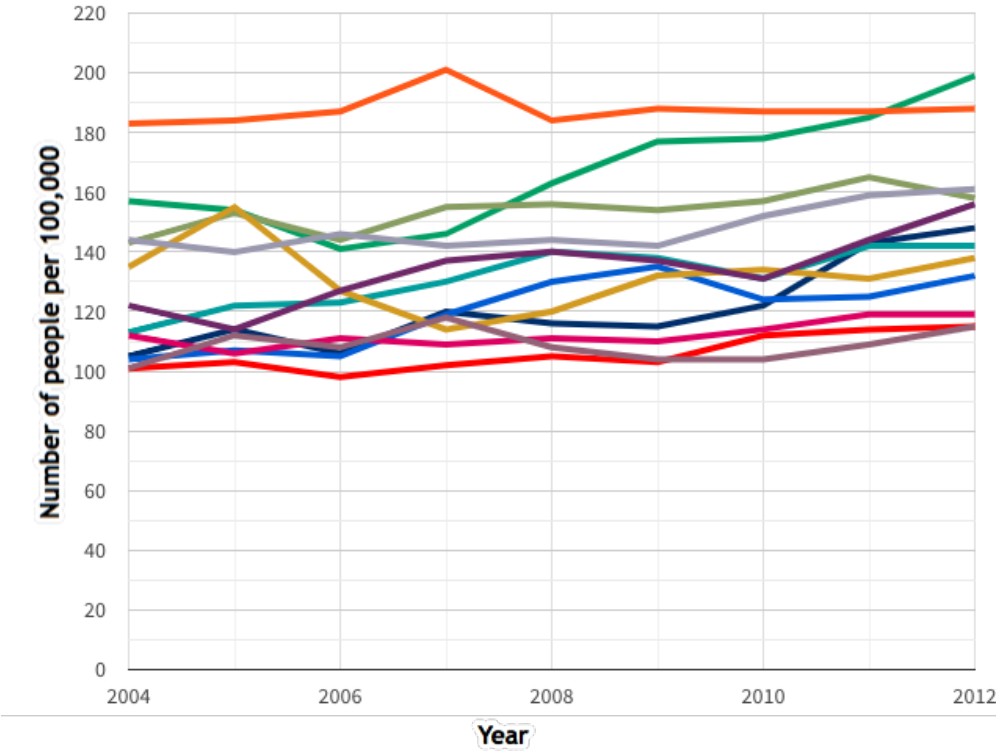

Figure 7 Number of lung cancer patients per 100,000 in each region of the UK in 2012. Scotland shown at the top of the graph in orange with 201 in 2007 falling to 188 in 2012. Taken from the British Lung Foundation[84].

2.1.1 Lung Cancer Management

Management of lung cancer requires a multi-modal approach including radiotherapy, chemotherapy, surgical resection or a combination of treatment strategies depending on cancer staging. The National Institute for Health and Care Excellence (NICE) published the Lung cancer: Diagnosis and Management

guideline in March 2019, recommending lobectomy (either open or thoracoscopic) for people with non-small cell lung cancer (NSCLC) who are well enough and for whom treatment with curative intent is suitable[86]. The number of NSCLC patients being offered surgery continues to rise with 17% of patients undergoing surgery in England in 2017, an increase of 8% since 2006 (Figure 8)[87]. A variety of factors have resulted in an increase in surgical resections including recommendations to invite older patients with multiple co-morbidities to consider surgery if they are prepared to accept the higher risks associated[88].

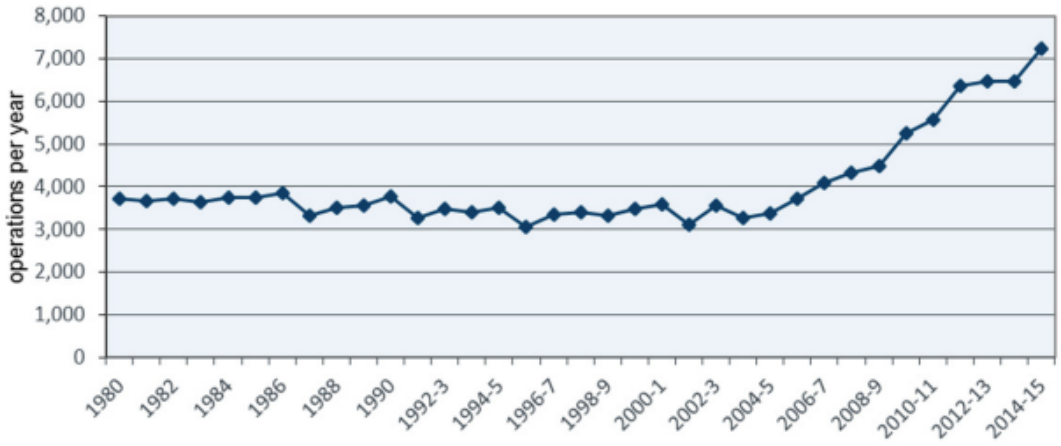

Figure 8 Number of lung cancer operations by year.
Number of operations for all lung cancers in England. Surgery for non-small cell lung cancers totalled 92.6% of all lung cancer surgeries. Data from Lung Cancer Clinical Outcomes Publication in 2016[89].

2.1.2 Lung Cancer Surgery Morbidity and Mortality

The historical surgical approach for performing lobectomy was that of an open thoracotomy, whereby a large incision is made to enable access to the rib cage before opening the intercostal space. Evolving techniques have led to the introduction of video-assisted thoracoscopy (VATS) with the theoretical advantage of a restricted surgical approach using three or four ports or a limited mini thoracotomy or a combination of both. The number of lung resections performed by VATs has continued to increase across the UK with VATS accounting for 58% of all cancer resections in 2018, with data from the National Thoracic Surgery Activity showing in-hospital survival around 99% for both surgical approaches[90 91]. Studies have indicated that VATs surgical resection have significantly less short and longer-term morbidity and a shorter length of stay

when compared with open thoracotomy[92-94]. The largest randomised study in the UK, comparing VATS and open for primary lung cancer, showed a significant reduction in overall hospital complications observed in the VATS group (32.85 v 44.3%, p=0.008) with VATS having a shorter hospital stay (median 4 days versus 5 days, p=0.008)[95 96].

Lobectomy is established as the standard procedure for early-stage lung cancer; however, there is the option of limited resection surgery (sub lobar resection), which is traditionally considered in those patients who would not tolerate lobectomy due to pre-existing cardiovascular or respiratory co-morbidities. The only randomised controlled study comparing lobectomy and limited resection did not demonstrate any statistical evidence for preservation of pulmonary function in limited resection compared with lobectomy[97]. Similar results were also demonstrated in studies by Takizawa, Harada and Saito[98-100]. A study by Zhang et al demonstrated better perioperative outcomes in sub-lobar resection in elderly patients with stage one NSCLC including less blood loss and shorter hospital stay[101].

Patients undergoing lung resection surgery are generally considered to be 'high-risk' surgical candidates for a number of reasons including; age (significant proportion are >60 years), a significant smoking history and a high prevalence of cardiovascular and respiratory co-morbidities. Major post-operative complications are primarily cardiac or respiratory in nature. Post-operative pulmonary complications (PPCs) include; pneumonia, PE, acute respiratory distress syndrome (ARDS), persistent air leak, bronchopleural fistula and lobar collapse. Incidence rates of PPCs are reported between 7% to 49% and have been shown to increase length of hospital stay and are associated with increased mortality[102-107].

Post-operative cardiac complications include; myocardial infarction (MI), cardiac arrhythmias, cardiac failure, and stroke[106]. The commonest cardiac complication following lung resection is atrial fibrillation (AF) with a reported incidence between 4% and 37%[108-111]. AF may significantly increase morbidity and mortality in the post-operative period and affect longer-term outcomes[108 109 112]. Post-operative MI rates range from 3% to 17%, with heart failure and pulmonary oedema less commonly seen[113]. Patients with post-operative complications

require increased medical support and intervention leading to significant use of hospital resources in the immediate post-operative period and longer-term.

Not only do patients present with post-operative complications, they also report a significant reduction in their quality of life (QoL). They describe a decline from their pre-operative functional ability, with worsening shortness of breath, reduced exercise capacity, reduced ability to carry out day-to-day activities, increased fatigue and lethargy and a poor overall QoL[114 115].

2.1.3 Predictors of Morbidity and Mortality Following Lung Resection

Predicting which patients will develop peri- and post-operative complications following lung resection remains challenging with no *single* predictive test or tool existing. Known risk factors include; male sex, increasing age, higher American Society of Anaesthesiologists (ASA) score, pre-existing renal dysfunction, steroid use, prior chemo-radiation therapy, pneumonectomy, and bilobectomy[116 117].

Current guidelines recommended using a combination of respiratory and cardiovascular function as a guide as to who should be offered surgery and as a predictor of those who may suffer post-operative complications. British Thoracic Society (BTS) and NICE recommend performing spirometry and transfer diffusion capacity for carbon monoxide (TLCO) in all patients considered for surgery with curative intent[86 88]. Both forced expiratory volume in one second (FEV_1) and TLCO can be corrected to predict post-operative lung function values ($ppoFEV_1$ and ppoTLCO) by calculating the amount of functional lung that will remain following surgery. Studies have demonstrated FEV_1, $ppoFEV_1$, TLCO, and ppoTLCO are all predictive of post-operative morbidity and mortality following lung resection[114 116-120].

Both BTS and NICE guidelines recommend the use of a global risk score to estimate the risk of death following surgery and recommend this is discussed with the patient as part of the consent process[86 88]. A variety of pre-operative scoring systems are available that include cardiovascular and respiratory parameters[121-123]. The Thoracic Revised Cardiac Risk Index (ThRCRI) is one such

score which differentiates patients into those who may proceed to surgery and those who require further cardiovascular examination.[124] The ThRCRI score incorporates four parameters; 1) history of ischaemic heart disease, 2) history of cerebrovascular disease, 3) serum creatinine level greater than 2mg/dl and 4) planned pneumonectomy[124]. Early studies demonstrated association between higher ThRCRI score and major cardiac events following lung resection[121 125]. However, the ThRCRI has a poor predictive value with an area under the receiver operator characteristic curve of 0.62, with further studies unable to demonstrate a relationship between higher ThRCRI and risk of cardiac complications[126 127]. Association between ThRCRI and patient reported outcomes and QoL has not been studied.

Thoracoscore is a logistic-regression derived model consisting of nine pre-operative and operative variables to predict risk of in-hospital mortality[128]. Further studies, carried out in the UK, have failed to validate Thoracoscore in predicting in-hospital mortality and it may be that Thoracoscore, originally developed in France, is not an accurate predictor for the UK population[128 129]. A major limitation of Thoracoscore is that it only predicts in-hospital mortality, whereas data shows that in-hospital mortality is relatively low and static at 1.8%[91]. It is unable to predict those who may suffer post-operative complications and is not an indicator of which patients will report poor QoL or a limitation in patient reported outcomes.

It would seem apparent that risk prediction following lung resection should incorporate both respiratory and cardiovascular function. Given that a large proportion of patients undergoing lung resection have cardiopulmonary dysfunction, the focus has shifted from assessment solely of pulmonary function towards a combination of cardiopulmonary function. The role of the RV in health and disease is now recognised and has been widely examined in cardiac disease and surgery[5-8 130-132]. The importance of the RV in pulmonary disease has also been examined with RV dysfunction well recognised in chronic obstructive pulmonary disease (COPD), PH and PE[4 133-139]. It would therefore seem feasible that the RV may be affected in lung resection surgery. The relationship between RV function and post-operative lung resection outcomes is examined in this chapter.

2.2 The Right Ventricular Response to Lung Resection

It is now widely recognised that lung resection surgery results in RV dysfunction peri- and post-operatively. Changes in the RV occur as a result of the use of OLV intra-operatively and the removal of lung parenchyma resulting in re-distribution of CO to the remaining lung with a resultant increase in PVR and afterload.

During lung resection surgery, the patient is traditionally placed on the lateral decubitus position with the surgical site exposed. One lung ventilation (OLV) is utilised to improve exposure to the surgical field and involves mechanical separation of both lungs to allow ventilation to only the dependant lung whilst allowing for collapse of the non-dependant lung. A number of physiological changes occur during OLV including alterations in oxygenation, alteration in lung mechanics and disruption in right heart function.

The non-ventilated lung remains perfused during OLV which generates a right to left shunt which may be partially corrected by hypoxic pulmonary vasoconstriction (HPV) and re-distribution of blood flow[140]. Hypoventilation and ventilation/perfusion mismatch may occur as a result of OLV and lead to hypoxaemia and hypercapnia[141]. Both hypoxaemia and hypercapnia result in further pulmonary vasoconstriction with increased elastance of the pulmonary vasculature which may leads to alterations in RV-PA uncoupling and RV dysfunction[141].

During OLV, HPV in the non-dependant non-ventilated lung aims to reduce the right to left shunt, in doing so an increase in PVR and afterload occurs increasing the RV workload[138]. As described in Chapter 1, the RV is very sensitive to changes in afterload. Intra-operative ventilation settings with high inspiratory tidal volumes and high peak inspiratory pressures may affect further alter RV function by increasing RV afterload.

A variety of studies have examined the right ventricular response to lung resection. Various techniques have been used including pulmonary artery catheters (PAC), TTE and more recently CMR imaging. Table 2 describes the PAC studies and Table 3 describes the imaging studies.

2.2.1 Studies using Pulmonary Artery Catheter

A host of studies, including patients undergoing pneumonectomy and lobectomy surgery, have used the PAC for assessing RV parameters in the peri- and post-operative period. The majority of studies have used exclusively PAC with one study using a combination of PAC and TTE. The studies primarily focused on the PAC derived parameters: pulmonary artery pressure (PAP), pulmonary vascular resistance (PVR), RV ejection fraction (RVEF) and RV end-diastolic volume index (RVEDVI), these parameters are discussed individually below.

2.2.1.1 Mean Pulmonary Artery Pressure

Five studies have examined mPAP, including studies at rest and exercise, with four studies demonstrating alterations during the study time period. In those measured at rest, Reed et al demonstrated an increase in mPAP one hour post-operatively, which was maintained at four to six hours but had returned to baseline by 24 hours[142]. Rams et al were unable to demonstrate changes in mPAP at rest but did demonstrate increased mPAP on exercise[143]. Similarly, Nishimura et al demonstrated an increase in mPAP with exercise at 6 months post-operatively[6]. These patients were then followed up at 42-48 months demonstrating an increase in mPAP at rest as well as on exercise[144].

Author Year *(n)*	Measure of RV function	Time Points	Change in function	Comments
Rams et al.[143] 1962 61 (pneumonectomy)	mPAP	Variable (30 days – 7years)	↑mPAP with exercise	PA pressures were higher in those who died post-op 24 patients with post-op PAC.
Reed et al.[145] 1992 15	RVEF, CO RVEDV, PVR, PAP	Pre-op PA occlusion Completion Post-op: 4h, 6h POD1 , POD2	Intra-op: ↑PVR Post-op: ↓PAP initial, ↔ PAP POD 1:↓RVEF, ↑RVEDV	3 patients had sustained arrhythmias that correlated with significant increase in RVEDV.
Nishimura et al[146] 1993 9	PAP, PCWP, RAP, PVRI	Pre-op 4-6months post-op	↑mPAP with exercise ↑PVRI at rest and with exercise	Open lobectomy or bilobectomy. "*haemodynamics after pulmonary resection as compared with the preoperative values better predict the postoperative quality of life in lung cancer*."
Reed et al.[142] 1993 10	RVEF, mPAP RVEDVI, PVR	Pre-op Post-op: 1h, 4-6h, 24h	↑PAP at 1hr maintained 4-6h, returned to baseline at 24h ↔RVEF, ↑RVEDVI	
Okada et al.[147] 1994 20	RVEF, RVEDVI PAP, PVR	Pre-op 1hr , 6hr POD1, POD2 Week 3	↑RVEDVI, ↓RVEF (at rest and exercise) ↑PAP/PVR during exercise only	10 exercise,10 rest RVEF is depressed post-operatively and has only partially recovered by week 3 .

Reed et al[148] 1996 41	RVEF, RVEDVI PRVI, PRSW	Pre-op POD1 POD2	Part 1: ↑RVEDVI, ↓RVEF, ↔ PRVI Part 2:↑RVEDVI, ↓RVEF, ↔ PRVI	Part 1: RVEDVI and RVEF in 35 patients undergoing lobectomy or pneumonectomy. Part 2 – 6 patients undergoing lobectomy had a prostaglandin infusion to reduce RV afterload.
Backlund et al.[149] 1998 24	PAP, RVEF RVEDVI, RVSWI PVRI	Pre-op Recovery POD1-3	Group P:↓RVEDVI (POD 1) ↔ RVEDD ↔ PVRI Group S:↑mPAP/PVRI (POD1-3), ↓RVEF(POD1-3), ↔RVEDVI/RVSWI, ↓RVEDD	Patients who developed AF had greater PVRI and a greater RVSP immediately post-op. Group P – FiO_2 35% until POD3. Group S – FiO_2 35% until POD1.
Miyazawa et al.[144] 1999 8	Rest and exercise: mPAP, PVRI, CO, CI	Pre-op 4-6 months 42-48 months	↑mPAP at exercise ↑PVRI at rest and exercise	Both lobectomy and bilobectomy.
Mikami et al.[150] 2001 23	RVSWI RVEF	Pre-op 6h, 12h 24h, 48h	↑RVEDVI in both groups VATS:↓RVEF	To determine if VATS lobectomy is better for those patients over 70. 13 VATS, 10 pneumonectomy.
Mageed et al. [151] 2005 30	mPAP, RVEDV, RVEF, RVSWI, PVRI	Pre-op Immediately post-induction 2h post-op	At 2hrs post-op:↓RVEF , ↔mPAP, ↔RVEDV, ↔RVSWI ↔PVRI	*"afterload is not the causative factor of RV dysfunction in the early postoperative period and that alteration in RV contractility may be the causal factor".*

Elrakhawy et al.[152] 2018 178	mPAP, PVR, RVEF, RVEDVI	Pre-op Post-op: 3h,6h,12h, 24h, 48h	Pneumonectomy:↓RVEF, ↑RVEDVI, ↑PVR Lobectomy:↓RVEF, ↑RVEDVI, ↑PVR	"*right ventricular dysfunction early after major pulmonary resection as evidenced by increased RV afterload. This dysfunction is more pronounced in pneumonectomy*".

Table 2 Studies assessing right ventricular function after lung resection using pulmonary artery catheter

↔ = no change, ↑ = increase, ↓ = decrease, PAC = pulmonary artery catheter, mPAP = mean pulmonary artery pressure, PA = pulmonary artery, Post-op = post-operatively, Intra-op = intra-operatively, RVEF = right ventricular ejection fraction, CO = cardiac output, RVEDV = right ventricular end-diastolic volume, RVEDVI = right ventricular end-diastolic volume index, PVR = pulmonary vascular resistance, Pre-op = pre-operatively, POD = post-operative day, PCWP = pulmonary capillary wedge pressure, RAP= right atrial pressure, PVRI = pulmonary vascular resistance index, RVESVI = right ventricular systolic volume index, RVESV = right ventricular systolic volume, LVEF = left ventricular ejection fraction, CI = cardiac index, VATS = video-assisted thoracoscopy, RVSP = right ventricular systolic pressure, PASP = pulmonary artery systolic pressure.

2.2.1.2 Pulmonary Vascular Resistance

PVR and pulmonary vascular resistance index (PVRI) have been widely examined following lung resection (Equation 1, Chapter 1)[142 144-146 148 149 151]. PVR has been shown to increase in the immediate post-operative period but begin to fall towards baseline and return to normal by POD2 (Figure 9)[142 145]. Studies examining PVRI over a longer post-operative course have shown PVRI increases at both rest and on exercise[146 147 144].

In a study by Backlund et al patients undergoing lobectomy were randomised to two groups post-operatively to assess the effect of oxygenation on pulmonary haemodynamics[149]. Patients who received shorter oxygen duration (until the morning of POD1 versus 35% oxygen for three days) had higher PVRI[149].

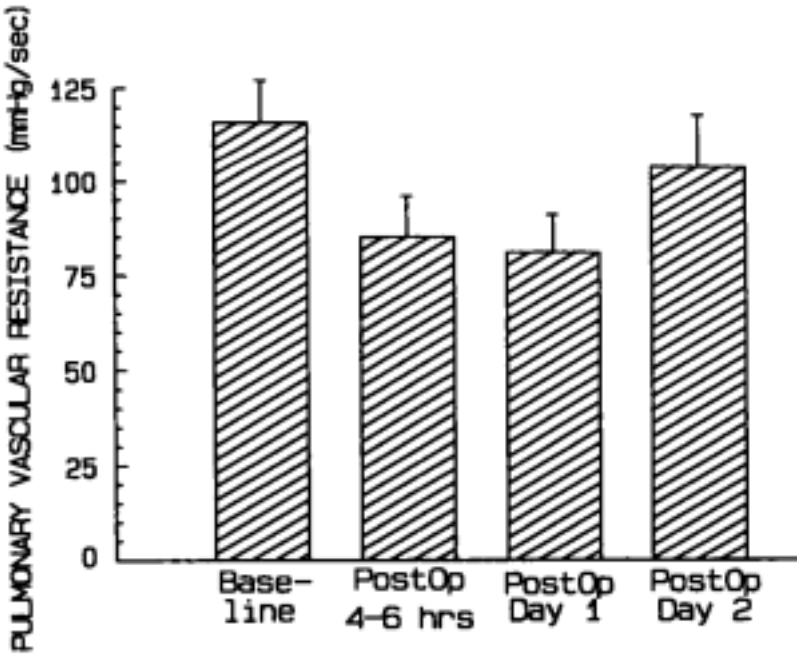

Figure 9 Pulmonary vascular resistance in the post-operative period.
Taken from Reed et al[145]. This demonstrates the derived PVR was significantly below baseline in the early post-operative period and on post-operative day 1 ($p<0.05$) but returned to normal by post-operative day 2. In keeping with most other reports yet contrary to accepted belief, PVR is not increased postoperatively.

2.2.1.3 Right Ventricular Ejection Fraction

Various studies have reported the impact of lung resection on RVEF[142 145 147-151 153]. Of the various parameters described in the literature, consistently RVEF has been depressed in the post-operative period from as early as POD2 to 48 months following surgery[145 142 147 148 151-153]. Reed at al were the first to utilise volumetric PAC to measure RVEF and demonstrated a significant reduction in mean (SD) RVEF from 45% (2) at baseline to 36% (3) on POD2 (Figure 10), of which similar findings have also been reported in other studies[145 142 147 148 151-153].

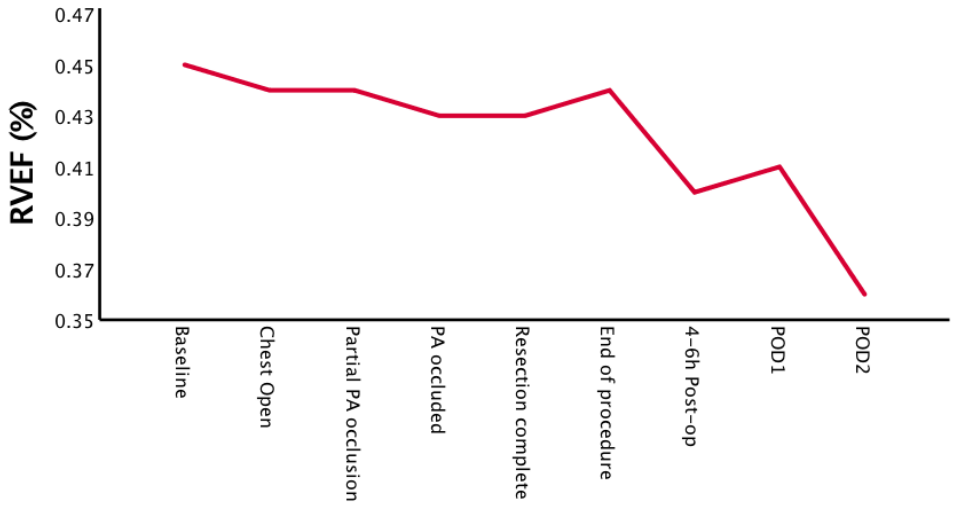

Figure 10 Right ventricular ejection fraction measured using volumetric pulmonary artery catheter following lung resection.
Adapted from Reed et al[145]. Note the reduction in RVEF at four to six hours which remains depressed from baseline at POD1 and 2 ($p<0.05$). Insufficient data available to allow for drawing of error bars.

2.2.1.4 Right Ventricular End-Diastolic Volume Index

Right ventricular end-diastolic volume (RVEDV) is the volume of blood present in the RV at the end of diastole and is considered a surrogate for preload. This can be indexed to body surface area (ml/m^2) to give the RVEDV index (RVEDVI). Various studies have shown an increase in RVEDV or RVEDVI in the post-operative period following lung resection[142 145 147 150 152 153].

2.2.1.5 Limitations of Volumetric Pulmonary Artery Catheters

Pulmonary artery catheters have been available since the 1940s but they became commonplace in the 1970s after the development of the first balloon tipped flow directed catheter which could be inserted in the intensive care unit (ICU) setting without the need for fluoroscopy[154]. Whilst the technique is safe, compared to non-invasive assessment there remains a slight morbidity and mortality risk. In a review by Hoeper et al. of 7218 catheterisations, two patients died directly from catheter related complications while 76 patients had serious adverse events (including pneumothorax, arrythmia, haematoma, and hypotension)[155].

As a consequence of the risks associated with insertion of a PAC and evidence suggesting a lack of benefit associated with their use[156], the use of PACs declined rapidly within the critical care setting. Despite the decline in PAC in clinical practice, studies examining the RV response to lung resection have continued to use PAC for measuring RV haemodynamics. Volumetric PACs (vPACs) have been compared with angiography in a small study with only 13 patients, the correlation between the two methods for RVEF was r = 0.83 and r = 0.71 for RVEDV (Bland Altman analysis was not performed in this study)[157]. Transoesophageal three-dimensional echocardiography (3DE) was compared with vPACs in 25 patients undergoing coronary artery bypass surgery[158]. Volumetric PACs were found to overestimate RV volumes with no correlation between RV volumes obtained by thermo-diluation and those obtained by 3DE. The bias for measuring RVEF was +15.6% with a precision of +/- 4.3%[158]. Hein et al compared vPAC with conductance catheters, a method considered gold standard for assessing RV volumes and function, in a pig model of RV infarction[159]. The conductance catheter demonstrated a decrease in RVEF and an increased in RVEDV during ischaemia which was not evident in the PAC data[159]. The validity and realibility of vPACs is questioned in the studies described above, and given that both PAH and RV ischaemia may be contributing mechanisms in RV dysfunction, the use of vPACs as a method to assess RV function after lung resection is questionable:

"Pulmonary artery catheter determined right ventricular ejection fraction and right ventricular end-diastolic volume: Another case of "The Emperor Has No Clothes"

Andrew B Leibowitz[160]

2.2.2 Studies Using Echocardiography.

Echocardiographic assessment of the RV is now commonplace and the studies in the literature examining the RV response to lung resection reflect the change in practice with the transition from PAC to TTE in the early 21st century. Studies report a range of parameters to assess RV function including standard TTE measurements TRJ velocity, right ventricular systolic pressure (RVSP), pulmonary artery systolic pressure (PASP) and newer techniques including tissue doppler and strain measurements.

2.2.2.1 Standard Transthoracic Echocardiography

Both TRJ and RVSP have been shown to increase following lung resection[161-163]. Amar et al describe two studies of the same patient cohort, the first demonstrating patients who developed SVT had a higher TRJ velocity (2.7+/-0.6m/s compared to 2.3+/-0.6m/s) on POD 2-6[161]. The authors further reported findings from the same cohort of patients revealing a significantly higher RVSP[1], on post-operative days two to six, in the pneumonectomy group compared with the lobectomy group (31+/-15 mmHg and 25+/-10mmHg respectively, $p<0.05$)[162]. In a study by Venuta et al only pneumonectomy patients showed an increase in TRJ 2.3+/-0.1m/s to 2.6+/-0.1m/s) and PASP (26mmHg +/- 2.3mmHg to 34.3mmHg +/-7.6mmHg) from pre-operative assessment to assessment at four years but no significant change in lobectomy patients[163].

Foroulis et al compared patients undergoing pneumonectomy and lobectomy using continuous wave Doppler TTE pre-operatively and at six months post-operatively, demonstrating an increase in the number of patients with TTE

[1] Of note RVSP is derived from TRJ. The first study used TRJ and the second RVSP, from the same cohort of patients, these studies ultimately demonstrating the same information.

detectable TR post-operatively in both pneumonectomy and lobectomy patients at six months[164]. These post-operative increases corresponded to a higher PASP (40.5+/-12.5mmHg) in the pneumonectomy group compared with the lobectomy group (32.9+/-5.3mmHg)[164]. Patient's undergoing a right sided pneumonectomy also had a higher PASP at follow-up compared to those with a left sided procedure. RV dilatation, defined as abnormal if basal dimensions >28mm, was associated with higher PASP pressures (48.47 +/- 11.32mmHg v 28.66+/-4.84mmHg) compared to those with normal RV dimensions[164].

2.2.2.2 Tissue Doppler Echocardiography

Tissue Doppler TTE has been utilised by two authors, the first study using such a technique by Colkesen et al showed a change in tricuspid valve velocities but no demonstrable change in volumes[165]. There was a significant rise in the tricuspid A wave velocity, decrease in tricuspid e' and tricuspid E deceleration time, indicating an impairment in RV relaxation and filling postoperatively. This study also demonstrated a significant increase in heart rate which can have an impact on the interpretation of Doppler values, and this should be considered when interpreting these findings. The second study using tissue doppler demonstrated the peak velocity of early diastolic filling (E wave) was significantly reduced on POD7 compared to POD2 (35.77 ± 7.4cm/s versus 45.93 ± 8.0, $p<0.05$).[166] Peak velocity of late diastolic filling (A wave) demonstrated a rise from pre-operative baseline at both POD2 and 7. A decrease in the height of the E wave and an increase in the height of the A wave represents impaired relaxation and is indicative of a stiff ventricle. The authors suggest these findings reflect both early systolic and diastolic RV dysfunction.

Author Year *(n)*	Measure of RV function	Time Points	Change in function	Comments
Amar et al[161] 1995 100	**TTE:** TRJ, RVSP	Pre-op POD1 POD 2-6	↑ TRJ in SVT group	"*Increase in right heart pressure predisposes to SVT after lung resection*".
Amar et al.[162] 1996 86	**TTE:** RVSP	Pre-op POD1 POD2-6	Pneumonectomy: ↑RVSP at POD2-6	Used same cohort of patients in Amar et al 1995.[161]
Foroulis et al.[164] 2004 52	**TTE:**PASP	Pre-op 6m	Pneumonectomy: ↑RVSP,↑RV dimensions Lobectomy: ↑RVSP	Elevated PASP is associated with RV dilatation in both groups. In the pneumonectomy group, patients with more debilitating dyspnoea at 6 months had higher PASP at this time.
Venuta et al.[163] 2007 51	**TTE:** PASP, RVDD	Pre-op 1 week, 3m, 6m 1yr	Pneumonectomy: ↑RVDD, ↑RVSP Lobectomy: No change	36 lobectomy, 15 pneumonectomy. "*RV modifications evident after pneumonectomy compared with lobectomy.*"
Colkesen et al.[165] 2009 19	**TTE:** Peak diastolic E/A, DT, IVRT	Pre-op 4 weeks	↓Tricuspid E ↑Tricuspid A	Utilised both traditional 2D TTE and tissue doppler techniques.
Kumbasar et al.[166] 2013 20	**TTE:** E/A, E', A', S'	Pre-op POD2	POD2: ↓E, ↑A, ↓S'	E/A, E', A', S' reflects systolic and diastolic dysfunction. No comparison made with standard TTE.
Wang et al. [167] 2016 **30**	**TTE:** Longitudinal, circumferential and radial strain. PAP	Pre-op 1 week	Pneumonectomy: ↑PAP, ↓ all strain Lobectomy:↓all strain	First study to analyse strain after lung resection.

Smulders et al. [168] 2007 15	**CMR:** RVEDV, RVEDVI, RV mass	Pre-op 5years	No change in RV volumes after left sided pneumonectomy ↓RVEDV in right-sided	Study primarily assessing anatomical and geometrical changes of the heart 25 control patients
McCall et al. [81] 2019 27	**CMR:** RVEF RV SV: ESV	Pre-op POD2 2m	POD2: ↓RVEF ↓RV SV:ESV, ↑RVESV 2 months: ↓RVEF ↓RV SV:ESV	SV: ESV derived index of right ventriculoarterial coupling First CMR study in the perioperative lung resection period

Table 3 Imaging studies of right ventricular function after lung resection.
Post-op = post-operatively, Intra-op = intra-operatively, RVEF = right ventricular ejection fraction, CO = cardiac output, RVEDV = right ventricular end-diastolic volume, RVEDV = right ventricular end-diastolic volume index, Pre-op = pre-operatively, POD = post-operative day, PCWP = pulmonary capillary wedge pressure, RAP= right atrial pressure, RVESVI = right ventricular end-systolic volume index, RVESV = right ventricular end-systolic volume, LVEF = left ventricular ejection fraction , VATS = video-assisted thoracoscopy, TTE= transthoracic echocardiography TRJ = tricuspid regurgitation jet, RVSP = right ventricular systolic pressure, PASP = pulmonary artery systolic pressure, TV = tricuspid valve, RVEDD = right ventricular end-diastolic diameter, CMR = cardiovascular magnetic resonance, m = months.

2.2.2.3 Strain Echocardiography

One study has utilised the novel technique speckle tracking echocardiography to assess myocardial strain following lung resection. Thirty patients who had undergone lung resection (10 pneumonectomy and 20 lobectomy) underwent TTE pre-operatively and one week post-operatively to assess radial strain (RS), circumferential strain (CS) and longitudinal strain (LS) in the RV[167]. In the lobectomy group a significant change was demonstrated post-operatively from pre-operative values with LS (17.06+/-3.34 versus 21.95+/-2.46, $p<0.05$) but no change in RS or CS.[167] In the pneumonectomy group significant changes were demonstrated in all three values; LS (11.48+/-2.51 versus 21.05+/-21.3, $p<0.05$), CS (-1665+/- 21.55+/-3.26, $p<0.05$) and RS (28.37+/-11.23 versus 41.56+/-10.11, $p<0.05$)[167].

2.2.3 Studies using Cardiovascular Magnetic Resonance Imaging.

Despite CMR being the gold standard for assessment of the RV, its role in assessing the RV response to lung resection has not been widely explored. Smulders et al was the first study to utilise CMR following lung resection, comparing patients five years after pneumonectomy with a control group (no pre-operative imaging was performed)[168]. Primarily, the study assessed the anatomical and geographical changes to the heart following lung resection. They demonstrated that left-sided pneumonectomy was associated with an increased LV-EDV and a decreased LVEF, but normal RV volumes. Right-sided pneumonectomy showed signs of RV hypertrophy and decreased RV-EDV with no change in LV volumes or function. In this study, RVEF was not measured.

Our research group was the first to perform serial CMR imaging of the right heart after lung resection. Twenty-eight patients were included in the study undergoing CMR at three time points: pre-operatively, POD2 and at two-months to assess RV and LV volumes. In addition to RV function, measures of RV-PA coupling were assessed with the ratio of SV to ESV calculated as an estimate of RV-PA coupling (originally described by Sanz et al as a non-invasive technique using CMR)[169]. The study showed no change in LVEF post-operatively but a reduction in median RVEF by POD2 (Figure 11)[81]. A deterioration in RV SV: ESV

was noted at POD2 from 1.0 to 0.8 and persisted at 2 months, (p=0.011) suggesting a deterioration in the coupling of afterload and contractility following lung resection[81].

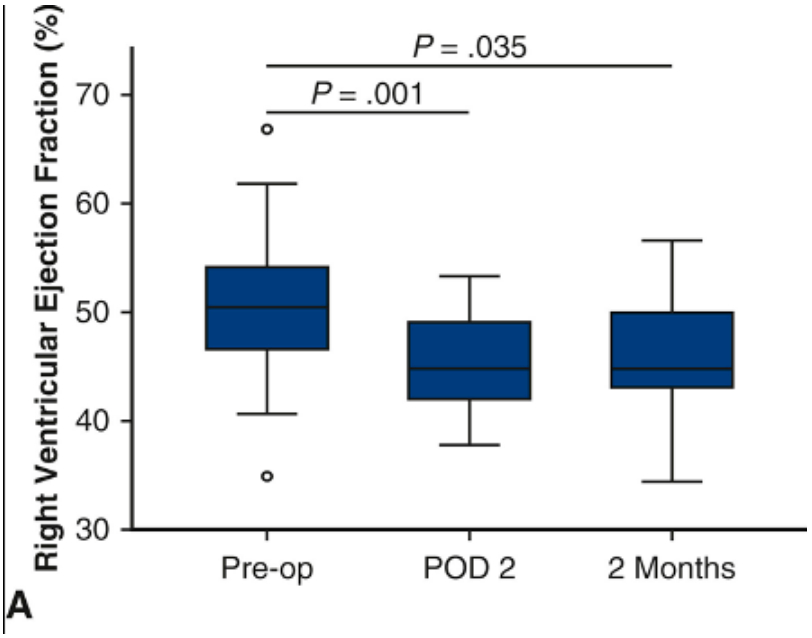

Figure 11 Right ventricular ejection fraction over time.
Taken from McCall et al[81]. The graph demonstrates a median relative decrease in RVEF by 10.9% from baseline on POD2 (p=0.01) which remained depressed at 2 months.

To assess the pulsatile aspect of afterload, flow imaging of the main PA and left and right branches of the PA was performed, allowing calculation of PA acceleration time (PAAT) and PA distensibility. Both these measures are indices of afterload that do not assume constant flow unlike PVR calculations. A reduction in PAAT was noted on POD2 in all vessels with the greatest decrease in the operative vessel indicative of increased afterload in the operative vessels (Figure 12).

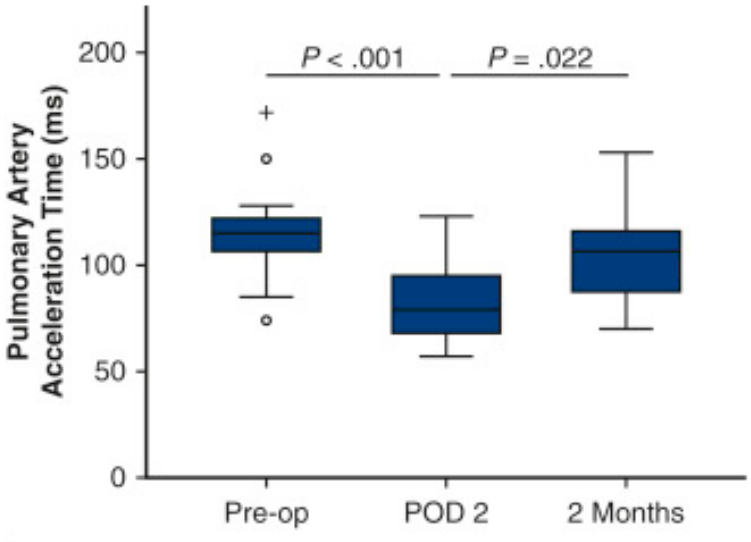

Figure 12 Pulmonary artery acceleration time over time.
Taken from McCall et al.[81] The graph shows a decrease in median PAAT in the main pulmonary artery from baseline (median 115ms) to POD2 (median 82.7) ($p<0.01$).

2.2.4 Right Ventricular Response to Lung Resection Conclusion

As described above, RV dysfunction occurs following lung resection. A variety of parameters have been used to demonstrate alterations in both RV function and volumes with no single parameter being yet considered the gold standard. As technology has changed over the course of the last 50 years, so have the methods for assessing the RV. Due to the risks and complications associated with the insertion of PAC, the change in practice to the use of TTE and more recently CMR are reflected in the literature. Newer techniques such as TDI echocardiography and CMR have allowed for more accurate assessment of the RV following lung resection; however, the studies utilising these techniques are so far limited and further work is required in these areas.

2.3 The Mechanism of Right Ventricular Dysfunction Following Lung Resection.

Although various studies have now demonstrated RV dysfunction does occur following lung resection, the aetiology remains unclear. Several hypotheses exist as to why it occurs, with the vast majority of the literature focusing on the role of increased RV afterload. The American Heart Association reports

"acute right heart failure may occur during or after noncardiac surgery as a result of the development of acute pulmonary hypertension or intraoperative myocardial ischaemia"[170].

This statement however only deals with elements of the underlying mechanism and in reality it is a more complex interaction between multiple aetiologies.

2.3.1 Increased Afterload

An increase in afterload is the most commonly hypothesised mechanism for RV dysfunction following lung resection[81 142 144 145 147 148]. PVR is a surrogate measure of afterload but no consistent changes in PVR or PVRI have been shown in the early post-operative period, with studies showing either no change or in some instances a reduction[142 144 145 147 148 151]. The studies by Reed et al were the first to refute the theory that the mechanisms of RV dysfunction are due solely to an increased afterload with changes in PVR and PAP returning to baseline by four to six hours after lung resection but with ongoing RV dysfunction present after twenty-four hours[142 145]. These changes in afterload were improved with an infusion of prostaglandin resulting in a vasodilator effect and a resulting decrease in PVR and PAP to baseline; however RV dilatation and dysfunction remained. It would seem from these studies that the RV dysfunction is not solely explained by a change in RV afterload alone given the difficulties and inconsistencies demonstrated in the studies using PVR or PAP as a surrogate of afterload[142 144-148].

Studies using only PAP or PVR to assess afterload may not reflect the complexity of RV afterload as PVR does not consider pulsatile flow. Pulsatile flow is responsible for a significant amount of the hydraulic work of the RV. True RV

afterload, or RV input impedance, is a combination of both static and pulsatile components and therefore any technique measuring afterload should reflect both components[11]. Glass et al utilised pulmonary artery wave intensity analysis (WIA) following lung resection to measure pulsatile afterload. Wave reflection occurs at a vessel bifurcation or where there is a change in vessel wall compliance or calibre[171]. Wave intensity analysis combines changes in area and flow through the pulmonary vessels during the cardiac cycle to derive wave intensity. This wave can be separated into compression waves that drive blood away from, or towards the heart. With decreased vessel compliance, a forward wave will be partially reflected back towards the heart, causing increased afterload[171]. Glass et al analysed wave reflection in patients undergoing lung resection surgery at three time points (pre-operatively, POD2 and two-months). In the post-operative period, an increase in blood flow through the non-operative PA compared with the operative PA was demonstrated ($p<0.001$) with increased wave reflection[171]. These changes were strongly associated with changes in RVEF at two-months post-operatively with moderate association with RV strain[171]. The results of this study suggest that if the non-operative PA is unable to cope or accommodate the increased blood flow that occurs following lung resection, RV strain may occur over time. Initially, the non-operative lung may be able to compensate for an increase in wave reflection but with an increase in CO, decompensation may occur. It is likely therefore that alterations in afterload (not reflected by assessment of PVR) are at least partly responsible for the changes described within the RV following lung resection surgery.

2.3.2 Alterations in Contractility

Alterations in contractility have been hypothesised as a potential cause for postoperative RV dysfunction[81 142 145 147-151 153]. Although RVEF is a good indicator of RV pump performance, it is poor index of RV contractile state as it is affected by more than contractility: it is 'load dependant' and can be influenced by changes in both preload and afterload. To overcome these difficulties, Reed et al used preload recruitable stroke work (PRSW), a load independent index of RV contractile performance combining stroke work and end-diastolic volume, as a measure of RV contractile performance following lung resection[142]. Despite a change in RV performance (as assessed by RVEF) in the post-operative period, this could not be correlated with a change in PRSW. Reed et al utilised PRSW in a

further study of patients undergoing lung resection and were again unable to demonstrate a decrease in PRSW despite a decrease in RVEF[148].

Strain (as described in Chapter 1) is a marker of myocardial contractility and is considered to be less load and angle dependant than fractional area change (FAC) or TAPSE (other utilised methods of measuring contractility)[172 173]. McCall et al reviewed a range of TTE parameters following lung resection surgery with RV global longitudinal strain (RVGLS) and RV free wall longitudinal strain (RVFWLS) able to identify RV dysfunction post-operatively (AUROCC's of 0.74 and 0.76 respectively) when compared to a gold-standard of CMR derived RVEF[174]. Wang et al demonstrated a reduction in radial, circumferential and longitudinal strain following lung resection[167]. The value of strain as a measure of contractility is thought to remain somewhat limited as it is still load dependant and therefore increases in afterload may result in a reduction in strain and result in false interpretation of contractility. Strain imaging, in both TTE and CMR, is still in its infancy and has not yet been validated in larger studies of patients undergoing lung resection. Contractility may be a contributing factor in RV dysfunction after lung resection, but no robust assessment of contractility has been demonstrated.

2.3.3 Myocardial Ischaemia and Infarction

Post-operative myocardial injury (PMI) following non-cardiac surgery has been widely described in the literature since the 1960s with ECG changes and post-operative troponin rises described[175-178]. Following lung resection, the incidence of MI is reported between 0.7-2% with incidences of PMI reported as high as 28%[179 180 181-184]. No direct link between myocardial ischaemia and RV dysfunction has been studied in patients undergoing lung resection. However, given that myocardial ischaemia and infarction are recognised complications of lung resection and may result in disruption of preload, afterload and contractility[185], it is plausible that ischaemia and infarction contribute in part to RV dysfunction after lung resection.

Myocardial injury following non-cardiac surgery is associated with increased post-operative morbidity and mortality but the aetiology is not clear[177 183 186]. Pre-operative coronary angiography showed no association with PMI and pre-

existing coronary artery disease again suggesting a number of factors may be at play than purely ischaemia alone[187]. The Peri-Operative Ischaemic Evaluation (POISE) trial suggested that many of the patients with myocardial injury in the post-operative period did not meet the traditional diagnostic criteria for MI[188]. In a post hoc analysis, a group of patients with troponin rise but without the criteria to diagnose MI, had poor post-operative outcomes[188]. With this in mind, authors have sought to introduce newer terms to describe peri-operative myocardial injury. Myocardial injury after non-cardiac surgery (MINS) is a newer term, defined by Botto et al as a myocardial injury caused by ischaemia, that may or may not result in necrosis, has prognostic relevance and occurs within 30 days after non-cardiac surgery[177]. MINS is defined by *high-sensitivity* cardiac troponin (hsTnT) *only* with symptomatic non-cardiac conditions associated with a raised troponin excluded (such as PE, chronic renal failure, sepsis and anaemia)[177]. This definition presumes that the myocardial injury is caused by ischaemia whereas The Fourth Universal Definition of Myocardial Infarction defines an MI as the detection of an elevated troponin value greater than the 99th percentile and does not specify which troponin assay is to be used, neither does it specify the aetiology[189]. It is widely hypothesised that MINS occurs as a result myocardial oxygen supply / demand imbalance induced by perioperative haemodynamics[190]. It is likely that the troponin rises demonstrated following lung resection occur as a result of a global myocardial injury, as described above, and do not reflect solely myocardial ischaemia or infarction.

2.3.4 Inflammatory Injury to the Myocardium

The inflammatory response to all types of surgery is well recognised. Surgery results in a ‘surgical stress’ reaction whereby a range of physiological reactions taken place in order to preserve homeostasis. The inflammatory response involves the activation of the cytokine cascade which triggers the release of both pro- and anti-inflammatory cytokines into the systemic circulation. Systemic inflammation plays a major role in the development of cardiovascular disease. The inflammatory response is an important contributor to myocardial injury after myocardial infarction and cardiac surgery, but the extent to which systemic inflammation is involved in the pathogenesis of PMI after non-cardiac surgery is not known.

Ackland et al demonstrated that PMI was associated with elevated neutrophil-lymphocyte ratio, suggesting systemic inflammation, characterised by relative lymphopaenia and higher concentrations of circulating monocytes, may predispose patients to PMI[191]. Circulating monocytes have been shown to play a major role in driving and maintaining inflammation in a wide range of chronic inflammatory conditions[192 193].

May et al utilised microRNAs (miRs) to explore the potential of an inflammatory response resulting in myocardial injury following non-cardiac surgery[194]. Given that miRNAs have been proposed as potential biomarkers that may identify patients with acute MI earlier than high sensitivity troponin assays, it is possible they could be used to identify those with peri-operative myocardial insult without a troponin rise after non-cardiac surgery[195]. The study compared a group of 24 patients with a troponin rise following non-cardiac surgery with a matched group of 24 patients with no troponin rise after surgery. The study demonstrated an increase in concentrations of cardiac-specific miRs that increase after acute coronary syndrome (ACS) following surgery; however these rises were independent of troponin concentration[194]. The authors report the identification of increased circulating miRs predominately associated with regulation of cardiac muscle contraction. May et al suggest adrenergic stress that occurs in the peri-operative period may lead to the release of miRs from cardiac cells, which in higher risk groups (such as older patients, patients with cardiac failure, diabetes mellitus, or renal disease) results in mitochondrial dysfunction, and myocardial injury displayed clinically by alteration in troponin (Figure 13)[194]. The study identified a decline in hsa-miR-146a-5p[2] suggesting dysregulation of inflammatory pathways may be a contributing factor to myocardial injury after non-cardiac surgery. By causing dysregulation, loss of cardioprotective mechanisms may occur and result in myocardial injury.

[2] hsa-miR-146a-5p suppresses the production of proinflammatory cytokines by inhibiting the expression of IRAK1, TRAF6 and NFk, which promote myocardial injury[192 193]

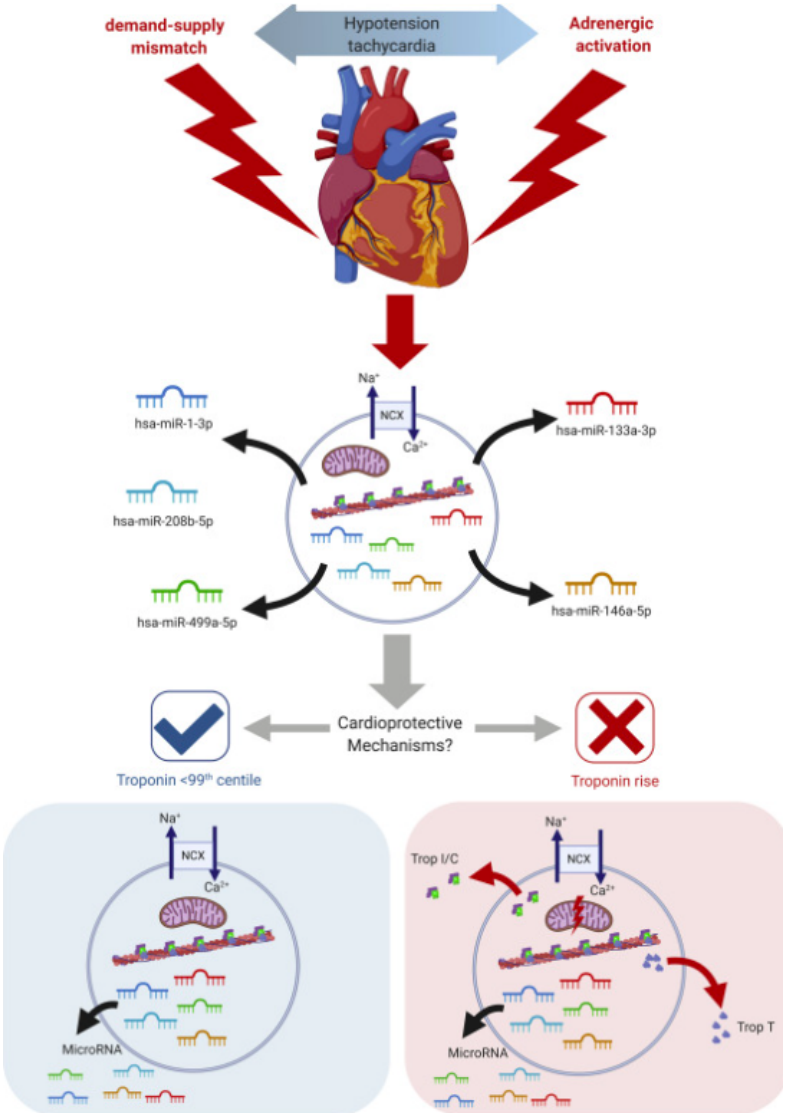

Figure 13 MicroRNA expression following non-cardiac surgery.
The diagram displays the potential mechanism of peri-operative myocardial injury proposed by May et al with oxygen demand-supply mismatch and a trigged adrenergic response resulting in hypotension and tachycardia. These physiological changes alter the release of pro and anti-inflammatory miRNAs which may have a protective or destructive mechanism within the myocardium. Such changes occur in all patients, where subsequent troponin leak is dependent on the integrity of endogenous cardioprotective mechanisms From May et al.[194]

An inflammatory response within the myocardium has been shown in both PE and PH, both conditions with alterations in afterload[198-208]. In the animal studies of PE the acute changes in afterload may be similar to that in lung resection with both banding or occlusion of the PA used experimentally to mimic the physiological changes encountered in a human model of PE. These sudden increases in afterload have been shown widely to result in a localised inflammatory response in the myocardium and are discussed in detail in Chapter 3[199 200 203 204]. It is therefore conceivable that the RV dysfunction that occurs

following lung resection may be due in part as a result of a myocardial inflammatory injury.

2.4 Conclusion

Lung cancer is a leading cause of death in the UK with recognised cardiorespiratory deterioration following lung resection surgery.[81 82 209] The literature has widely described a deterioration in RV function following lung resection surgery; however, the mechanism of this dysfunction remains unclear with a range of potential aetiologies still to be explored[81 165 167 171 174 209-217].

Chapter 3 – Right Ventricular Inflammation after Lung Resection – Literature Review

3.1 Introduction

As described in the previous chapter, RV dysfunction is now widely recognised following lung resection. Literature suggests intra-operative clamping of the lobar pulmonary artery (PA), use of one lung ventilation, activation of HPV and removal of lung parenchyma (and associated vasculature) results in increased RV afterload and thereafter RV dysfunction. However, as discussed in chapter two, PVR returns to baseline within 24 hours, yet RV dysfunction persists well beyond this time. An increase in RV afterload may therefore not account solely for the changes demonstrated in the RV after lung resection. As discussed in Chapter two, a range of aetiologies including myocardial ischaemia, altered contractility and a triggered myocardial inflammatory response may contribute.

Few studies have sought to demonstrate the mechanism of RV dysfunction following lung resection beyond that of an alteration in static afterload (as assessed by PVR) and as a result, in this literature review comparisons have been sought with other clinical conditions that may mimic elements of the physiological disruption encountered in the RV following lung resection. One such condition is PE. PE usually occurs as a result of bloods clots in the deep vasculature, primarily the legs, which detach and embolise to the pulmonary arterial tree, occluding pulmonary blood.[218] Animal studies mimic the haemodynamic effects of PE by banding of the PA, analogous to the surgical ligation that is performed during lung resection surgery, or by injection of microspheres into the internal jugular vein leading to obstruction of the PA.[203] [219-226]

Mechanisms of RV dysfunction in PE are widely examined in the literature, with one well explored mechanism being that of an increased inflammatory response that is triggered following occlusion of the pulmonary arterial tree. The release of inflammatory modulators combined with an increase in PVR, results in pulmonary hypertension (PH) and impaired RV function. I hypothesise that an analogous inflammatory response is triggered, following surgical ligation of the

pulmonary vessels during lung resection, that contributes to RV dysfunction post-operatively.

3.1.2 Myocardial Inflammation

At any anatomical site, inflammation initially occurs at the site of injury in an attempt to limit the tissue effects of such an injury. Acute inflammation is the initial response and is characterised by the influx and accumulation of systemic leucocytes at the site of the injury. If this initial response does not eliminate the injury stimulus, a chronic inflammatory process is triggered and may last for weeks, months or years. The five cardinal signs of inflammation were first described by the Roman writer Celsus[227], as i) rubor or redness, ii) calor or increased heat due to increased blood flow to the site of the injury, iii) tumour or swelling due to a fluid influx, iv) dolour or increased pain with the Greek writer Galen[228] adding v) function *laesa* or disturbance of function.

The initial changes of myocardial tissue during acute myocardial inflammation include an increase in blood flow and permeability of the venules and capillaries, increase in cell membrane permeability of cardiomyocytes, swelling of cardiomyocytes due to increased water content and widening of the intercellular cleft with an increase in intracellular space and water content[229]. Myocardial inflammation occurs in a wide variety of pathological conditions including PE, rheumatoid arthritis , systemic lupus erythematous, and sarcoidosis[230] [231] [232].

3.2 Methods

To explore the role of RV inflammation in RV dysfunction following lung resection, the following search strategy was utilised using the Ovid Medline (R) database, 1946 to Present with Daily Update; (search performed November 2018):

1. *right ventricular inflammation.mp*
2. *(RV inflammation or right ventricular inflammation or right ventricle inflammation or right ventricle inflammatory response).tw*
3. *left ventricular inflammation.mp*
4. *LV inflammation or left ventricular inflammation or left ventricle inflammation or left ventricle inflammatory response).tw*
5. *Ventricular inflammation.mp*
6. *(Inflammation of the ventricles or ventricle inflammation or ventricle inflammatory response).tw*
7. *inflammation or myocarditis.tw*
8. *right ventricular dysfunction.mp*
9. *RV dysfunction or right ventricle dysfunction.tw*
10. *Ventricular dysfunction.mp or Ventricular dysfunction*
11. *Heart inflammation.mp*
12. *1 or 2 or 3 or 4 or 5 or 6 or 7 or 8 or 9 or 10 or 11*
13. *lung resection.mp*
14. *(lung resection surgery or surgery of the lung or lung surgery or lung cancer surgery or lobectomy or thoracotomy or pneumonectomy or video assisted thoracoscopy or VATS).tw*
15. *13 or 14*
16. *12 and 17*
17. *limit 16 to English*

This search did not yield any results. It was apparent that my hypothesis that an inflammatory response following lung resection surgery contributes to RV dysfunction is novel. As a consequence, the literature search was altered to examine the role of RV inflammation in PE and acute afterload given the similarities described above. The following strategy was utilised using the Ovid Medline (R) database, 1946 to Present with Daily Update; (search performed November 2018):

1. *right ventricular inflammation.mp*
2. *(RV inflammation or right ventricular inflammation or right ventricle inflammation or right ventricle inflammatory response).tw*
3. *left ventricular inflammation.mp*
4. *(LV inflammation or left ventricular inflammation or left ventricle inflammation or left ventricle inflammatory response).tw*
5. *Ventricular inflammation.mp*
6. *(Inflammation of the ventricles or ventricle inflammation or ventricle inflammatory response).tw*
7. *inflammation or myocarditis.tw*
8. *right ventricular dysfunction.mp*
9. *RV dysfunction or right ventricle dysfunction.tw*
10. *Ventricular dysfunction.mp*
11. *Heart inflammation.mp*
12. *1 or 2 or 3 or 4 or 5 or 6 or 7 or 8 or 9 or 10 or 11*
13. *acute afterload.mp*
14. *pulmonary embolism.mp*
15. *PE or blood clot or lung clot or lung thrombus.tw*
16. *13 or 14 or 15*
17. *12 and 16*
18. *limit 17 to English*

One hundred and thirty-two results were returned (Figure 16). Studies were included if they reported parameters relating to RV inflammation. Only studies reporting the effects of acute increase in afterload were included. Studies examining circulating systemic inflammatory markers and chronic increased afterload (greater than seven days) were excluded. Following examination of the study title, 63 results were removed and a further 54 removed after reading the available abstract (Figure 16). References of all relevant studies were reviewed for relevant work with three additional studies identified. Eighteen studies were included for full-text review based on the inclusion and exclusion criteria (Figure 14).

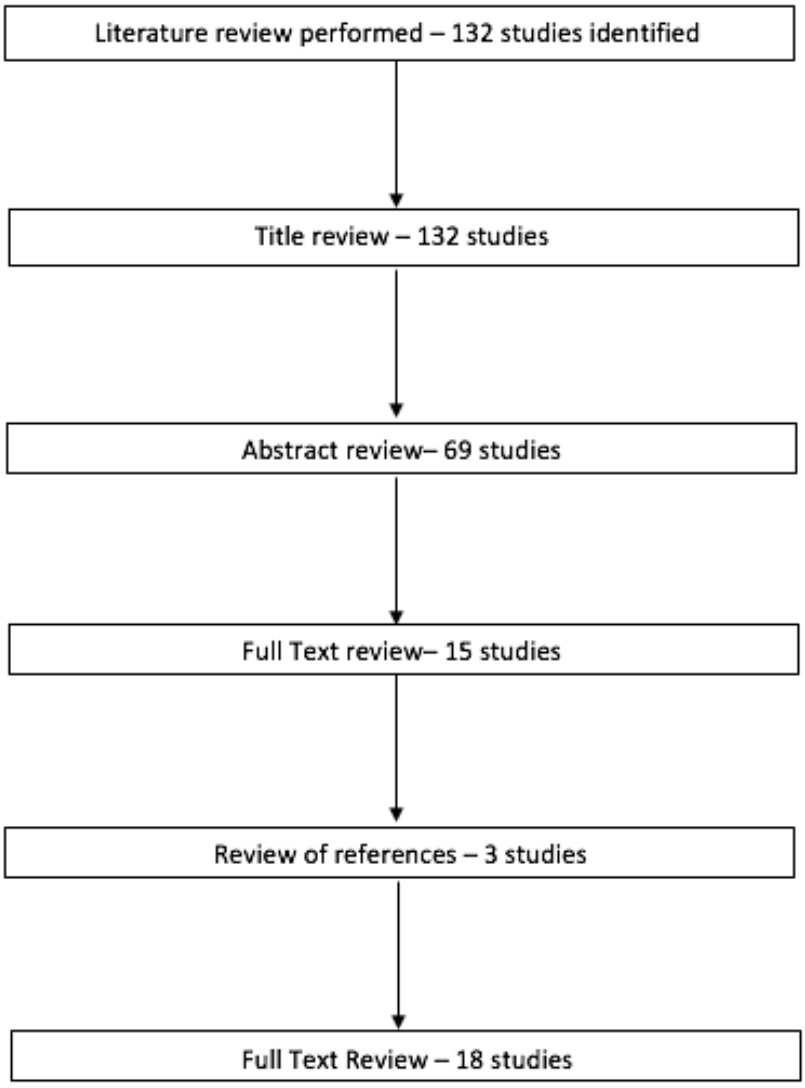

Figure 14 Flow chart of Literature review
Performed November 2018.

An updated literature review was performed in August 2022 using the strategy detailed above. Using the initial search strategy (which resulted in zero studies in November 2018), 56 studies were identified. Following examination of the study title, 52 studies were removed. Of the four studies remaining, abstract review was performed with no studies included for full text review. The second search strategy was utilised from November 2018 to present with 323 studies returned (Figure 15). There was a considerable increase in potential studies identified from 2018 to 2022. Examination of titles and abstract revealed a number of studies reporting findings of patients with COVID-19 from 2020 onwards with associated myocardial dysfunction (all of which were excluded). Two papers were identified for full text review and are included in the

discussion of the literature search. In total, 20 studies are discussed in this chapter.

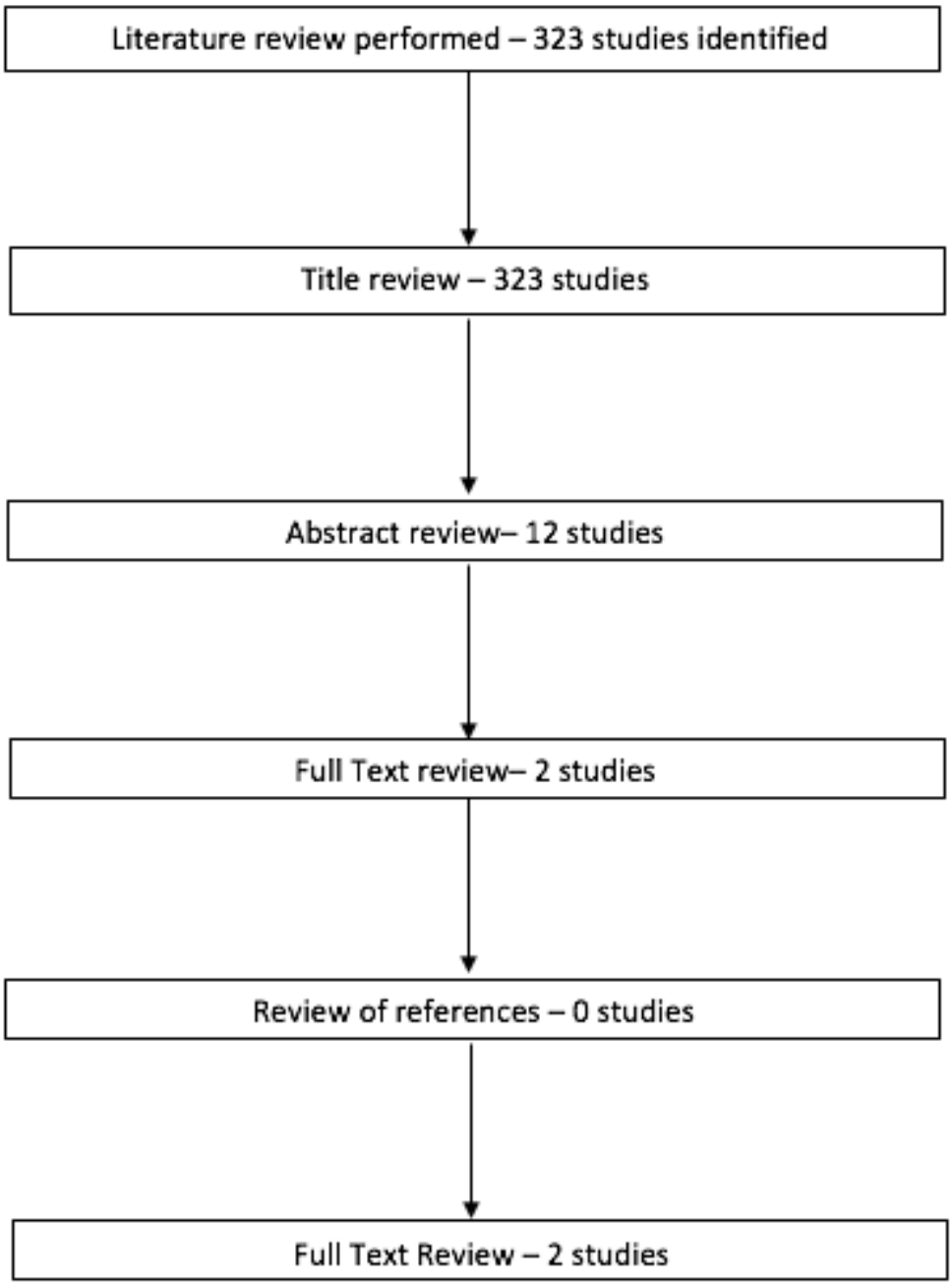

Figure 15 Flow chart of updated literature review
Performed August 2022 covering the period November 2018 to present.

3.3 Results

For discussion, the studies have been divided into PE and other causes of acute afterload. Where appropriate, these have been further sub-divided into animal and human studies. A summary is provided in Tables 4 and 5.

3.3.1 Pulmonary Embolism

The literature review reflects the variety of techniques implemented to demonstrate an RV inflammatory process following PE. Inflammation can be measured in a variety of different ways including histopathological examination, gene expression, or the expression of common inflammatory cell signalling pathways.

3.3.1.1 Human Studies

Only five human studies examining the role of RV inflammation in PE were identified (Table 4). Of the five, four were autopsy studies examining histological evidence of inflammation within the myocardium (both LV and RV). Only one study prospectively recruited patients with a diagnosis of PE and RV dysfunction.

The first published work acknowledging the potential role of inflammation in the pathogenesis of RV dysfunction following pulmonary embolism reported two human autopsy cases. Iwadate et al performed microscopic examination and immunostaining of myocardial tissue obtained at autopsy in two patients with PE as the cause of the deat[233]. Microscopic examination of the RV in both cases showed a number of polymorphonuclear neutrophils and mononuclear cells infiltrating the entire RV free wall (Figure 16). Immunostaining of RV tissue displayed positive CD68 staining of almost all of the infiltrating RV mononuclear cells. Microscopic examination of the LV showed some mild congestion of the ventricle in one of the cases and minor patchy subendocardial fibrosis in the second, but no evidence of inflammatory cells as displayed in the RV. Unlike tissue analysis of the RV, no immunostaining of LV tissue was performed. One weakness of this study is the absence of the ability to compare the number of inflammatory cells present in both the LV and RV. It is feasible that

inflammatory cells were present within the LV but were not examined using immunostaining and subsequently not reported. As with any case series, there are numerous biases, meaning these findings cannot be generalised to the wider population and it is important that they are not over interpreted.

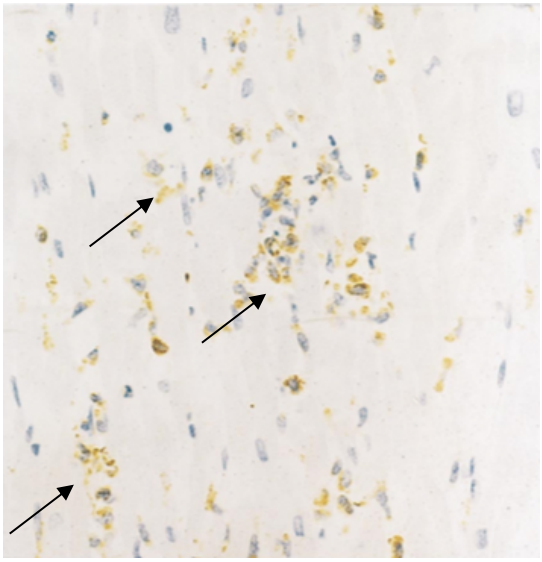

Figure 16 Microscopic examination of the right ventricular free wall following pulmonary embolism
A pathological specimen of RV free wall myocardium from an autopsy case of a patient who died following pulmonary embolus. Shown is a specimen of the right ventricular free wall stained with anti-CD68-pan-macrophage marker with x100 magnification. The arrows indicate macrophage infiltration (yellow). Taken from Iwadate et al[233].

A further autopsy study by Iwadate et al compared the autopsy findings of 20 patients with PE recorded as the cause of death and 10 control autopsies[234]. A significantly higher number of macrophages were demonstrated in the right ventricle wall of the PE group, compared with the control group ($p<0.01$) (Figure 17). On comparison of the left and right ventricles in the PE group, the mean number of macrophages in 100 high-power fields was, 7.61+/-12.9 cells in the RV and 1.41 +/-1.62 cells in the LV ($p<0.05$). However, only nine cases showed a significantly larger number of macrophages in the RV. The authors hypothesise that those with no morphological changes may have died immediately after PE, therefore allowing no time for macrophage infiltration, unlike those with a longer period from occlusion of the PA to death.

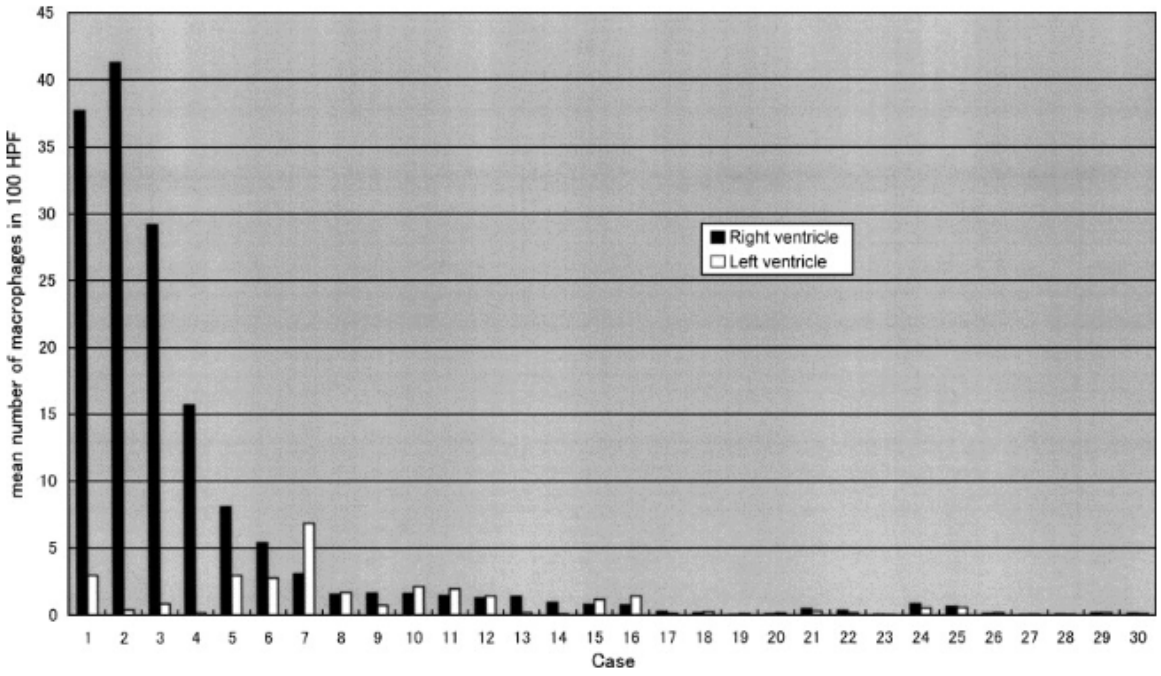

Figure 17 Semi-quantitative examination of the number of macrophages per 100 high power field in 30 autopsy cases.
Taken from Iwadate et al[234]. The graph demonstrates the mean number of macrophages per 100 high power field with cd68 pan-macrophage marker staining of the RV myocardium taken at the time of autopsy. Cases numbered 1-20 had a confirmed diagnosis of PE as the cause of death, cases 21-30 were control autopsies.

Author Year (n)	Measure of Inflammation	Findings	Comments
Iwadate et al.[233] 2001 2	Immunostaining: CD-68, CD20, CD45R0 Anti-human neutrophil elastase	+ve staining of CD68 in both cases in RV. +ve staining of anti-human neutrophil elastase in RV.	Small study (case series). No immunostaining performed of the LV.
Iwadate et al.[234] 2003 20 (10 controls)	Immunostaining: CD-68	↑macrophages in the RV in PE cohort compared with controls.	Nine in PE cohort with a significantly larger n. of macrophages in RV versus LV ($p<0.001$).
Begieneman et al.[235] 2008 41 (22 PE, 11 PH, 8 controls)	Immunostaining: MPO CD68 CD45 Complement C3d	PE (versus control): ↑neutrophil granulocytes, lymphocytes, macrophages in both and LV, ↑CD3 PH: ↔ all inflammatory cells.	↔ PH group suggestive *acute* afterload may be cause of inflammatory response. ↑ inflammatory cells, more in RV ($p<0.001$).
Orde et al.[230] 2011 28	Immunostaining: CD68 CD3 CD20 Anti-human neutrophil elastase	PE (versus control): ↑RV wall thickness ↑macrophages, T-lymphocytes, neutrophils. Myocyte necrosis in 64%.	28 isolated RV pathology (27 PE diagnosis) with 28 matched controls. RV changes focal or patchy.
Jimenez et al[236] 2018 **34**	No direct measurement	RV dysfunction on TTE present in 59% of diclofenac group versus 76% placebo group ($p=0.46$) at 48 hours. 35% in both groups has dysfunction at 7 days.	Study of Iv diclofenac versus no treatment for PE. Diclofenac 1st dose immediately, then 2 further 12hrs apart. Poor recruitment 34 over 3yrs.

Table 4 Human autopsy studies of pulmonary embolism and ventricular inflammation.
(n) – number, CD – cluster of differentiation, +ve – positive, RV – right ventricle, LV – left ventricle, PE – pulmonary embolus, PH – pulmonary hypertension, ↑ - increase, ↔ no change. IV – intravenous. Hrs-hours. Yrs. – years.

Begieneman et al performed an autopsy study in 41 patients (22 with PE, 11 with chronic PH, and eight controls with no evidence of either PE or PH) demonstrating a significant increase in inflammatory cells (neutrophil granulocytes, lymphocytes, and macrophages) in both the RV and LV in the PE group when compared with control[235]. When comparing the number of inflammatory cells between the RV and LV, the RV displays a significantly higher number than the LV ($p<0.001$)[235]. The increase in inflammatory processes in the LV was unlike the previous autopsy studies that only demonstrated the presence of these cells in the RV. It is recognised that PH occurs as a result of elevated PVR, due to a range of aetiologies, which may result in progressive RV dysfunction and ultimately failure. Interestingly despite a chronic increase in afterload in this subset of patients in this study, no inflammatory cells were present in either the LV or RV. This suggests that an *acute* change in afterload is the trigger for the inflammation demonstrated in the PE subgroup.

All four human autopsy studies demonstrated an increase in inflammatory immunostaining in the RV following PE. Two of the four studies did not demonstrate any inflammatory response in the LV. The study by Begieneman et al was the only one to demsontrate notable inflammatory deposition in the LV of those who died of PE[235]. This differs from the animal studies discussed later in the chapter, where inflammatory cells were only demonstrated in the RV[203]. The authors of these studies suggest the mechanism of inducing PE in these rat studies, infusion of microshperes for a limited time (up to a maximum of 18 hours), may not have been long enough to result in inflammation in the LV. It is suggested by the authors of the study that as their samples were taken at the time of human autopsy (typically within hours or days of death compared with hours in animal studies), changes to the LV may have been allowed to occur unlike in animal studies that examine myocardium within 24 hours of PE.

The only study to recruit patients prospectively examined the role of IV diclofenac in improving RV dysfunction in patients with PE [236]. The study did not demonstrate any improvement in TTE parameters of RV function in those treated with IV diclofenac within the first 24 hours of diagnosis[236]. The study reports recruiting difficulties, with only 34 patients enrolled over a three-year period. The authors report 118 patients would be required in each group to demonstrate

a difference in RV function and as such their study with 34 patients is markedly underpowered.

There are limitations in drawing conclusions from only five studies with a combined total of 125 human participants. Overall, the studies suggest inflammation is present within the myocardium following an acute increase in RV afterload, more so within the RV than the LV.

3.3.1.2 Animal Studies

Most animal studies examining this topic utilised a model of PE whereby polystyrene microspheres were injected into the jugular vein. This results in pulmonary vascular obstruction similar to PE. [198 203 221 222 223-225 237] Studies primarily focused on either the diagnosis of myocardial inflammation using immunohistology and gene expression and the association with RV dysfunction, or the improvement in RV dysfunction following administration of anti-inflammatory modulators. The major findings of each study are shown in Table 5.

Author year (n)	Methods	Measurement of inflammation	Findings	Comments
Jones et al.[221] 2003 48	Rat 1.Treatment efficacy 2. Angiography 3. Pleural fluid histology	No direct measurement of inflammation made. RV function: MAP, RAP, RVSP, LVSP.	Placebo (vs control): ↓MAP, ↓RVSP severe RV hypokinesis. Ketorolac (vs placebo): ↑MAP,↑RVSP.	Furegrelate (a thromboxane synthase) was also examined. It demonstrated improvement in RVSP, and MAP compared with placebo but not to the extent of that shown by Ketorolac.
Watts et al.[203] 2006 122	Rat 1. Mild PE 2. Mod PE 3. Sham 4. Mod PE anti-PMN antibody	Immunohistology: MPO activity, Neutrophil-specific esterase, CD68. Chemokine expression: CINC-1, CINC-2, MIP-2, MCP-1, MIP-1α.	Mild PE (vs sham): ↔ MPO/neutrophils/ monocytes/macrophages. Mod PE (vs sham and anti-PMN): ↑ in all RV chemokines and immunohistology.	Largest areas of inflammatory infiltrate in basal RV. Significantly less MPO staining/inflammatory cells in the RV of anti-PMN treated rats ($p<0.002$).
Zagorski et al.[222] 2008 unclear	Rat 1. Mild PE 2. Mod PE 3. Sham	DNA microarray analysis Real time PCR RNA microarray at 2, 6 and 18hours.	Number of genes altered: Mild: 6h – 2, 18h - 83 Mod: 6h – 821,18h – 5939.	Strong bias towards expression of pro-inflammatory pathways in moderate PE.
Zagorski et al.[223] 2007 120	Rat 1. Sham 2. PE 3. PE plus anti-CNC Abs	Immunohistology: MP0 and MMP activity Chemokine expression Neutrophil-specific esterase.	PE (vs sham): Influx neutrophils at 18h ↑CINC-1, -2 at 6 and 18h ↑MPO. PE with anti-CNC Abs (vs PE): ↓MPO.	RVSP improved in treatment group compared with PE only. Troponin decrease in treatment group.

Watts et al.[224] 2008 Unclear	Rat 1. PE 2. Sham	Histopathology of RV tissues Immunohistology: MPO, MMP-9, CD68 Microarray: M1 and M2 mononuclear cells	PE (vs sham): MPO ↑ 24h, ↔ day 4, MMP-9 ↑ 24h to 6w, CD68 ↑ 24h to 6w, M1 ↑ 24h, M2 ↑ 6 weeks	Response over 6 weeks. Histology changes in basal RV. RV dysfunction shown with a ↑RVSP.
Watts et al.[225] 2009 42	Rat 1. Sham 2. PE (saline) 3. PE (ketorolac)	Gene expression: CINC-1, CXCL1, COX-2, Sele, ICAM-1 Immunohistology: MP0	PE (vs sham): ↑ in all gene expression at 6 and 18h PE with ketorolac (vs saline): ↓ in all gene expression at 6 and 18h	Ketorolac treated rats no RV dysfunction. White plaque formation in RVOT in PE, improved with ketorolac. Sparing of apex and LV.
Zagorski et al.[237] 2009 10	Rat 1. PE 2. Control	Histological appearance of tissue Gene expression of tissue	PE compared with control: ↑gene expression	RVOT noted highest increase in gene expression. Apex spared.
Fortuna et al.[238] 2007 35	Dog 1. Sham 2. Doxycycline only 3. PE 4. PE (doxycycline)	Immunohistology of plasma: MMP -2, MMP -9, Pro-MMP -9	PE (vs sham):↑MMP-9, pro-MMP-9,↔MMP-2 PE + doxycycline (vs PE): ↓MMP-9	Effects of doxycycline at 5 30 and 120 mins after PE induced. ↑↑ RV function at 120mins in doxycycline.
Neto-Neves et al.[239] 2011 30	Dog 1. Sham (saline) 2. Sham (doxycycline) 3. PE (saline) 4. PE (doxycycline)	Immunohistology of plasma: MMP-2 and MMP-9	PE (vs sham): ↑MMP-9, ↔MMP-2 PE(doxy) (vs PE only): ↓MMP-9, ↔MMP-2	Doxycycline treatment was associated with an improvement in RV function.

Uzuelli et al.[240] 2007 26	Dog 1. Sham 2. Mild PE 3. Moderate PE 4. Severe PE	Immunohistology of plasma: MMP -2 and MMP-9	Severe PE(vs sham): ↑MMP-9 Mild/Mod PE: ↔MMP-9 All groups: ↔ MMP-2	↑mPAP and PVRI all PE groups. ↑↑ 120mins.
Neto-Naves et al.[241] 2013 58	Lamb 4 control groups and 4 PE groups received either: 1. Saline 2. Dobutamine 3. Doxycycline 4. Doxycycline and dobutamine	Immunohistology of RV tissue: MMP-2 and MMP-9	PE (vs control): ↓ MMP-2, ↑MMP-9 PE + doxycycline (vs PE): ↑MMP-2, ↔ MMP -9	TTE at baseline, 30 and 120mins. DDRV, SDRV, global systolic function measured. Pre-treatment with doxycycline improved RV function.
Wu et al.[242] 2018 96	Rat 1. Control 2. Control (saline) 3. PE 4. PE (simvastatin)	Immunohistology of RV tissue: MMP-2 and MMP - 9	PE (vs control): ↑MMP-9, ↔MMP-2 all time points PE (simvastatin) (vs PE): ↓MMP-9, ↔MMP-2 all time points	Primarily examined lung inflammatory processes. Improvement in mPAP and PVRI in group 4 versus group 3.
Lu et al.[243] 2018 149	Rat Two-part study: • Part 1 – Inflammatory response after PE • Part 2 – Inflammatory response after treatment with cyclosporin and anti-CD147.	Immunohistology: CyPA, CD147, MPO, MMP-2, MMP-9	PE (vs sham): ↑ all immunohistology PE and cyclosporin (vs PE):↓ In all except CD147 (no change) PE and anti-CD147 (vs PE): ↓ all immunohistology	RV dysfunction improved with cyclosporin anti-CD147.

Zhou et al.[202] **2021** **36**	Rat 1. Sham 2. PE 3. PE plus low dose SP-8356 4. PE plus high dose SP-8356	Immunohistology: CyPA, CD147, MPO, MMP-2, MMP-9	PE (vs sham): ↑ all immunohistology PE and cyclosporin (vs PE):↓ In all except CD147 (no change) PE and anti-CD147 (vs PE): ↓ all immunohistology	SP-8356 is CD147 inhibitor RV dysfunction improved with low and high doses of SP-8356 Apoptosis of cardiomyocytes ↓in SP-8356 groups

Table 5 Animal studies of pulmonary embolism and right ventricular inflammation

n) – number, vs – versus, CD – cluster of differentiation, +ve – positive, RV – right ventricle, LV – left ventricle, PE – pulmonary embolus, PH – pulmonary hypertension, ↑ - increase, ↔ no change, ↓ - decrease, MAP – mean arterial pressure, RAP – right atrial pressure, RVSP – right ventricular systolic pressure, LVSP – left ventricular systolic pressure, mPAP – mean pulmonary artery pressure, PVRI – pulmonary vascular resistance index, PA – pulmonary artery, IVC – inferior vena cava, MPO – myeloperoxidase, anti- PMN – anti-polymorphonuclear neutrophil antibodies, CINC – cytokine induced neutrophil chemoattractant, DNA – deoxyribonucleic acid, PCR – polymerase chain reaction, CCL – chemokine C ligand, CXCL – chemokine XC ligand, RVOT – right ventricular outflow tract, MMP – matrix metalloproteinase, COX – cyclooxygenase, mins – minutes, CyPA – cyclophilin A, DDRV- diastolic linear dimension of the right ventricle, SDRV - systolic displacement of the lateral wall of the right ventricle.

3.3.1.2.1 Expression of Inflammation Within the Myocardium in Animal Studies of PE

This section describes the main findings from the studies which have sought solely to describe the expression of inflammation within the myocardium and its link to RV dysfunction. Of the four studies described, three examined immunohistology of either plasma or myocardial tissue.

Watts et al[224] analysed the inflammatory response from 24 hours up to six weeks in a rat model of PE. The study focused on the inflammatory histological changes in the RV outflow tract. These rats displayed white plaque development at 24 hours which persisted through to week 6 within the RV outflow tract (Figure 18). No changes were shown in either the apical RV or LV segments emphasising a purely RV inflammatory response to PE. The in-vivo RV outflow muscle contractile forces, measured using an isometric tension transducer to produce length-tension curves, were noted to be significantly reduced compared with control. Human hearts examined following PE have also demonstrated injury to the RV outflow tract[244]. The RV outflow tract may well display more noticeable changes as it has thinner muscularity and delayed contraction when compared with the apical myocardium. The outflow tract may be susceptible to greater stretch and increased shear forces when subjected to an acute rise in PVR as seen with PE.

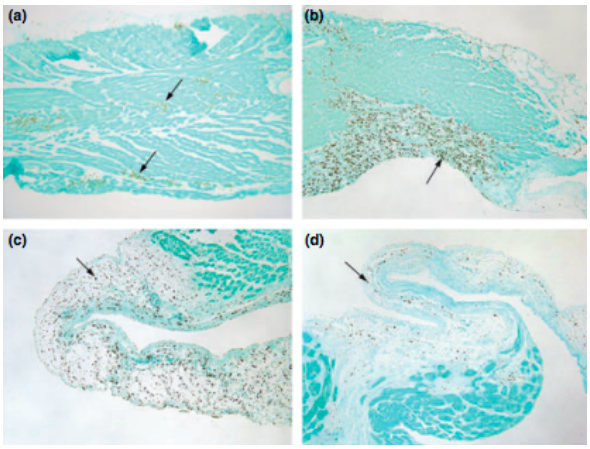

Figure 18 Histological examination of the RV outflow tract in a rat PE model.
Taken from Watts et al[224]. CD68 staining was used to identify monocyte/macrophage cells (demonstrated with black arrows). Image (a) shows a cluster of CD68+ cells in the RVOT at day 1(black arrow) with a thinned RVOT at week 1 in image (c) (black arrow).

Myocardial tissue was also examined for matrix metalloproteinases (MMP) in the study by Watt et al[224], a group of enzymes with a fundamental role in the remodelling of the extracellular matrix (ECM). Neutrophils and macrophages release granules containing MMP-9. They have been shown to be involved in the inflammatory cell process due to their regulation of inflammatory mediators such as chemokines and cytokines as well as the transmission of leukocytes from the vascular bed to injured tissues[245]. An increase in myeloperoxidase (MPO) and MMP-9 were elevated as early as day 1 and corresponded with plaque formation in the RV outflow tract[224]. The high MPO level declined on day 4 and returned to baseline after one week of PE being induced, whereas both MMP-9 and CD68 levels were high throughout the 6-week period[224]. These immunohistological changes suggest the potential of a biphasic inflammatory response occurring in the RV after PE with a significant elevation in mononuclear cells M1, a characteristic pro-inflammatory phenotype at 24 hours followed by a significant elevation in M2 cells, a characteristic healing phenotype, at 6 weeks. A dog study of PE showed similar rise in MMP-9 associated with RV dysfunction[240].

Zagorski et al was the only study to examine targeted inflammatory gene expression using DNA micro-assay analysis of RV tissues in rats induced with PE[222]. The study demonstrated the highest number of gene alterations occurred in rats with moderate PE compared with mild PE and control groups. Pro-inflammatory pathway gene expression was highest at 18 hours following induction of PE compared with mild PE and the control group.

3.3.1.2.2 Improvement in RV Dysfunction in Rat Models of PE Using Anti-inflammatory Modulators.

The majority of studies described in this chapter not only demonstrated an initial inflammatory response within the myocardium with associated RV dysfunction, but subsequently sought to demonstrate an improvement in RV function following administration of anti-inflammatory modulators.

Two studies utilised ketorolac, a non-steroidal anti-inflammatory or COX inhibitor used clinically for its anti-inflammatory, anti-pyretic and analgesic effects, to blunt the inflammatory response to induced PE. The study by Jones et al randomised rats to receive ketorolac or placebo at five hours and then

fourteen hours after the induction of PE. In the ketorolac group, an improvement in RV systolic function was shown compared with the saline only treatment group (Figure 19)[221] with those rats demonstrating only mild RV dilatation on angiography unlike the saline group which had evidence of severe RV hypokinesis, tricuspid regurgitation (TR) and LV filling delay in response to PE. Within this study, a group of rats were randomised to receive furegrelate sodium (a thromboxane a2 inhibitor) which also improved RV systolic function compared with placebo (Figure 19). The same group examined the role of ketorolac in a further study, on this occasion administered at the time of induction of PE[225]. In rats treated with ketorolac a significant reduction in inflammatory gene expression was noted, as well as an improvement in RV function.

Although the first study did not demonstrate histological evidence of RV inflammation following PE, by successfully demonstrating an improvement in RV function following the administration of two different anti-inflammatory drugs, there is the suggestion that RV dysfunction following PE is a result of an inflammatory process. This was further validated in their second study whereby inflammatory gene expression was reduced with early anti-inflammatory treatment whilst protecting RV contractile function.

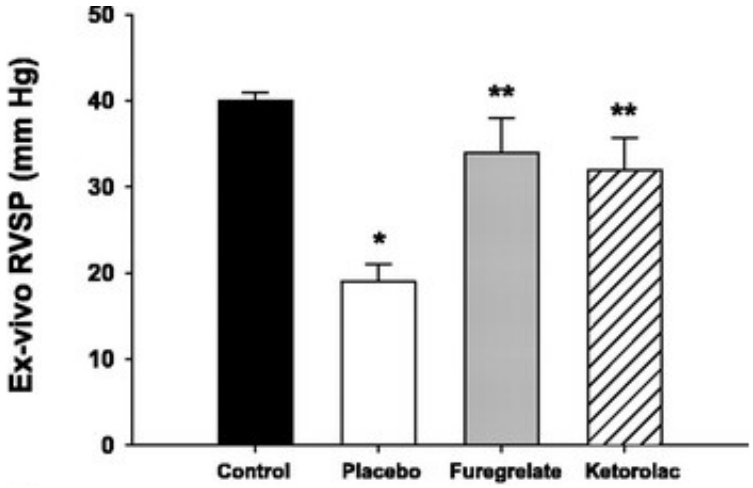

Figure 19 Ex-vivo right ventricular systolic pressure in rats induced with PE.
Taken from Jones et al.[221] The graph demonstrates a decrease in RVSP in the PE plus placebo group compared with the healthy control group (no PE). An increase in RVSP in those rats treated with both Ketorolac and Furegrelate compared with placebo is also shown. (*p<0.05 vs control, **p<0.05 vs placebo).

Doxycycline, a non-specific MMP inhibitor and broad-spectrum tetracycline antibiotic, was utilised in three studies[238 239 241]. Dogs induced with PE demonstrated increase in MMP-9 associated with evidence of modest RV dysfunction (increase mPAP and PVRI). These changes in RV function improved with the administration of doxycycline (fifteen minutes prior to the induction of PE with a significant increase in both mPAP and PVRI as well as a reduction in MMP-9). A similar study by the same group demonstrated an improvement in RV function as early as five minutes after the injection of IV doxycycline with the greatest improvement at 120 minutes after injection[239].

An animal study by Neto-Naves et al[241] performed TTE imaging to aid diagnosis of RV dysfunction. Lambs induced with PE and treated with doxycycline prior to PE demonstrated an improvement in afterload (mPAP and PVRI) compared with those treated only with saline or dobutamine. Pre-treatment with doxycycline provided protection against RV dysfunction and an improved responsiveness to dobutamine. This study adds further weight to those described in the sections above and goes a step beyond; demonstrating clinical improvement in RV function with anti-inflammatory treatment. This study suggests that by directly blunting the inflammatory response of PE within the myocardium with MMP inhibitors, clinical RV function will improve.

It would appear from the three studies utilising doxycycline as a potential treatment strategy in PE that MMP-inhibitors have a protective effect against cardiac injury and as a result improve responsiveness to inotropes. The authors suggest a possible mechanism of improving RV function is that doxycycline may reduce RV afterload. MMP-9 has been shown to be involved in the modulation of vascular tone through the release of endothelin-1, which is a potent vasoconstrictor involved in PH and PE and may increase PVR as a result of receptor activation[246 247 248-250]. Doxycycline has been shown to reduce haemodynamic changes associated with acute PE[251]. It is possible therefore that by inhibiting MMP, doxycycline reduces PVR and RV afterload, with an improvement in RV function. Doxycycline is a non-specific MMP inhibitor and therefore it would also be of interest to note the actions of specific MMP inhibitors in PE.

Antibodies, including anti-polymorphonucleocytes (anti-PMN) and anti-cytokine induced neutrophil chemoattractant (anti-CINC), have been utilised in a group of studies to improve RV function after PE. Watts et al utilised anti-PMN antibody to reduce the influx of neutrophils and achieve functional agranulocytosis prior to inducing PE in rats[203]. In the first instance the study demonstrated a 95-fold increase in MPO activity in the RV in rats with moderate PE with only a small increase in MPO activity in the LV. Histological examination was also performed demonstrating a massive influx in neutrophils in the RV of the moderate PE group only. No neutrophil influx was demonstrated in any sections of the LV in any of the groups (Figure 20). The largest infiltration of inflammatory cells occurred in the basal portion of the RV with sparing of the apex. In the same study, rats treated with anti-PMN antibody prior to PE being induced, had no evidence of RV dysfunction and a 75% reduction in MPO activity compared to those with PE only. This group also tended to have a lower troponin rise compared with the PE group. This suggests blocking the neutrophil accumulation with anti-PMN antibody reduces cardiac inflammation and improves cardiac contractile function with a reduction in cardiac myocyte death (shown with a reduction in troponin release). This strongly suggests that excessive inflammatory responses with neutrophil infiltration of the myocardium contributes to RV dysfunction after PE (Figure 21).

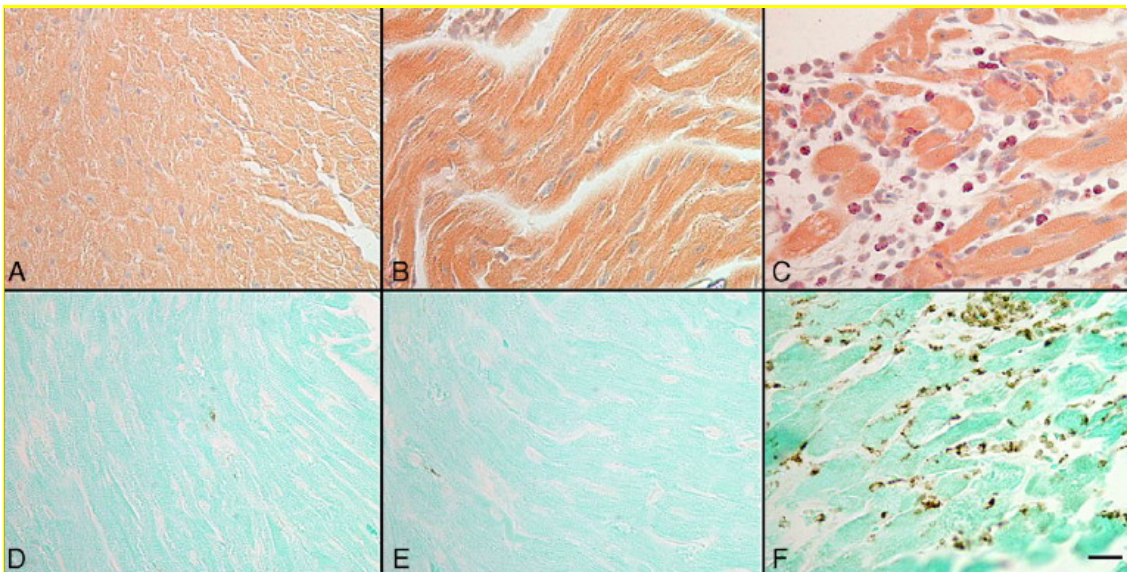

Figure 20 Histological examination of right ventricular samples in experimental PE. Taken from Watts et al.[198] Samples A,B, and C are stained with neutrophil specific esterase and samples D,E and F with CD68. Samples A and D are taken from a sham rat, B and E from a rat with mild PE and C and F from a rat with moderate PE. All samples taken 18hours after PE was induced. The increase in neutrophils in Figure C is shown with an increase in the number of cells stained pink and purple. The increase in cells stained brown in Figure F represents an increase in the number of macrophages and monocytes.

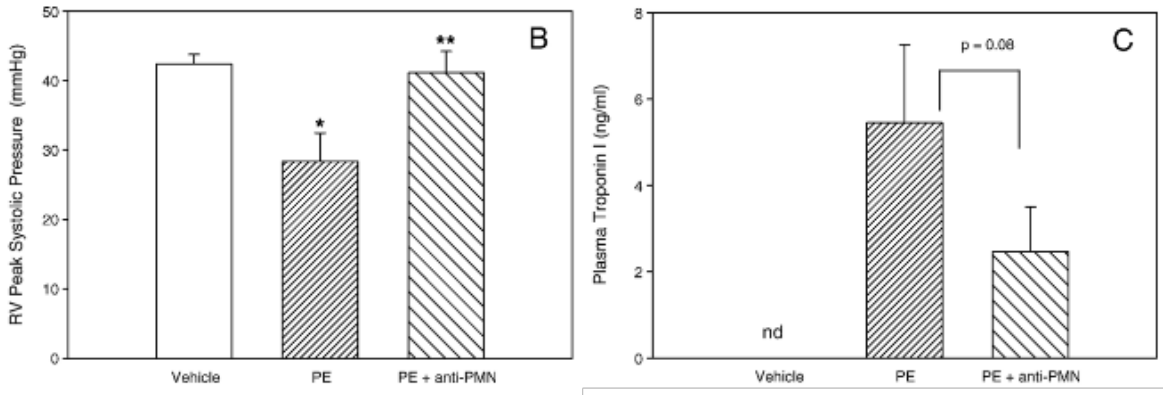

Figure 21 Right ventricular systolic pressure and troponin rises in rats induced with PE. Taken from Watts et al[198]. Note RVSP value remains similar to that of a healthy rat (vehicle) in those rats treated with anti-PMN before PE is induced (Graph B). A higher troponin value is demonstrated in rats with PE only compared with those treated with anti-PMN. * indicates a value that is significantly different ($p<0.05$) from the vehicle group. ** indicates a value that is significantly different from the PE group.

Similar apical sparing described is recognised clinically. In human studies of acute massive PE using transthoracic echocardiography assessment of the RV describe 'McConnell's sign' whereby the RV apex demonstrates hyperactivity combined with akinesia of the mid free wall[244 252 253]. Various theories exist as to why this clinical sign may exist including tethering of the RV apex to a contracting and hyperdynamic LV, a bulging free wall due to an abrupt increase in afterload or localised ischaemia of the free wall due to increased wall stress[244].

Zagorski et al[223] used anti-CNC (cytokine-induced neutrophil chemoattractant) to modulate the inflammatory response to PE. A 50% reduction in MPO inflammatory activity was demonstrated in the rats treated with anti-CNC compared with the PE only group ($p<0.05$). An improvement in RV function (increase in RVSP and +dp/dt)[3] in those treated with anti-CNC antibodies was also demonstrated.

Lu et al studied the effects of cyclosporin A (a calcineurin inhibitor used in variety of inflammatory conditions) and anti-CD147 in rats with PE[243]. The study

[3] +dp/dt is a derivative of pressure over time used as a measure of ventricular pressure and a marker of ventricular contractility. It can be measured on TTE using doppler.

demonstrated an increase in inflammatory pathways with a significant increase in the CyPA-CD147 signalling pathway with associated RV dysfunction on TTE in those rats with PE only. CyPA is a protein secreted from cells in response to inflammation, and CD147, a matrix metalloproteinase inducer, is an extracellular signal receptor for CyPA[254 255]. The CyPA-CD147 interaction is associated with a range of inflammatory disease processes[256 257]. Rats treated with either cyclosporin or anti-CD147 or combination of both demonstrated a decrease in inflammatory mediator release with an improvement in RV dysfunction on TTE compared with no treatment ($p<0.01$). Treatment was also associated with a reduction in troponin I release suggesting these treatment strategies may modulate the inflammatory response and result in less cardiomyocyte damage.

Zhou et al also demonstrated the ability to modulate the CyPA-CD147 signalling pathway[202]. Sp-8356, a novel inhibitor of cd147-cyclophilin pathway, restored RVSP, cardiac troponin and MMP levels to that off the sham group. Direct visualisation of the cardiac myocytes demonstrated a reduction in apoptosis in those rats treated with SP-8356.

3.3.2 Syndromes of an Acute Increase in Afterload

Studies examining the inflammatory response as a result of acute afterload increase out-with PE are limited. Only one study used an animal model of acute afterload by performing banding of the PA. This technique is similar to that adopted during lung resection surgery whereby the lobar branch of the PA is clamped prior to dissection and as a result the RV findings in this study may well be more closely analogous to those in patients undergoing lung resection surgery.

Dewachter et al[258] induced RV failure in a canine group by performing prolonged PA banding to examine both the functional and inflammatory response to RV failure before and after an infusion of intravenous epoprostenol (a synthetic analogue of the naturally occurring prostacyclin, used as the mainstay of treatment in patients with PH and shown to reduce PVR and improve clinical outcomes). Following 90 minutes of PA banding, canines demonstrated a deterioration in RV contractility (shown by a decrease in Ees/Ea ratio) and

neutrophil and macrophage infiltration of the RV, both of which improved with epoprostenol. The study examined a wide variety of inflammatory signalling pathways and their response to prostacyclin treatment. An inverse correlation was demonstrated between RV arterial-coupling (Ees/Ea) and pro-inflammatory cytokines, as well as RV macrophage and neutrophil infiltrations suggesting a potential link between activation of an inflammatory process in the RV during acute afterload and RV-arterial decoupling.

3.4 Conclusion

This literature review has consistently demonstrated histological evidence of inflammation within the RV in both animal and human studies following PE and an acute increase in afterload. The strongest evidence of RV inflammation is found within the laboratory animal studies. These studies have widely demonstrated the activation of a range of pro-inflammatory pathways within RV myocardial tissue. Not only is inflammation present within the tissue, but clear association with clinical markers of RV dysfunction have been demonstrated with PA catheter monitoring and TTE imaging. The evidence from human studies is more limited given only a handful of studies have sought to demonstrate histological evidence of RV inflammation; however, RV inflammation was clearly demonstrated.

As discussed earlier in this chapter, lung resection surgery can be compared with other aetiologies that occur as a result of an acute increased afterload, such as that seen in animal models of PE. It is therefore conceivable that the histological changes that occur within the RV myocardium and associated RV dysfunction may be present in patients undergoing lung resection surgery who are subjected to an acute increased in afterload upon institution of OLV, clamping of the lobar branches of the PA and resection of lung parenchyma and associated vasculature. It is plausible that an inflammatory response may contribute to the RV dysfunction that occurs following lung resection.

Those studies examining the role of anti-inflammatory modulating therapies demonstrated again in the first instance that RV inflammation occurs following PE and is associated with RV dysfunction. The results of these studies also showed utilising anti-inflammatory modulating therapies directly targets the

inflammatory pathways, thereby reducing the inflammation within the RV and subsequently improving clinical evidence of RV dysfunction. Of particular interest were those studies who were able to reduce the inflammatory response and prevent RV dysfunction using anti-inflammatory modulating therapies pre-treatment, prior to the induction of PE. Ongoing areas of interest are the development of treatment modalities that may block the neutrophil influx into the RV tissue to ameliorate the acute inflammation caused by neutrophil activation whilst still allowing for normal wound-healing with monocyte activation. One such difficulty in clinical PE is the inability to pre-treat with anti-inflammatory therapies given the acute nature of the insult.

Building on this hypothesis, the purpose of this thesis is to test the hypothesis that an inflammatory injury is trigged in the RV in patients undergoing lung resection. By demonstrating such changes, it may be plausible in the future that patients undergoing lung resection patients could receive pre-operative anti-inflammatory modulating drugs to prevent RV inflammation and the subsequent dysfunction widely reported in the peri- and post-operative periods. Unlike in PE, the inflammatory response following lung resection is likely to be more predictable and opportunity may be available in the pre-operative period to blunt the inflammatory response prior to the inflammatory trigger. Further work is required to validate this hypothesis as currently no evidence exists in the literature to support this.

Chapter 4 Measuring Myocardial Inflammation

4.1 Introduction

Myocardial inflammation can be measured using a variety of techniques with advances in technology improving detection; however, most techniques still rely on the identification of at least one of the five cardinal signs of inflammation (as described in chapter 3). The main techniques used in clinical practice are discussed below.

4.2 Endomyocardial Biopsy

The current gold standard for diagnosing myocarditis, or inflammation of the myocardium, is the use of endomyocardial biopsy (EMB)[259]. EMB is usually performed under fluoroscopy guidance with the right interval jugular vein the most commonly used approach. Once the vein is cannulated, a PA catheter and bioptome are passed into the right atrium and across the tricuspid valve to the RV[260]. Biopsies are ideally obtained from the apical RV septum with three to five specimens obtained. Tissue samples are then analysed for evidence of lymphocyte, histiocytic or eosinophil infiltration or evidence of myocyte necrosis. The sensitivity and specificity of EMB varies depending on the clinical indication[260].

Despite being the gold standard, EMB is often considered a second line investigation in diagnosing myocardial inflammation due to the high-risk nature of the procedure, with complication rates reported around 1-3.3%[261-264]. The risks include cardiac chamber perforation leading to pericardial tamponade, arrhythmias, pneumothorax, damage to blood vessels and heart valves, haematoma, emboli and the creation of an arteriovenous fistula[263]. Although multiple biopsies are taken, missing the affected myocardium can result in a diagnostic result in around only one quarter of cases[265]. Fluoroscopy guidance also results in radiation exposure to both patient and staff undertaking the procedure. Due to the invasive nature of EMB and the development of well-validated non-invasive techniques, EMB is rarely performed in the investigation of cardiac inflammation, out-with heart transplantation where it is used for surveillance of organ rejection. The use of CMR guided EMB in animal studies has

been described in the literature and may potentially improve EMB results and safety in future clinical practice[266 267]. The use of EMB in human clinical research carries significant risks and due to its invasive nature was not considered appropriate for use in this perioperative population.

4.3 Transthoracic Echocardiography

Conventional transthoracic echocardiography (TTE) does not demonstrate any specific features of cardiac inflammation but may be utilised to evaluate cardiac dysfunction as a result of inflammation. Non-specific features, such as disproportionate thickening of the myocardium and increased echogenicity, can indicate the presence of myocardial oedema[268]. It has been suggested that conventional echocardiography may miss myocardial inflammation in those patients with patchy or minor degrees of inflammation[268].

Newer echocardiography techniques, such as 2D speckle tracking echocardiography, may have a role in demonstrating cardiac inflammation as studies have demonstrated alterations in 2D-echocardiographic strain in those with myocarditis[268-270]. Alterations in echocardiographic features, including global systolic longitudinal strain and strain rate, correlated with CMR and EMB evidence of myocarditis[268 269]. Of note, these studies were examining the LV for evidence of myocardial inflammation and make no reference to imaging of the RV using these techniques.

TTE offers the advantage of being widely available, minimally invasive and cost effective; however, it is widely recognised that TTE evaluation of the RV is challenging due its retrosternal position and complex geometry. The non-specific features of myocardial inflammation and challenging imaging make TTE a less well-suited imaging modality for imaging RV inflammation.

4.4 Cardiovascular Magnetic Resonance

Cardiovascular magnetic resonance is a non-invasive method for identifying myocardial inflammation. Different CMR techniques can be utilised to measure these changes and are described below. The advantages and disadvantages of each are also described (Table 6).

4.4.1 Gadolinium Enhancement

Gadolinium is a chemical element which is present in CMR contrast agents which are widely used to assess myocardial tissue. After an intravenous (IV) bolus is administered, the contrast agents transfer from the intravascular to the extravascular space (known as wash-in)[271]. Disease which causes expansion of the extravascular-extracellular space, or myocyte cell membrane rupture, provides an increased distribution volume for contrast agents and allows for their accumulation in scarred or fibrotic tissue. The different contrast kinetics result in differences between normal and diseased tissues which can be viewed by CMR. Gadolinium enhancement techniques use T1- weighted pulse sequences (T1- weighted pulse sequencing is discussed previously in Chapter 2).

Acute inflammation leads to the presence of hyperaemia (increase in blood flow to the tissues) which may be represented on CMR by an increase in the early uptake of intravenous contrast agent[272 273]. In early gadolinium enhancement (EGE), images are obtained within 0-2minutes of the contrast agent injection. Oedematous myocardial tissue, as seen in acute myocarditis or acute MI, will enhance rapidly. EGE has a reported sensitivity between 63 and 85% and specificity of 68-100% for detecting myocarditis[274].

Late gadolinium enhancement (LGE) is assessed fifteen to twenty minutes after the injection of contrast. LGE imaging is performed when the magnetisation of normal tissue is close to zero. In normal myocardium, contrast would be expected to have washed out at this time point, whereas in areas of increased extracellular/interstitial space, the contrast washout is delayed and appears hyperintense on imaging (Figure 22)[271]. Timing in LGE is essential as early imaging may lead to poor discrimination between the blood pool and the myocardium[271]. Dosing of contrast is also of importance in LGE as the window to acquire images may be brief in low doses, where higher doses may result in excessive brightening of the blood pool, reducing the ability to detect tissue necrosis and scarring[271]. LGE is useful for detecting fibrosis that is patchy in appearance whereas diffuse myocardial fibrosis is more difficult to distinguish as the global myocardial signal intensity may be nulled, appearing normal[275]. ‘Nulled’ describes tissue that produces little or no signal and makes no significant contribution to the reconstructed image[49]. LGE has been shown to

have a sensitivity of 59%, specificity of 86%, and accuracy of 68% for detecting myocarditis[274 276-278].

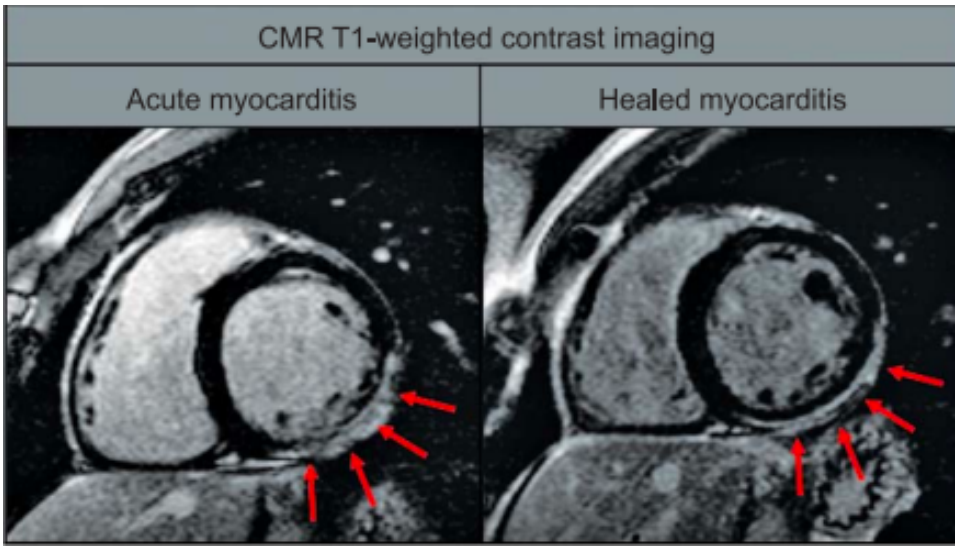

Figure 22 Cardiac magnetic resonance image of a patient with myocarditis using LGE techniques.
Image taken from Yilmaz et al[229]. The images shown are T1-weighted short-axis gradient-echo images in a patient with biopsy proven myocarditis. The red arrows demonstrate subepicardial LGE in the inferolateral segments indicating myocardial damage in the image on the left. The image on the right demonstrates extent of LGE after 3 months.

CMR Technique	Advantages	Disadvantages
Early Gadolinium Enhancement (EGE)	Hyperaemia easily visualised	Variable image quality Widely affected by artefact Few studies validated against histology Not widely available
Late Gadolinium Enhancement (LGE)	Can detect scar and necrosis Validated against histology Widely available technique	Not specific for inflammation Focal disease Timing of imaging critical
Native T1 mapping	Can detect a variety of pathologies No contrast required Short acquisition times	Affected by cardiorespiratory motion Different T1 acquisition techniques produce different T1 values
T2 weighted	No contrast agent Short acquisition protocols	Not routinely used in clinical practice Cannot always detect diffuse oedema Lack of familiarity with scan protocols Signal dropout and motion artefact common
Extracellular Volume (ECV) Quantification	Correlates with histological findings Distinguish between diffuse and discrete fibrosis Represents a physiological parameter Reproducible between different field strengths and scanning techniques	Contrast required Values affected by contrast dosing

Table 6 Advantages and disadvantages of cardiac magnetic resonance techniques for visualising cardiac inflammation.

4.4.2 T1 Weighted Imaging

The T1 relaxation time is a measure of how fast the nuclear spin magnetisation returns to equilibrium state after a radiofrequency pulse has been applied in the MRI scanner[55]. The general principle of T1 mapping is to acquire multiple images with different T1 weightings and to fit the signal intensities of the images to the T1 relaxation equation (Figure 23 and Equation 3). Each tissue type has a range of normal T1 values[279-281]. Inflammation and ischaemia of myocardial tissue results in an increased tissue water content which alters the molecular component of the tissues and affects the T1 value[282-285]. Inflammation of the myocardium will result in an increased native T1 value due to the increased water content of the tissue. A series of T1 images are acquired to generate a T1 map. Each pixel present on the map has a specific T1 value allowing for quantification of tissue characteristics[286].

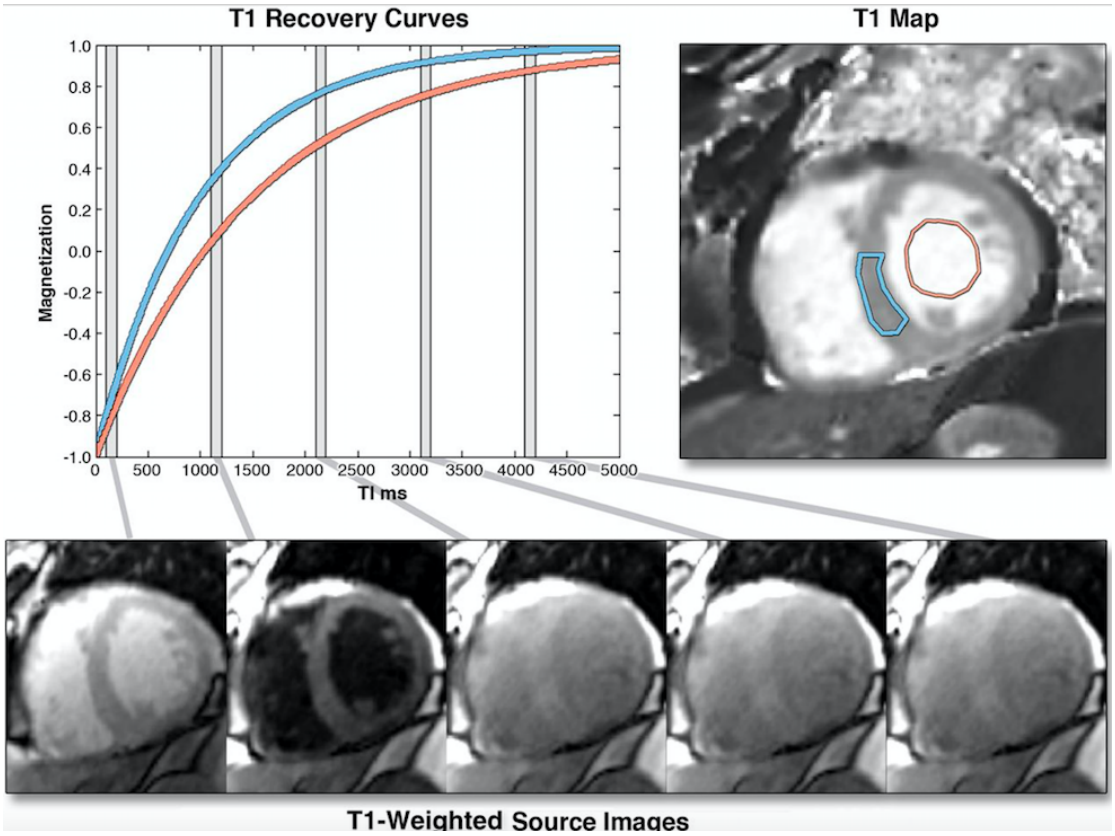

Figure 23 Magnetisation Inversion Recovery for T1 mapping.
The graph on the left shows 2 inversion recovery curves for a septal region of interest (blue) and the blood pool (red), generated from images, shown in the bottom row, taken at different times after an inversion pulse at time t=0. The T1 for each pixel location can be used to generate a T1 map, as shown in the top-right image. Taken from Taylor et al[55].

$$A - B * \exp(-t/T1)$$

Equation 3 T1 relaxation equation.
A and B are fitting parameters related to the equilibrium magnetisation and type of preparation, t is the time after preparation (i.e. either T1 or time after saturation pulse) and T1 is the T1 relaxation time[55].

There are a variety of CMR scanning protocols for measuring T1, the 'look-locker' technique, 'modified look-locker' (MOLLI), 'shortened MOLLI' (SMOLLI) and the 'saturation recovery single-shot acquisition' (SASHA), each with their own advantages and disadvantages. The look-locker techniques collect the images after an inversion pulse is created to create multiple images along the inversion curve, each with a defined T1 value[55]. SASHA differs in that it uses a saturation recovery technique to produce T1 maps. The most widely used clinical technique for T1 mapping is MOLLI acquisition; single-shot images are acquired intermittently in diastole during 3 to 5 heartbeats after the inversion pulse with images spaced by the R-R interval along the T1 recovery curve (Figure 24)[55].

Since the development of the MOLLI recovery sequence, pre-contrast T1 mapping techniques have become standard in the non-invasive measurement of myocardial inflammation[273]. Native T1 allows imaging of myocardial inflammation without the need for IV contrast which is advantageous in patients with chronic renal failure. However, without contrast, early changes in the myocardium may be missed. T1 maps rely on the alignment of the anatomy between all the images in the sequence with any cardiac and respiratory motion affecting the quality of the T1 images produced. It is also important to standardise the interpretation of the T1 maps as different reporting software may result in variation in T1 values.

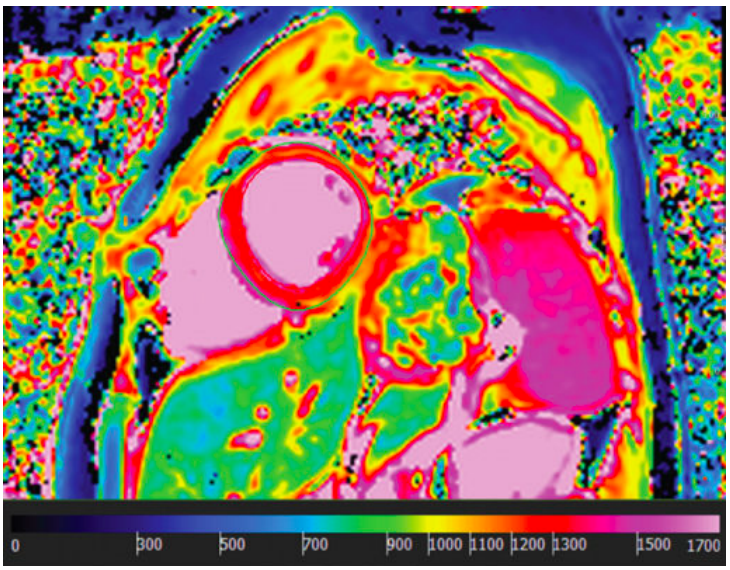

Figure 24 Example of a Modified Look-Looker T1 map acquired in a healthy volunteer. Taken from Ibrahim et al[287].

4.4.2.1 T1 and Extracellular Volume Mapping

ECV comprises the interstitial and intravascular spaces and can be measured using T1 mapping techniques following the administration of intravenous gadolinium (Figure 25). The administration of contrast shortens the T1 relaxation time and resultant T1 value, therefore areas of scarring and fibrosis will produce smaller post-contrast T1 values[288]. ECV is calculated from the formula in Equation 2, Chapter 1. ECV is a physiological parameter derived from the ratio of T1 signal values, is more reproducible allowing for better comparisons of images at different time points. ECV is considered to be independent of field strength, unlike native T1, with a meta-analysis of normal values for ECV found the pooled mean was 25.9% (95% CI: 25.2% to 26.3%) at 1.5Tand 25.9% (95% CI: 25.4% to 26.5%) at 3T[288 289]. It is a marker of myocardial tissue remodelling and is often due to an excess collagen deposition. ECV correlates with histological collagen and is useful in assessing both discrete and diffuse fibrosis and has been shown to correlate better with histological findings than contrast T1 mapping alone.[290] It may have a diagnostic benefit in early disease, in particular, diffuse fibrosis that may not be detected by LGE[290].

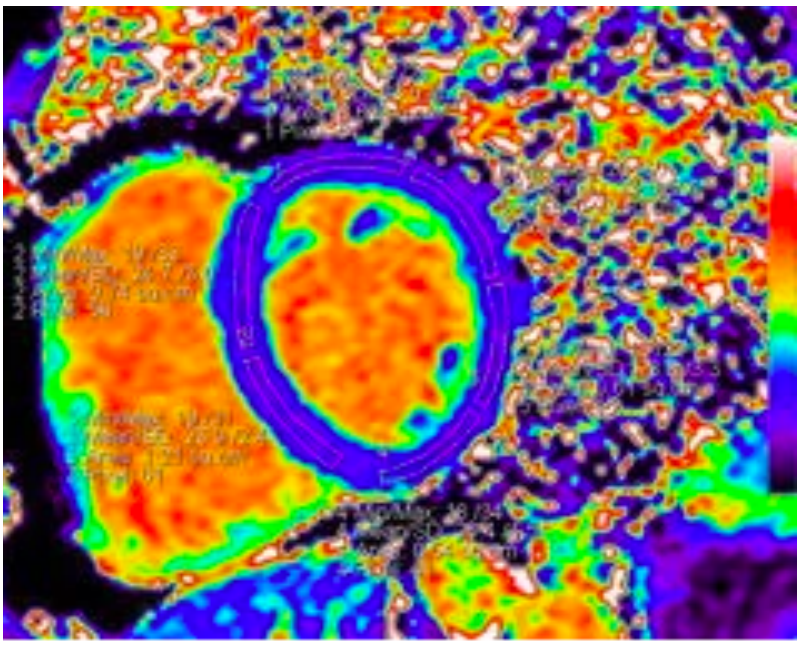

Figure 25 Example of a Modified Look Locker Extracellular volume map in a healthy volunteer
Taken from Cao et al[291].

4.4.3 T2 Weighted Imaging

T2 or the spin-spin relaxation time, is the exponential time constant responsible for the decay of transverse magnetisation following the application of a RF pulse[292]. During T2 imaging, tissues with a higher water content will have a longer T2 value and display a bright signal intensity. As a result, longer T2 relaxation times displayed in a wide range of acute cardiovascular conditions including myocarditis and oedema[278 293 294]. T2, similar to T1, has the advantage of detecting both regional and global increases in myocardial water content. It has a sensitivity between 45-100% and specificity of 50-100% for detecting myocarditis[274].

T2 has a relatively short acquisition time and does not require contrast administration. If gadolinium enhancement images are also required, the timing of T2 imaging is essential and must be taken prior to administration as contrast enhancement of T2 images will result in false results[295]. Signal dropout and motion artefact may occur if the images are acquired during phases of rapid cardiac motion. Image quality may be severely hampered by a lower signal to noise ratio and therefore affect its reliability in visualising and quantifying

oedema[292]. Signal to noise ratio (SNR) is a performance metric of MRI imaging. It is the ratio of signal present in the image, to the amount of noise present, noise being static fluctuation in signal intensity that results in a grainy or irregular appearance on the MRI image. Noise can occur as a result of molecular movement in the human body, and electrical resistance from the electronic components of the MRI system. T2 weighted images are affected by a lower SNR as they use a longer echo time (the time between the application of RF excitation pulse and the peak of the signal induced in the coil)[295]. Reproducibility, image quality and subjective assessment of T2-weighted images have limited its widespread adoption in clinical practice[295].

4.5 Nuclear Scintigraphy Imaging

The positron emission tomography (PET) technique uses positron emitting radiotracers to image metabolic processes. They typically use a radiotracer, such as gallium-67, which accumulates in areas with increased glycolytic activity. Inflammation is characterised by an increase in glucose metabolism with an overexpression of glycolytic enzymes in inflammatory cells (macrophages, monocytes, and neutrophils)[229 258]. PET scanning allows for the direct visualisation of inflammation by directly quantifying the metabolic activity of inflammatory cell infiltrates.

PET has been shown to have a high sensitivity for detecting acute inflammation, can differentiate between acute and chronic inflammation and has shown to have good agreement with CMR, the current gold standard for imaging cardiac inflammation. Patients require to fast between 12 and 18 hours prior to PET imaging in order to suppress the physiological glucose metabolism of the heart. PET imaging has the advantage of being non-invasive; however it is expensive, not widely available and requires radiation exposure[273 296]. A promising technique is the combination of PET/MRI to produce high quality cardiac images; however this technique is expensive and as of yet not widely available[297].

4.6 Laboratory Blood Tests

Many of the laboratory blood tests available, such as troponin, creatine kinase-MB (CK-MB) and naturetic peptides, are non-specific indicators of myocardial

injury and ischaemia and are used in combination with imaging techniques to monitor the inflammatory response and myocardial function over time. C-reactive protein is described as an acute phase protein and can be used as an earlier indicator of infection or inflammation. It is a non-specific marker of inflammation and can be raised for a range of reasons including infection, post-operative, and chronic inflammatory conditions[298 299].

Newer laboratory tests, including microRNAs (miRs) have shown potential as being specific for an inflammatory process alone. miRs are small non-encoding RNA molecules involved in a wide range of both physiological and pathological processes involving inflammation. They have been shown to have a high specificity and sensitivity for inflammatory process such as myocarditis, pulmonary embolism and pulmonary hypertension[300-303]. microRNA analysis is expensive and not currently in mainstream laboratory use therefore they are primarily utilised as research tool. microRNAs are discussed in greater detail in Chapter 10.

4.7 Conclusion

There are a variety of techniques that can measure myocardial inflammation with advantages and disadvantages of each. Although the gold standard for detecting myocardial inflammation is EMB, its invasive nature and complication rates limit its use. CMR offers a non-invasive imaging technique that is widely available with a range of imaging techniques for myocardial inflammation. Each of the CMR techniques described in this chapter have their merits. The ability to combine both T1 mapping and ECV quantification in one is clearly advantageous when examining myocardial inflammation. This combination allows the ability to detect both discrete and diffuse areas of fibrosis, has been shown to detect a wide variety of cardiac pathologies, and shows direct correlation with histological evidence of myocardial inflammation. This technique has gained widespread popularity and a variety of scanning techniques have been studied and improved over time to produce high quality images. Despite T2 weighted images offering the ability to detect oedema and fibrosis, its low signal to noise ratio and lack of familiarity in clinical practice reduce its appeal. The combination of PET/MRI is a promising technique but as of yet is not widely available. PET/MRI is not available within this hospital site and therefore cannot

be utilised in the early peri-operative period of this study (where transferring patients would be unsafe and logistically challenging). Laboratory blood tests are widely available but are non-specific markers of inflammation and may be used in combination with one of the techniques described but not as the sole determinant of myocardial inflammation.

Chapter 5 – Materials and Methods

5.1 Introduction

The remainder of this thesis describes the results of a prospective observational imaging study using CMR T1 mapping and ECV to investigate the novel hypothesis that an inflammatory myocardial injury occurs during lung resection surgery and may be a contributing factor to RV dysfunction in the peri-operative period. This chapter details the methods used for both imaging and biomarker studies.

5.2 Generic Methods

5.2.1 Ethical Approval

The study received ethical approval from the West of Scotland Research Ethics Committee (REC Reference: 18/WS/0006, Approval date 1st February 2018, substantial amendment approval date 20th April 2018).

5.2.2 Study Setting

The study was performed at the Golden Jubilee National Hospital/West of Scotland Heart and Lung Centre (GJNH) Clydebank. GJNH is a tertiary referral cardiothoracic centre and one of the largest thoracic centres in the UK[91]

5.2.3 Patient Population

Patients were selected following review by lead surgeon (Mr Mohammed Asif, consultant thoracic surgeon) at either the Monday morning or Wednesday afternoon outpatient clinic. An initial screen of potential participants was performed by the lead surgeon during the clinic appointment based on the inclusion and exclusion criteria.

Not all patients attending the clinic who met the inclusion and exclusion criteria were approached. Inclusion to the study was also dependant on the day of surgery and only those undergoing surgery on a Tuesday could be approached due to the availability of CMR in the hospital. Those patients who did not meet any exclusion criteria were approached at the end of the clinic and provided

initially with verbal information about the study, and then written information in the form of a patient information sheet to review prior to their admission for surgery the following Monday. Those patients who provided written informed consent participated in the study.

Inclusion criteria were; aged 16 years of age or over, planned elective lung resection by video-assisted thoracoscopy (VATS) or open lobectomy. Exclusion criteria were; patients who were pregnant, any ongoing participation in any investigational research which would undermine the scientific basis of the study, wedge, segmental or sob-lobar lung resection, pneumonectomy, isolated right middle lobectomy, atrial fibrillation at baseline, contraindications to cardiovascular magnetic resonance imaging (CMR) including cardiac pacemaker, artificial heart valve, neurostimulator, aneurysm clips, metal injuries to the eye or loose metal in the body, or contraindications to intravenous Gadolinium administration including acute or chronic renal failure, and known contrast allergy.

5.2.3.1 Justification of Inclusion and Exclusion Criteria

Lobectomy is the most common lung resection procedure performed[135 304135 304135 304133 302133 301]. Although pneumonectomy is more likely to cause greater physiological disruption, pneumonectomy represents less than 6% of lung resections nationally, limiting the application of study results. VATS resection rates have rapidly increased in recent years and now account for 70% of resections within the Golden Jubilee National Hospital. Lesser resections than lobectomy, including isolated right middle lobectomy, have been excluded as the lesser physiological disruption may be hypothesised to be inadequate to significantly influence RV function.

Patient's whose eGFR were below 60ml/min were not included in the study due to the risk of deteriorating renal function following contrast injection. If a patient developed either acute or chronic kidney disease following inclusion, they remained in the study but CMR was performed without the use of IV contrast.

5.2.4 Anaesthetic Protocol

The study did not aim to alter the anaesthetic, surgical or post-operative management of patients undergoing lung resection surgery. In order to try and standardise care, an anaesthetic protocol was designed based on the practice of the lead anaesthetist (Dr Mark Stevens, consultant cardiothoracic anaesthetist, GJNH) and broadly aligned with the wider anaesthetic department. In the event that Dr Stevens was not present, the named anaesthetist for the case used this anaesthetic protocol to ensure continuity in peri-operative practice.

Anaesthetic induction was performed with IV propofol, and anaesthesia maintained with an inhalational anaesthetic and an infusion of intravenous remifentanil. Lung isolation was achieved with a double lumen endo-tracheal tube. Ventilation was performed with a lung protective approach; tidal volume <8mls/kg, positive end expiratory pressure (PEEP) 0-10cmH_20, maximum airway pressure (P_{max}) limited to 30cmH_20, with fraction of inspired oxygen ($Fi0_2$) titrated to maintain oxygen saturations between 92-98%. For analgesia, an epidural catheter was placed pre-operatively for planned open thoracotomy or surgery with an increased likelihood of conversion to open and paravertebral catheters for VATS. Paravertebral catheters were sited intra-operatively by the operating surgeon. For both techniques, a bolus of local anaesthetic was administered in theatre and an infusion of local anaesthetic continued in the post-operative period. Patients received multi-modal post-operative analgesia as per local guidelines including regular oral paracetamol, oral anti-inflammatory (if no contraindications) and regular and as required oral opioids for break-through pain.

5.2.5 Data Collection

Data were collected by the author and research nursing staff during the patient's hospital admission and at their two-month follow-up appointment. All anonymised data was collated and stored in a password protected spreadsheet by the author.

5.2.5.1 Baseline Demographic Data

Routine patient demographics were collected at the time of recruitment from both face-to-face patient interview and from data extracted from patient's clinical records. All information was recorded in case report forms (Appendix 1, page 235).

Routine pre-operative pulmonary function tests were performed in all patients prior to attending the Golden Jubilee National Hospital for surgery according to national guidelines. These are reported as either absolute values or percentage predicted. Percentage predicted compares the values obtained to those obtained from population studies of healthy subjects matched for age, sex, height and ethnicity[305].

Thoracoscore, a validated multivariate model used to predict the risk of in-hospital death in patients undergoing thoracic surgery, was calculated from the parameters of; age, gender, American Society of Anaesthesiologists (ASA) score, performance status, dyspnoea score, priority of surgery, class of procedure, indication for procedure (malignancy or benign) and co-morbidity score[128].

5.2.5.2 Self-Reported Exercise Tolerance and Functional Status

Participants completed a written questionnaire to assess functional status and quality of life (QoL). Functional status was reported using three techniques, the World Health Organisation performance status (WHO-PS), the New York Heart Association (NYHA) heart failure classification and the Medical Research Council dyspnoea scale (MRC-DS) (Appendix 2, page 240)[306-309]. QoL was assessed using the EuroQOL 5 domain score (EQ5D) which comprises of: mobility, self-care, usual activities, pain/discomfort and anxiety/depression. Within each domain are five levels: no problems, slight problems, moderate problems, severe problems, and extreme problems. Permission was obtained from EuroQOL to use the EQ-5D questionnaire (December 2017). Questionnaires were completed pre-operatively and at clinic visit two-months post-operatively. Those patients unable to attend the post-operative clinic, answered the questionnaire via telephone. The MRC and EQ-5D have both been validated for use via telephone[310 311].

5.2.5.3 Cardiovascular Magnetic Resonance Imaging

Contrast-enhanced CMR was performed pre-operatively, at post-operative day two and at two-month clinic follow-up. Two-months was chosen as the second post-operative scanning time point for a range of reasons; 1) previous work from our research group demonstrated a reduction in RVEF that persisted at two-months post-operatively, 2) patient's routinely attend the hospital for follow-up at two-months post-operatively and therefore undertaking CMR scanning at that time point would ensure no further visits to the hospital out-with their routine standard care and 3) animal models of PE demonstrated the development of RV fibrosis at six-weeks post-operatively and this may be reflected in this patient population on CMR at this time point. Full details of the protocol and image analysis are detailed in section 5.3 page 118.

5.2.5.4 Laboratory Sampling

Blood sampling was performed at a number of time points peri-operatively. The initial blood sample was taken pre-operatively, immediately before induction of anaesthesia, followed by a sample immediately post-operatively in the recovery area, and then at six hours, twelve hours and on post-operative day (POD) one to three depending on the length of the participants' admission to hospital. Full details of blood sampling analysis are discussed below.

5.2.5.5 Intra-Operative Clinical Data

Intra-operative clinical data was collected using the RECALL Anaesthetic Intraoperative Management System (AIMS) electronic charting system (Informatics Clinical Information Systems Limited, Glasgow). To determine duration of anaesthesia, a substitute measure of end-tidal carbon dioxide ($ETCO_2$) presence was taken; as the appearance of $ETCO_2$ represents intubation and the disappearance that of extubation. Duration of OLV was obtained directly from the RECALL chart if recorded by the primary anaesthetist. In the absence of this data being prospectively recorded, duration was estimated from manual inspection of the airway pressure and tidal volume versus time curves.

5.2.5.6 Post-Operative Clinical Data

Critical care stay parameters are automatically and continuously recorded whilst a patient remained with the critical care post-operative areas (either the intensive care unit or the high dependency unit). This data is recorded using the ICU clinical information system (Centricity, CIS; GE Healthcare©, Buckinghamshire, UK) which records continuous parameters such as HR and blood pressure (BP) approximately every two minutes. Fluid and medication administration, urine output and cumulative fluid balance are also recorded. Fluid balance is automatically calculated by the system and a 24-hour fluid balance is reset each morning at 07.59.

Meaningfully defining length of high dependency unit (HDU) stay was difficult as discharge from the critical care environment can depend on a variety of factors including bed availability, and the time of day. To overcome this issue, length of stay began at the time of the first recorded oxygen saturation on the CIS and ended with the end of continuous oxygen saturation. The change from continuous recording to intermittent recording of monitoring is reflective of the patient requiring a lower level of post-operative care (from level two care to level one care) and therefore was the determinant of length of critical care stay.

Length of hospital stay was defined as the number of days in hospital following surgery, including the day of surgery. At the Golden Jubilee National Hospital, some patient's may be admitted for several days prior to their surgery for further investigations. As the Golden Jubilee National Hospital is a tertiary referral centre for the West of Scotland, some patients travel large distances to attend for their treatment and therefore can be admitted several days prior to surgery. To account for these unique features the length of stay was calculated for each patient *post-operatively*.

Predicted post-operative pulmonary function was calculated by using the standard equation (Equation 1) for both forced expiratory volume in one second (FEV1) and carbon monoxide diffusion factor (DLCO)[312].

$$PPO\ Value = \frac{pre - operative\ value}{T} \times R$$

Equation 4 Predicting post-operative values.
PPO = predicted post-operative value, T = total number of functioning segments prior to resection, R = number of functional segments following resection.

5.2.6 Data Synthesis and Statistics

Statistical analyses were performed using SPSS for Mac, version 25 (IBM, Corp, Armonk, New York, United State of America). A p-value of <0.05 was considered statistically significant; no adjustments were made for multiple comparisons. Data are presented as mean (SD) or median (IQR) as appropriate to distribution. Normality was assessed by visual inspection of data distribution and confirmed with the Shapiro-Wilk test (p<0.05). Transformations were made where possible for non-normal data distribution and where not possible, a non-parametric test was used. Participants with missing data will be included in data analysis as missing data is likely to be as a result of 'missing data completely at random'[313]. Removal of patients with missing data would result in a significant loss of data and associated loss of power in a study with a small number of participants.

Changes over time for normally distributed data were assessed using the one-way repeated measures analysis of variance (ANOVA) and for non-parametric data using Friedman's test. Comparisons of parametrically distributed data in related groups were made using a paired t-test. Comparisons of parametrically distributed data in unrelated groups were made using an independent t-test or one-way analysis of variance as appropriate. Comparisons of non-parametrically distributed data between unrelated groups was using the Mann-Whitney U-test or Kruskal-Wallis test as appropriate. Categorical variables were compared using the Chi-squared test.

All linear associations were visually inspected and assessed using the Spearman's or Pearson's correlation coefficient as appropriate. Inter and intra-observer variability was assessed using the intraclass correlation coefficient (ICC) for agreement and consistency, and the coefficient of variation (COV). ICC and COV

were interpreted as outlined in Table 7. Bland-Altman plots were created to assess bias and any differences between observers or measures[314].

Intraclass correlation coefficient	Coefficient of Variation	Interpretation
0 - 0.4	>15%	Poor
0.41- 0.6	10-15%	Moderate
0.61-0.8	<10%	Good
0.81-1.00	<10%	Excellent

Table 7 Interpretation of the intraclass correlation coefficient and coefficient of variation. Coefficient of variation is defined by three different values unlike intraclass correlation coefficient therefore a coefficient of variation of <10% would be classified as both good and excellent. Table adapted from data from Reed et al, Kawel et al and Koo et al[315-317].

5.3 Cardiovascular Magnetic Resonance Assessment of Right Ventricular Function and Inflammation.

5.3.1 Methods

Cardiovascular magnetic resonance imaging was performed pre-operatively, on POD2 and at two-month clinic follow-up. Pre-operative CMR imaging was performed the day prior to surgery where possible. In some cases, CMR imaging was performed on the morning of surgery. In these instances, surgery was scheduled to be performed as an afternoon case to allow adequate patient preparation. CMR imaging took place on the afternoon of POD2 where possible, in those patients unable to participate on POD2 due to medical reasons, CMR imaging was performed instead on POD3.

5.3.1.1 Power Analysis

The primary outcome of the study was to determine if RV inflammation can be assessed by T1 mapping following lung resection. The primary endpoint is the number of CMR studies which have an Image Quality Score (IQS) of two or more. Images will be scored against three grades; 1 – poor image quality unable to interpret, 2 – satisfactory/variable image quality but able to interpret or 3 –

good image quality able to interpret. Similar grading systems have been used in other studies measuring T1 values in the myocardium[318].

Whilst feasibility of measurement of T1 is the primary outcome of the study, a power calculation was performed on the main secondary outcome – *Is increased T1 present in the RV following lung resection*? There are no previous studies assessing the role of T1 mapping in this population. In PH, Spruijt et al[319] reported T1 values of 1060+/-70ms in PH versus 957+/-70ms in controls with an effect size of 1.37. Reiter et al[320] found similar effect size differences with T1 values of 1298±78ms in PH versus 1193±31ms in controls with an effect size 1.25. In MI, a greater difference in native T1 between infarcted myocardium and remote zone (myocardium not directly affected by the infarct) is described; Carrick et al (collaborators in our institution) demonstrated T1 values of 1097+/-52ms versus remote zone 961+/-25ms effect size 2.36[321].

The author hypothesises however that the observed effect size in native T1 observed post-operatively will be modest in comparison to PH. Due to the pilot nature of this study, the author had no indicative value from which to calculate power, however as a guide, the effect size for the change in RVEF seen in the serial CMR study from our research group was 0.9[81]. Based on a two-sided, paired t-test with a significance level of 5% and power of 80%, 12 patients would be required to demonstrate an effect size of 0.9. Assuming a minimal sample size of 12 patients, and allowing a margin of 20% for drop outs, 15 patients would be recruited.

Power analysis may have limited value in an observational pilot study. In this study, sample size was limited by the patient population, the ability for patient's to undergo CMR scanning in the immediate post-operative period, the inclusion and exclusion criteria and the time available for enrolment.

5.3.1.2 Image Acquisition

All CMR imaging was performed at the Golden Jubilee National Hospital using a 1.5 Tesla Siemens Avanto (Siemens, Germany) whole body scanner by band seven Health and Care Professionals Council accredited advanced practitioner radiographers. All study participants completed a standard CMR safety

questionnaire prior to recruitment and consent to the study. This questionnaire was verified by a member of the scanning team prior to the participant entering the CMR scanning room to ensure no absolute contraindications to CMR imaging (Appendix 3, page 244).

Participants were asked to dress in a hospital gown and position themselves onto the examination table lying supine. An intravenous cannula was inserted by a member of the research team to allow for injection of intravenous contrast during the scan. Adhesive monitoring pads were placed on the participant's chest to allow continuous three lead ECG monitoring during the scanning procedure. A padded chest coil was then placed on the patient's chest to allow transmission pf radiofrequency signals. The participant was given ear defenders and provided with an emergency buzzer they could use throughout the procedure if they required assistance. The table was then placed within the bore of the scanner to allow image acquisition. Prior to image acquisition, function of the microphone and headphone communication system was checked to allow communication between participant and the scanning team. A member of the research team was present in the CMR control room throughout the procedure. This sequence was followed for both POD2 and two-month follow-up CMR.

During surgical lung resection, surgical clips and linear stapling devices are utilised. To ensure this equipment was compatible with immediate post-operative MR imaging, a record of all the intra-operative surgical equipment used by the main operating surgeon was collected by the research team and cross-checked for MR compatibility with the manufacturer. All equipment confirmed to be MR safe by the manufacturer was placed on a checklist of MR safe equipment and was 'signed off' by Dr Des Alcorn (consultant radiologist). The research team collected intra-operative equipment for each individual participant at the time of their surgery and this was cross-checked with the checklist by the author. Any new equipment not present on the checklist required MR safety checking with the manufacturer before being signed off by Dr Alcorn prior to scanning. Once participants were all safely scanned on POD2, they were safe to undergo their two-month follow-up scan unless they had undergone further surgical procedures in the interim or met another exclusion criteria.

Image acquisition on POD2 varied slightly from the above sequence due to some key post-operative features. In the immediate post-operative lung resection period, patients require a chest drain for collection of any air or fluid that may have collected in the thoracic cavity during surgery. At the Golden Jubilee Hospital, the Thopaz (Mendela, Switzerland) thoracic drainage system is used which is not MR safe. Any participant who still required chest drainage on POD2 had their Thopaz drainage system changed to an underwater seal chest drain immediately prior to CMR scanning as this drainage system is compatible with MR imaging. During scanning, the chest drain was secured to the side of the scanning table.

Where feasible, all infusions were discontinued for the duration of the scan to minimise the number of patient connections whilst in the scanner. For those participants with either a thoracic epidural or paravertebral catheters for analgesia, these were discontinued and disconnected prior to the participant leaving the ward area. Prior to discontinuing them for the duration of the scan, the patient was given oral analgesia to ensure they remained comfortable throughout transfer and the scan itself. On return to the ward, the catheters were immediately reconnected, and a 'top-up' bolus of analgesia given. All patients scanned on POD2 were accompanied by a member of the medical research team who were present in the CMR control room throughout the scan.

A dedicated CMR protocol used for all imaging (Appendix 4, page 245). Electrocardiogram-gated fast imaging steady state-free precession cines were used throughout. Standardised imaging parameters included repetition time; echo time; flip angle; voxel size; and field of view = 4.3ms, 1.2ms, 60°, 1.4 x 1.4 x 6mm, 340mm. Six-millimetre imaging slices were used with a 4mm interslice gap. Short axis imaging was performed during breath holds and initiated at the atrioventricular valve plane and propagated sequentially to the cardiac apex to ensue complete coverage of both ventricles. Cine sequences, steady-state free precession sequences aligned to two-chamber view (CV), 3 CV, 4 CV and short-axis (SA), black blood and late gadolinium enhancement images were obtained. Native and post-contrast T1 mapping were also performed. T1 mapping images were acquired at mid-ventricular short-axis sections by using an optimised MOLLI)sequence. Pre-contrast T1 maps were obtained in both SA and horizontal long axis (HLA) prior to the injection of IV contrast. Post-contrast T1 maps were

obtained 12-15minutes after injection of IV contrast in both the SA and HLA views. The contrast agent used was Gadovist® (Bayer HealthCare, United Kingdom) injected at a dose of 0.15mmol/kg as per manufacturer's guidelines.

On completion of the scan, the images were saved to the hard drive of the MRI scanner and the hospital imaging network. At completion of the study, all images were anonymised and randomised by a member of the research team not involved in the blinded analysis and images were stored on an encrypted external hard drive.

5.3.1.3 Image Analysis

To ensure incidental findings that could be of clinical importance were not overlooked, safety reporting of all anonymised scans at two-month follow-up were reported by Professor Colin Berry (consultant cardiologist with level 3 European Association of Cardiovascular Imaging certification in CMR imaging). A clinical report was generated and made available in the patient record.

Post-processing software (circle cvi42, Calgary, Canada) using manual planimetry was used to determine both left ventricular and right ventricular volumes. Randomised and anonymised images were dual reported by the author and a co-investigator. For the assessment of intra-observer variability, all randomised and anonymised scans underwent repeat analysis by the author. This was performed more than one month after the first analysis.

The methods for determining both LV and RV volumes are standardised in clinical CMR practice[322]. To determine both RV end-diastolic and end-systolic volume, the full image stack was evaluated. The RV end-systolic image was chosen as the image with the smallest RV blood pool (Figure 26)[322]. RV end-diastole was determined as the image with the largest RV blood pool (Figure 27)[322]. Following identification of end-diastole and systole, the endocardial border of the RV was contoured in both phases (Figure 28). The RV outflow tract up to the pulmonary valve (where visible) was included in the analysis. As per standard clinical recommendations, the RV trabeculations were ignored and a smooth endocardial border drawn, in an attempt to improve reader

reproducibility.[322] A similar process took place for the LV volumes with the papillary muscles included as part of the myocardial blood pool (Figure 29).[322]

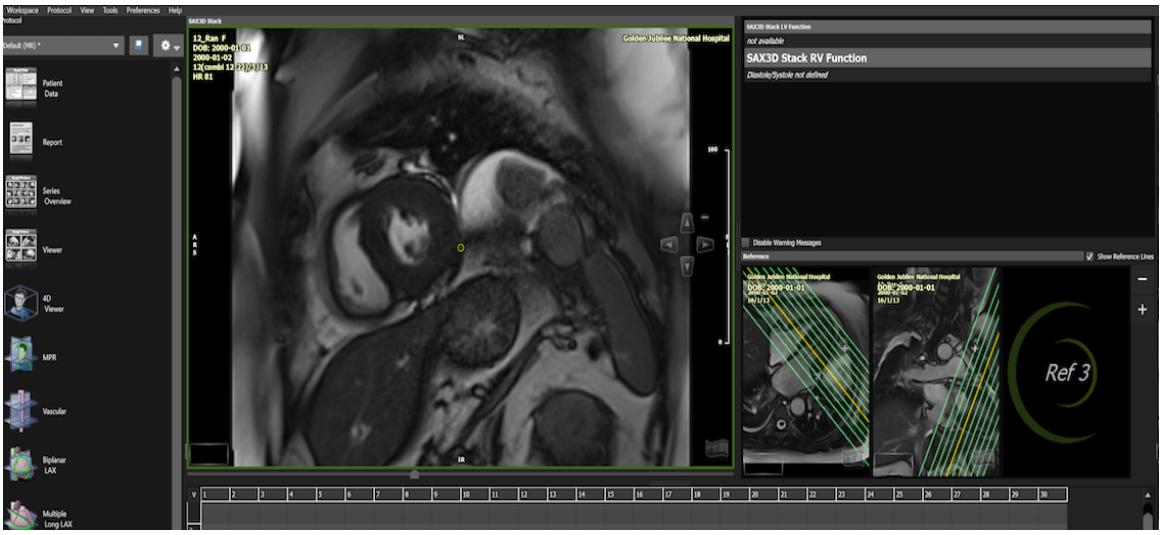

Figure 26 Determining end-systole in Circle CVI.
A screenshot from the Circle CVI software for CMR analysis. The central image is a mid-ventricular short axis slice at end systole (when the blood pool is at its smallest). The two smaller central images are the horizontal long axis which can be used as a slice reference point.

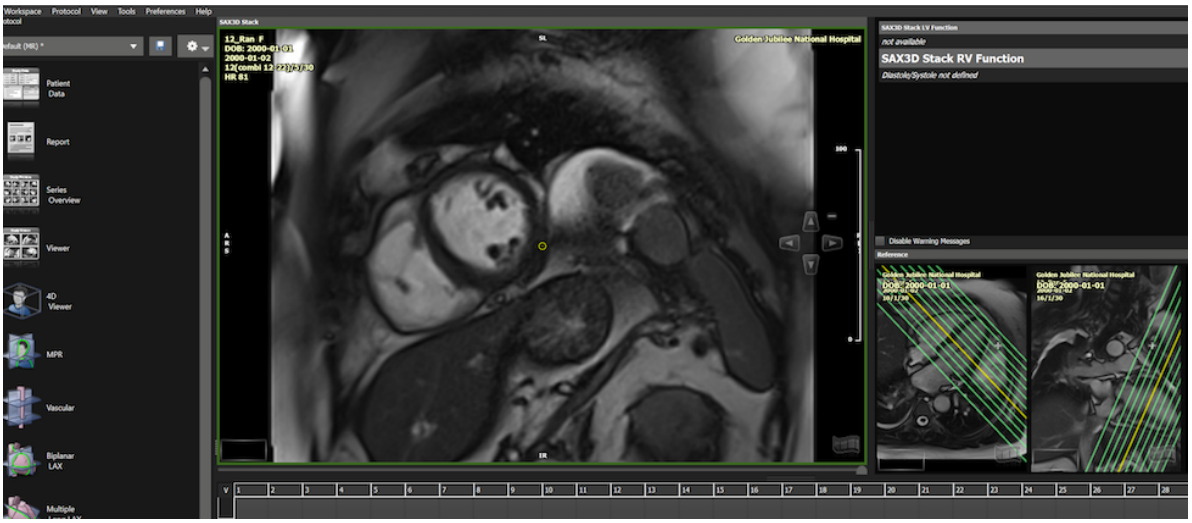

Figure 27 Determining end-diastole in Circle CVI.
A screenshot from the Circle CVI software for MRI analysis. The central image is a mid-ventricular short axis slice at end diastole (when the blood pool is at its largest). The two smaller central images are the horizontal long axis which can be used as a slice reference point.

Defining the most basal ventricular slice can be a challenging aspect of CMR image analysis. In an attempt to overcome difficulties identifying this for both the RV and LV, once the most basal ventricular slice was identified, this was then cross-referenced with the horizontal long axis view to ensure the slice was

ventricular and not atrial in origin. The basal slice for the LV was determined as the most basal slice surrounded by 50% or more of ventricular myocardium.

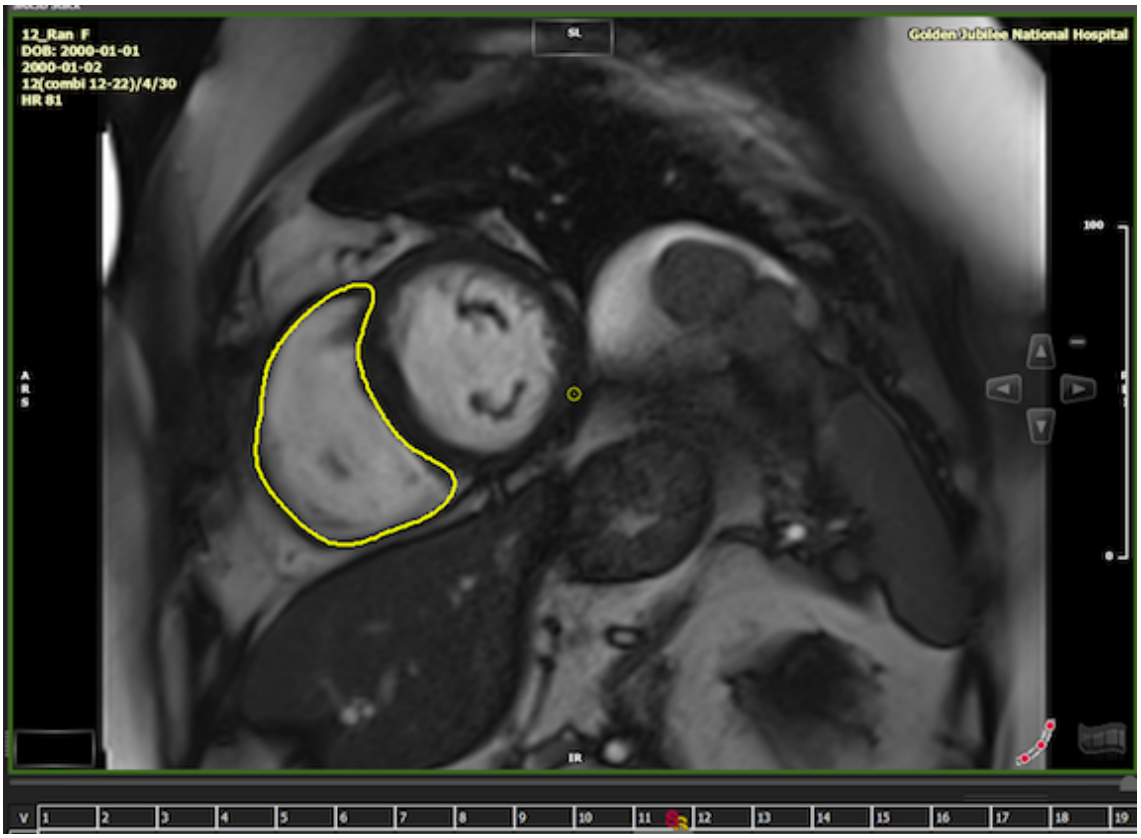

Figure 28 Contouring of the right ventricle in Circle CVI.
A screenshot demonstrating the RV contouring process. The yellow line demonstrates contouring of the endocardial border of the RV in end-diastole.

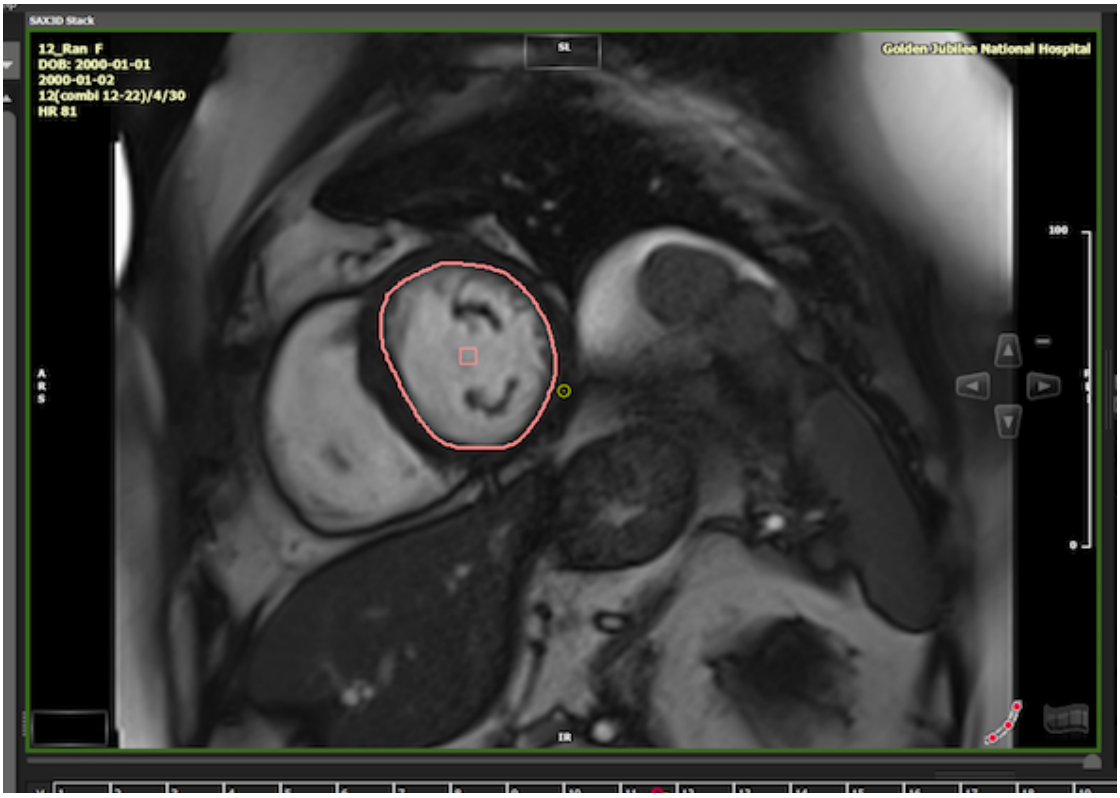

Figure 29 Contouring of the left ventricle in Circle CVI.
A screenshot demonstrating the LV contouring process. The red line demonstrates contouring of the endocardial border of the LV in end-diastole.

Right and left end diastolic and end systolic volumes (EDV and ESV respectively) were calculated using an automated calculation utilising the sums of discs method. Right and left ventricular SV and EF were automatically computed using the equations demonstrated below (Equation 5 and 6).

$$Stroke\ volume\ (ml) = End\ diastolic\ volume\ (ml) - End\ systolic\ volume\ (ml)$$

Equation 5 Calculation of stroke volume

$$Ejection\ Fraction\ (\%) = \left(\frac{Stroke\ volume\ (ml)}{End\ diastolic\ volume\ (ml)}\right) \times 100$$

Equation 6 Calculation of ejection fraction

T1 maps were produced and analysed using the circle cvi42 software. Prior to measuring T1, images were evaluated and graded depending on image quality and interpretability. Both Siemens-generated native and post contrast T1 maps

and raw native and contrast maps were evaluated. For the raw maps, the native MOLLI sequences were initially loaded and reviewed for the presence of artefact (Figure 30). When artefacts occurred and may potentially have contributed to a variation in the T1 value, the images with the affected segments were removed producing new raw maps (Figure 31).

Contours (including epicardial and endocardial borders, ventricular insertion points, and blood pool) were drawn on all raw images present in the sequence to produce a corrected T1 map. This process was performed for the raw post-contrast images. Both Siemens-generated and raw maps were evaluated with a score of 1 to 3 assigned for each individual pre- and post- contrast map (Table 8 and Figure 32). Images with a score of 1 were excluded and T1 values were not calculated.

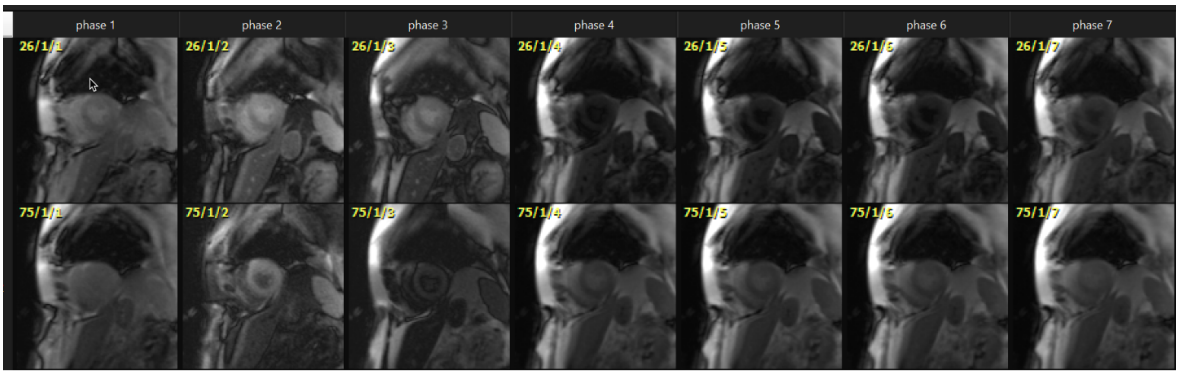

Figure 30 Example of a Modified Look Locker T1 Sequence
Images shown demonstrate a MOLLI pre-contrast sequence loaded into the series overview feature on circle cvi42 analysis software. Each individual image is analysed for image quality and artefact. If artefact present the individual image is removed from the sequence and a new raw T1 sequence generated for T1 map analysis.

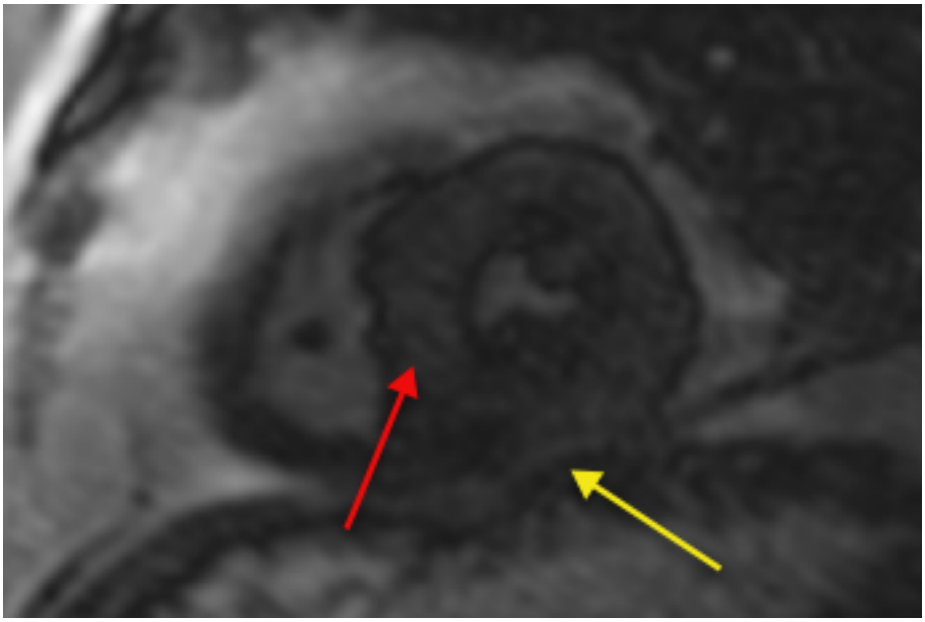

Figure 31 Example of artefact affecting image quality of a pre-contrast T1 map.
The red arrow is artefact within the septum. The yellow arrow is artefact with blood margins at the LV free wall. This is most likely respiratory artefact due to inadequate breath holding.

Image Score	Comment
1	Poor image quality; unable to interpret Presence of significant artefact Poorly defined borders
2	Variable image quality, able to interpret Presence of some artefact Blurring of borders
3	Good image quality, able to interpret No artefact Clear border definition

Table 8 T1 Maps Image Quality Score

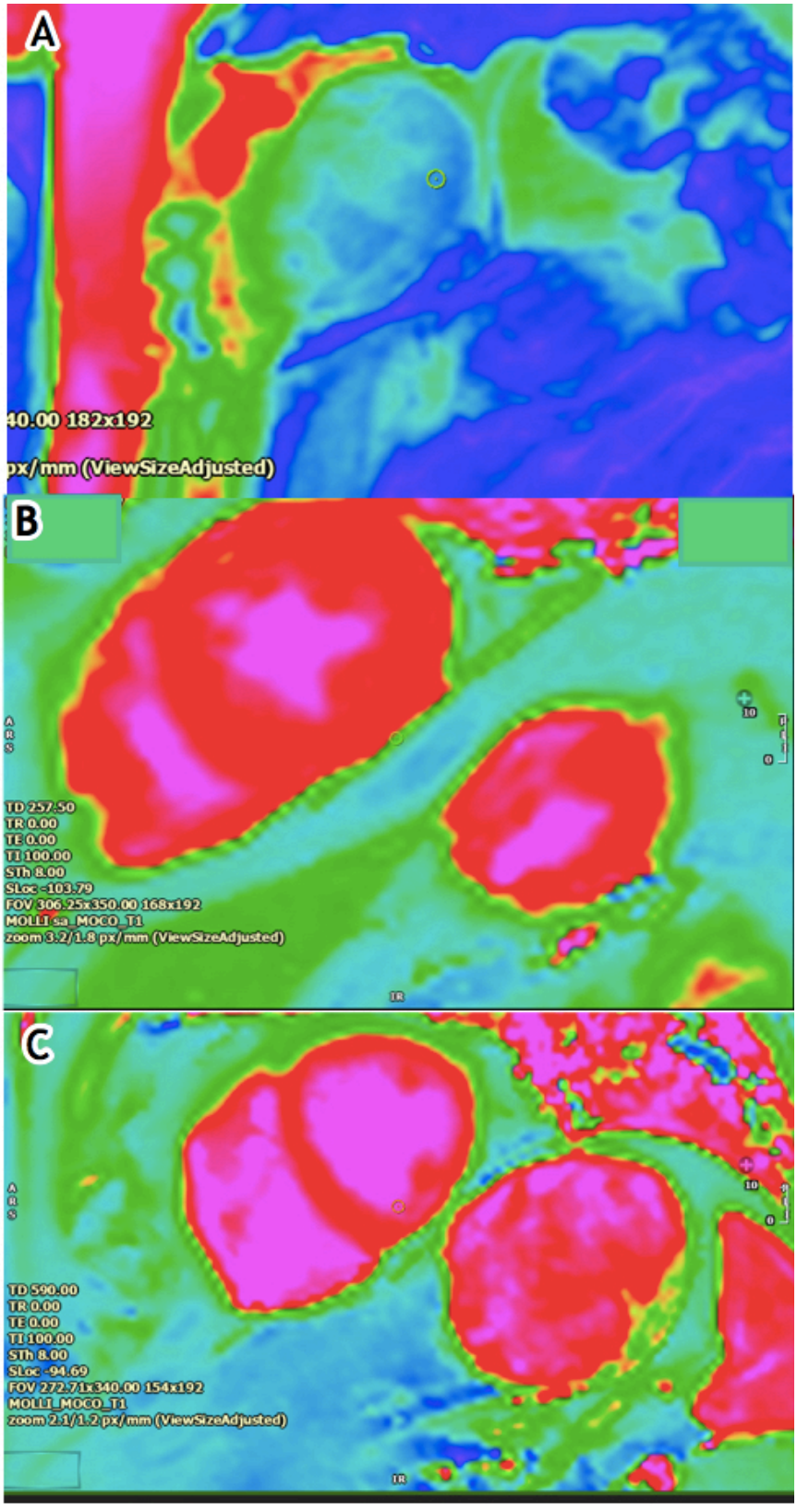

Figure 32 Examples of T1 maps image quality scoring.
images A-C are regenerated T1 maps all viewed on circle CVi42 software. Image A has an image quality score of 1 (poor) as there are major artefacts present with poor definition between blood and myocardium. Image B has an image quality score of 2 (satisfactory) as there is sufficient contrast between blood and myocardium. Image C has an image quality score of 3 (good) with no artefacts with good contrast between the myocardium and blood.

T1 values were calculated on regenerated maps. Short-axis T1 maps were loaded onto the T1 analysis platform. Epicardial and endocardial borders of the LV were defined along with the superior and inferior VIPs. The SA axis slice was segmented according to the American Heart Association (AHA) 16-segment model using the anterior RV-LV insertion point as a reference point (Figure 33).[323] Segmental AHA regions of interest (ROI) were delineated by user-defined semi-automated border delineation (circle cvi42, Calgary, Canada). To calculate T1 values, a ROI was drawn using a free hand ROI tool and standardised to be of similar shape and size. Care was taken to allow adequate margins of separation from tissue interfaces such as blood pool or epicardial fat and myocardium. ROIs were drawn on the septum, LV free wall, and the superior and inferior VIPS. The ROIs for the VIPs were defined at the border of myocardial segments 7/8 and 9/10 for anterior and inferior right ventricular insertion respectively (Figure 34). The same sequence was performed for the post-contrast T1 maps. An example of a pre and post-contrast map from this study are shown (Figures 34 and 35). ECV was calculated using the standardised ECV equation (Equation 2 Chapter 1) and ECV maps produced (Figure 36 and 37). For inter-observer variability, ten randomised and anonymised scans were selected for dual-reported analysis.

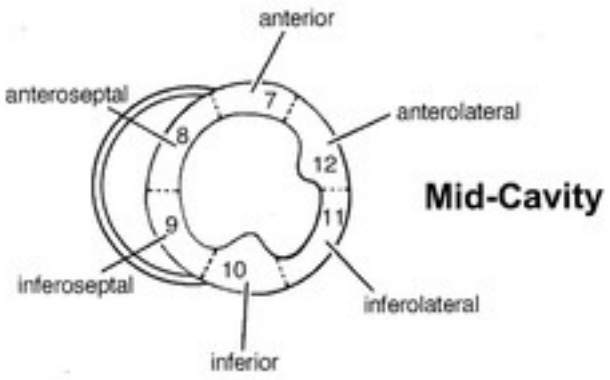

Figure 33 Mid-cavity short axis slice segmentation
Image demonstrates the six segments at the mid-cavity as per the American Heart Association Standardized Myocardial Segmentation and Nomenclature for Tomographic Imaging of the Heart.[323] This diagram is used to demonstrate the name, location and landmarks present in the mid-cavity short axis slice.

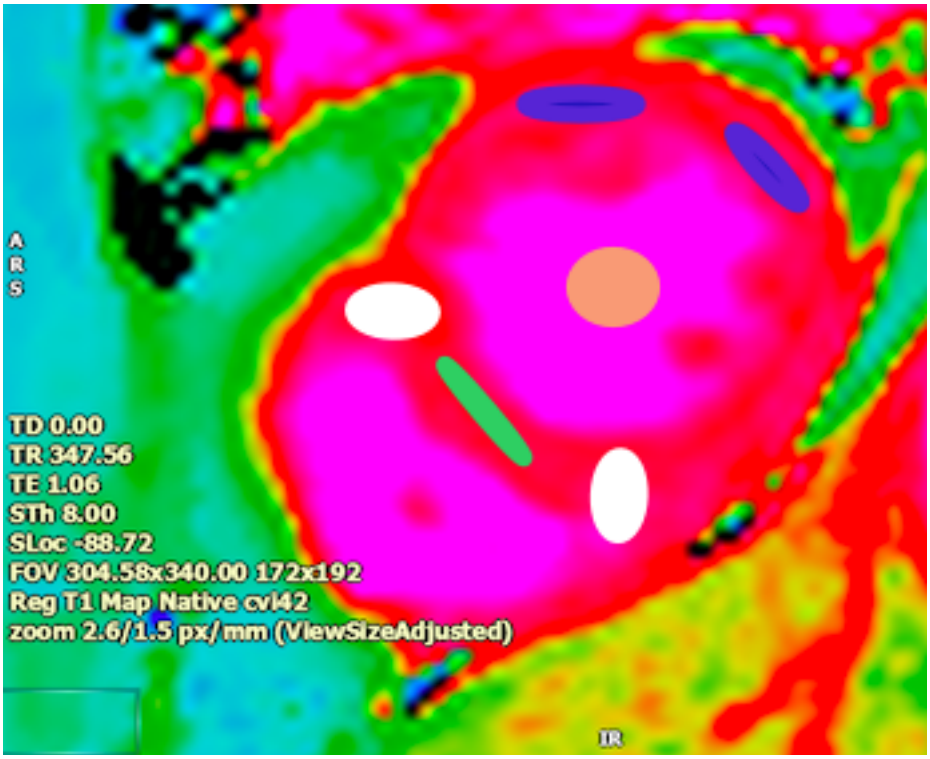

Figure 34. Example of a pre-contrast map displaying regions of interest within the myocardium.
A pre-contrast regenerated T1 map regions of interest in the septum (green), left ventricular (blue), blood pool (orange) and superior and inferior ventricular insertion points (VIP)(white).

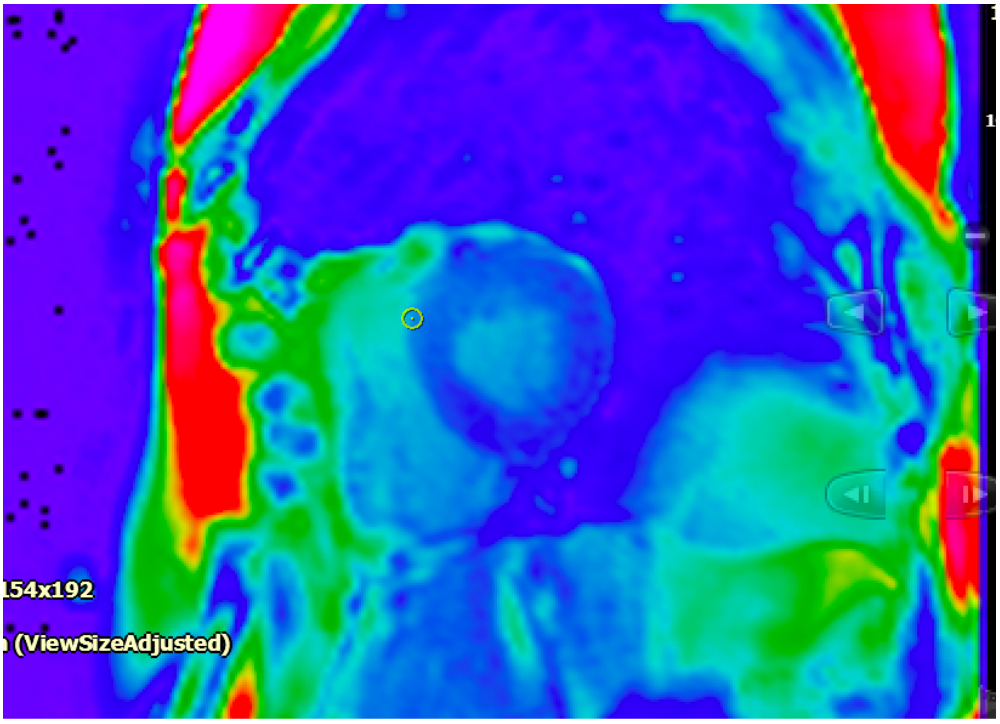

Figure 35 Example of a post-contrast regenerated T1 map.

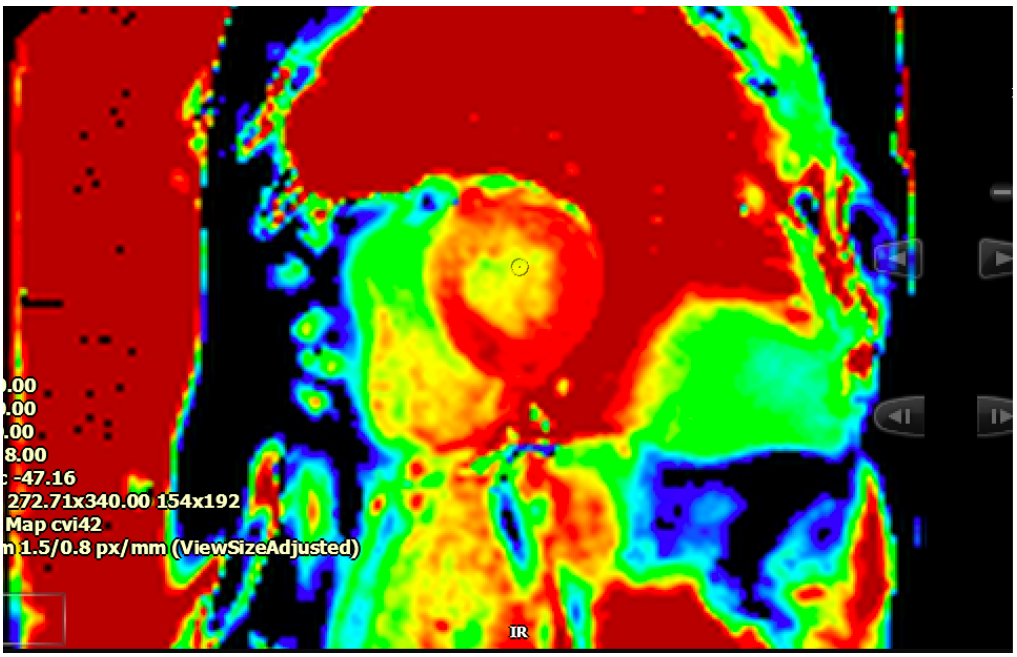

Figure 36 Example of an extracellular volume map.

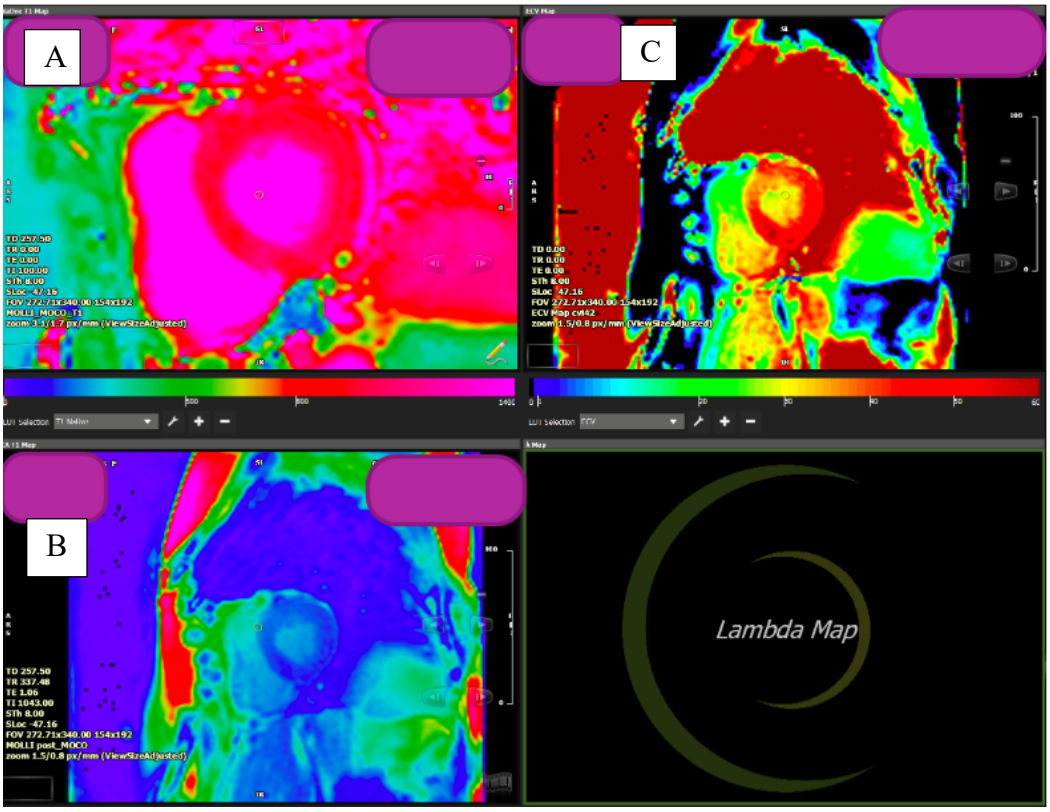

Figure 37 Circle CVi42 software T1 map analysis panel displaying regenerated pre-contrast T1 map(A), post-contrast T1 map (B) and a corresponding ECV map(C).

5.4 Biomarkers of Myocardial Dysfunction

5.4.1 Methods

Standard procedure for patients undergoing lung resection surgery involves the placement of an arterial cannula allowing continuous measurement of haemodynamic parameters and for blood sampling without the need for further venepuncture. Where possible, samples for biomarker analysis were drawn from the arterial cannula along with routine post-operative blood samples. When samples were required after the removal of the arterial cannula, a peripheral venous sample was obtained.

Blood sampling was performed pre-operatively (prior to the induction of anaesthesia), immediately post-operatively (once extubated in the recovery area), six, twelve and twenty-four hours post-operatively and then on the mornings of post-operative day two, and three if the participant remained in hospital at this point. A further sample was taken at two months when the patient returned for routine post-operative clinic follow-up. Blood was collected using the BD Vacutainer® system with 3x4ml EDTA (purple top) tubes obtained. BNP, NT-proBNP, and TnT were measured as described below. The remaining samples were immediately centrifuged, plasma aliquoted and stored at -80^{0}C in the research laboratory of the Golden Jubilee National Hospital.

As part of routine care for lung resection surgery, routine blood samples, including haematocrit, urea, creatinine, eGFR, and CRP, are measured at various time points (pre-, peri- and post-operatively). These samples were collected as part of the patient's routine pre- and post-operative care and processed in the haematology and biochemistry laboratories at the Golden Jubilee National Hospital using standardised laboratory protocols.

BNP, NT-proBNP, and TnT were measured immediately using the Alere Triage® system (Alere, Stockport, UK). This is a point of care fluorescence-based immunoassay system. The Triage SOB Profiler® and Triage NT-Pro BNP panels were used to perform assessment of BNP, NT-Pro BNP, and TnT. Prior to study recruitment, all members of the research team underwent training by Ms Janice McIvor (Alere specialist support team). A sample of blood was transferred from

the EDTA tube, using the provided transfer pipette, to the test device and the manufacturers guidelines were followed throughout the testing process. This processed was performed for each panel. High and low reference frozen control samples were performed on a monthly basis as per manufacturer recommendations for both panels.

5.5 Conclusion

This chapter describes the generic methods of this study and the CMR protocol used. All patients underwent a standardised anaesthetic and surgical technique as per routine standard of care for patients' undergoing lung resection surgery for primary lung cancer. Out with standard routine care patients underwent CMR on three separate peri-operative time points and blood sampling for a range of biomarkers performed in the pre and post-operative period as per the study protocol.

Chapter 6 - Generic Results

The results described here apply to the cohort recruited for the imaging and biomarker studies described in chapter 5. Patient demographics, operative characteristics, post-operative outcomes and both; volumes and cardiac function assessed by CMR, are described.

6.1 Patient Demographics and Operative Characteristics.

From 13th April 2018 to 10th December 2018, 15 patients were recruited to the study by the author (Figure 38).

One patient (RV13) was excluded from further participation in the study as a result of an incidental diagnosis of hypertrophic cardiomyopathy being made following pre-operative CMR scanning. Pre-operative biomarkers BNP and NT-proBNP were also markedly elevated in this patient. Following multidisciplinary team discussion between the research team, operating surgeon and anaesthetist, it was determined that the patient should be removed from the study due to these significant abnormal findings. The patient did not undergo CMR scanning on POD2 or at two- months and no further biomarker sampling was performed. Baseline demographic data on the remaining 14 patients is presented in Table 9.

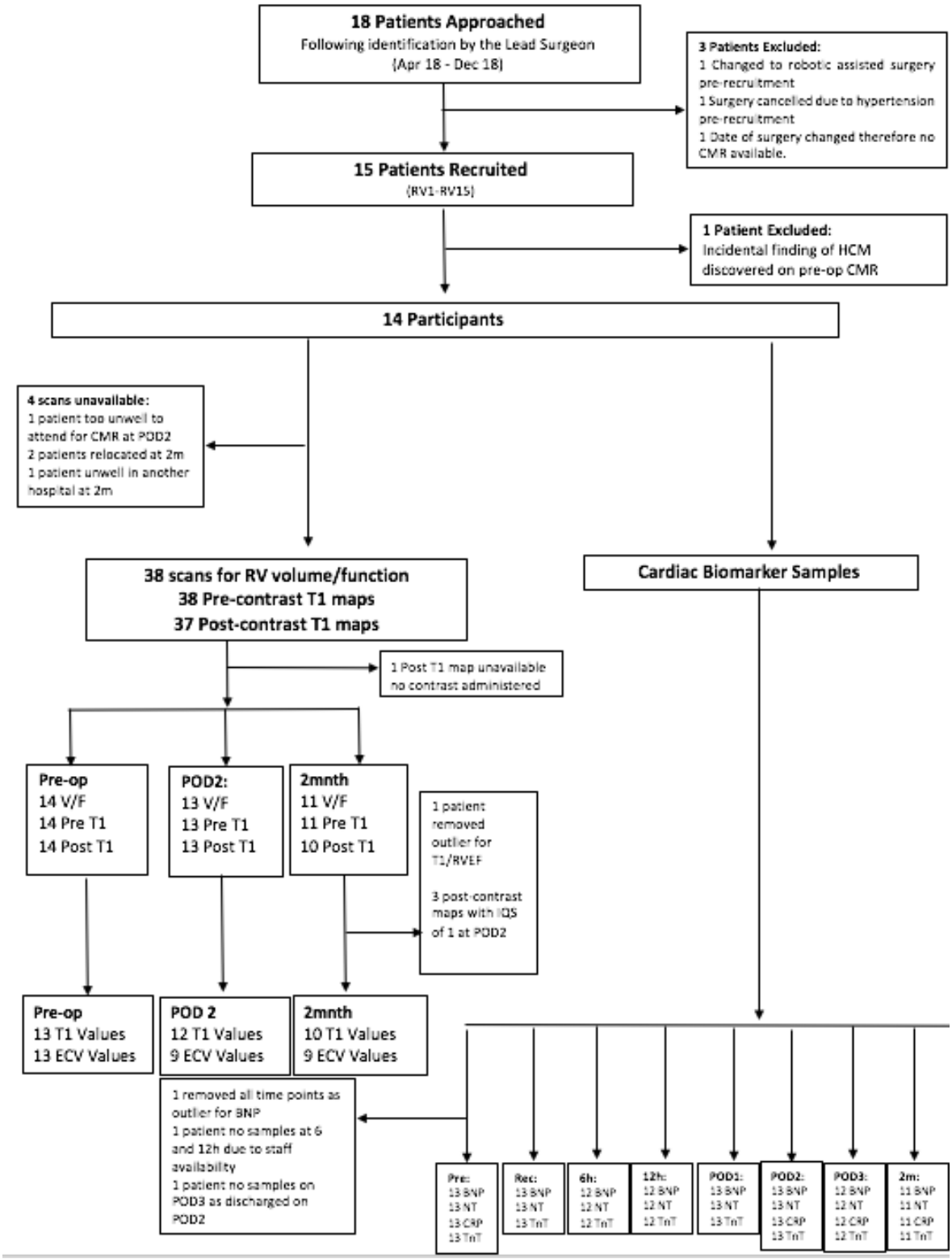

Figure 38 Study Consort Diagram
Apr – April, Dec – December, 18 – 2018, CMR – cardiac magnetic resonance, RV – right ventricle, V/F – volume and function analysis, Pre T1 – pre contrast T1 map, Post T1 – post contrast T1, ECV, extraceullar volume, NT – NT-proBNP, TnT – troponin, Pre – pre-operative, Rec – recovery, 6h – six hours post-operatively, 12h – twelve hours post-operatively, POD – post-operative day, 2m – two months post-operatively.

Demographic	*n*	Descriptive Statistics
Age (years)	*14*	67 (57, 82)
Female Sex	*14*	8 (57%)
Weight (kg)	*14*	73 (18)
Height (cm)	*14*	164 (7)
Smoking Status	*14*	
Current Smoker		4 (29%)
Ex-Smoker		9 (64%)
Never Smoked		1 (7%)
Pack Years History	*13*	43 (20)
Pre-Op Pulmonary Function		
$Sa0_2$ on Air (%)	*14*	95 (95,97)
FEV_1 (L)	*14*	2 (2, 4)
FEV_1/FVC	*14*	74 (62, 86)
%Predicted FEV_1 (%)	*14*	96 (81,111)
DLCO (ml/kPa/min)	*14*	5 (5, 6)
%Predicted DLCO (%)	*14*	70 (59,85)
Co-morbidity		
History of cancer (other than lung)	*14*	1 (7%)
COPD	*14*	4 (29%)
Hypertension	*14*	6 (43%)
Ischaemic Heart Disease	*14*	3 (21%)
Diabetes Mellitus	*14*	2 (14%)
Peripheral Vascular Disease	*14*	1 (7%)
Obesity	*14*	1 (7%)
Alcoholism	*14*	1 (7%)
Left ventricular dysfunction	*14*	1 (7%)
Pre-operative Medication		
Aspirin	14	3(21%)
Ace inhibitor	14	1(7%)
Beta-blocker	14	3(21%)
Calcium Channel Blocker	14	6(43%)
Inhaled Bronchodilators	14	3(21%)
Oral Steroid	14	1(7%)
Statin	14	5(36%)
Non-steroid anti-inflammatory	14	0
ASA Score	14	
1		3 (21%)
2		7 (50%)
3		4 (29%)
Thoracscore (%)	14	2.8 (1, 8)

Table 9 Baseline demographic data.
Values are number (%), mean (SD) or median (IQR) as appropriate.
n represents the number of patients with data available for each parameter.
SaO_2 = percentage arterial oxygen saturation, FEV_1 = forced expiratory volume in 1 second, FVC = forced vitality capacity, DLCO = diffusion capacity for carbon monoxide, COPD = chronic obstructive pulmonary disease, ASA = American Society of Anaesthesiologists.

Fourteen patients underwent lobectomy or bilobectomy (incorporating the right middle lobe and right upper- or lower-lobe); of these, one patient underwent a planned open procedure. All fourteen patients had a diagnosis of primary lung cancer with the operative characteristics described in Table 10. All patients received intravenous induction of anaesthesia and were maintained with Sevoflurane and an infusion of shorting acting opioid Remifentanil.

Characteristic	*n*	Descriptive Statistics
Surgery	*14*	
Lobectomy		13 (93%)
Bilobectomy		1 (7%)
Right sided procedure		7 (50%)
VATS		13 (93%)
No. of segments resected		4 (3, 7)
Anaesthesia	*14*	
Duration of Anaesthesia (mins)		160 (107, 282)
Duration of OLV (mins)		111 (50, 180)
Lung Cancer Stage	*14*	
T1N0		6 (43%)
T1N1		1 (7%)
T1N2		0
T2N0		3 (21%)
T2N1		0
T2N2		1 (7%)
T3N0		2 (14%)
T3N1		1 (7%)

Table 10 Operative data
Values are number (%), mean (SD) or median (IQR) as appropriate.
n represents number of patients with data available for each parameter.
VATS = video-assisted thoracoscopic surgery, OLV = one lung ventilation.

No patients required intensive care unit admission post-operatively and the mean (SD) HDU stay was 25 (24) hours. Median (IQR) hospital stay was 5 (4, 7) days. One patient developed a post-operative arrhythmia (AF) on POD2 which responded to medical management (amiodarone). This patient was deemed, by the study investigator and the medical team, unsafe to attend for the POD2 CMR due to cardiovascular instability. Post-operative clinical data is summarised in Table 11.

Characteristic	*N*	Study Demographics
Analgesia		
Intra-op NSAID	*12*	8 (66%)
Intra-op Dexamethasone	*12*	6 (50%)
Paravertebral Catheter	*14*	13 (93%)
Epidural Catheter	*14*	1 (7%)
Post-op NSAID	*12*	4 (33%)
Fluid Administration (ml)	*14*	
Intra-op		1000 (1000, 2000)
Recovery		100 (0, 200)
Cumulative fluid balance by morning POD1		900(200, 1700)
Vasopressor Requirements	*14*	
Intra-op		2 (14%)
Recovery		0
POD1		0
Arrhythmia	*14*	
Atrial Fibrillation		1 (7%)
Length of Stay	*14*	
HDU (hours)		25 (20, 90)
Hospital (days)		5 (2, 8)
Lung Function	*14*	
ppoFEV1 %		75.8 (18.2)
ppoDLCO%		56.3 (13.9)
Follow-up		
Number attending for post-operative follow-up	*14*	11(79%)
Time from operative day to follow up (Days)	*11*	64 (8.0)

Table 11 Post-operative data
Values are number (%), mean (SD) or median (IQR).
n represents number of patients with data available for each parameter.
NSAID – non-steroid anti-inflammatory, pre-op – pre-operatively, intra-op - intra-operatively, post-op – post-operatively. HDU -high dependency unit. POD - post-operative day, ppoFEV1% = predicted post-operative forced expiratory volume in one second (as a percentage), ppoDLCO% = predicted post-operative diffusion capacity of the lungs for carbon monoxide (as a percentage).

Eleven patients attended for two-month follow-up. Of the three who did not undergo CMR at two-months, one patient had moved to another country, one patient had moved to another part of this country and one was undergoing chemotherapy as an in-patient in another hospital and was too unwell to attend.

All three patients unable to attend the Golden Jubilee Hospital agreed to complete quality of life questionnaires by telephone. Three patients had lung cancer recurrence at one year and one patient died within one year of the study.

From 20th April 2018 to 19th December 2018, 272 patients underwent lung resection at the Golden Jubilee National hospital. This period encompassed the complete study duration. Table 12 demonstrates a comparison of those participating in the study and those not taking part during the study time period. The study sample appear representative of the total lung resection patient population at the Golden Jubilee National Hospital during the study period. The only parameter of note is a difference in length of hospital stay.

Characteristics	Study Participants	Non-Study Participants	p value
Age (years)	67 (57,82) *(n=14)*	67 (56, 84) *(n=272)*	0.95*
Female Sex	8 (57.1%) *(n=14)*	152 (55.9%) *(n=272)*	0.93*
Thoracoscore	0.76(0.57, 7.68) *(n=14)*	1.08(0.11, 9.55) *(n=270)*	0.38*
Right sided procedure	7 (50%) *(n=14)*	171 (63.6%) *(n=69)*	0.23**
Open Procedure	1 (7.14%) *(n=14)*	53 (19.6%) *(n=270)*	0.24**
Hospital length of Stay (days)	5 (2, 8) *(n=14)*	8.5 (2, 184) *(n=247)*	**0.01***

Table 12 Characteristics of study participants and non-study participants undergoing lung resection at the Golden Jubilee National Hospital during the study period.
Values are number (%) and median (IQR).
* Mann-Whitney U-test, **Chi-squared test.
Significant result in bold.
Where the dataset is in incomplete (n) represents the number of patients with data available.

6.2 Functional Status and Quality of Life

Functional status and QoL was assessed using self-reported questionnaires pre-operatively and at two-months post-operatively. All patients completed the questionnaire at both time points. As described in section 6.1 three patients completed the post-operative questionnaire by telephone as they were unable to

attend hospital for their two-month post-operative appointment. The mean (SD) time to two-month follow-up was 64 days (8.0).

6.2.1 Functional Status

Overall, patients reported a reduction in their overall functional capacity and QoL following surgery (Table 13). Patients reported increased WHO-PS compared with preoperative (p=0.02 chi-squared for trend). Patients also reported worsening MRC and NYHA scores, but these did not reach statistical significance (chi-squared for trend, p=0.08 and p=0.06 respectively).

Functional Status	Pre-op *(n=14)*	Post-op *(n=14)*	p-value
WHO-PS Score			
1	10 (71.4%)	2 (14.3%)	
2	2 (14.3%)	7 (50%)	
3	2 (14.3%)	4 (28.6%)	
4	0	1 (7.1%)	0.02
5	0	0	
MRC Score			
1	8 (57.1%)	2 (14.3%)	
2	5 (35.7%)	5 (35.7%)	
3	1 (7.1%)	5 (35.7%)	
4	0	1 (7.1%)	
5	0	1 (7.1%)	0.08
NYHA Class			
I	7 (50%)	2 (14.3%)	
II	5 (35.7%)	5 (35.7%)	
III	2 (14.3%)	7 (50%)	0.06
IV	0	0	

Table 13 Self-reported functional status pre- and post-operatively.
Values are number (%). Chi-squared for trend test comparing change in score from pre- to post-op. Pre-op – pre-operatively, post-op – post-operatively, WHO-PS - World Health Organisation performance status, MRC - Medical Research Council, NYHA - New York Heart Association. Definitions of each score given in Appendix 2, page 240.

There were no associations demonstrated between pre- or post-operative lung function tests and patient reported scoring WHO-PS, MRC, or NYHA (Table 14).

	WHO_PS *(n=14)*	MRC *(n=14)*	NYHA *(n=14)*	GHS *(n=14)*	EQ50 Index *(n=14)*
Pre FEV1% *(n=14)*	r=0.18 p=0.95	r=-0.45 p=0.10	r=-0.36 p=0.20	r=0.44 p=0.11	r=0.36 p=0.21
Pre DLCO% *(n=14)*	r=-0.17 p=0.83	r=-0.33 p=0.24	r=-0.27 p=0.36	r=0.23 p=0.43	r=0.50 p=0.07
ppoFEV1% *(n=14)*	r=-0.03 p=0.92	r=-0.44 p=0.12	r=-0.45 p=0.10	r=0.43 p=0.12	r=0.50 p=0.07
ppoDLCO% *(n=14)*	r=-0.14 p=0.63	r=-0.40 p=0.16	r=-0.35 p=0.26	r=0.21 p=0.47	**r=0.61** **p=0.02***

Table 14 Associations between pre- and post-operative predicted lung function and patient reported outcomes at two-months post-operatively.
Spearman's correlation coefficient. * - significant
PreFEV1% - pre-operative forced expiratory volume in one second as a percentage, PreDLCO% - pre-operative diffusion capacity of the lungs for carbon monoxide (as a percentage), ppoFEV1% - predicted post-operative forced expiratory volume in one second (as a percentage), ppoDLCO% - predicted post-operative diffusion capacity of the lungs for carbon monoxide (as a percentage), WHO_PS – World Health Organisation Performance Status, MRC – medical research council, NYHA – New York Heart Association, GHS – Global Health Score, EQ50 – EuroQOL five dimension scoring tool.

6.2.2 Quality of Life

Quality of life was assessed using the EQ-5D-5L questionnaire with patients ranking each domain individually. Individual domains were analysed for changes from pre-operative reporting. There was an increase in the number of patients describing difficulties with their usual day to day activities at two-months (p=0.01 chi-squared for trend, Table 15). There was no significant increase in the number of patients reporting difficulty with mobility, self-care, pain, or anxiety at two-months (all p>0.10, chi squared for trend, Table 15).

The EQ5D Summary Index was calculated using a specific UK algorithm where each individual EQ5D component is given a value and added to a combined score. Patients reported a lower summary index post-operatively when compared with baseline (Paired t-test, p=0.01, Table 15). There was association between QoL summary index and ppoDLCO% (Spearman's test, r=0.61, p=0.02, Table 14) but this was not associated with any other measure of pre- or predicted post-operative lung function test (Table 14).

The global health score (GHS) is obtained by asking the patient to grade their overall or 'global' health on a visual analogue score from 0-100. A deterioration in GHS was demonstrated at two-months (paired t-test, p=0.01, Table 15). There

was no association between pre-, nor predicted post-operative pulmonary function and post-operative GHS (Table 14).

EQ5D Domain	Pre-op Value	Post-op Value	p-value
Mobility			
1	7 (50%)	6 (42.9%)	
2	4 (28.6%)	2 (14.3%)	
3	3 (21.4%)	6 (42.9%)	
4	0	0	
5	0	0	0.41*
Self-Care			
1	12 (85.7%)	9 (64.3%)	
2	1 (7.1%)	2 (14.3%)	
3	0	2 (14.3%)	
4	0	0	
5	1 (7.1%)	1 (7.1%)	0.43*
Usual Activities			
1	8 (57.1%)	2 (14.3%)	
2	4 (28.6%)	2 (14.3%)	
3	1 (7.1%)	9 (64.3%)	
4	0	0	
5	1 (7.1%)	1 (7.1%)	**0.01***
Pain/Discomfort			
1	6 (42.9%)	3 (21.4%)	
2	4 (28.6%)	4 (28.6%)	
3	3 (21.4%)	6 (42.9%)	
4	0	0	
5	1 (7.1%)	1 (7.1%)	0.57*
Anxiety			
1	11 (78.6%)	7 (50%)	
2	0	4 (28.6%)	
3	3 (21.4%)	2 (14.3%)	
4	0	1 (7.1%)	
5	0	0	0.10*
ED50 SI	0.84	0.73	**0.04****
GHS (0 – 100)	79 (26)	63 (25)	**0.01*****

Table 15 Self-reported quality of life scores pre-operative and post-operatively.
Values are number (%) or mean (SD).
* = chi-squared for trend test for comparison of each domain pre- and post-operatively. ** = paired t-test comparing pre- and post-operative scores, *** = Wilcoxon signed rank test comparing pre- and post-operatively.
Significant results in bold.
EQ5D - EuroQOL 5 Domain Score, EQ5D SI - EuroQOL 5 Domain Score Summary Index, GHS – Global Health Score. Definitions of each domain are given in Appendix 2.

6.3 Cardiovascular Magnetic Resonance Imaging Study Findings

6.3.1 Study Protocol

The study protocol was well tolerated with 13 (93%) patients undergoing CMR at POD2, and 11 (79%) at two-months. One patient was unable to take part on POD2 due to the development of AF with a rapid-ventricular response. The study investigators and the treating medical team felt transfer to CMR would be unsafe. AF with uncontrolled ventricular rate also makes performing and interpretation of CMR difficult. Thirty eight scans were available for analysis; 14 pre-operative, 13 POD2 and 11 at two-months.

6.3.2 Assessment of Reproducibility of Volume and Function

All RV parameters showed excellent intra-observer correlation with intraclass correlation coefficients (ICC, two-way mixed effect model for absolute agreement) >0.90 for all parameters (Table 16). Similarly, all LV parameters showed excellent intra-observer correlation with ICCs >0.98 (data not shown).

	ICC (95% CI)	p-value
RVEF	0.97 (0.63, 0.99)	<0.01
RVSV	0.99 (0.37,0.95)	<0.01
RVEDV	0.90 (0.65, 0.97)	<0.01
RVESV	0.97 (0.92, 0.99)	<0.01

Table 16 Intra-observer reproducibility for right ventricular function.
ICC – intraclass correlation coefficient, two-way mixed model, absolute agreement.
CI – confidence interval. RVEF – right ventricular ejection fraction, RVSV – right ventricular stroke volume, RVEDV – right ventricular end-diastolic volume, RVESV- right ventricular end systolic volume.

6.4 Changes in Cardiac Function

Heart rate increased from baseline on POD2 and at two-months. CO did not show any significant change at POD2 or two-months (Table 17).

6.4.1 Right Ventricular Volume and Function

There was a significant change in RVEF over time (Friedman's test $p<0.01$). Median RVEF decreased from 62% (56, 63) pre-operatively to 52% (45, 59) on POD2 and remain depressed at 51% (45, 58) at two-months (Figure 39 and Table 17). There was an increase in RVEDV and RVESV values post-operatively from baseline, but these did not reach significance (Figure 40 and Table 17).

	Pre-op *(n=14)*	**POD2** *(n=13)*	**2mnth** *(n=11)*	**p-value**
HR	73 (12)	81 (8) †	82 (8) †	0.02*
CO	5.1 (1.5)	5.5 (1.3)	5.2 (1.2)	0.46
RVEDV	126 (111, 155)	134 (116,160)	141 (116,156)	0.24
RVESV	52.0 (48, 64)	63.1 (57, 84)	62.7(53, 79)	0.12
RVSV	73 (56, 89)	75 (56, 86)	77 (48,83)	0.26
RVEF	62 (56, 63)	52 (45, 59) †	51 (45, 58) †	<0.01*
LVEDV	148 (81)	124 (68)	129 (66)	0.46
LVESV	71 (16)	69 (18)	65 (16)	0.90
LVSV	78(68, 90)	77 (65, 91)	70 (61, 83)	0.26
LVEF	59 (14)	59 (12)	59 (13)	0.90

Table 17 Changes in cardiovascular magnetic resonance parameters over time
Values are mean (SD) or median (IQR) as appropriate. † = significant difference from pre-op.
* = one-way repeated measures of ANOVA, ** = Friedman's test,
HR = heart rate, CO = cardiac output, RV = right ventricle, LV = left ventricle, EDV = end-diastolic volume, ESV = end-systolic volume, SV = stroke volume, EF = ejection fraction.

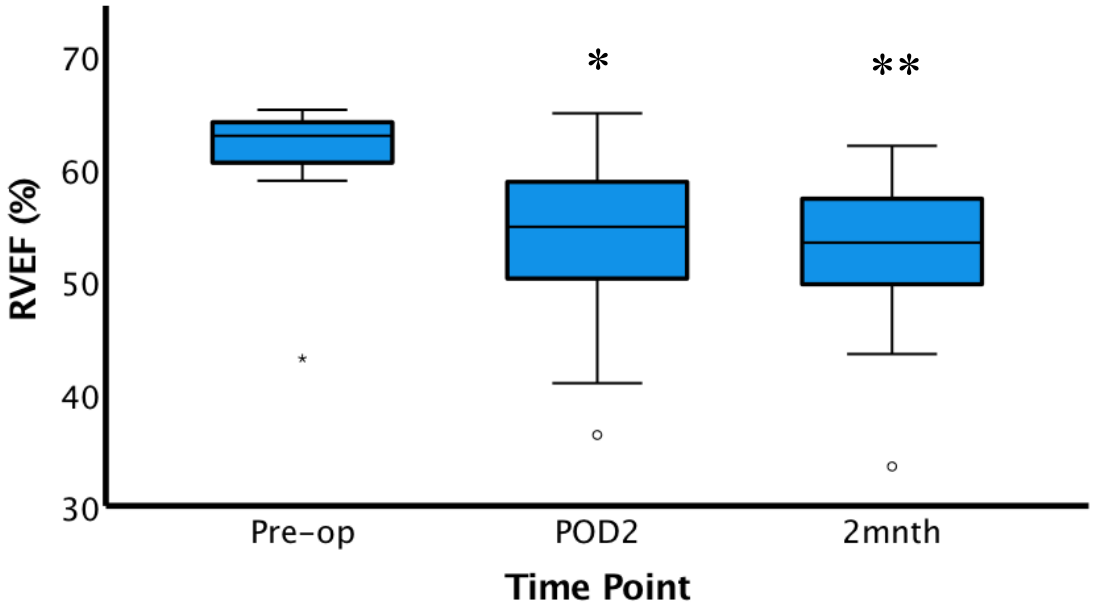

Figure 39 Change in right ventricular ejection fraction over time
Boxes (error bars) represent median (IQR).
Change over time assessed by Friedman's'. Pairwise comparison made with Wilcoxon signed ranked test. * p=0.02. ** p=0.03. versus pre-op
RVEF – right ventricular ejection fraction. Pre-op – pre-operative, POD – post-operative day. 2mnth – 2 months post-operatively.

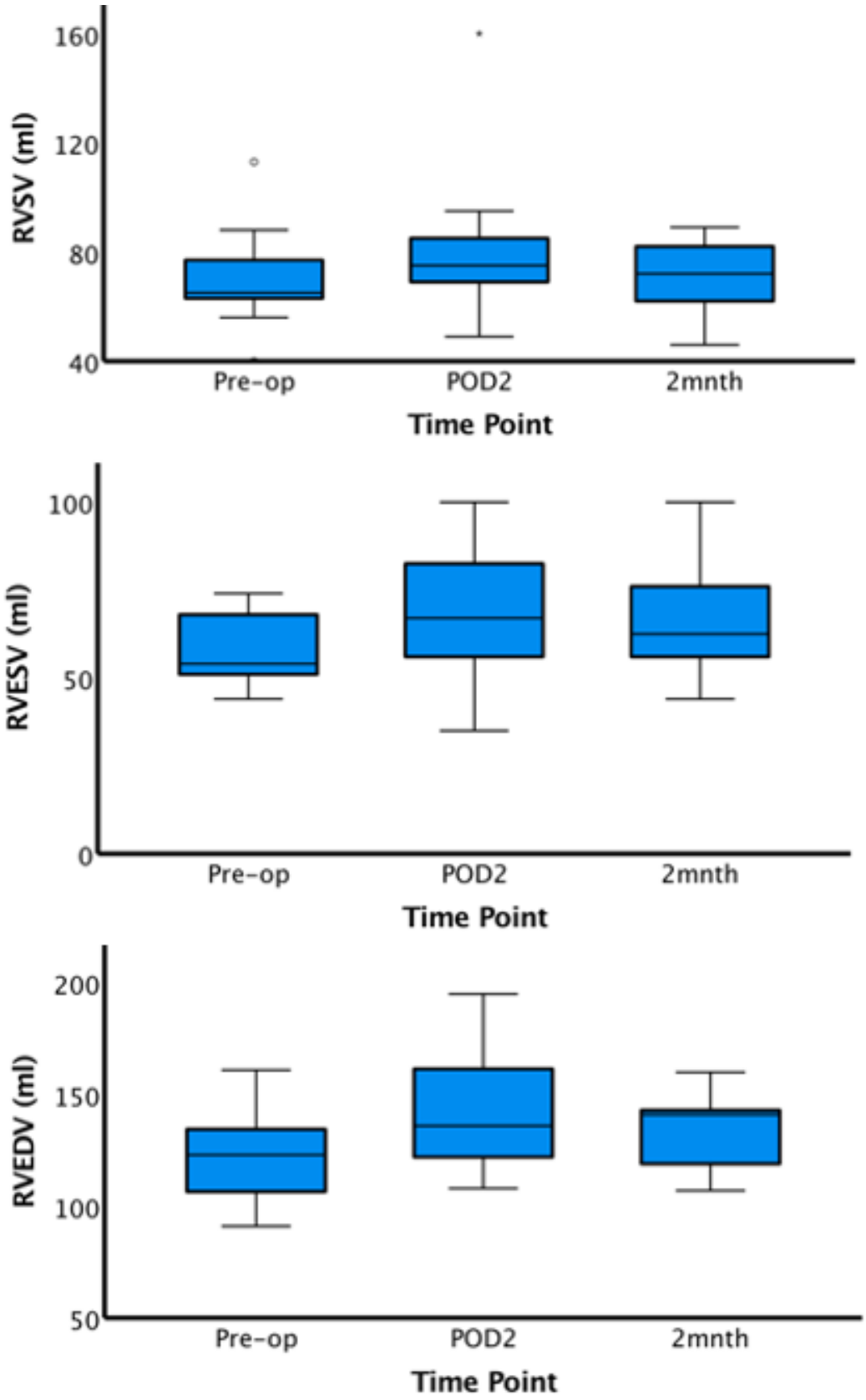

Figure 40 Change in right ventricular volumes over time.
Bar (error bars) represent median (IQR). No statistically significant changes.
RVSV – right ventricular stroke volume, RVESV – right ventricular end-systolic volume, RVEDV – right ventricular end diastolic volume, ml – millilitres. Pre-op – pre-operative, POD2 – post-operative day two, 2mnth – 2 months post-operatively.

On visual inspection of the data, there was an outlier (RV2) identified as the lowest RVEF by the author at all three time-points (Figure 41). On further analysis of this patient's data, it appeared that they were also an outlier for native T1 values (described in Chapter 8) and changes in cardiac biomarkers (described in Chapter 9). As a result, a sensitivity analysis was performed without this patient for change in RV function and volumes over time. A significant reduction in RVEF was still demonstrated (Table 18 and Figure 42).

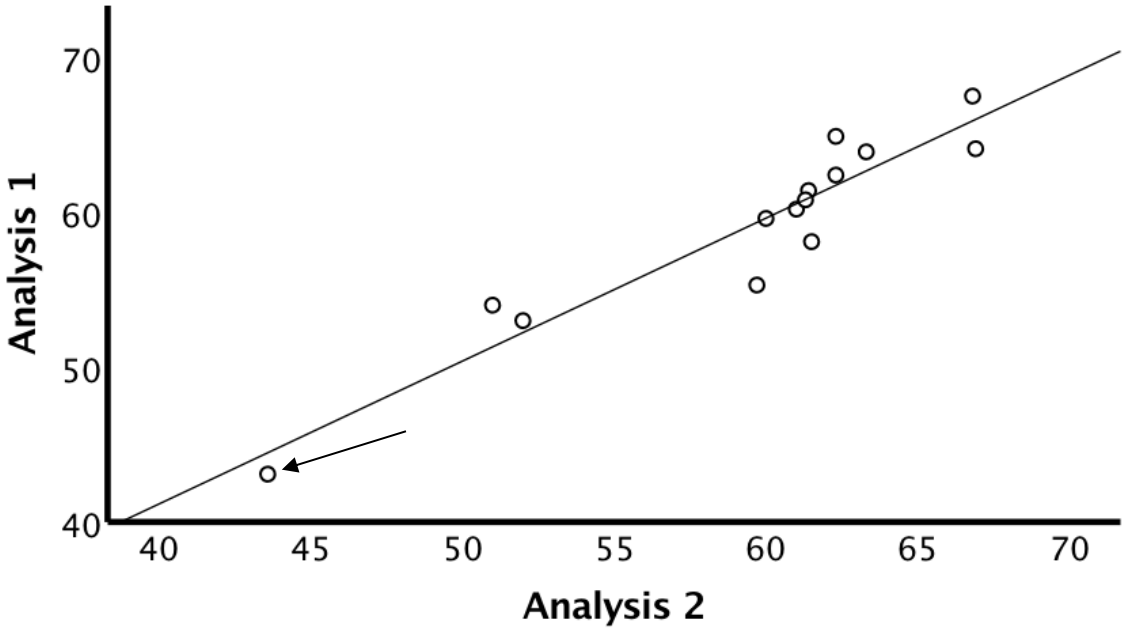

Figure 41 Association of pre-operative right ventricular ejection fraction and delta right ventricular function
Arrow indicates outlier. Spearman's correlation coefficient.
RVEF – right ventricular ejection fraction, ∆RVEF = change in right ventricular ejection fraction from baseline to post-operative day two.

	Pre-op *(n=13)*	POD2 *(n=12)*	2mnth *(n=10)*	p-value
RVEDV	126 (111, 143)	143 (126, 160)	138 (122, 155)	0.29
RVESV	54 (51, 65)	67 (55, 80)	63(54, 78)	0.26
RVSV	65 (60, 81)	75(63, 98)	72 (60, 81)	0.23
RVEF	61 (57, 64)	52(48, 57) †	52 (46, 57) †	<0.01*

Table 18 Changes in cardiac magnetic resonance parameters over time without outlier.
Values are median (IQR).
Friedman's' test. † - significant difference from pre-op. * denotes significance.
RV – right ventricle, EDV – end-diastolic volume, ESV – end-systolic function, SV – stroke volume, EF – ejection fraction, Pre-op – pre-operative, POD2 – post-operative day two, 2mnth – two-months post-operatively.

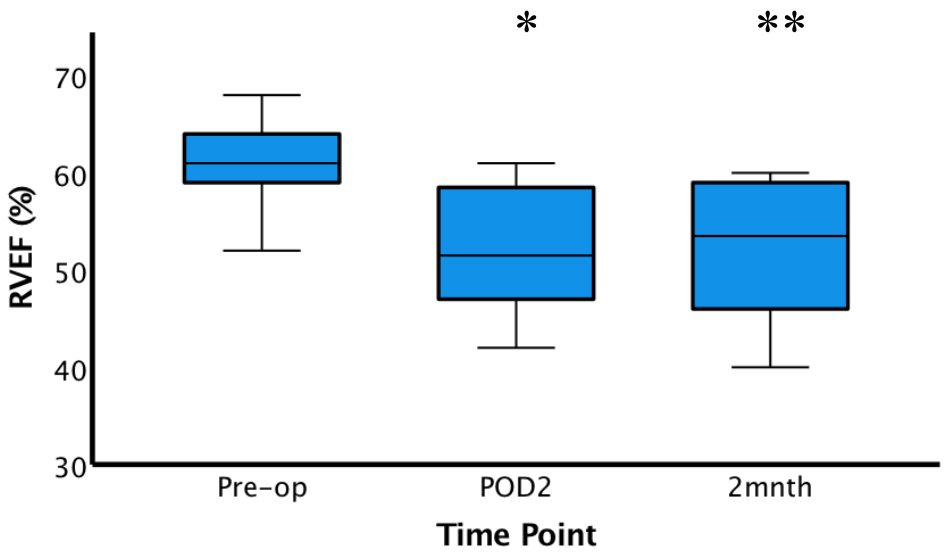

Figure 42 Change in right ventricular function over time with outlier removed
Bars (error bars) represent median (IQR).
Change over time assessed by Friedman's p <0.01. Pairwise comparison made to pre-operative values with Wilcoxon signed ranked test. * p = 0.02. ** p = 0.03.
RVEF – right ventricular ejection fraction. Pre-op – pre-operative, POD – post-operative day. 2mnth – 2 months post-operatively.

6.4.2 Left Ventricular Volume and Function Over Time.

There was no significant change in LVEF over time (One-way repeated measures ANOVA, p=0.90, Figure 43). Similarly, there was no change in LV- EDV, ESV or SV over time (Table 17). On visual inspection of the data, one patient was noted to be an outlier at all three time points for low LVEF (data not shown) and was known pre-operatively to have pre-existing LV dysfunction.

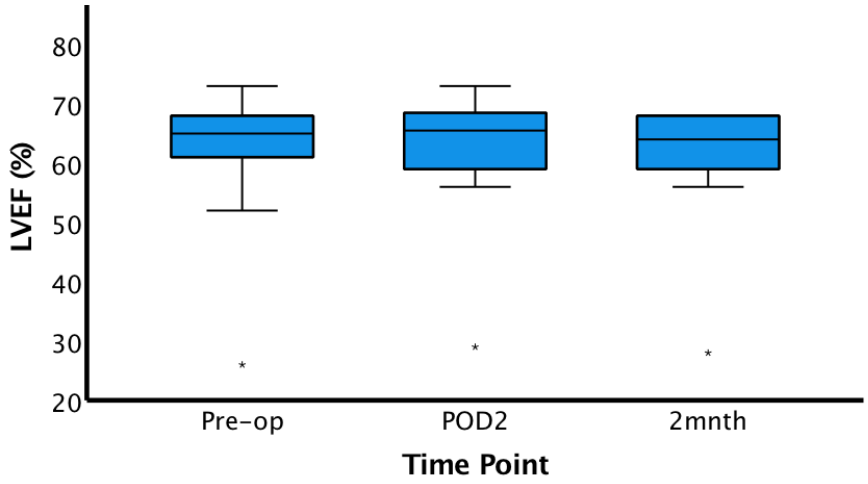

Figure 43 Change in left ventricular function over time
Bar represents median (IQR). No statistically significant change.
LVEF – left ventricular ejection fraction, Pre-op – pre-operative, POD – post-operative day. 2mnth – 2months post-operative.

6.5 Discussion

This study recruited 15 patients to examine the role of RV inflammation after lung resection with 14 patients included for image, biomarker and patient reported functional outcome analysis. The study protocol was well tolerated both pre-operatively and at POD2, with three patients unable to attend for their two-month follow-up. Despite their non-attendance, there was still 100% questionnaire completion rate at two-months. On analysis of the CMR data, one patient appeared as a significant outlier for pre-operative RVEF and as a result, data presented for RV function and volume over time also includes a sensitivity analysis.

The cohort of patients recruited to the study were representative of the those undergoing lung resection surgery at the Golden Jubilee National Hospital during the study period, suggesting this study population is representative of the lung resection patient population within the West of Scotland and limits the risk of selection bias in this study findings. Hospital length of stay did differ between both groups with the study group demonstrating a statistically shorter hospital stay. The data provided for all patients undergoing lung resection during the study time period records only the length of stay in days but does not provide information regarding the reasons for a prolonged length of stay. As described in Chapter 5, in this study I defined length of stay from the day of operation, the

same time frame will not have been used in data collected from the lung cancer patient population as it will begin from the day of admission to hospital and may impact the results shown.

This study demonstrates a significant decrease in RV cardiac function following lung resection surgery, both on post-operative day two and two-months. These findings are consistent with results from the same thoracic centre who reported the first CMR study of RV dysfunction following lung resection surgery[81]. In keeping with our studies, there was no change in LV function during the study time period[81]. Of note, one patient was noted to be an outlier for LVEF on visual inspection of the data, however, this patient was known to have LVEF pre-operatively. Patients with multiple co-morbidities were included in the study and therefore this patient remained within the study despite being an outlier for LVEF.

A decrease in functional capacity is demonstrated with the subjective WHO-PS, MRC-DS and the NYHA classification scoring systems. An MRC score of three or more is considered to indicate severe disability as a result of dyspnoea. Half of the study patients report a post-operative MRC score of three or more compared with only one pre-operatively. A smaller proportion of patients reported a worse WHO-PS and NYHA score at two-months. The decline in functional capacity following lung resection has been well described in other studies with the results of this study consistent with those previously reported. [74 81 114]

A significant decrease in the ability to perform day-to-day usual activities is reported at two-months, with a trend towards an increase in difficulties with mobility and self-care, but not to a significant level. Patients did report a significant change in their overall health score at two-months. The deterioration in ED50 Summary Index score by two-months (from 0.84 to 0.73) is considered statistically significant but is also likely to be clinically significant based on minimally clinically important difference (MCID) grading.[324-326] The MCID has been defined as the smallest change in a patient reported outcome that is perceived by patients as clinically significant.[325] In lung cancer, the MCID for the ED50 Summary Index has been reported between 0.08 and 0.16 with a mode of 1.0.[325] The reported change in ED50 summary Index in this study falls within this range and therefore may be considered clinically significant. These trends are in

keeping with a decline in health-related QoL demonstrated in other work.[74 81 114 116]

This study demonstrates no association between pre-operative or post-operative predicted lung function and patient reported outcomes, with inconsistent associations between pulmonary function and post-operative patient reported function. The lack of consistent association between post-operative pulmonary function and post-operative functional status and QoL further supports the hypothesis that changes following lung resection are not solely due to respiratory status and other factors, such as cardiovascular function, need to be considered.

6.6 Strengths and weaknesses

A strength of the study is the use of the reference method for assessing cardiac volumes, CMR. The excellent ICC (>0.9 for all parameters) reported in both measurement of the RV and LV is consistent with previous CMR studies .[327 328] Despite this, studies describing the use of CMR to explore cardiac function in this patient population are lacking, with the current study being only the third to utilise CMR to assess heart function following lung resection.[81 168] A further strength of this study is the serial measurement of myocardial function over three peri-operative time points, with it being only the second CMR to utilise serial measurements.[81] The main finding of this chapter, the decrease in RV function post-operatively following lung resection, is consistent with both human and animal studies assessing RV function after lung resection.[81 145 147 148 211]

The study protocol was well tolerated by patients throughout confirming similar to previous work from our research group, that performing CMR imaging of the myocardium is feasible in the immediate post-operative period and is able to provide accurate and reproducible reporting of myocardial function after lung resection.[81] Despite patients being unable to attend the hospital in person for follow-up, a strength of the study was the ability to complete patient reported questionnaires to allow for a complete comparison in all 13 patients at two time points. As the results have shown, the importance of asking and reporting patient reported outcomes following lung resection surgery can give an insight into the impact of surgery on patients' and their day to day lives.

A weakness of the study is the missing data, primarily at two-months post-operatively and as a result the findings reported from POD2 may therefore be more robust in comparison to those reported from two-months. In this thesis, I opted to not remove patients with missing data as this would limit the number of participants in this small study with loss of significant amount of data and loss of power (as discussed in section 5.2.6, page 118). It is likely the missing data is as a result of 'missing data completely at random'[313]. The small sample size combined with multiple comparisons of pulmonary function and functional outcomes as well as loss of data at two months make the findings described at high risk of a type 1 error.

6.7 Conclusion

This chapter describes the generic results of the study examining the RV inflammatory response to lung resection. Fifteen patients were recruited to the study with one patient removed prior to analysis due to an incidental finding of hypertrophic cardiomyopathy. The study reports a reduction in RVEF in the early peri-operative period which persists two-months post-operatively, consistent with previous observations. The decline in functional status following lung resection demonstrated in this study are confirmatory of previous studies in the lung resection patient population and highlight the impact of surgery in the post-operative period.

Chapter 7 – Feasibility and Reproducibility of T1 Mapping in Lung Resection Surgery

7.1 Introduction

This chapter describes feasibility and intra- and inter-observer reproducibility of T1 CMR mapping of the myocardium following lung resection surgery. Feasibility and reproducibility are assessed at all three time points with both pre- and post-contrast images analysed. Data from both regenerated and Siemens T1 maps is also reported (as described in Chapter 5).

7.2 Feasibility of T1 mapping

7.2.1 Assigned Image Quality Scores

Thirty-eight scans were available for pre-contrast analysis (14 pre-operatively, 13 POD2 and 11 at two-months post-operatively) and 37 scans for post-contrast analysis (14 pre-operatively, 13 POD2 and 10 at two-months post-operatively). One patient inadvertently received subcutaneous rather than intravenous contrast and therefore no post-contrast T1 image was produced. Image Quality Scores (IQS) of one, two or three (described in Chapter 5, Table 8 and Figure 32) were assigned to all scans on both the regenerated maps and the Siemens generated maps respectively (as described in Chapter 5).

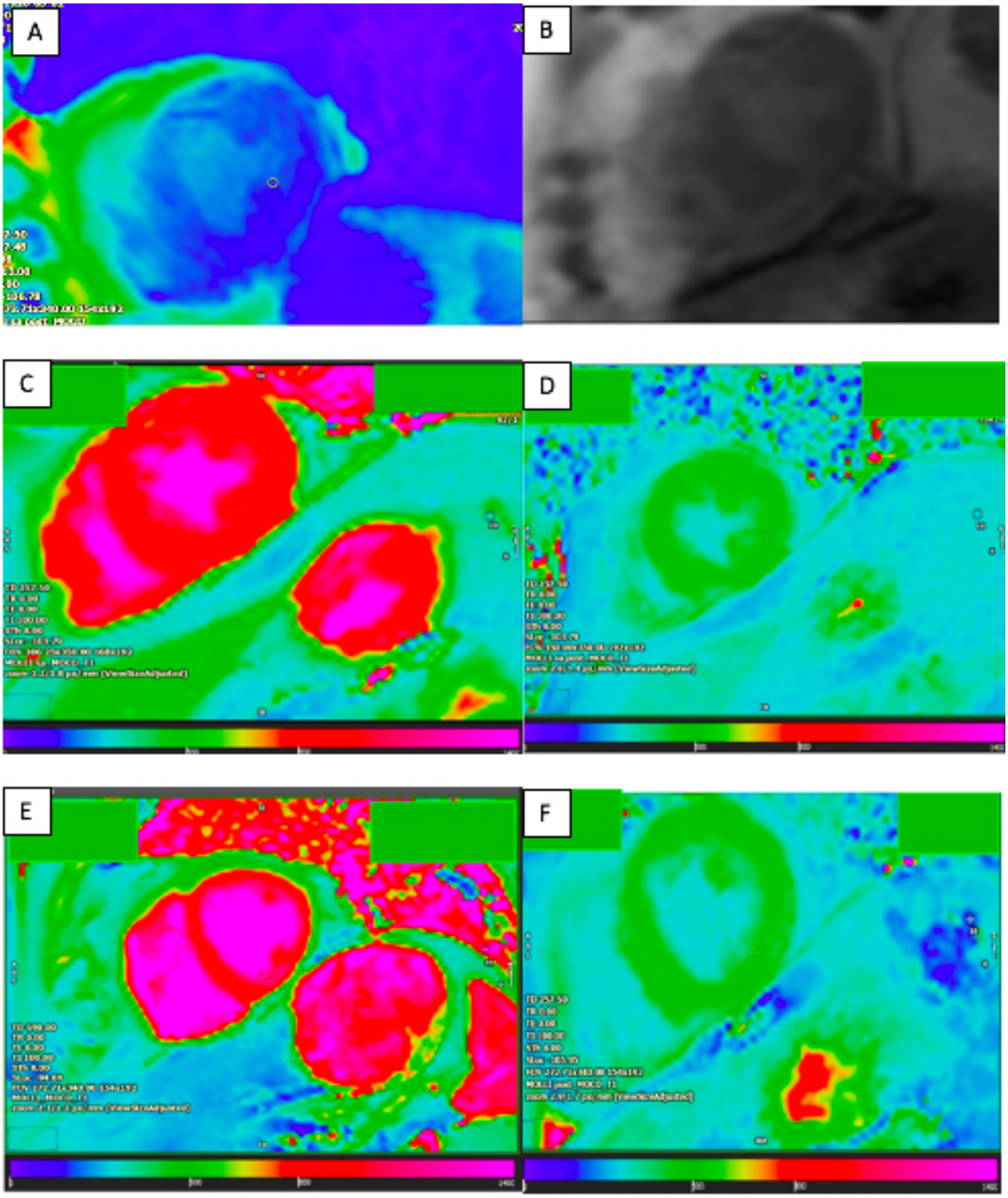

Figure 44 Examples of pre- and post-contrast maps with image quality scores one to three. Image A is the post-contrast regenerated T1 map from a CMR performed on POD2. Note the poor image quality with difficulties defining the epicardial and endocardial borders and therefore inability to define regions of interest within the myocardium. Image B is an individual image slice from the T1 map sequence from the same patient. This is combined with multiple images to produce the T1 map shown in image A. Pre-contrast (C) and post-contrast (D) images are taken from a patient at two-months post-operatively. In comparison to the image shown in A and B, the epicardial and endocardial borders are present, and it is possible to define regions of interest within the myocardium. Pre-contrast (E) and post-contrast (F) images are taken from a patient pre-operatively. Images E and F demonstrate clear epicardial and endocardial borders with the ability to clearly define regions of interest within the myocardium.

7.2.1.1 Regenerated Maps

Mean (SD) IQS for the pre-contrast regenerated image was 2.5(0.6) and 2.3(0.7) for post-contrast images. No pre-contrast regenerated image was assigned a value of one. Three regenerated post-contrast maps had an IQS of one and were removed from further T1 analysis (Figure 45). This meant 38 (100%) pre contrast regenerated images had an IQS of two or more and were deemed suitable for analysis, as were 34 (92%) post-contrast images. All three images assigned an IQS of one were performed at the POD2 time-point.

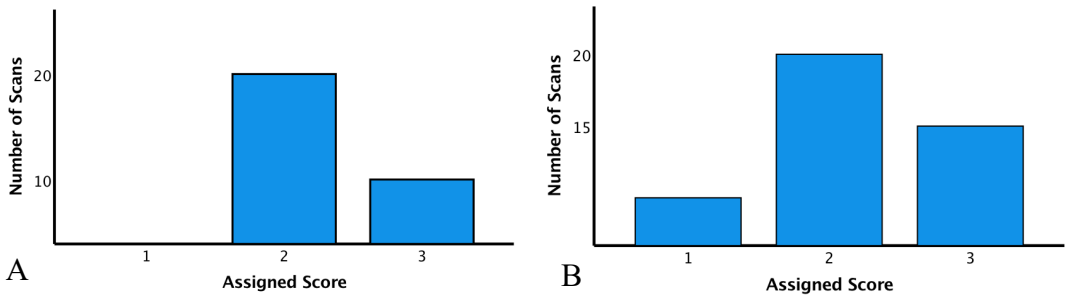

Figure 45 Pre (A) and post contrast (B) regenerated Image Quality Scores.

7.2.1.2 Siemens Generated Maps

Six pre-contrast and five post-contrast Siemens generated scans had an IQS of one (Figure 46). Mean (SD) IQS for pre-contrast Siemens generated maps was 2.3 (0.6) and 2.2 (0.7) for post-contrast. Thirty-two of 38 (84%) pre- and post-contrast Siemens generated images had an IQS of two or more and would be suitable for T1 map analysis.

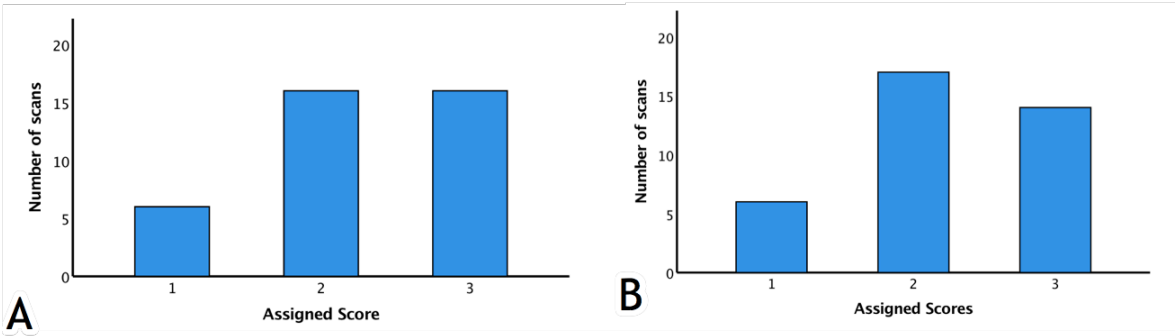

Figure 46 Pre (A) and post-contrast (B) Siemens generated Image Quality Scores

7.2.1.3 Comparison of Regenerated and Siemens Generated Map Scores

Higher quality pre-contrast T1 maps were produced with regenerated maps compared with Siemen's generated (median IQS 2.5 versus 2.3, t-test p=0.03). A similar, non-significant trend was observed post-contrast (IQS 2.3 versus 2.2, t-test p=0.08).

7.2.1.4 Reproducibility of Assigned Image Quality Scores

A second observer analysed ten anonymised scans and assigned each pre- and post- contrast image an IQS score. Of the ten, five were pre-operative images, and five were post-operative (two POD2 and three two-months post-operatively). Ten pre-contrast and 9 post-contrast images had an IQS of two or more. The ICC score for agreement (two-way mixed model, absolute agreement) was 0.89 (0.75, 0.93, p<0.01).

7.3.2 Feasibility by Regions of Interest

It was possible to identify a ROI in the LV free wall, septum, and superior and inferior ventricular insertion point (VIP) in all scans with an IQS of two or more. It was only possible to measure T1 in the RV free wall in two of the 38 pre-contrast scans and not possible in any of the 37 post-contrast scans. When attempting to draw a ROI in the RV, the thin free wall made it difficult to define an appropriate sized area that did not include blood pool (Figures 47).

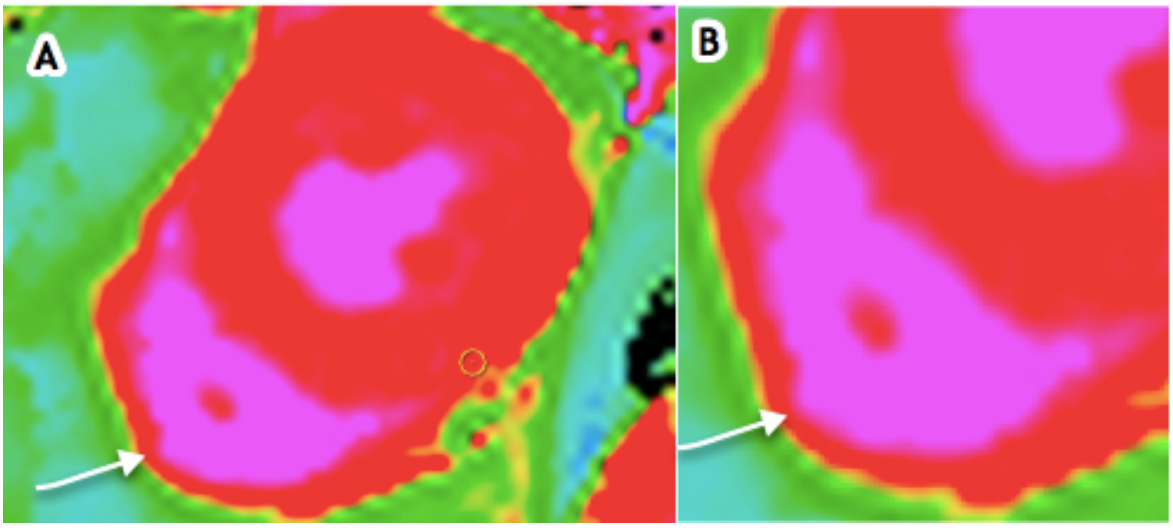

Figure 47 Example of the thin right ventricular free wall on T1 map
The pre-contrast images are both taken from a patient pre-operatively. Image A shows the complete right ventricle. Image B is a close up of image A highlighting the thin free wall of the right ventricle making it impossible to define a ROI in RV free wall without risk of including of including blood pool unlike those seen in the septum and VIP.

7.3 Reproducibility of T1 measurements

7.3.1 Intra-observer Reproducibility

All available randomised blinded scans underwent analysis by the author on two separate occasions more than a month apart. Excellent intra-observer reproducibility was demonstrated in the three areas of the myocardium (RVIP, septum and LV wall) at all time points, and both pre- and post-contrast (ICC >0.9 for all, two-way mixed model, absolute agreement, Table 19).

Parameter	ICC (95% CI)	p-value
Native VIP		
Pre-op	0.96 (0.89, 0.99)	<0.01
POD2	0.94 (0.25, 0.98)	<0.01
2months	0.97 (0.91, 0.99)	<0.01
Post-Contrast VIP		
Pre-op	0.92 (0.76, 0.97)	<0.01
POD2	0.93 (0.76, 0.97)	<0.01
2months	0.98 (0.88, 0.99)	<0.01
Native Septum		
Pre-op	0.97 (0.90, 0.99)	<0.01
POD2	0.99 (0.98, 0.99)	<0.01
2months	0.99 (0.98, 0.99)	<0.01
Post-Contrast Septum		
Pre-op	0.97 (0.92, 0.99)	<0.01
POD2	0.99 (0.98, 0.99)	<0.01
2months	0.97 (0.73, 0.99)	<0.01
Native LVFW		
Pre-op	0.97 (0.91, 0.99)	<0.01
POD2	0.97 (0.91, 0.98)	<0.01
2months	0.97 (0.90, 0.99)	<0.01
Post-Contrast LVFW		
Pre-op	0.91 (0.76, 0.94)	<0.01
POD2	0.98 (0.95, 0.99)	<0.01
2months	0.98 (0.92, 0.99)	<0.01

Table 19 Intra-observer variability for T1 at all time points
ICC calculated as two-way mixed effect, absolute agreement.
ICC – intraclass correlation coefficient, CI - confidence interval, Pre-op – pre-operative, POD2 – post-operative day two, VIP – ventricular insertion point, LVFW – left ventricular free wall.

7.3.2 Inter-observer Reproducibility

Ten randomly chosen blinded and anonymised scans were analysed by a second observer. Excellent inter-observer reproducibility was demonstrated in five of the six parameters examined (two way mixed model, absolute agreement, Table 20 and Figures 48-49). Post contrast VIP had very good reproducibility with an ICC of 0.86 (p=0.01, two way mixed model, absolute agreement, Table 20).

Parameter	ICC (95% CI)	p-value
Pre-contrast VIP	0.92 (0.63, 0.97)	<0.01
Post-contrast VIP	0.86 (0.74, 0.97)	0.01
Pre-contrast LV	0.90 (0.65, 0.97)	<0.01
Post-contrast LV	0.97 (0.86, 0.99)	<0.01

Table 20 Inter-observer reproducibility for T1
ICC calculated as two-way mixed effect, absolute agreement.
ICC – intraclass correlation coefficient, CI - confidence interval, Pre-op – pre-operative, POD2 – post-operative day two, VIP – ventricular insertion point, LV – left ventricle.

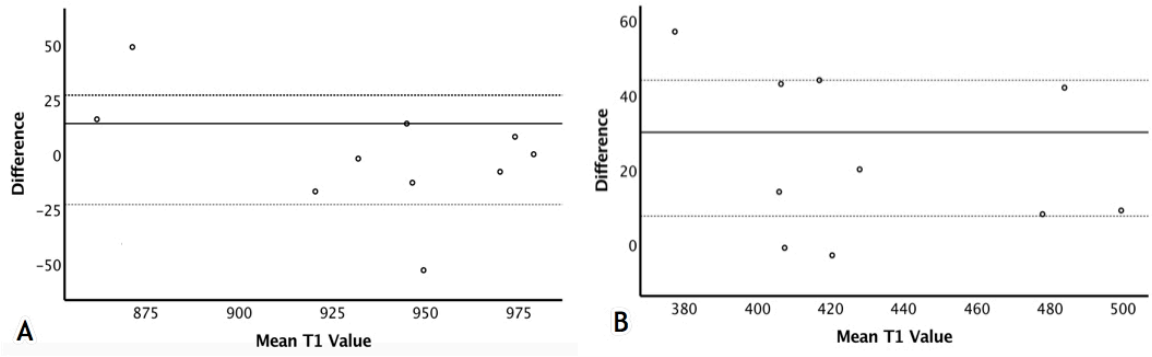

Figure 48 Bland-Altman plot of inter-observer reproducibility for pre- and post-contrast right ventricular insertion point T1 values.
A – Pre-contrast T1 values. B – post- contrast T1 values. Solid line in Graph A represents mean bias (7ms) and dashed lines in Graph A represent 95% limits of agreement (-22, 26ms). Solid line in Graph B represents mean bias (28ms) and dashed lines in Graph B represent 95% limits of agreement (-11, 41ms).

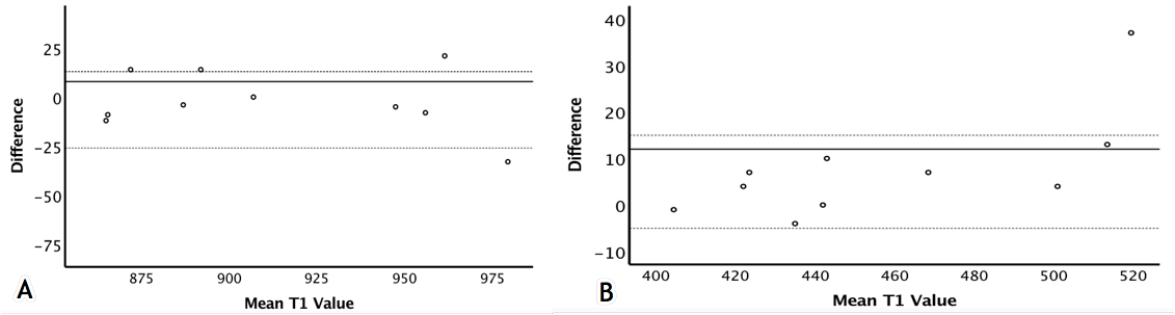

Figure 49 Bland-Altman plot of inter-observer reproducibility for pre- and post-contrast left ventricular free wall T1 values.
A – Pre-contrast T1 values. Solid line in Graph A represents mean bias (8ms) and dashed lines in Graph A represent 95% limits of agreement (-26, 9ms). Solid line in Graph B represents mean bias (11ms) and dashed lines in Graph B represent 95% limits of agreement (-5, 16ms).

7.4 Discussion

This is the first study to measure myocardial T1 in patients undergoing lung resection surgery. It demonstrates pre- and post-contrast T1 measurement is feasible in this cohort.

In this thesis, I used a one to three image quality grading system, similar to other image quality scores described for T1 and ECV maps[329-332]. A large proportion of the scans in this study were assigned an IQS of two or more and were therefore suitable for T1 map analysis. The number of scans removed from analysis are in keeping with other studies[333-337]. Other studies in the literature have also described poorer image quality in post-contrast T1 maps, with Garcia-Alvarez et al reporting 11% of their scans were removed due to a poor quality post-contrast image. Similarly in this thesis, four percent of post-contrast scans were removed as a result of an IQS of one[329 333].

Studies in the literature report measuring T1 values in either automatically generated T1 maps[338-342] (described as Siemens generated maps in this study) and maps regenerated following analysis of each individual MOLLI generated raw T1 image or slice[333 334 343-345]. In this study, I assigned IQS to both maps; regenerated T1 maps were assigned a higher IQS compared with Siemens generated maps. Going forward, I have elected therefore to describe the results of T1 analysis performed on regenerated maps due to the higher image quality, as this technique will aid in reducing the influence of artefact on measured T1 values.

In the small group of T1 maps assigned an IQS of one, these all occurred during the second CMR scanning time-point. This occurred at POD2 or three and is therefore unsurprising as image quality is likely to be affected by a number of factors related to lung resection surgery including the ability to breath-hold adequately in the immediate post-operative period, the presence of chest drains, and the likely shift of the mediastinum within the chest wall following removal of pulmonary segments. In the only other serial RV function CMR study following lung resection, reproducibility was affected in the post-operative period[81].

This study demonstrated both excellent intra- and inter-observer reproducibility for measuring both pre and post contrast T1 in a range of areas within the myocardium (ICC >0.86 for all comparisons and parameters) further supporting its suitability for measuring myocardial tissue characteristics in patients post lung resection and comparing well to values described in other populations. In other studies measuring T1, intra-class reproducibility has been reported ranging from 0.82-0.96 for the VIP[336 345], 0.84-0.96 for the septum[345 346], and 0.79-0.89 for the LV[345 347]. Inter-class reproducibility ICC have been reported ranging from 0.73-0.93 for the VIP[333 336 345 348], 0.84-0.96 for the septum[345 346 348 349] and 0.62-0.91for the LV [345 346].

I was unable to perform T1 analysis in the RV free wall as it was a thin-walled structure and therefore prone to generating spurious T1 values due to the inclusion of the blood pool and myocardium. In the patient group, the RV wall typically measured less than five mm (as expected in normal RV myocardium)[350].The standard operating procedure (SOP) for measuring ROI within the myocardium in this thesis did not dictate a certain size of ROI should be drawn each time. Instead, as in keeping with other studies, both observers aimed to draw the largest ROI possible without including blood pool[342]. It is unsurprising that both observers were unable to draw ROI within the RV wall, as one third of the images in this thesis were taken pre-operatively in patients with relatively healthy hearts. This is in keeping with other studies who have demonstrated difficulties when attempting, or who have opted not to measure T1 in a comparatively normal RV[285 319 329 351 352].

Kawel-Bohen et al were able to measure T1 in the RV free wall in a group of healthy volunteers[342]. By altering their scanning protocol to acquire T1 maps only during systole (when the RV myocardium thickens and so provides a larger target), they were able to successfully draw ROIs in the RV free wall in 10 of their 18 patients in the short axis (SA). The average size of ROI in the study by Kawel-Bohen et al measured 0.42 +/- 0.28cm^2 [342]. Despite similarly altering the CMR scanning protocol to include the acquisition of T1 maps during systole only, a small number of images were incidentally acquired during diastole and in those maps obtained in systole both obervers were still unable to draw ROI in the RV free wall in the majority of cases[342]. Of note, in the study by Kawel-Bohen et al the T1 measured in the RV wall of normal healthy subjects was significantly

higher than that measured in the LV (956+/-25ms versus 1016+/-61ms, $p<0.001$)[342]. The authors suggest this may be as a result of the increased collagen content of the normal RV myocardium. In other studies, where the RV T1 value has been higher than the LV, authors have acknowledged the value may be higher as a result of inadvertent inclusion of blood pool[338 353].

Difficulties have also been demonstrated in measuring a ROI in the RV of patients with lower BMI. In a healthy volunteer study, ROIs could not be drawn on some patients with a lower BMI[342]. There is a linear correlation between BMI and RV myocardial mass, and this may explain in part some of the difficulties encountered in obtaining RV free wall measurements as almost 50% of this study patients had a low BMI (18.5kg/m^2 or less as per the WHO BMI classification)[354 355].

A group of studies have successfully measured T1 and ECV values in the RV free wall in patients with PH; however it should be noted in patients with PH the RV myocardium is thickened due to chronic RV pressure overload[319 334 335 343 344 346 349 356 357]. A thickened RV allows for a ROI to be drawn within the myocardium without including partial volume artifact unlike those with a thin-walled RV. Habert et al describe measuring a RV wall ROI in their study when RV wall thickness was at least ten times than of the ROI; in my patient population with RV wall thickness of less than five 5mm, both observers were unable to draw a ROI of adequate size[334]. Other studies measuring either T1 or ECV in PH have opted not to measure the RV free wall due to the thin myocardium despite a diagnosis of PH[333 336 345 348].

Of the nine studies successfully reporting the measurement of T1 or ECV in the RV wall, the majority used either higher spatial resolution (two studies used a MOLLI technique on a 1.5T scanner but with either a higher resolution sequence[335] or a novel sequencing technique named accelerated and navigator-gated look-locker imaging [ANGIE][356]) or a higher field strength (two used a 3T scanner[349 357] and one a 9.4T scanner[344]). Of note, Patel et al measured T1 in the horizontal long axis (HLA) and not the SA[335]. Despite a number of studies utilising a commonly used MOLLI sequence, there are a magnitude of sequence parameters within each MOLLI sequence which may differ from study to study including scanning features such as flip angle, inversion and recovery times and

spatial resolution as well as patient factors such as HR and ability to adequately breath hold[358]. These parameters could therefore affect the reporting of T1 and ECV values and should be taken into consideration when making comparisons between studies. Those studies measuring values in the RV free wall reported inter-class correlations both pre and post-contrast ranging from 0.75-0.95 and 0.8-0.94 respectively[335 346 349 356].

Consistently in the literature, T1 or ECV have been measured in RVIP in patients with PH either with or without measurements in the RV free wall[319 333 336 343-346 348 349 357]. The insertion points have also been used in other disease processes other than PH, with alteration in values associated with markers of RV dysfunction[359-361]. It is proposed that the initial increase in afterload leads to mechanical stress with paradoxical septal motion and subsequent changes within the VIPs[344 362 363]. Garcia-Alvarez et al performed histological analysis of myocardial tissue taken from the RVIP in an animal model of PH as well as CMR examination of the myocardium[333]. The RVIP in animals with PH showed an increased percentage of interstitial collagen deposits associated with fibre disarray within the myocardium (44.5 ± 5.5% of the RVIP myocardium containing deposits in PH vs. 26.5 ± 7.5% RVIP myocardium containing deposits in sham; $p < 0.05$, Figure 50).

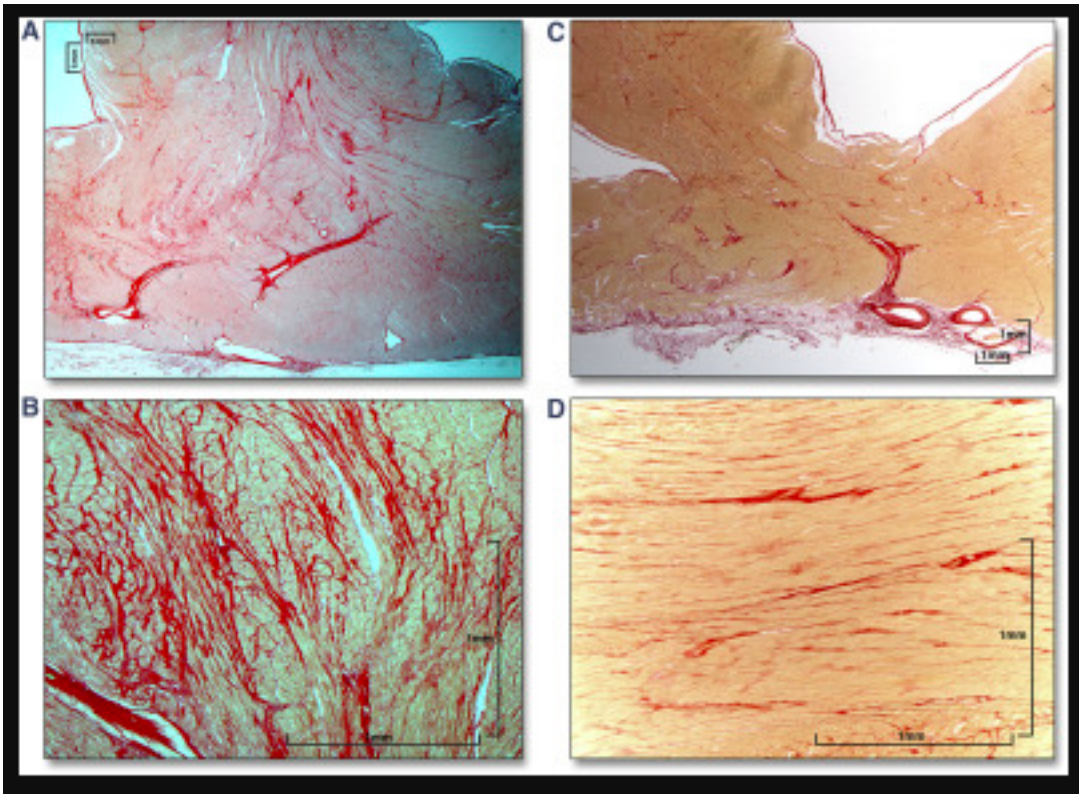

Figure 50 Morphological analysis of collagen density in animal model of pulmonary hypertension.
Images A and B are taken from animal model of PH. Images C and D are from sham-operated control. Cross sections were taken at the level of the papillary muscles. The red staining in the images demonstrate increased interstitial collagen within the VIPs. Taken from Garcia-Álvarez et al[333].

A study by Al-Wakeel-Marquard et al utilised a line of interest (LOI) as a method to measure T1 values and subsequently ECV within the RV[329]. The study measured ECV in both healthy controls and patients with congenital heart disease using both the traditional ROI measurement and the novel LOI. To overcome difficulties encountered with ROI, a curved 10mm LOI was drawn in the centre of the RV (Figure 51). LOI showed good correlation with the well-established ROI method for measuring T1 within the myocardium; however in almost half of the control subjects, RV ECV analysis was not performed due to insufficient RV wall thickness[329]. In future studies, utilising a LOI method may be considered to allow for measurement of T1 within the thin-walled RV free wall; however further validation is required.

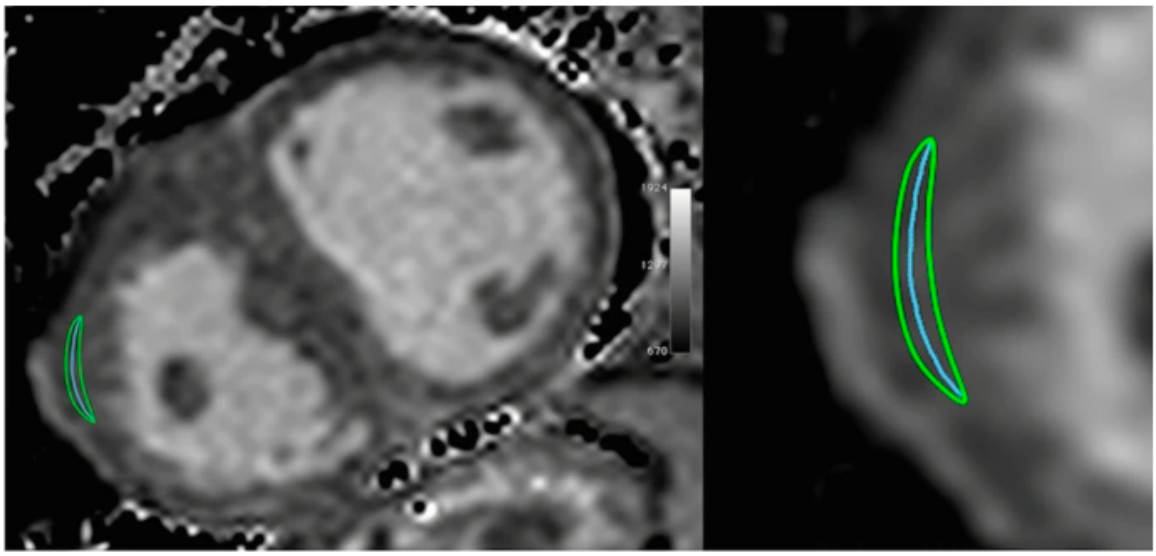

Figure 51 Illustration of the novel technique of a line of interest to measure T1 within the right ventricle.
The image on the left demonstrates an example of a native T1 map from a patient with congenital heart disease. The image on the right demonstrates measurement of both a region of interest (green) and corresponding line of interest (blue) in the right ventricle in short axis orientation. Taken from Al-Wakeel-Marquard et al[329].

7.5 Strengths and Limitations

This thesis reports the findings of a small, single-centre prospective study. Performing both intra- and inter-observer analysis is a strength of this study, with excellent ICCs for both, supporting this as a feasible technique in assessing the myocardium following lung resection surgery. A strength of the study was the measurement of T1 by two observers who were blinded to patient's demographics and study time point. However, only a proportion of scans underwent this dual analysis meaning numbers are small.

This study measured T1 values in only one plane, the short-axis. This plane was chosen as it has been shown in a healthy volunteer study as the optimal plane for measuring T1 when compared with both the transverse plane and the HLA plane[329 342]. However, a limitation may be the failure to include T1 measurements in the transverse and HLA planes which may have allowed the acquisition of T1 values in the RV free wall and improve the reporting of T1 values by including other measurements.

T1 analysis was performed retrospectively and as a result were only able to improve the images in this thesis by removing sequences with artefacts from raw

images and reproducing a regenerated map for analysis. Kawel-Bohen et al reviewed the T1 images in their study for the presence of artefact at the time of acquisition and patients were immediately rescanned and new T1 maps produced. The authors report this technique ensured good quality images were available for analysis[342]. Image acquisition could potentially have been improved in the patients who had an IQS of one or two, by performing real time T1 map analysis. However in this thesis the author has taken a pragmatic approach, given the potential for lengthy scan times with a number of breath holds in a cohort of patients who have undergone recent thoracic surgery, with a balance between obtaining appropriate images and patient experience. Using such a technique should be considered in future studies to improve image acquisition and the possibility of measuring T1 in the RV free wall whilst remaining mindful of the impact of CMR scanning in patients immediately post-operative.

7.6 Conclusions

It is feasible to measure myocardial CMR T1 values in patients undergoing lung resection surgery. By demonstrating the ability to produce high quality T1 maps with excellent intra- and inter-observer reproducibility, I have shown that the measurement of pre and post-contrast T1 in the myocardium is a valid method for assessing the characteristics of the myocardium post-lung resection surgery.

Chapter 8 Results of T1 and Extracellular Volume Analysis Following Lung Resection Surgery

This chapter describes the changes in T1 and extracellular volume (ECV) values over three study time points. Associations between T1, ECV, LV and RV function, and volume are examined. This chapter also describes the association between T1, ECV and pre-, peri- and post-operative outcomes as well as patient reported functional outcomes. This chapter describes the results from thirteen patients as participant RV2 was previously removed due to being identified as an outlier for not only RVEF (as described in Chapter 6) but also T1 (Figure 52 and 53). During clinical reporting at two-months this patient was highlighted as CMR findings may be consistent with a diagnosis of haemochromatosis and was subsequently referred for post-operative medical follow-up.

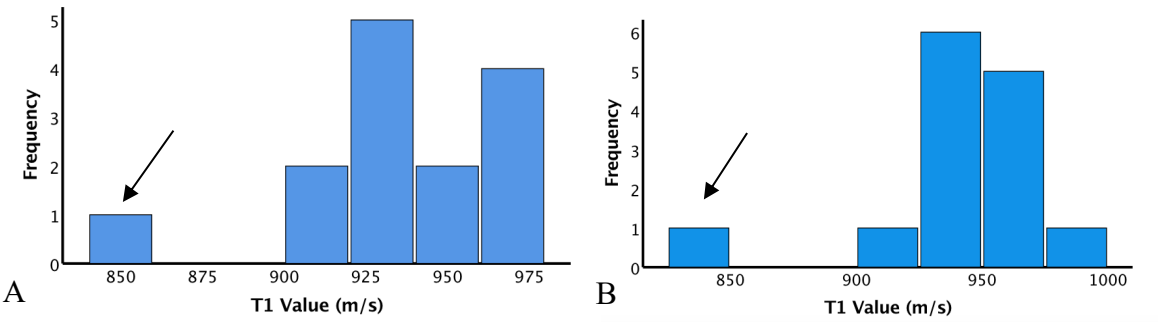

Figure 52 Identification of an outlier for T1 in both the right ventricular insertion point and the septum.
Graph A demonstrates T1 values in the right ventricular insertion point with outlier highlighted with the arrow. Graph B demonstrates T1 values in the septum with the same outlier highlighted with the arrow.

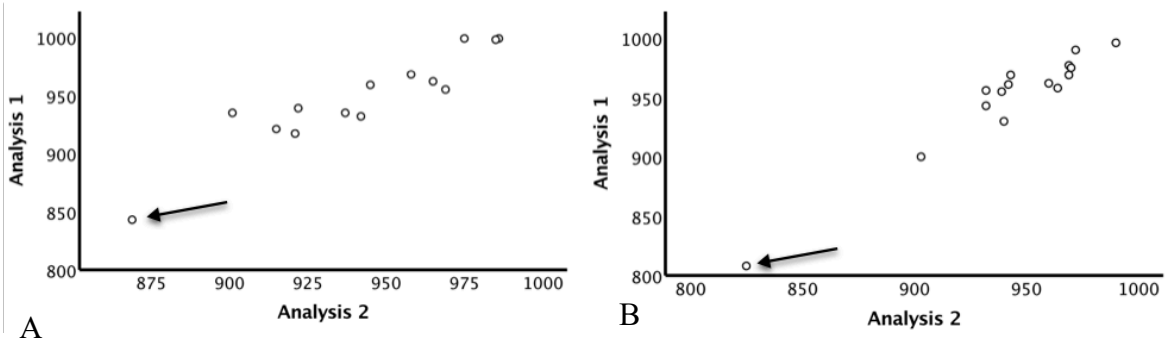

Figure 53 Scatter plot demonstrating outlier for T1 at the right ventricular insertion point and septum pre-operatively.
Graph A demonstrates T1 values in the right ventricular insertion point with outlier highlighted with the arrow. Graph B demonstrates T1 values in the septum with the same outlier highlighted with the arrow.

8.1 Change in T1 and Extra-cellular Volume Over Time

8.1.1 Right Ventricular Insertion Points

8.1.1.1 Right Ventricular Insertion Point T1 Value

Superior and inferior RV insertion point T1 values were averaged to give a combined RVIP T1 value (standard practice described in the literature).[345 364] Superior and inferior values are discussed in Section 8.1.1.3 (Table 22, and Figure 56). A significant change in native T1 values were demonstrated over time (Friedman's $p<0.001$, Figure 54 and Table 21). An increase in native T1 value was demonstrated at both POD2 and two-months from pre-operative values (Wilcoxon signed rank test, $p=0.002$ and $p=0.02$ respectively, Figure 54).

	Pre-op *(n=13)*	POD2 *(n=12)*	2mnth *(n=10)*	p-value
RVIP T1	938(923, 965)	1045(1000, 1070)†	959(949, 984)†	<0.01*
RVIP ECV	28(27, 29)	36(34, 38)†	31 (29, 32)†	<0.01*
Septum T1	943(935, 969)	975(970, 997)†	975(948, 989)	0.03*
Septum ECV	27(26, 30)	33(31, 35)†	30(28, 33)	0.07
LVFW T1	955(922, 966)	952(907, 977)	963(950, 973)	0.64
LVFW ECV	26(25, 29)	28(25, 30)	26(25, 29)	0.76

Table 21 T1 and ECV values in all regions of interest within the myocardium.
Values are median (IQR). T1 values are m/s, ECV values are given as %.
Friedman's test to assess for change over time. Wilcoxon Signed Rank test to assess for change from pre-op. * denotes significance over time. **† -** significant change from baseline value.
Pre-op – pre-operative, POD2 – post-operative day two, 2mnth – two-months post-operatively, RVIP – right ventricular insertion point, LVFW – left ventricular free wall, ECV – extra cellular volume.

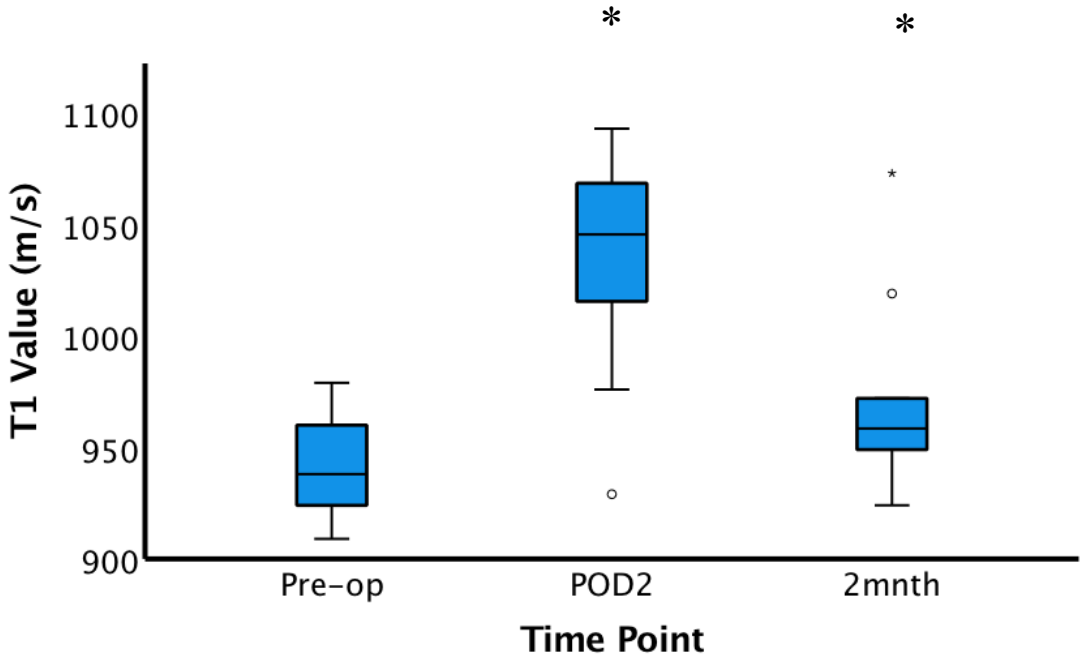

Figure 54 Change in T1 at the right ventricular insertion point over time.
Bar represents median (IQR).
Comparisons made with pre-operative value using Wilcoxon Signed Rank test
** denotes p <0.01 , * denotes p <0.05
Pre-op – pre-operative, POD2 – post-operative day two, 2mnth – two-months post-operatively.

8.1.1.2 Right Ventricular Insertion Point Extracellular Volume Values

ECV was calculated as per Equation 2, Chapter 1. As per native RVIP T1 values superior and inferior insertion point ECV values were combined and averaged to

give a combined RVIP ECV value. As was shown with native T1, a significant change in RVIP ECV over time was demonstrated (Friedman's test, p=0.001, Figure 55 and Table 21) with an increase in RVIP ECV at both POD2 and at two-months compared to baseline (Wilcoxon signed rank test, p=0.005 and p=0.007 respectively, Figure 55).

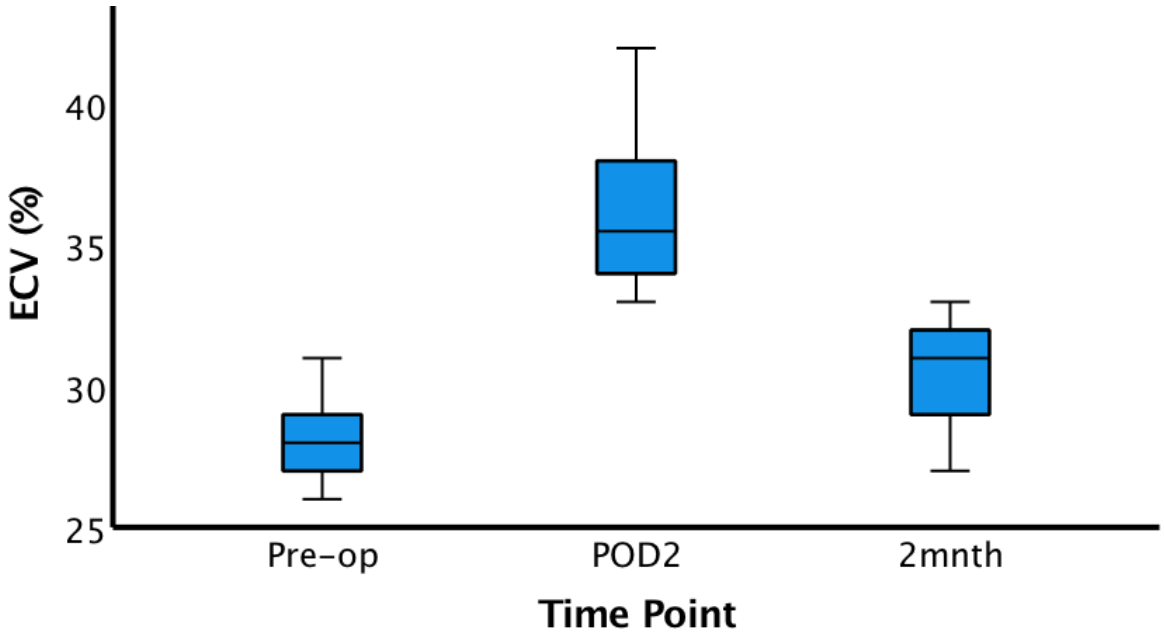

Figure 55 Change in right ventricular insertion point ECV values over time.
Bar represents median (IQR). * denotes p <0.001, ** p < 0.005
Comparisons made with pre-operative value using Wilcoxon Signed Rank test.
Pre-op – pre-operative, POD2 – post-operative day two, 2mnth – two-months post-operatively.

8.1.1.3 Relationship Between Superior and Inferior Ventricular Insertion Points

Median values for superior and inferior T1 values are displayed in Table 22. The superior and inferior RVIP were strongly associated with one another at pre-operative and POD-2 measurements (Spearman's, r=0.74 and r=0.60, p=0.01 and 0.03 respectively, Figure 56) with two-month post-operative measurements showing a moderate association (Spearman's, r=0.43, p=0.11, Figure 56).

	Anterior RVIP T1	Inferior RVIP T1	p-value
Pre-op	933 (914, 953)	945 (922, 971)	0.07
POD2	1040 (968, 1061)	1052 (1001,1091)	0.08
2month	949 (939, 963)	975 (948,1028)	0.07

Table 22 Comparison of superior and inferior right ventricular insertion point T1 values at all three study time points
Values given are median (IQR). Comparisons made with Mann Whitney U Test. All T1 values given in m/s.
Pre-op – pre-operative, POD2 – post-operative day two, 2month – two months post-operatively, RVIP – right ventricular insertion point.

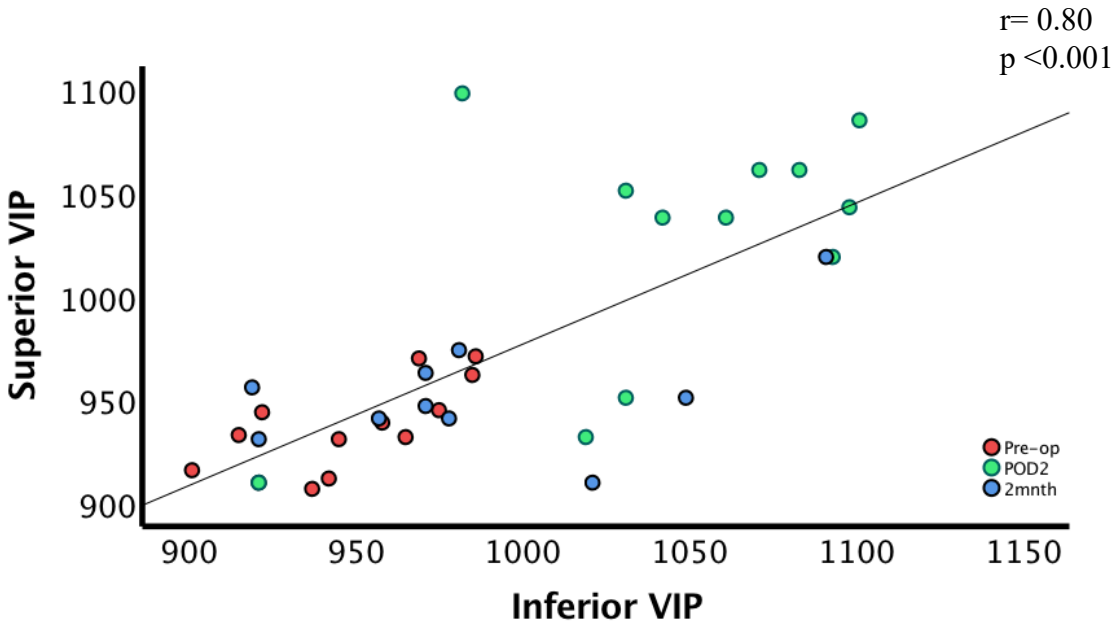

Figure 56 Association between superior and inferior right ventricular insertion point T1 value at all time points.
Spearman's correlation coefficient.
VIP -ventricular insertion point, Pre-op – pre-operatively, POD2 – post-operative day two, 2mnth – two-months post-operatively. Values are in m/s.

8.1.2 Septal T1 and Extracellular Volume Values

As with the RVIP T1, there was an increase in native T1 measured in the septum over time (Friedman's test, p=0.03, Figure 57, Table 21). ECV measured in the septum did change over time but did not reach significance (Friedman's test, p=0.07, Table 21).

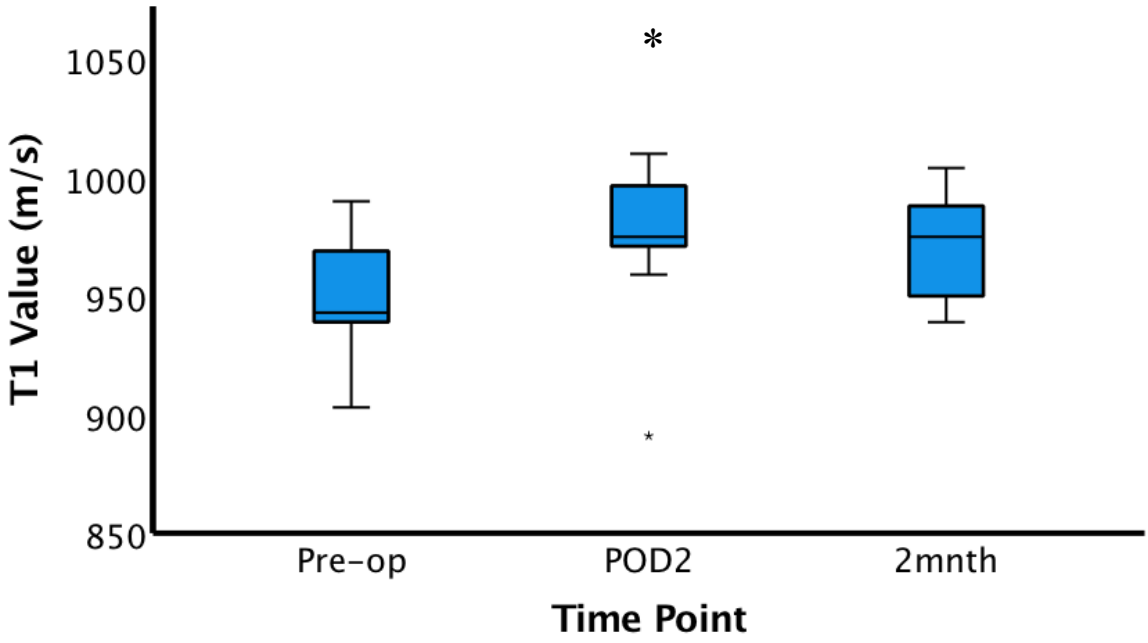

Figure 57 Change in septal native T1 value over time.
Bar represents median (IQR).
Comparisons made with pre-operative value using Wilcoxon Signed Rank test. * - p=0.004.
Pre-op – pre-operative, POD2 – post-operative day two, 2mnth – two-months post-operatively.

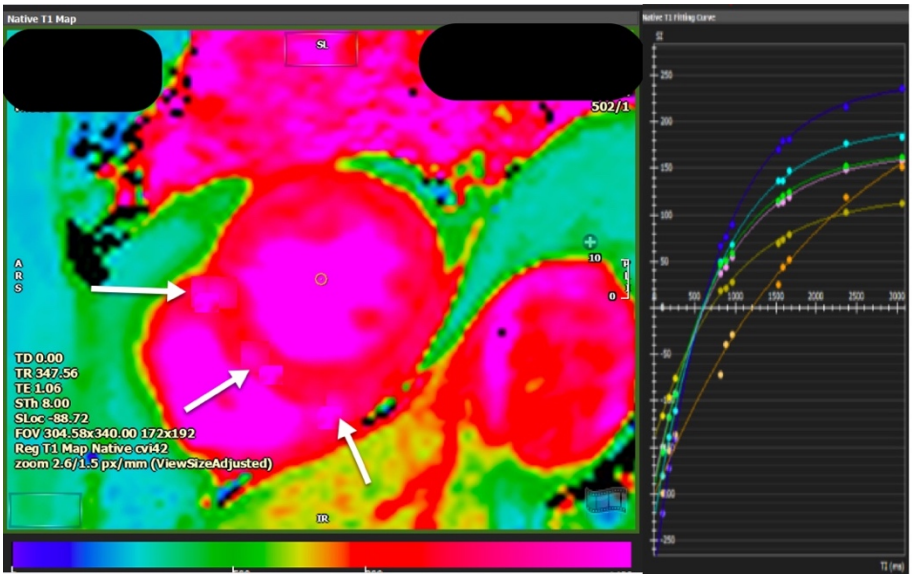

Figure 58 Native T1 map demonstrating increase in T1 at the right ventricular insertion points and septum on post-operative day two.
This native T1 map is from a 58-year-old female on post-operative day two following right lower lobectomy for a T2N0M0 staged lung cancer. The arrows indicate increased T1 at the right ventricular insertion points (1070ms) and septum (1010ms).

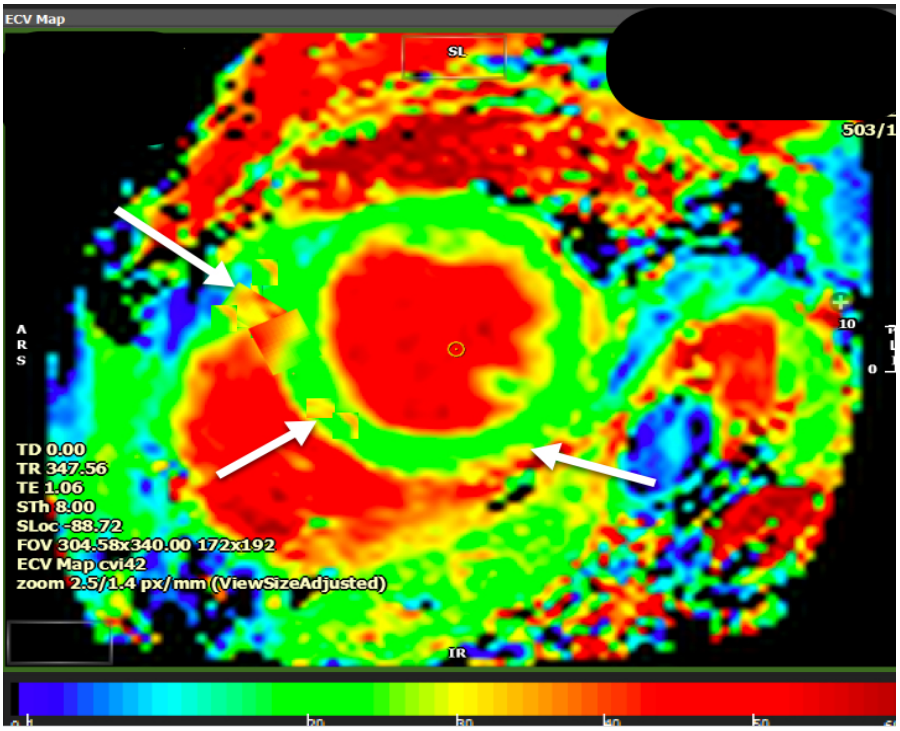

Figure 59 Extracellular volume map showing increased ECV in the right ventricular insertion points and septum on post-operative day two.
This ECV map is the corresponding ECV map for the patient described in Figure 58. The arrows indicate increased ECV at the right ventricular insertion points (40%) and septum (35%).

8.1.3 Left Ventricular Free Wall T1 and Extracellular Volume Values

Two ROIs were drawn within the LV free wall and combined to give an average LV value.[364] There was no change in LV T1 over time (Friedman's test, p=0.64, Table 21). There was no change in LV free wall ECV over time (Friedman's test, p=0.76, Table 21).

8.2 Changes in T1, ECV and Cardiac Function

Associations between T1, ECV and CMR indices of cardiac function were explored. Relative changes (in relation to baseline values) in T1 and ECV and RVEF were also examined. ΔT1, ΔECV and ΔRVEF describe relative T1, ECV and RVEF values compared to baseline pre-operative value unless otherwise stated.

8.2.1 T1, ECV and Changes in Right Ventricular Function

8.2.1.1 Right Ventricular Insertion Point T1 and RV Function and Volume

The associations between post-operative native T1 at the RVIP and RVEF are shown in Tables 23 and 24. There was a strong negative association between ΔT1 and ΔRVEF at POD2 (Table 24 and Figure 60), though this association was absent with absolute T1 and absolute RVEF at POD2 (Table 23). No association was shown between T1, ΔT1 and RVEF or ΔRVEF at two-months (Tables 23 and 24). RV volumes (ESV and EDV) were not associated with T1 at the RVIP at any time point (Spearman's, $r<0.44$, $p>0.21$, data not shown).

	Right Ventricular Insertion Points	
	POD2 T1 *(n=12)*	**2mnth T1** *(n=10)*
POD2 RVEF *(n=12)*	r= -0.22 p= 0.50	
2mnth RVEF *(n=10)*		r= 0.40 p= 0.29

Table 23 Associations between absolute right ventricular function and absolute right ventricular insertion point T1 value.
Spearman's correlation coefficient.
POD2 – post-operative day two, 2mnth – two months post-operatively, RVEF – right ventricular ejection fraction.

	Right Ventricular Insertion Point	
	ΔPOD2 T1 *(n=12)*	**Δ2mnth T1** *(n=10)*
ΔPOD2 RVEF *(n=12)*	**r= -0.66** **p= 0.02***	
Δ2mnth RVEF *(n=10)*		r= 0.54 p= 0.11

Table 24 Association between delta right ventricular ejection fraction and delta right ventricular insertion point T1 value.
Spearman's correlation coefficient.
POD2 – post-operative day two, 2mnth – two-months post-operatively, ΔPOD2 - $\Delta_{POD2\text{-}pre\text{-}op}$, Δ2mnth - $\Delta_{2mnth\text{-}pre\text{-}op}$. * denotes significance.

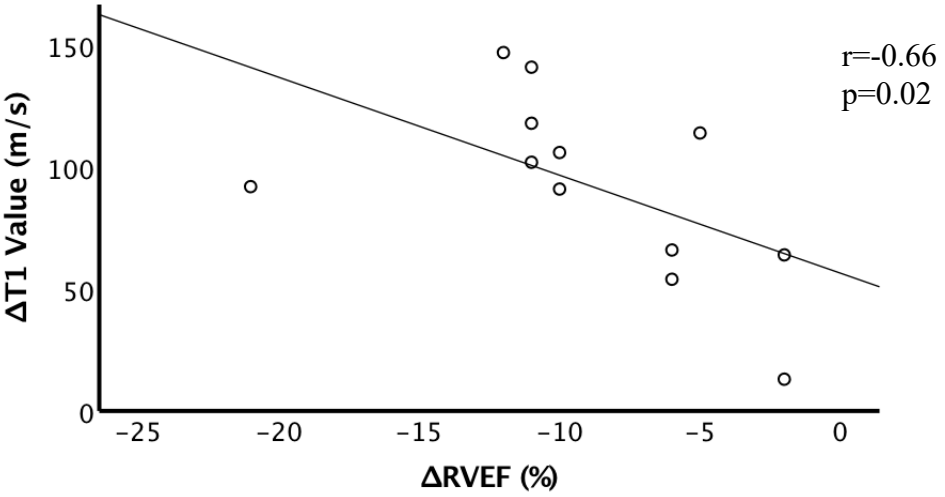

.

Figure 60 Association between delta T1 and delta right ventricular function at post-operative day two.
Spearman's correlation coefficient.
RVEF – right ventricular ejection fraction.

8.2.1.2 Septal T1 and RV Function and Volume

No associations were demonstrated between septal T1 and RVEF or septal ΔT1 and ΔRVEF at any post-operative time point (Tables 25 and 26). RV volumes (ESV and EDV) showed no associations with T1 at the septum at any time point (Spearman's, r<0.44, p>0.21, data not shown).

	Septum	
	POD2 T1 *(n=12)*	**2mnth T1** *(n=10)*
POD2 RVEF *(n=12)*	r= -0.22 p= 0.48	
2mnth RVEF *(n=10)*		r= -0.45 p= 0.20

Table 25 Association between absolute right ventricular ejection fraction and absolute septal T1 values
Spearman's correlation coefficient.
RVEF - right ventricular ejection fraction, POD2 – post-operative day two, mnth – two-months post-operatively, n - number.

	Septum	
	ΔPOD2 T1 *(n=12)*	**Δ2mnth T1** *(n=10)*
ΔPOD2 RVEF *(n=12)*	r=-0.06 p=0.84	
Δ2mnth RVEF *(n=10)*		r=-0.13 p=0.72

Table 26 Association between delta right ventricular ejection fraction and delta septal T1 value.
Spearman's correlation coefficient.
RVEF - right ventricular ejection fraction, POD2 – post-operative day two, mnth – two-months post-operatively, ΔPOD2 - $\Delta_{POD2\text{-}pre\text{-}op}$, Δ2mnth - $\Delta_{2mnth\text{-}pre\text{-}op}$,

8.2.1.3 Right Ventricular Insertion Point ECV and RV function and volume

Despite changes in RVIP ECV described in this study, no associations were observed between ECV and the documented changes in RVEF at any post-operative time period (Tables 27 and 88). As with T1, RV volumes (ESV and EDV) demonstrated no association with either ECV at the RVIP at any time point (Spearman's $r<0.39$, $p>0.27$ for all parameters, data not shown).

	Right Ventricular Insertion Point	
	POD2 ECV *(n=9)*	**2mnth ECV** *(n=9)*
POD2 RVEF *(n=13)*	r= 0.19 p= 0.63	
2mnth RVEF *(n=10)*		r= -0.13 p= 0.75

Table 27 Associations between absolute right ventricular ejection fraction and right ventricular insertion point extracellular volume.
Spearman's correlation coefficient.
POD2 – post-operative day two, mnth – two-month post-operatively, RVEF – right ventricular ejection fraction,

	Right Ventricular Insertion Point	
	ΔPOD2 ECV *(n=9)*	**Δ2mnth ECV** *(n=9)*
ΔPOD2 RVEF *(n=12)*	r= 0.13 p= 0.67	
Δ2mnth RVEF *(n=10)*		r= -0.12 p= 0.75

Table 28 Associations between delta right ventricular function and right ventricular insertion point extracellular volume
Spearman's correlation coefficient.
POD2 – post-operative day two, 2mnth – two-months post-operatively, ECV – extracellular volume, ΔPOD2 - $\Delta ECV_{POD2\text{-}pre\text{-}op}$, Δ2mnth- $\Delta ECV_{2mnth\text{-}pre\text{-}op}$.

8.2.1.4 Septal ECV and RV Function and Volume

No associations were identified between septal ECV and RVEF or ΔECV and RVEF at each post-operative time point (Tables 29 and 30). RV volumes (ESV and EDV) demonstrated no association with ECV or ΔECV at the septum at either post-operative time point (Spearman's $r<0.39$, $p>0.27$ for all parameters, data not shown).

	Septum	
	POD2 ECV *(n=9)*	**2mnth ECV** *(n=9)*
POD2 RVEF *(n=12)*	r= 0.13 p= 0.75	
2mnth RVEF *(n=10)*		r= -0.31 p= 0.42

Table 29 Association between absolute right ventricular ejection fraction and absolute septal extracellular volume.
Spearman's correlation coefficient.
POD2 – post-operative day two, 2mnth – two-months post-operatively, RVEF – right ventricular ejection fraction.

	Septum	
	ΔPOD2 ECV *(n=9)*	**Δ2mnth ECV** *(n=9)*
ΔPOD2 RVEF *(n=12)*	r= 0.28 p= 0.47	
Δ2mnth RVEF *(n=10)*		r= 0.21 p= 0.58

Table 30 Associations between delta right ventricular ejection fraction and delta septal point extracellular volume.
Spearman's correlation coefficient.
POD2 – post-operative day two, 2mnth – two-months post-operatively, ECV – extracellular volume, ΔPOD2 - $\Delta ECV_{POD2\text{-}pre\text{-}op}$, Δ2mnth- $\Delta ECV_{2mnth\text{-}pre\text{-}op}$.

8.2.1.5 T1, ECV and Heart Rate

Despite an increase in HR in the post-operative period from pre-operative values, this was not associated with changes in T1, ΔT1, ECV or ΔECV (Spearman's $r<0.39$, $p>0.19$ for all parameters, data not shown).

8.3 Change in T1, ECV and Baseline Demographics

Association between patient demographics and T1, ΔT1, ECV and ΔECV across the myocardium were sought including comparisons with age, oxygen saturations, preoperative FEV1% and DLCO %, post-operative predicted FEV1% and DLCO% and Thoracoscore (Tables 31 and 32).

8.3.1 Right Ventricular Insertion Point T1 and Baseline Demographics

Poorer lung function demonstrated strong associations with both T1 and ΔT1. Strong associations with both pre-operative DLCO% and ppoDLCO% and absolute T1 and ΔT1 on POD2 were demonstrated (Tables 31 and 32). Those with poorer pre-operative DLCO demonstrated higher absolute T1 values but not ΔT1 (Tables 31 and 32). These strong associations were also demonstrated with lower predicted post-operative lung function and both higher T1 and ΔT1 values (Tables 31 and 32 and Figure 61). Thoracoscore and pre-operative oxygen saturations levels were not associated with T1 or ΔT1 at either post-operative time point (Tables 31 and 32).

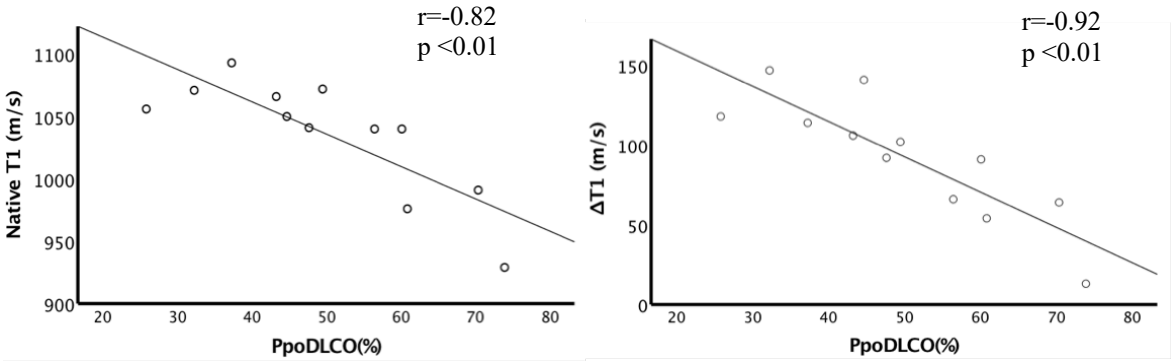

Figure 61 Association between T1 at the right ventricular insertion point on post-operative day two and predicted post-operative lung function.
Graph A demonstrates association between absolute native T1 and predicted post-operative DLCO(%). Graph B demonstrates association between relative native T1 and predicted post-operative DLCO(%).Spearman's correlation coefficient. DLCO - diffusion capacity for carbon monoxide given as a percentage. ∆ - delta T1 (POD2-pre-op).

	Right Ventricular Insertion Point			
	POD2 T1 *(n=12)*	**2mnth T1** *(n=10)*	**POD2 ECV** *(n=9)*	**2mnth ECV** *(n=9)*
Age *(n=13)*	r=-0.49 p=0.10	r=0.07 p=0.84	r=-0.43 p= 0.25	r=0.15 p=0.70
Pre-op Sats (%) *(n=13)*	r=-0.35 p=0.26	r=0.13 p=0.73	**r=-0.71** **p=0.03***	r=-0.03 p=0.95
Pre-op FEV_1(%) *(n=13)*	r=-0.41 p=0.19	r=-0.10 p=0.77	r=-0.01 p=0.99	r=-0.08 p=0.85
Pre-op DLCO (%) *(n=13)*	**r-0.74** **p <0.01 ***	r=-0.17 p=0.63	r=-0.49 p=0.15	r=-0.43 p=0.22
ppoFEV1 (%) *(n=13)*	r=-0.45 p= 0.13	r=-0.20 p=0.59	r=-0.25 p=0.51	r=0.13 p=0.75
ppoDLCO (%) *(n=13)*	**r=-0.82** **p<0.01***	r=-0.25 p=0.49	r=-0.51 p=0.16	r=-0.20 p=0.62
Thoracoscore *(n=13)*	r=0.03 p=0.92	r=-0.09 p=0.81	r=-0.25 p=0.51	r=0.04 p=0.99

Table 31 Associations between absolute right ventricular insertion point T1, absolute extracellular volume and baseline demographics.
Spearman's correlation coefficient. * - denotes significance.
FEV_1% - forced expiratory volume in one second, ppoFEV_1(%) – predicted post-operative forced expiratory volume in one second, DLCO (%) - diffusion capacity for carbon monoxide given as a percentage, pre-op – pre-operative, sats – saturations, POD2 – post-operative day two, 2mnth – two-months post-operatively, ECV – extracellular volume, n – number.

	Right Ventricular Insertion Point			
	ΔPOD2 T1 *(n=12)*	**Δ2mnth T1** *(n=10)*	**ΔPOD2 ECV** *(n=9)*	**Δ2mnth ECV** *(n=9)*
Age *(n=13)*	r= -0.24 p= 0.54	r= 0.27 p= 0.45	**r= -0.74** **p= 0.02***	r= 0.08 p= 0.84
Pre-op Sats (%) *(n=13)*	r= -0.53 p= 0.08	r= 0.34 p= 0.33	r= -0.40 p= 0.29	r= 0.07 p= 0.86
Pre-op FEV_1(%) *(n=13)*	r= -0.47 p= 0.12	r= 0.30 p= 0.41	r= -0.17 p= 0.64	r= 0.03 p= 0.93
Pre-op DLCO (%) *(n=13)*	r= -0.18 p= 0.61	r= -0.34 p= 0.34	r= -0.27 p= 0.48	r= -0.31 p= 0.41
ppoFEV1 (%) *(n=13)*	r= -0.53 p= 0.07	r= 0.09 p= 0.80	r= -0.17 p= 0.66	r= 0.09 p= 0.83
ppoDLCO (%) *(n=13)*	**r= -0.92** **p <0.01***	r= -0.15 p= 0.68	r= -0.39 p= 0.30	r= -0.04 p= 0.90
Thoracoscore *(n=13)*	r= -0.24 p= 0.45	r= 0.25 p= 0.48	r= -0.54 p= 0.13	r= -0.03 p= 0.95

Table 32 Associations between delta right ventricular insertion point T1, extracellular volume and baseline demographics,
Spearman's correlation coefficient. * denotes significance.
FEV_1% - forced expiratory volume in one second as a percentage, ppoFEV_1(%) – predicted post-operative forced expiratory volume in one second, DLCO (%) - diffusion capacity for carbon monoxide given as a percentage, pre-op – pre-operative, sats – saturations, POD2 – post-operative day two, 2mnth – two-months post-operatively, ECV – extracellular volume, n – number, ΔPOD2 T1 - $\Delta T1_{POD2\text{-}pre\text{-}op}$, Δ2mnth T1- $\Delta T1_{2mnth\text{-}pre\text{-}op}$, ECV – extracellular volume, ΔPOD2 ECV - $\Delta ECV_{POD2\text{-}pre\text{-}op}$, Δ2mnth ECV- $\Delta ECV_{2mnth\text{-}pre\text{-}op}$.

8.3.2 Right Ventricular Insertion Point Extracellular Volume and Baseline Demographics

Of the baseline demographics, only age and oxygen saturation levels demonstrated association with RVIP ΔECV and ECV respectively. Lower age was associated with higher ΔECV on POD2 (Table 32) whilst lower pre-operative saturation levels were associated with higher absolute ECV on POD2 (Table 31). Similar trends were demonstrated with predicted post-operative lung function and RVIP ECV as were shown with RVIP T1, with poorer predicted post-operative lung function associated with higher ECV; however these did not reach significance (Tables 31 and 32).

8.3.3. Septal T1 and Baseline Demographics

Similar associations were demonstrated with T1 measured in the septum as were shown with RVIP T1 with a trend towards poorer lung function (both pre and

predicted post-operatively) being associated with higher T1 values (Table 33). Strong associations were demonstrated between POD2 T1 and both pre-op DLCO% and ppoDLCO% (Figure 62 and Table 33). A similar trend was shown between both lower pre-operative FEV1% and ppoFEV1 demonstrating association with higher absolute T1 values in the septum but this did not reach significance (Table 33). There was no association between ΔT1 measured in the septum and any baseline demographic parameter at either POD2 or two-months post-operatively (Table 34).

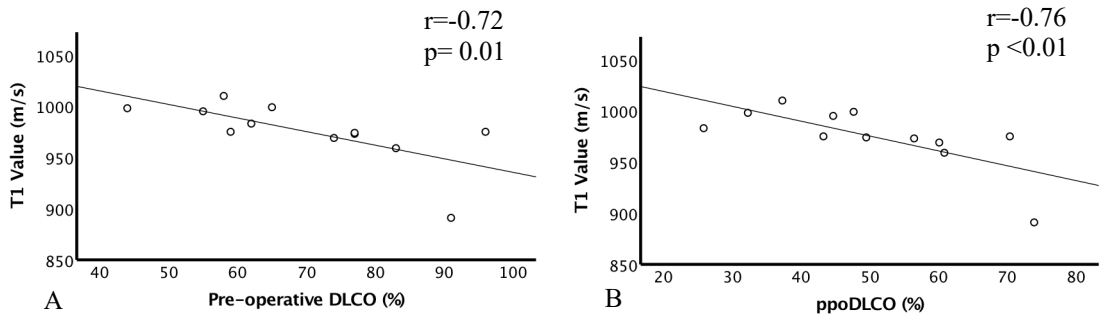

Figure 62 Association between absolute septal T1 values on post-operative day 2 and pre-operative and predicted post-operative lung function.
Graph A demonstrates association between pre-operative measured diffusion capacity for carbon monoxide given as a percentage and absolute T1 measured at the septum on POD2. Graph B demonstrates an association between predicted post-operative measured diffusion capacity for carbon monoxide given as a percentage and absolute T1 measured at the septum on POD2. Spearman's correlation coefficient.

	Septum			
	POD2 T1 *(n=12)*	**2mnth T1** *(n=10)*	**POD2 ECV** *(n=9)*	**2mnth ECV** *(n=9)*
Age *(n=13)*	r=-0.03 p=0.93	r=-0.52 p=0.12	r=-0.36 p=0.34	r=-0.14 p=0.73
Pre-op sats (%) *(n=13)*	r=-0.51 p=0.11	r=-0.03 p=0.93	**r=-0.85 p<0.01***	r=-0.04 p=0.91
Pre-op FEV_1(%) *(n=13)*	r=-0.43 p=0.19	r=-0.26 p=0.47	r=-0.27 p=0.48	r=-0.03 p=0.95
Pre-op DLCO (%) *(n=13)*	**r=-0.72 p=0.01**	r=-0.25 p=0.49	r=-0.49 p=0.18	r=-0.43 p=0.25
ppoFEV1 (%) *(n=13)*	r=-0.55 p=0.06	r=0.24 p=0.51	r=-0.28 p=0.47	r=0.44 p=0.24
ppoDLCO (%) *(n=13)*	**r=-0.76 p<0.01***	r=-0.14 p=0.70	r=-0.54 p=0.14	r=-0.12 p=0.76
Thoracoscore *(n=13)*	r=0.24 p=0.49	r=-0.34 p=0.34	r=-0.22 p=0.57	r=0.32 p=0.41

Table 33 Associations between absolute T1, absolute extracellular volume in the septum and baseline demographics.
Spearman's correlation coefficient. * - denotes significance.
FEV_1% - forced expiratory volume in one second as a percentage, ppoFEV_1(%) – predicted post-operative forced expiratory volume in one second, DLCO (%) - diffusion capacity for carbon monoxide given as a percentage, pre-op – pre-operative, sats – saturations, POD2 – post-operative day two, 2mnth – two-months post-operatively, ECV – extracellular volume, n – number.

	Septum			
	ΔPOD2 T1 *(n=12)*	**Δ2mnth T1** *(n=10)*	**ΔPOD2 ECV** *(n=10)*	**Δ2mnth ECV** *(n=10)*
Age *(n=13)*	r=0.29 p=0.36	r=-0.51 p=0.11	r=-0.05 p=0.90	r=-0.16 p=0.65
Pre-op Sats (%) *(n=13)*	r=-0.23 p=0.48	r=0.08 p=0.81	r=-0.31 p=0.36	r=0.02 p=0.94
Pre-op FEV_1(%) *(n=13)*	r=-0.36 p=0.26	r=-0.04 p=0.92	r=-0.14 p=0.68	r=0.05 p=0.89
Pre-op DLCO(%) *(n=13)*	r=-0.04 p=0.90	r=0.17 p=0.61	r=-0.47 p=0.14	r=-0.23 p=0.51
ppoFEV1 (%) *(n=13)*	r=-0.42 p=0.14	r=0.34 p=0.31	r=-0.19 p=0.59	r=-0.12 p=0.73
ppoDLCO (%) *(n=13)*	r=-0.29 p=0.34	r=0.10 p=0.90	r=-0.31 p=0.35	r=-0.04 p=0.90
Thoracoscore *(n=13)*	r=0.20 p=0.54	r=0.02 p=0.95	r=-0.24 p=0.47	r=0.14 p=0.69

Table 34 Associations between delta T1 and delta extracellular volume in the septum and baseline demographics
Spearman's correlation coefficient.
FEV_1% - forced expiratory volume in one second as a percentage, ppoFEV_1(%) – predicted post-operative forced expiratory volume in one second, DLCO (%) - diffusion capacity for carbon monoxide given as a percentage, pre-op – pre-operative, sats – saturations, POD2 – post-operative day two, 2mnth – two-months post-operatively, ECV – extracellular volume, n – number, ΔPOD2 T1 - $\Delta T1_{POD2\text{-}pre\text{-}op}$, Δ2mnth T1- $\Delta T1_{2mnth\text{-}pre\text{-}op}$, ECV – extracellular volume, ΔPOD2 ECV - $\Delta ECV_{POD2\text{-}pre\text{-}op}$, Δ2mnth ECV- $\Delta ECV_{2mnth\text{-}pre\text{-}op}$.

8.3.4 Septal Extracellular Volume and Baseline Demographics

Of the baseline demographics, only pre-operative oxygen saturations demonstrated association with absolute ECV measured at POD2 (Table 33). Similar trends were demonstrated with septal ECV on POD2 and pre-operative DLCO % and ppoDLCO% as was demonstrated with septal T1; however on this occasion these did not reach significance (Tables 33). ΔECV demonstrated no association with any baseline parameter at either POD2 or at two-months post-operatively (Table 34).

8.4 Change in T1, ECV and Peri-operative Parameters

To explore the impact of surgical and anaesthetic technique on post-operative T1 values, associations were sought between aspects of peri-operative care

during lung resection surgery and post-operative T1, ΔT1, ECV and ΔECV values (Tables 35 and 36).

8.4.1 Right Ventricular Insertion Point T1 and Peri-operative Parameters

The median (IQR) number of pulmonary segments resected was 4 (4, 5) with a larger number of resected segments being associated with higher POD2 T1 values at the RVIP (Spearman's, r=0.60, p=0.03, Figure 63 and Table 35). The number of segments resected did not demonstrate association with T1 at two-months or ΔT1 at either POD2 or two-months at the RVIP (Tables 35 and 36). The median (IQR) duration of OLV was 101 minutes (87, 162) and the median duration of surgery was 142 minutes (134, 196). Neither duration of OLV or surgery were associated with T1 or Δ T1 (Tables 35 and 36).

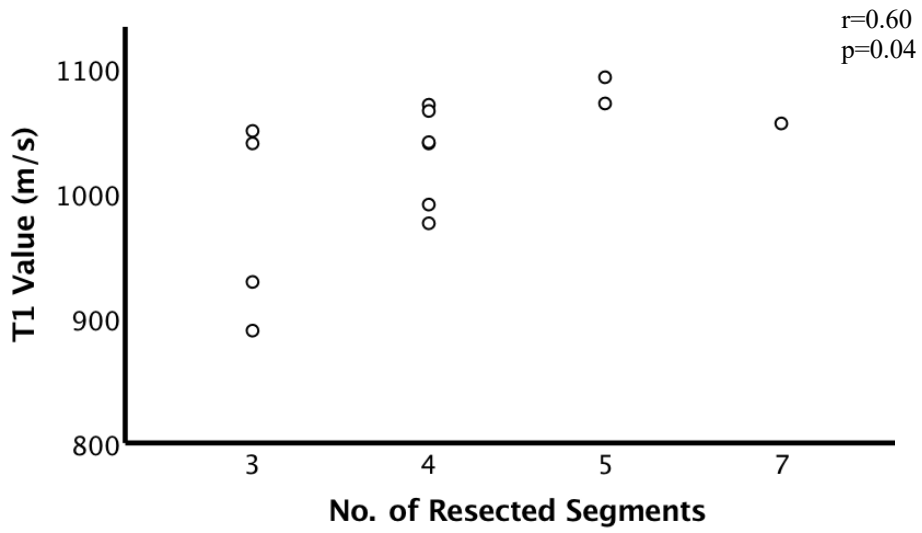

Figure 63 Association between the number of pulmonary segments resected and absolute T1 value at post-operative day two in the right ventricular insertion point.
Spearman's correlation coefficient.

The mean (SD) intra-op fluid administered was 802ml (325); as fluid is typically given in 500ml aliquots, all thirteen patients had fluid administration documented in in multiples of 500ml. As a result, fluid administration could not be treated as a continuous variable and therefore fluid administration was grouped into three groups; 500ml or less, 501-999ml and 1000ml or more. There

was no association between volume of fluid administered and T1 or ΔT1 at any time point (Kruskal-Wallis test, p>0.15 for all parameters, data not shown).

	Right Ventricular Insertion Point			
	POD2 T1 *(n=12)*	**2mnth T1** *(n=10)*	**POD2 ECV** *(n=9)*	**2mnth ECV** *(n=9)*
Segments resected ***(n=13)***	**r=0.60** **p=0.04***	r=0.17 p=0.65	r=0.66 p=0.06	r=-0.26 p=0.50
Duration OLV ***(n=13)***	r=0.13 p=0.68	r=-0.12 p=0.75	r=0.03 p=0.95	r=-0.08 p=0.98
Duration of surgery ***(n=13)***	r=0.07 p=0.83	r=0.15 p=0.79	r=0.28 p=0.46	r=0.11 p=0.79

Table 35 Associations between absolute T1 and extracellular volume in the right ventricular insertion point and peri-operative factors.
Spearman's correlation coefficient. * denotes significance.
OLV – one lung ventilation, POD2 – post-operative day two, 2mnth – two-months post-operatively, ECV – extracellular volume.

No association was demonstrated between intra-operative NSAID or dexamethasone use and any T1 or ΔT1 at any time point (Kruskal-Wallis test, p>0.45 for all parameters, data not shown).

8.4.2 Right Ventricular Insertion Point Extracellular Volume and Peri-operative Parameters

As with RVIP ECV, a trend was demonstrated towards a larger number of resected segments and higher ECV and ΔECV values on POD2; however these did not reach significance (Tables 35 and 36). No other intra-operative parameter demonstrated association with ECV or ΔECV at either POD2 or two-months post-operatively (Tables 35 and 36). No association was demonstrated between intra-operative NSAID or dexamethasone use and any ECV or ΔECV at any time point (Kruskal-Wallis test, p>0.69 for all parameters, data not shown).

	Right Ventricular Insertion Point			
	ΔPOD2 T1 *(n=12)*	**Δ2mnth T1** *(n=10)*	**ΔPOD2 ECV** *(n=9)*	**Δ2mnth ECV** *(n=9)*
Segments resected *(n=13)*	r=0.32 p=0.31	r=-0.13 p=0.97	r=0.54 p=0.14	r=-0.46 p=0.19
Duration OLV *(n=13)*	r=0.25 p=0.44	r=-0.19 p=0.60	r=0.28 p=0.48	r=0.13 p=0.75
Duration of surgery *(n=13)*	r=-0.33 p=0.48	r=-0.22 p=0.54	r=0.48 p=0.18	r=0.09 p=0.82

Table 36 Associations between delta T1 and extracellular volume in the right ventricular insertion point and peri-operative factors.
Spearman's correlation coefficient.
OLV – one lung ventilation, POD2 – post-operative day two, 2mnth – two-months post-operatively, ΔPOD2 T1 - $\Delta T1_{POD2\text{-}pre\text{-}op}$, Δ2mnth T1- $\Delta T1_{2mnth\text{-}pre\text{-}op}$, ECV – extracellular volume, n – number, ΔPOD2 ECV - $\Delta ECV_{POD2\text{-}pre\text{-}op}$, Δ2mnth ECV- $\Delta ECV_{2mnth\text{-}pre\text{-}op}$.

8.4.3 Septal T1 and Extracellular Volume and Peri-operative Parameters

As with RVIP, higher ΔT1 values in the septum were associated with a higher number of segments resected; however this did not reach significance (Spearman's test, r=0.55, p=0.06). No other peri-operative factors demonstrated any association with either T1 or ΔT1 values in the septum (Spearman's test $r<0.43$, $p>0.13$ for all parameters, data not shown). As with RVIP ECV, peri-operative parameters were not associated with ΔECV in the septum (Spearman's test, $r<0.42$, $p>0.22$, data not shown).

No association was demonstrated between intra-operative NSAID or dexamethasone use and any T1, ΔT1, ECV or ΔECV in the septum at any time point (Kruskal-Wallis test, $p>0.72$ for all parameters, data not shown).

8.4 Change in T1 and Post-operative Outcomes

Association between post-operative outcomes and T1, ΔT1, ECV and ΔECV in the RVIP and septum were sought. One patient developed AF in the post-operative period and as a result was unable to undergo the CMR protocol in the early post-operative period and therefore no T1 and ECV values are available for analysis

(as described in Chapter 6). No patients in the study required post-operative vasopressors.

The mean (SD) HDU length of stay was 35 (24) hours and the median (IQR) length of hospital stay was 5 (4, 6) days. No association was demonstrated between any myocardial T1 or ECV value (or delta value) and either length of HDU stay or length of hospital stay (Tables 37 and 38).

No association was demonstrated between post-operative NSAID use and T1, ΔT1, ECV or ΔECV measured in the RVIP and septum at any time point (Kruskal-Wallis test, p>0.19 for all parameters, data not shown).

	Right Ventricular Insertion Point			
	POD2 T1 *(n=12)*	**2mnth T1** *(n=10)*	**POD2 ECV** *(n=9)*	**2mnth ECV** *(n=9)*
HDU Stay *(n=13)*	r= -0.13 p= 0.66	r= 0.14 p= 0.68	r= -0.36 p= 0.28	r= -0.51 p= 0.11
Hospital Stay *(n=13)*	r= 0.10 p= 0.74	r= -0.24 p= 0.48	r= 0.24 p= 0.47	r= -0.11 p= 0.75

Table 37 Associations between absolute T1 and extracellular volume in the right ventricular insertion point and post-operative outcomes.
Spearman's correlation coefficient.
n- number, HDU – high dependency unit, POD2 – post-operative day two, 2mnth – two-months post-operatively, , ECV – extracellular volume.

	Right Ventricular Insertion Point			
	ΔPOD2 T1 *(n=12)*	**Δ2mnth T1** *(n=10)*	**ΔPOD2 ECV** *(n=9)*	**Δ2mnth ECV** *(n=9)*
HDU Stay *(n=13)*	r= -0.28 p= 0.38	r= -0.18 p= 0.61	r= -0.04 p= 0.90	r= 0.27 p= 0.42
Hospital Stay *(n=13)*	r= 0.45 p= 0.14	r= -0.15 p= 0.69	r= 0.17 p= 0.62	r= -0.05 p= 0.88

Table 38 Associations between delta T1 and extracellular volume in the right ventricular insertion point and post-operative outcomes
Spearman's correlation coefficient.
n – number, HDU – high dependency unit, POD2 – post-operative day two, 2mnth – two-months post-operatively, ΔPOD2 T1 - $\Delta T1_{POD2\text{-}pre\text{-}op}$, Δ2mnth T1- $\Delta T1_{2mnth\text{-}pre\text{-}op}$, ECV – extracellular volume, ΔPOD2 ECV - $\Delta ECV_{POD2\text{-}pre\text{-}op}$, Δ2mnth ECV- $\Delta ECV_{2mnth\text{-}pre\text{-}op}$.

8.5 Change in T1, ECV and Patient Reported Post-Operative Outcomes

Associations between T1, ΔT1, ECV and ΔECV measured at the RVIP and septum and patient-reported functional outcomes and QoL at two-months post-operatively were examined.

8.5.1 Right Ventricular Insertion Point T1 and Patient Reported Post-Operative Outcomes

Higher T1 and ΔT1 values in the immediate post-operative period were associated with poor patient reported outcomes at two-months (Table 39). A moderate association was demonstrated with RVIP $\Delta T1_{POD2\text{-}pre\text{-}op}$ and NYHA score at two-months (Table 39). Strong associations were also demonstrated with higher POD2 RVIP T1 and $\Delta T1_{POD2\text{-}pre\text{-}op}$ values associated with a lower post-operative QOL Summary Index at two-months (Table 39 and Figure 63). Of the individual EQ5D variables, mobility, self-care and anxiety showed strong association with both POD2 RVIP T1 and $\Delta T1_{POD2\text{-}pre\text{-}op}$ ($r>0.62$, $p<0.03$ for all parameters, data not shown).

	Right Ventricular Insertion Point			
	POD2 T1 *(n=12)*	**2mnth T1** *(n=10)*	**ΔPOD2 T1** *(n=12)*	**Δ2mnth T1** *(n=10)*
WHO *(n=13)*	r=0.14 p=0.67	r=0.07 p=0.84	r=0.35 p=0.27	r=0.30 p=0.41
NYHA *(n=13)*	r=0.32 p=0.31	r=-0.03 p=0.93	**r=0.58** **p=0.05***	r=-0.07 p=0.84
MRC *(n=13)*	r=0.49 p=0.10	r=0.14 p=0.71	r=0.49 p=0.10	r=0.04 p=0.91
QOL Summary Index *(n=13)*	**r=-0.64** **p=0.02***	r=0.09 p=0.82	**r=-0.77** **p<0.01***	r=-0.16 p=0.65
GHS *(n=13)*	r=-0.22 p=0.49	r=-0.36 p=0.31	r=-0.31 p=0.33	r=-0.17 p=0.63

Table 39 Associations between right ventricular insertion point T1 and patient reported outcomes at two-months.
Spearman's correlation coefficient. *denotes significance.
POD – post-operative day, 2mnth – two-months post-operatively, WHO – world health organisation, MRC – medical research council, NYHA – New York Heart Association, QOL – quality of life, GHS – global health score, n – number, ΔPOD2 - $\Delta T1_{POD2\text{-}pre\text{-}op}$, Δ2mnth - $\Delta T1_{2mnth\text{-}pre\text{-}op}$.

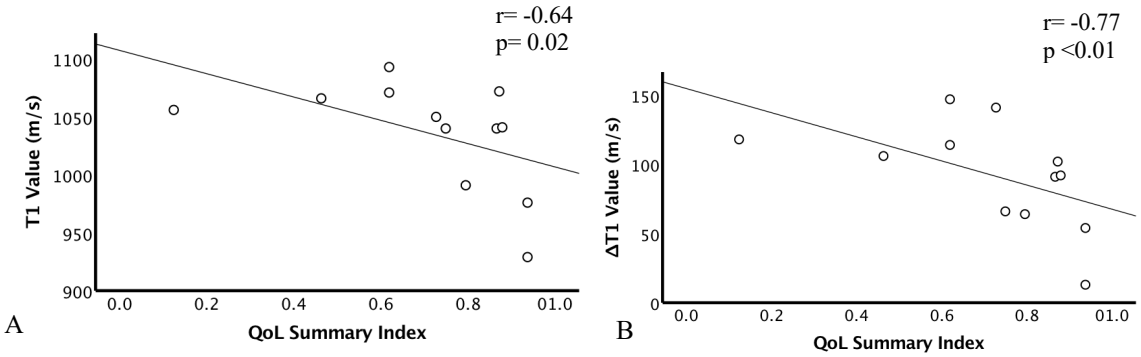

Figure 64 Association between absolute T1 (A), delta T1 (B) on post-operative day two and quality of life summary index score at two-months post-operatively.
Spearman's correlation coefficient.
QoL – quality of life.

8.5.2 Septal T1 and Patient Reported Post-Operative Outcomes

As with RVIP T1, T1 at the septum on POD2 also showed strong association with QOL Summary Index (Table 40). Once again, the individual EQ50 variables mobility, self-care and anxiety demonstrated strong individual associations with T1 ($r>0.61$, $p<0.03$ for all parameters, data not shown). Higher septal T1 measured at two-months also demonstrated moderate association with higher NYHA reported scores at two-months. Of note this was the only septal T1 value measured at two-months that demonstrated an association with patient-reported outcomes (Table 40).

	Septum			
	POD2 T1 *(n=12)*	**2mnth T1** *(n=10)*	**ΔPOD2 T1** *(n=12)*	**Δ2mnth T1** *(n=10)*
WHO *(n=13)*	r=-0.06 p=0.86	r=-0.10 p=0.79	r=0.32 p=0.31	r=0.23 p=0.52
MRC *(n=13)*	r=0.19 p=0.56	r=0.32 p=0.37	r=0.29 p=0.37	r=0.36 p=0.31
NYHA *(n=13)*	r=0.30 p=0.35	**r=0.82 p<0.01***	r=-0.05 p=0.88	r=0.48 p=0.16
QOL Summary Index*(n=13)*	**r=-0.57 p=0.05***	r=0.46 p=0.19	r=-0.38 p=0.23	r=-0.20 p=0.56
GHS *(n=13)*	r=-0.10 p=0.77	r=-0.47 p=0.17	r=0.10 p=0.77	r=-0.17 p=0.63

Table 40 Associations between septum T1 values and patient reported post-operative outcomes.
Spearman's correlation coefficient. *denotes significance.
POD – post-operative day, 2mnth – two-month post-operatively, WHO – world health organisation, MRC – medical research council, NYHA – New York Heart Association, QOL – quality of life, GHS – global health score, n – number, ΔPOD2 - $\Delta T1_{POD2\text{-}pre\text{-}op}$, Δ2mnth - $\Delta T1_{2mnth\text{-}pre\text{-}op}$.

8.5.3 Right Ventricular Insertion Point Extracellular Volume and Patient Reported Post-Operative Outcomes

Unlike RVIP T1, no associations were shown between RVIP ECV and patient reported outcomes at two-months (Table 41).

8.5.4 Septal Extracellular Volume and Patient Reported Post-Operative Outcomes

Associations between septal ECV and patient reported outcomes were not observed with only POD2 ECV and WHO grade at two-months demonstrating a moderate association (Table 42).

	Right Ventricular Insertion Point			
	POD2 ECV *(n=9)*	**2mnth ECV** *(n=9)*	**ΔPOD2 ECV** *(n=9)*	**Δ2mnth ECV** *(n=9)*
WHO *(n=13)*	r= -0.63 p= 0.07	r= -0.37 p= 0.33	r= -0.11 p= 0.77	r= 0.02 p= 0.96
NYHA *(n=13)*	r= -0.18 p= 0.63	r= 0.23 p= 0.55	r= 0.25 p= 0.51	r= 0.33 p= 0.36
MRC *(n=13)*	r= -0.36 p= 0.34	r= -0.17 p= 0.66	r= 0.09 p= 0.98	r= 0.29 p= 0.42
QOL Summary Index *(n=13)*	r= -0.09 p= 0.82	r= 0.26 p= 0.56	r= -0.31 p= 0.42	r= -0.03 p= 0.93
GHS *(n=13)*	r= 0.34 p= 0.37	r=-0.13 p= 0.74	r= -0.02 p= 0.96	r= -0.40 p= 0.26

Table 41 Associations between right ventricular insertion point extracellular volume and patient reported outcomes at two-months.
Spearman's correlation coefficient.
POD – post-operative day, 2mnth – two-months post-operatively, WHO – world health organisation, MRC – medical research council, NYHA – New York Heart Association, QOL – quality of life, GHS – global health score, ECV – extracellular volume, n – number, ΔPOD2 - $\Delta T1_{POD2\text{-}pre\text{-}op}$, Δ2mnth - $\Delta T1_{2mnth\text{-}pre\text{-}op}$.

	Septum			
	POD2 ECV *(n=9)*	**2mnth ECV** *(n=9)*	**ΔPOD2 ECV** *(n=9)*	**Δ2mnth ECV** *(n=9)*
WHO *(n=13)*	**r=0.67** **p=0.05***	r=-0.43 p=0.21	r=0.27 p=0.46	r=-0.13 p=0.73
NYHA *(n=13)*	r=-0.18 p=0.61	r=-0.17 p=0.64	r=-0.16 p=0.66	r=-0.14 p=0.70
MRC *(n=13)*	r=-0.17 p=0.67	r=0.02 p=0.96	r=0.03 p=0.94	r=-0.07 p=0.86
QOL Summary Index *(n=13)*	r=0.13 p=0.72	r=0.23 p=0.52	r=0.04 p=0.92	r=0.29 p=0.41
GHS *(n=13)*	r=0.38 p=0.28	r=-0.07 p=0.85	r=0.08 p=0.82	r=0.04 p=0.92

Table 42 Associations between septal extracellular volume and patient reported outcomes at two-months.
Spearman's correlation coefficient. *denotes significance.
POD – post-operative day, 2mnth – two-months post-operatively, WHO – world health organisation, MRC – medical research council, NYHA – New York Heart Association, QOL – quality of life, GHS – global health score, ECV – extracellular volume, n – number, ΔPOD2 - $\Delta T1_{POD2\text{-}pre\text{-}op}$, Δ2mnth - $\Delta T1_{2mnth\text{-}pre\text{-}op}$.

8.6 Sensitivity analysis: Change in T1 and Image Quality Score

As image quality could possibly affect the measured T1 values both pre- and post-contrast, due to inclusion of artefact in poorer quality images leading to artificially high values, associations were sought between assigned IQS and both T1 and ECV values. As described in Chapter 7, images were scored and grouped one to three. IQS was not associated with either T1 or ECV values measured anywhere in the myocardium at any study time point. (Kruskal-Wallis test, $p>0.20$ for all parameters, individual association data not shown).

8.10 Discussion

The main finding of this study is an increase in myocardial T1 and ECV, primarily in the RVIP, in the immediate post-operative period following lung resection surgery. The rises in native T1 and ECV are most notable at POD2 before trending towards baseline pre-operative values at two-months. Similar changes in the septum are shown, albeit a lesser response than the RVIP, with no changes shown in the LV across the study time period. Delta T1 in the RVIP is associated with delta RVEF in the immediate post-operative period and poorer patient reported outcomes at two-months. To my knowledge, this is the first study to measure myocardial T1 and ECV following non-cardiac surgery and demonstrate a possible inflammatory or oedematous response within the myocardium in response to such surgery.

The values for both native T1 and ECV of the LV, septum and RVIP were in keeping with the reference ranges described in the literature for global T1 and ECV using a 1.5T Siemens scanner and a MOLLI technique (as used in this study)[365 366]. Although the native T1 values measured on POD2 still fall within the defined ‘normal’ region, it is the rise from baseline values that are striking rather than the absolute value. In this study, a difference of 108ms were noted in the RVIP with a smaller rise of 32ms in the septum at POD2 from baseline. The absolute T1 and ECV values described in other disease processes, such as PH, are typically larger than described in this study; however the mean differences between normal control subjects and PH patients are similar to the difference between pre-op and post-op described in this study[334 344 349 358 364]. In a meta-

analysis examining T1 and ECV in PH, T1 values were noted to be significantly higher in the RVIP in patients with PH compared with controls with a median (IQR) difference of 108ms (89,128ms) demonstrated. As in this study a similar but lesser difference was seen in the septum showing a median (IQR) difference of 56ms (41 to 72ms)[358]. In this current study, superior and inferior RVIP demonstrated moderate to strong association with inferior RVIP demonstrating higher T1 values. These findings are consistent with other studies measuring T1, ECV and LGE at the RVIPs[337 367 368].

CMR scanner related factors can affect the measurement of T1 and ECV including field strength, dose of contrast agent, as well as the timing between injection and subsequent measurement of T1[350 365]. However, in this study the same study protocol and 1.5T scanner was used for all patients allowing for comparison across the study time period. Within patient comparison, with the same protocol and physical scanner is a significant strength of this study. Higher T1 and ECV values may also occur due to technical aspects of CMR scanning and analysis, such as inadvertently including blood pool within the ROI. As described in Chapter 7, care was taken during CMR analysis to ensure blood pool was not included in the ROI. By scoring the study images one to three and removing those images deemed poor, the image quality was improved and the likelihood of including artefact reduced. Sensitivity analysis showed image quality was not associated with raised T1 or ECV further supporting that the elevated results demonstrated in this study were due to pathological changes and not image interpretation.

Higher T1 and ECV values may occur for a number of patient related reasons including age and sex, and physiological factors such as heart rate (HR). This study reported a trend towards higher T1, delta T1, ECV and delta ECV values in the RVIP both pre-operatively and at POD2 and lower age; but this relationship was absent at two-months and was not present in the septum. The absence of a continuing trend at two-months could be explained by the number of scans available at this time point. Studies in the literature have reported conflicting associations between age and T1 and ECV values[350 365 366 369 370]. The Multi-Ethnic Study of Atherosclerosis (MESA) study reported a small positive correlation with increasing age and higher ECV values; however this study was performed in a population with multiple co-morbidities and a significant result was only shown

in older males[369]. In a healthy volunteer study, increasing age demonstrated association with lower T1 values for both men and women with a decrease in T1 by 8m/s per decade, but no change in ECV[370]. It has been suggested that increases in ECV should be expected with older age as both myocardial mass and fibrosis increase with age whereas others suggest an expected higher ECV with younger age due to increase in myocyte size and volume fraction with a decrease in the relative amount of interstitium[369-371].

In the current study, the author was able to make within-patient comparisons in a cohort of thirteen patients across three different time points. This study design would mitigate against patient factors influencing the T1 and ECV results, therefore as result of the study design, age alone is unlikely to be a factor in the rise demonstrated post-operatively[280]. Higher HR is associated with an increase in T1 values; however the change in T1 for a HR of 70 compared to that of a HR 80 has been shown to be only in the region of 10ms (932ms versus 941ms)[280 365 372]. Despite an increase in HR demonstrated in this study in the post-operative period (an increase from a mean (SD) value of 71bpm (11) at baseline to 81(8) at POD2 and 82(8) at two-months, this was not associated with increased T1 values. The significant rises in T1 in this study would not be expected to occur solely as a result of an increase in HR of 15% from baseline.

The two commonest biological determinants of an increase in native T1 are oedema (with an increase of tissue water content as a result of inflammation or acute infarction) or due to an increase of interstitial space (such as fibrosis or infarction with resultant scar tissue)[290]. ECV is a marker of myocardial tissue remodelling and an increased ECV is most often due to excessive collagen deposition (such as myocardial fibrosis).

The T1 and ECV changes in PH described in the literature are widely thought to be as a result of a chronically increased afterload with increased RV wall tension causing leftward shift of the IVS during systole[319 344]. The shift in the septum may increase mechanical stress on the VIP[319 344]. Paradoxical movement of the IVS has also been shown to result in increased strain at VIPs in non-PH conditions[373 374.] Increased traction, compression, and shear forces, at the RVIPs and IVS are believed to be particularly prone to remodelling processes[337 339]. Paradoxical movement of the septum alone without RV remodelling has been shown to

increase LGE at the VIP with a case report of a patient with an atrial septal defect (ASD). The case was that of a 50-year-old woman with a new diagnosis of secundum ASD. Prior to surgery, speckle TTE demonstrated paradoxical motion of the IVS towards the RV in early systole with CMR demonstrating LGE at the posterior VIP without evidence of PH on RHC or RV hypertrophy on imaging[374]. Following surgery to repair the ASD, repeat imaging showed no evidence of LGE at the VIP with a return to normal septal motion on TTE. The authors of the case report propose these changes may be as a result of either i) a reversible aetiology, ii) contrast pooling due disruption or disarray of myocardial fibres without overt fibrosis or myocardial damage or iii) an inflammatory process[374].

In this current study, the changes reported in the RVIP and septum may be as a result of the aetiologies described above and may be reflective of oedema, inflammation or fibrosis, or a combination of these factors. Changes in native T1 occur as a result of tissue expansion which may be as a result of increased water or collagen; however the characteristics of T1 alone on CMR do not allow differentiation between these possible aetiologies. Possible aetiologies for the increase in T1 and ECV in this study are a result of an alteration in afterload or contractility. In lung resection surgery, it has been widely demonstrated that acute increases in afterload do occur in the peri-operative period with clamping of the lobar branches of the PA and the use of OLV[142 145 148 171]. In response to these acute increases in afterload, mechanical stress may result in paradoxical movement of the septum with septal wall "bouncing." The movement of the septum may result in strain at the VIPs, represented in this study with an increase in native T1 within the RVIP, and to a lesser extent the septum. Teng et al analysed eccentricity index (EI), as a measure of septal shift occurring as a result of abnormal ventricular interactions, following lung resection using both CMR and TTE[375]. Although the study failed to demonstrate any overall change in systolic and diastolic EI post-operatively from pre-operative values, septal shift was evident in a proportion of patients and both EI parameters measured on CMR on POD2 demonstrated moderate association with RVEF on POD2[375]. This is the first study that has attempted to quantify septal movement following lung resection and despite the lack of overall change in EI, the association with RV dysfunction suggests abnormal septal movement may be a contributing factor. As discussed in Chapter 3, animal models of PE demonstrated that acute increases

in afterload trigger an acute inflammatory response that leads to disruption of the myocardial tissue resulting in altered myocardial contractility which may contribute to RV dysfunction. It is feasible that a similar aetiology is also occurring in this patient population due to an acute increase in afterload.

It is described in the literature that the changes in ECV in PH occur as a result of a fibrotic process with histological evidence of fibrosis[335 344]. Given the changes in ECV reported in this study occur in the early post-operative period, the pathological process is unlikely to be that of fibrosis in such a limited time period and is more likely representative of an oedematous process which results in disruption of the intracellular matrix of the cardiomyocytes.

Delta T1 at POD2 was associated with delta RVEF at the same study time point. By demonstrating an association between inflammatory changes in the myocardium and a deterioration in RV function, these findings further support the hypothesis that an inflammatory response may be a contributing mechanism to RV dysfunction following lung resection surgery. When observing RV function after lung resection, McCall et al reported changes in RVEF relative to baseline allowing for interpretation in context of pre-operative RVEF[376]. These authors suggest that an *absolute* change in RVEF of 5% on POD2 may be less significant if RVEF pre-operatively was 70% compared, with a pre-operative RVEF of 35% (a relative change of 7.1% versus 14.3%)[376]. In the setting of this study, by similarly measuring and reporting acute relative changes from baseline rather than absolute values are likely to be more reflective of the magnitude of the injury to the myocardium.

There are inconsistent associations between RV function and septal T1 and delta T1 in and RVIP and septal ECV and delta ECV in this study. The relationships at two-months post-operatively are not consistent with those seen on POD2. At two-months post-operatively, absolute RVIP T1 and delta RVIP T1 demonstrated a trend towards a positive relationship with absolute RVEF whereas absolute septal T1 and septal delta T1 demonstrated a trend towards a negative relationship with absolute RVEF. In this study, both RVIP and septal T1 values were returning towards baseline values and had fallen considerably from the values reported at POD2; this may account for the lack of association at this time point. The positive relationship demonstrated is not in keeping with the

hypothesis described in this study with no obvious biological explanation it may be a potentially spurious result. An alpha error may occur in this study due to the number of associations made.

Inconsistences between T1, ECV and RV function in PH are described in the literature[319 335 336 345 348 349 356]. Of those studies exploring associations between T1, ECV and CMR derived RV function (six in total including RVIP and septum), only half demonstrated a positive association between changes in T1 and RVEF[167 319 336 345 348 349]. Of the six examining septal changes and RV function, only one study demonstrated a significant association with septal T1 or ECV and RVEF[334].

Associations between ECV and a range of outcomes were not demonstrated in this study despite associations existing for native T1. Given that native T1 is a variable in the ECV equation, it would be expected that ECV may demonstrate similar associations to T1 given that both T1 and ECV rise following lung resection surgery. The trend in changes in ECV are similar to those demonstrated with T1 for some parameters (including pre-operative lung function, predicted post-operative lung function, pulmonary segments resected, and post-operative patient reported outcomes), whilst others appear to show no relationship (including post-operative RV function). Overall, there was a lack of association between absolute ECV, delta ECV and absolute RVEF and delta RVEF at both post-operative time points. Both absolute and delta ECV at the RVIP demonstrated a trend towards a very weak positive relationship with both absolute and delta RVEF. The opposite was shown at two-months, with a trend towards a very weak negative relationship. Similar trends were demonstrated with the values measured at the septum as described with the RVIP. Given that ECV does change over time, a pathological process may be occurring within the myocardium with possible oedematous changes within the RVIP and septum; however these changes do not appear to be associated with the demonstrated RV dysfunction. It may be plausible that the pathology resulting in alterations in ECV does not impact myocardial function to the same extent as the pathological process driving the increase in native T1.

Similar differences in the associations between native T1 and ECV signal and outcomes were shown in a study examining T1 and ECV at the RVIP in patients heart failure with preserved ejection fraction[337]. Despite demonstrating an

increase in both native T1 and ECV at the RVIP, only anterior RVIP native T1 was independently related with outcome and was shown to be a better predictor of outcome than ECV by multivariable analysis[337]. The authors of the study propose these findings are as a result of different pathophysiological changes resulting in variations in T1 and ECV associations with native T1 more sensitive to subtle myocardial changes within the intracellular component of the myocardium[337]. ECV is predominantly reflective of changes in the extracellular space whereas the signal for native T1 time depends on intracellular, extracellular and interstitial factors, therefore changes within the intracellular compartment (i.e. within myocytes) may not be reflected in ECV[55 377]. They go on to suggest that progressive RV afterload and mechanical stress may result in disruption of the cellular matrix in the myocardium with an accumulation of fluid. These changes then result in disruption to the cardiomyocyte energy state with a decrease in intracellular levels of phosphocreatine and adenosine triphosphate. These alterations result in cardiomyocyte membrane instability and intracellular fluid shift[337 378]. As a result of changes primarily in the intracellular compartment of the myocardium, increases in native T1 were more sensitive to the subtle alterations to the intracellular component. Techniques, such as MRS, have the ability to examine cardiomyocyte energy state and metabolism and could be considered for future studies to offer further insight into changes at an intracellular level[57 58].

Another possible explanation in this current study for the difference reported in association between T1 and ECV and clinical outcomes is the availability of data for both native T1 and ECV parameters for analysis. Given that the post contrast T1 maps had a higher number of poor IQS and therefore were removed from analysis, a number of ECV values were missing, particularly at POD2 time point. Twelve pre-contrast scans were available for analysis at POD2 therefore 12 T1 values were available whereas three POD2 post-contrast scans had an IQS of one and were excluded leaving only nine scans to calculate an ECV value at that time point. A reduction in one quarter of available results in a small study like this will have a significant impact on the study's power. At two-months post-operatively, ten pre-contrast scans and nine post-contrast scans were available, allowing for nine calculated ECV values. The lack of ECV data may account for the lack of associations presented in this study. Given the changes shown in

native T1 and the excellent T1 image quality with native T1 maps, it may be considered to only use native T1 imaging in future studies and therefore avoid the use of IV contrast and the necessity to exclude patients with pre-existing renal dysfunction. One disadvantage of such a technique is the challenges of comparing native T1 values across different CMR scanners whereas ECV comparisons are not affected by the individual CMR scanner employed (as discussed in Chapter 4).

Unfortunately, due to the small size of this study, robust interpretation of the clinical implications of altered myocardial T1 and ECV is limited. Due to the large number of associations made, these must be considered to be primarily hypothesis generating and will require validation in a larger study. Of the surgical and anaesthetic factors examined, the number of segments resected was associated with native T1 post-operatively with a larger number of resected segments associated with both higher absolute and delta T1 values. Studies have demonstrated the extent of lung resection may have an impact on the degree of post-operative RV dysfunction[162 163 211]. It is plausible that with a larger pulmonary resection, there is a greater increase in post-operative afterload resulting in the increased inflammatory response (increase in T1 in this study). The larger the surgical resection may result in a larger intrinsic myocardial injury. It is feasible that alterations in myocardial T1 would be present in other surgeries which employ OLV, such as oesophagectomy, or indeed it may be that all surgical insults result in a triggered inflammatory response in the myocardium. Insights from other surgical procedures, with similar characteristics to lung resection surgery, may help to ascertain the underlying mechanisms resulting in raised T1 and ECV in the post-operative period. Given that this is the first study to observe T1 changes in the post-operative period, I am unable to draw any comparisons with other similar surgical insults. Neither pre-operative or Intra-operative anti-inflammatory use was associated with either T1 or ECV in either the RVIPs or septum at any study time point..

This study demonstrated a strong association between poorer pre-operative and predicted post-operative lung function and higher T1 values in the RVIP and septum. Associations between RV dysfunction and lung function have been shown in other studies with those with poorer pre-existing lung function showing a greater degree of postoperative RV dysfunction[376]. Higher PA pressures have

also been shown to be associated with lower TLCO% in patients with severe chronic lung disease suggesting a link between poor pulmonary function and RV-PA dynamics[379]. It would seem that in this study, those with both poor pre-operative and predicted post-operative lung function are likely to sustain a more significant myocardial inflammatory injury. It may be as a result of pre-existing poor lung function, the RV-PA dynamics are already distorted with reduced pulmonary vascular flow and RV contractile reserve and therefore further injury to the cardiac-pulmonary system during lung resection surgery results in a more significant impact with less ability to compensate[184].

In PH, data showing association between myocardial T1 and ECV values and longer-term outcomes are lacking. Asano et al demonstrated higher RV T1 values are predictive of hospitalisation and survival rates in PH; however Saunders et al reported RV T1 values were not associated with mortality in PH[345 349]. Higher myocardial T1 values have been shown to be predictive of poorer outcome in patients with heart failure with anterior RVIP values independently associated with survival[337 380]. In this study, neither T1 or ECV showed association with length of critical care stay or hospital stay and given that only one patient died in the year following recruitment to the study, no associations with T1 or ECV and survival were sought.

However in this study T1 and ECV did demonstrate association with patient reported post-operative outcomes and QoL. Patients with higher T1 and ECV values at POD2 reported a poorer quality of life at two months with patients reporting a decline in their ability to self-care and mobilise. Data available in the literature demonstrating an association between T1 or ECV values and patient reported outcomes is limited with studies primarily focusing on association between physiological or imaging evidence of myocardial dysfunction and T1 and ECV. A small number of studies have shown association between poorer NYHA scores and increased global ECV in cardiomyopathy and heart failure patient populations[381 382].

8.11 Strengths and Limitations

This the first use of native T1 mapping in the post lung resection surgery population. The study recruited a modest number of patients, with a small

number of dropouts at two months post-operatively and as a result of poorer quality post contrast images in the immediate post-operative period, the number of CMR T1 maps available for analysis was reduced and therefore may impact on the results shown.

The patients in this thesis did not undergo right heart catheterisation (RHC) as part of the study protocol and as a result, I may fail to observe associations between T1, ECV and RHC derived RV function parameters demonstrated in other studies utilising RHC as well as CMR. The ability to utilise RHC may help to unravel the theories regarding potential underlying mechanisms, in particular the increase in afterload and altered contractility hypothesis. In PH, mPAP has been shown to demonstrate association with both native T1 and ECV, and it is possible these associations could be demonstrated in this thesis patient population[340]. Tello et al measured RV-arterial coupling using a pressure-volume catheter and sought association with T1 in patients with PH[343]. The study measured end-systolic elastance (Ees) as a measure of RV contractility, and the ratio of Ees to PA elastance (Ees: Ea – i.e. coupling) as an assessment of RV contractility adaptability in the face of increased afterload. These measures of contractility demonstrated association with global T1 and VIP values[343]. Given that an increase in T1 may result in an alteration in contractility, future studies exploring this hypothesis further may wish to consider the ability to measure contractility using a pressure-volume catheter. In PH, RHC is used as part of routine investigation for patients with possible PH and is therefore able to provide observations of myocardial function as part of standard of care. Patient's undergoing lung resection surgery do not routinely have RHCs inserted; however this could be considered in future research.

In this study, I opted to only utilise CMR for measuring RV function and did not undertake TTE analysis as part of the study protocol. In other studies measuring T1 and ECV, associations have been shown with TTE, in particular newer techniques including strain[334]. Habert et al showed global RV ECV was strongly associated with TAPSE ($r=-0.64$, $p=0.03$), S' wave ($r=-0.71$, $p<0.01$), and septal strain ($r=-0.71$, $p=0.01$) in a PH cohort[334]. As described previously, strain may be a less load dependant measure of cardiac function in comparison with RVEF and therefore by examining strain parameters, surrogate markers of contractility may be explored. It is feasible that it may have been possible to demonstrate

association with TTE derived measures of contractility and T1. In this study, I sought only to use CMR as it is the gold standard for assessment of the RV and TTE presents challenges when assessing the RV, particularly in a lung resection cohort (as described in Chapter 1 and 4).

As described, this is a small single centre study with a large number of associations sought between myocardial evidence of inflammation and pre-, intra- and post-operative measures. As a result, the results presented should be considered as hypothesis generating and require a larger study to test the validity in a wider lung cancer patient population.

Additionally, no histological analysis was performed in this study and therefore I cannot completely exclude the possibility that the increases in T1 could be explained by inclusion of blood or myocardium within the ROI. Other studies have shown alterations in T1 correlate with histological evidence of inflammation or oedema in a range of pathologies[283 344 383-385]. A study performing both CMR and histological sampling of the myocardial tissue could be considered in an animal model of lung resection surgery to demonstrate correlation between T1 and histological changes in the myocardium.

8.12 Conclusions

This is the first study to demonstrate an increase in myocardial T1 in the early post-operative period following lung resection surgery. Increases in both T1 and ECV are present in the RVIP and septum with absence of changes within the LV. Relative changes in RVIP T1 are associated with relative changes in RVEF suggesting a link between an intrinsic myocardial injury, as a result of lung resection surgery, and resultant RV dysfunction. The alterations in T1 and ECV suggest an early inflammatory insult occurs; potentially as a result of one-lung ventilation, clamping of the lobar branches of the PA or due to the surgical insult itself with resection of multiple lung segments or a combination of both factors.

Not only does native T1 and ECV demonstrate association with evidence of RV dysfunction on CMR, association is also demonstrated with post-operative patient reported outcomes and poorer QoL. The reported decline in functional

status and QOL are in keeping with other studies in this patient population; however this is the first study to show a possible link between patient reported outcomes and associated myocardial injury following lung resection. It has been widely reported that predicted post-operative lung function alone is a poor indicator of poorer post-operative functional outcomes however, CMR parameters of myocardial dysfunction may have the potential to identify those at risk of longer-term poor functional outcomes.

Further larger studies are required to validate these results and explore the plausible inflammatory hypothesis. It is feasible that future work may seek to explore potential therapeutic pathways to ameliorate the inflammatory response. A potential role may exist for anti-inflammatory modulation prior to, or during lung resection surgery to blunt the inflammatory process displayed within this study.

Chapter 9 Biomarkers of Myocardial Function Following Lung Resection

9.1 Introduction

This chapter describes the results of the biomarkers BNP, NT-proBNP, TnI, and CRP. BNP, NT-proBNP and TnI were analysed at eight times points (pre-operatively, immediately post-operatively in recovery, six- and 12 hours post-operatively, POD one to three and at two-months post-operatively). CRP was analysed pre-operatively, POD two and at two-months post-operatively. This chapter also compares BNP and NT-proBNP following lung resection to determine time of the peak rise of both biomarkers in the post-operative period. Finally, it describes associations between biomarkers and CMR measures of cardiac function and CMR measures of myocardial inflammation.

As biomarkers were measured at eight peri-operative time points, in order to limit the number of comparisons and reduce the risk of Type-1 error, the author limited the number of associations explored. Associations were sought and are reported at the following time points; pre-operatively, peak post-operative time point for each individual patient, POD2 and POD3 (POD3 was also included as a small number of patients underwent CMR scanning on this day as they were unable to attend for CMR on POD2), and at two-months post-operatively.

Biomarker results were unavailable for one patient at six and twelve hours post-operatively as no staff were present to perform venepuncture and immediate analysis of the samples. Results were unavailable at two-months in three patients as they were unable to attend for follow-up (as described in Chapter 6). Biomarker results were available in all 14 patients at all other time points. CRP was unavailable for three patients at two-months for the same reasons described above. CRP was available in all 14 patients at pre-operative and POD2 time points.

On visual inspection of the data, one patient appeared as an outlier with a *reduction* in BNP in the immediate post-operative period demonstrated. On closer inspection of the data, the pre-operative BNP value was measured at 10.3pg/ml, this fell to 7.9pg/ml at six hours post-operatively before rising back

to baseline values at twelve hours (10.5pg/ml) and remaining at these values until POD2 where it rose slightly to 12.5pg/ml before dropping again to lower than pre-operative values at POD3 (5pg/ml). This contrasted with the thirteen other patients in the study who demonstrated an increase in the immediate post-operative period before returning to baseline values later in the post-operative period. The patient (RV2) was also an outlier for RVEF and T1 (as described in Chapter 6 and Chapter 8) and subsequently was also removed from further analysis in this chapter. This chapter describes results of the remaining 13 patients.

9.2 Changes in biomarkers over time

The change in BNP, NT-proBNP, troponin and CRP over the study time period are explored (Table 43).

9.2.1 BNP

BNP increased over time ($p=0.02$, Friedman's test, Table 43 and Figure 65) with a significant rise at all time points from baseline (all $p<0.04$, Wilcoxon Signed Rank, Table 43 and Figure 65).

9.2.2 NT-proBNP

NT proBNP increased over time (Friedman's test, $p < 0.001$, Table 40 and Figure 66) with a significant rise from baseline at post-operative days one, two and three before returning back towards baseline at two-months (Wilcoxon Signed Rank, $p<0.03$, Table 43 and Figure 66).

	Pre-op	Recovery	6hr	12hr	POD1	POD2	POD3	2mnth	p-value
BNP	27 (20, 59)	50† (27, 75)	63† (30, 115)	88† (34,148)	82† (41,132)	74† (43,179)	128† (44, 179)	87† (15, 154)	0.02*‡
NT-pro	92 (45, 188)	66 (41,187)	100 (62, 316)	149 (80, 271)	202† (104, 305)	263† (128 ,637)	518† (281, 906)	268 (75, 591)	<0.01*‡
TnI	<0.05	<0.05	<0.05	<0.05	<0.05	<0.05	<0.05	<0.05	1.0‡
CRP	3 (3, 13)					98† (40, 134)		26† (3, 56)	<0.01*‡

Table 43 Biomarkers over time
Results are median (IQR). Friedman's test analysis at all time points. Pairwise comparison between each individual post-operative time point and baseline value assessed via the Wilcoxon Signed rank test. All units in pg/ml. * - denotes significance, † significant increase from baseline. ‡ denotes change in value over time assessed by Friedman's test
Pre-op - pre-operative. 6h - six hours. 12h - 12 hours. POD - post-operative day, 2mnth – two-months post-operatively, BNP - b-type natriuretic peptide. NT-pro - n-terminal proBNP. TnI - troponin I.. CRP - c-reactive protein.

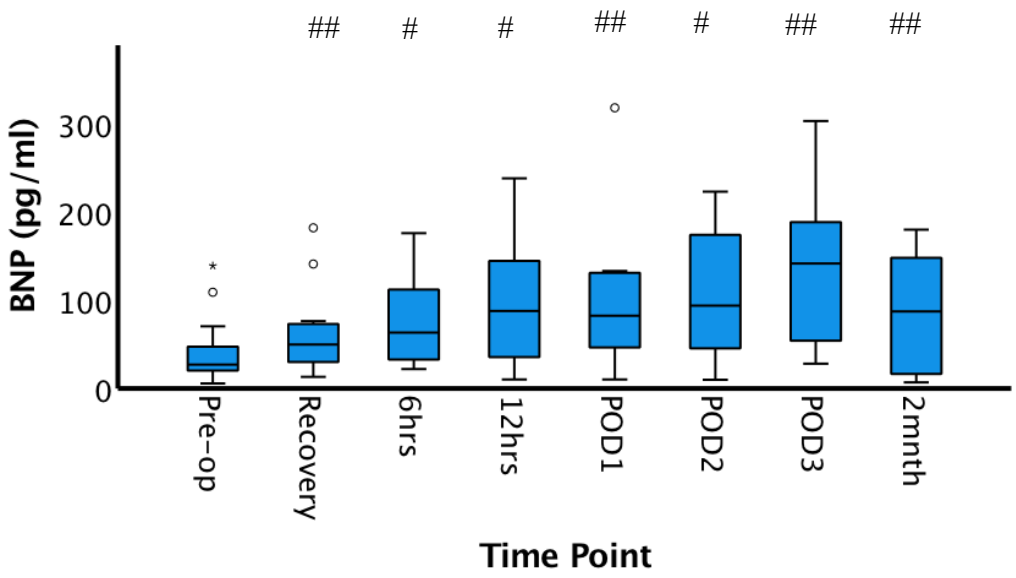

Figure 65 Change BNP over time
Box plots represent median (IQR) . ## = p< 0.01, # = p< 0.05.
Pairwise comparison between each individual post-operative time point and baseline value assessed via the Wilcoxon Signed rank test.
BNP = B-type natriuretic peptide. Preop - pre-operative, hrs – hours, POD2 - post-operative day two, 2mnth – two-months post-operatively.

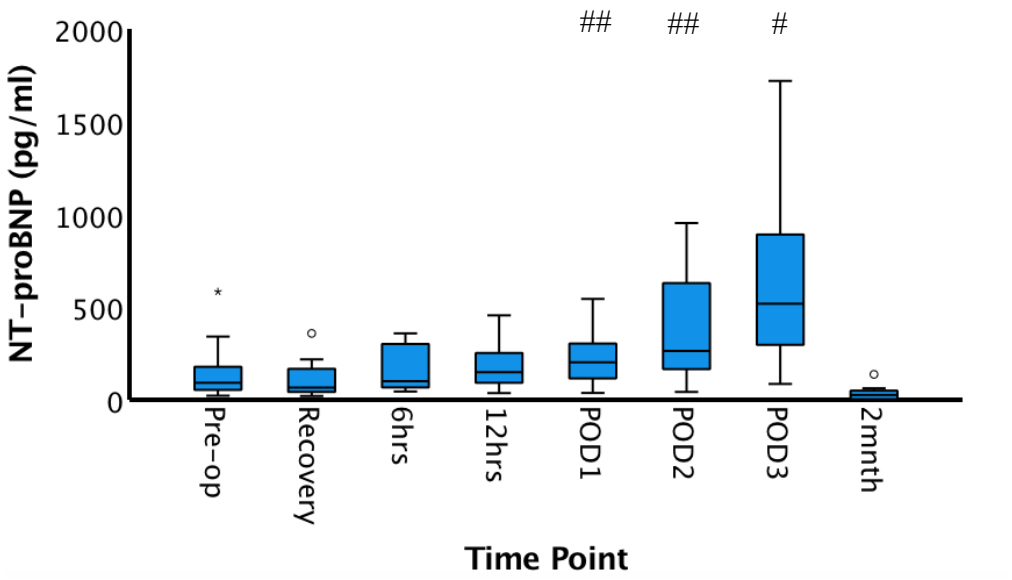

Figure 66 Change in NT-proBNP over time
Box plots represent median (IQR). # = p< 0.01, ## = p< 0.05.
Pairwise comparison between each individual post-operative time point and baseline value assessed via the Wilcoxon Signed rank test.
NT-proBNP = N-terminal pro B-type natriuretic peptide. Preop - pre-operative, hrs – hours, POD2 - post-operative day two, 2mnth – two-months post-operatively.

9.2.3 Troponin

There was no change in troponin over the study time period with all patients displaying a troponin of <0.05pg/ml at all study time points.

9.2.4 C-Reactive Protein

There was an increase in CRP at both POD2 and two-months with the most notable rise being in the early post-operative period (Friedman's p<0.01, Figure 67).

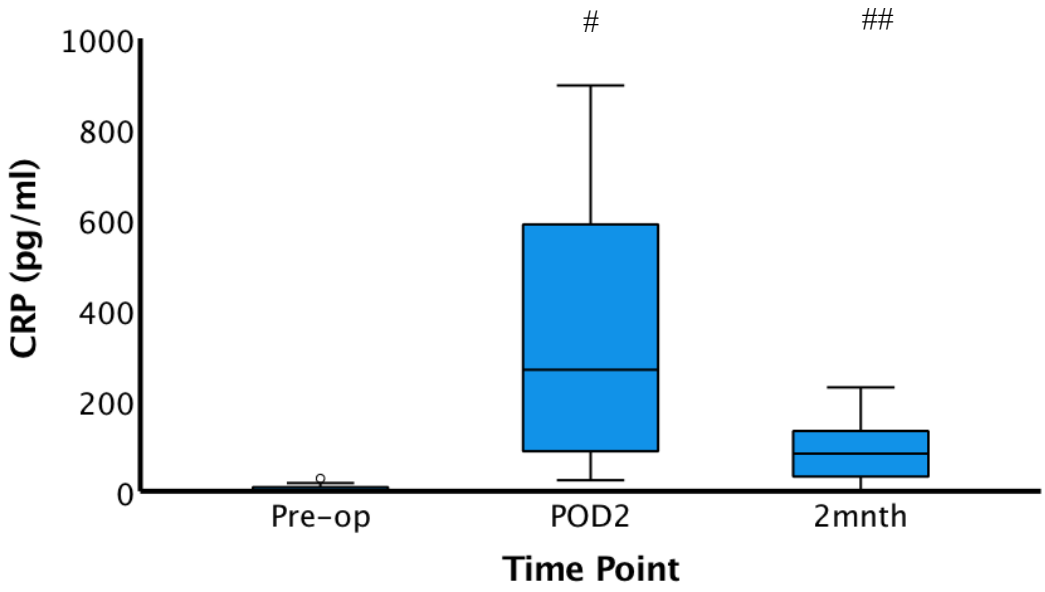

Figure 67 Change in C-reactive protein over time
Box plots represent median(IQR). # = p< 0.01, ## = p< 0.05.
Pairwise comparison between each individual post-operative time point and baseline value assessed via the Wilcoxon Signed rank test.
CRP - C-reactive protein. Preop - pre-operative, hrs – hours, POD2 - post-operative day two, 2mnth – two-months post-operatively.

9.3 Comparison of Peak BNP and NT-proBNP in the Post-Operative Period

The peak time point was defined as the study time point at which the biomarker value demonstrated the first peak in each patient. The median (IQR) time to BNP peak rise was 12 hours (6, 24) with a median peak BNP value of 116pg/ml (58, 201) at this time point (Figure 68). The trend in BNP was that of a drop on POD1 and POD2 before rising again on POD3.

The median time for peak rise for NT-pro BNP was 72 hours (36, 72 hours) with a peak value of 452pg/ml (246, 907pg/ml) (Figure 68). Peak BNP and peak NT-proBNP values demonstrated good correlation (Spearman's, r=0.60, p=0.03, Figure 69).

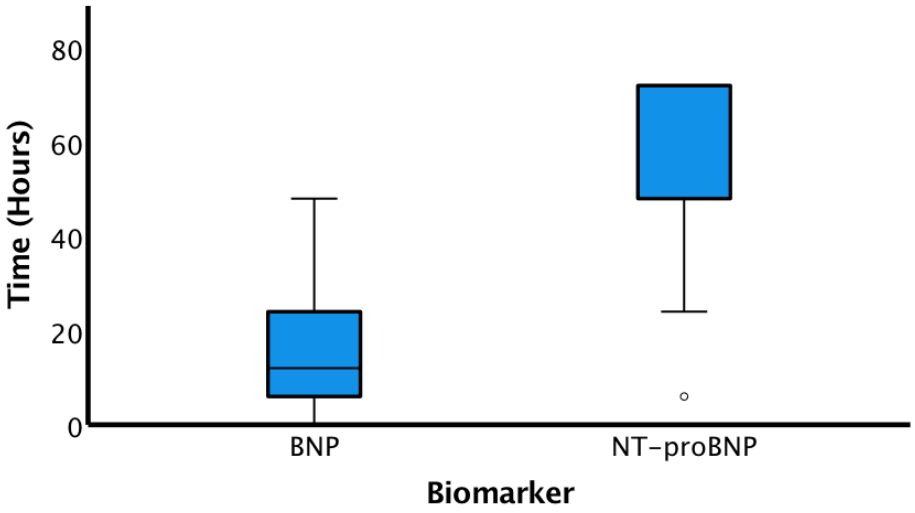

Figure 68 Time to peak BNP versus NT-proBNP in hours.
Box plots represent median (IQR). Wilcoxon signed-rank test p= 0.01.
BNP – B type natriuretic peptide, NT-proBNP – N-terminal pro B-type natriuretic peptide.

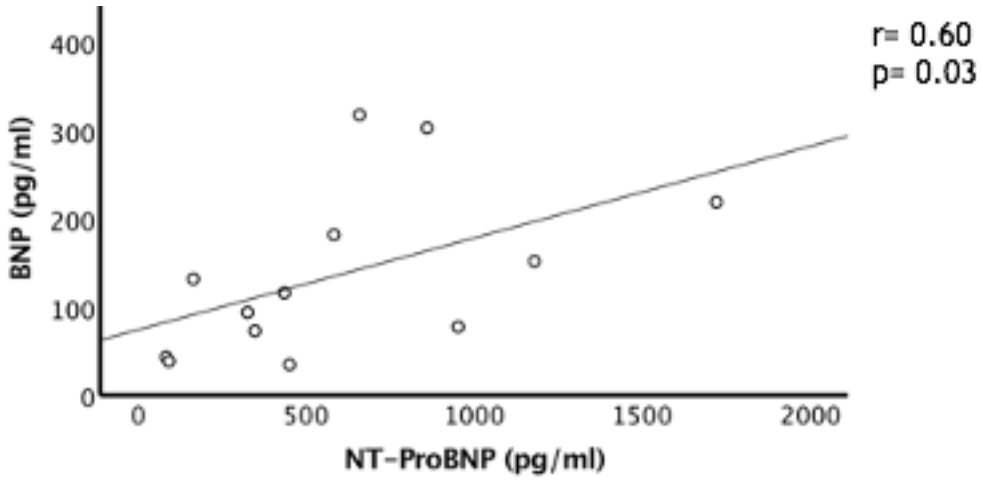

Figure 69 Association between peak BNP and NT-proBNP.
Spearman's correlation coefficient.
BNP – B type natriuretic peptide, NT-proBNP – N-terminal pro B-type natriuretic peptide.

9.4 Association of Biomarkers and CMR Measures of Cardiac Function

9.4.1 BNP

Associations were sought between BNP, ΔBNP and CMR markers of both LV and RV function and volumes.

9.4.1.1 BNP and Right Ventricular Volume and Function

Pre-operatively, higher BNP values were associated with measurements of pre-operative RV function and volume including a moderate negative association with RVEF (Spearman's test, r=-0.62, p=0.02, Figure 70), a strong positive association with RVESV (Spearman's test r=0.60, p=0.03) and a trend towards a moderate positive association with RVEDV which did not reach statistical significance (Spearman's test, r=0.52, p=0.09).

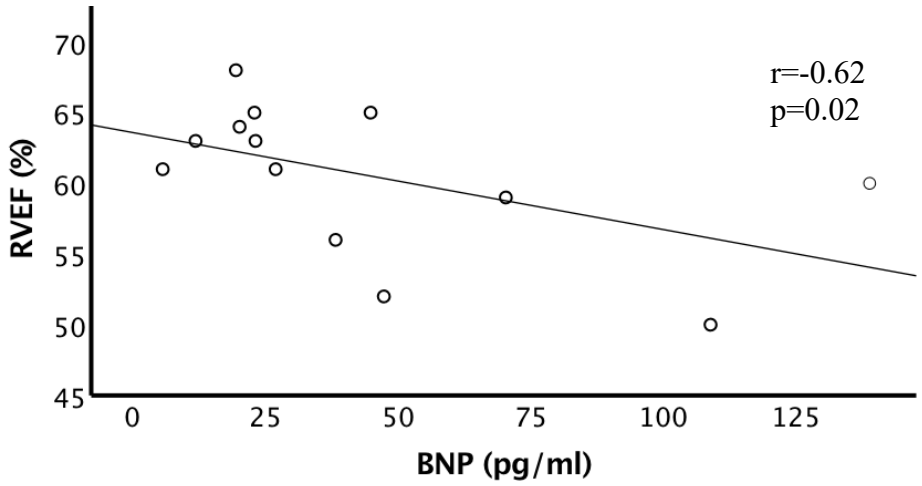

Figure 70 Association between pre-operative RVEF and pre-operative BNP
Spearman's correlation coefficient.
RVEF – right ventricular ejection fraction, BNP – B-type natriuretic peptide.

Post-operatively, those patients with higher BNP (POD2 and POD3) demonstrated lower RVEF at POD2, however these relationships did not reach significance (Table 44, Figure 71). ΔBNP measured at the same time period was not associated with POD2 ΔRVEF (Table 45). At two-months, lower RVEF demonstrated association with higher BNP, but again did not reach significance (Table 44). No association was shown between ΔBNP and ΔRVEF at two-months (Table 45).

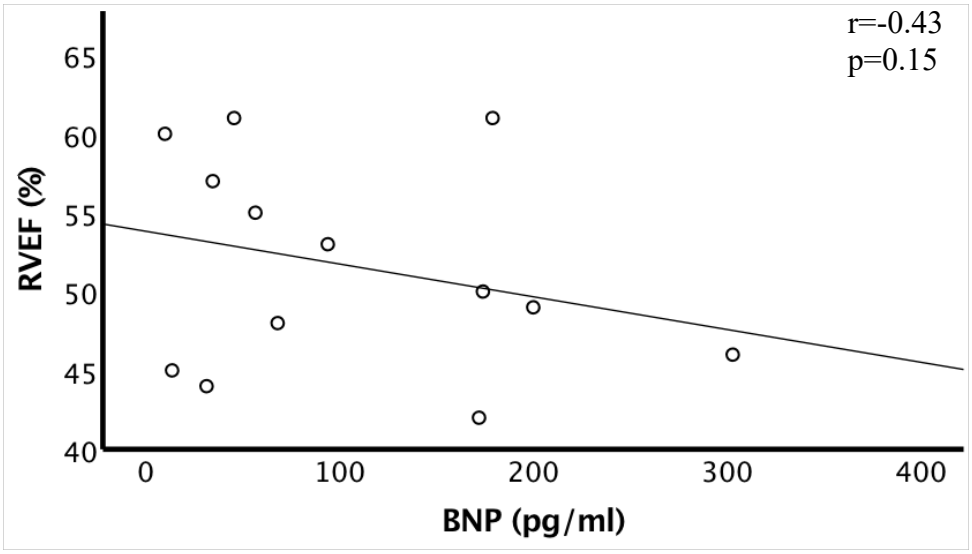

Figure 71 Association between right ventricular ejection fraction on day two and BNP on day two.
Spearman's correlation coefficient.
RVEF – right ventricular ejection fraction, BNP – B-type natriuretic peptide.

On POD2, RV volumes (ESV and EDV) did not demonstrate association with BNP (Spearman's test, r<0.49 and p>0.09 for all parameters, data not shown). Strong associations were demonstrated with RV volumes measured at two months and BNP; two-month RVEDV and two-month BNP (Spearman's test, r =0.62, p=0.05) and two-month RVESV and two-month BNP (Spearman's test, r=0.69, p=0.03).

	Peak BNP *(n=12)*	**POD2 BNP** *n=(13)*	**POD3 BNP** *n=(13)*	**2mnth BNP** *n=(10)*
POD2 RVEF *(n=12)*	r= -0.10 p= 0.75	r= -0.43 p= 0.15	r= -0.40 p= 0.22	
2mnth RVEF *(n=10)*				r= -0.52 p= 0.12

Table 44 Associations between absolute right ventricular ejection fraction and BNP.
Spearman's correlation coefficient.
RVEF – right ventricular ejection fraction, 12hr – twelve hours post-operatively, POD – post-operative day, 2mnth – two months post-operatively.

	ΔPeak BNP *(n=12)*	**ΔPOD1 BNP** *n=(13)*	**ΔPOD2 BNP** *n=(13)*	**Δ2mnth BNP** *n=(10)*
ΔPOD2 RVEF *(n=12)*	r= 0.25 p= 0.42	r= 0.35 p= 0.26	r= 0.15 p= 0.65	
Δ2mnth RVEF *(n=10)*				r=-0.37 p=0.26

Table 45 Associations between delta right ventricular ejection fraction and delta BNP.
Spearman's correlation coefficient.
RVEF – right ventricular ejection fraction, 12hr – twelve hours post-operatively, POD – post-operative day, 2mnth – two months post-operatively, ∆12hr -(12hours-pre-op), ∆POD1 - (POD1-pre-op), ∆POD2 - (POD2-pre-op), ∆2mnth- (2month-pre-op).

9.4.1.2 BNP and Left Ventricular Volumes and Function

Similar results were shown with measures of LV function and volumes with higher pre-operative BNP values once again demonstrating strong association with lower pre-operative LVEF (Spearman's test, r=-0.73, p=0.004, Figure 72), and a strong association with higher pre-operative LVESV and LVEDV (Spearman's test, r=0.72 and 0.68, p=0.06 and 0.01 respectively). No association was shown between LVEF and BNP at any post-operative time point (Table 46). LV volumes (ESV and EDV) at POD2 and two-months did not demonstrate association with

BNP at any time point (Spearman's r <-0.49, p>0.13 for all parameters, data not shown).

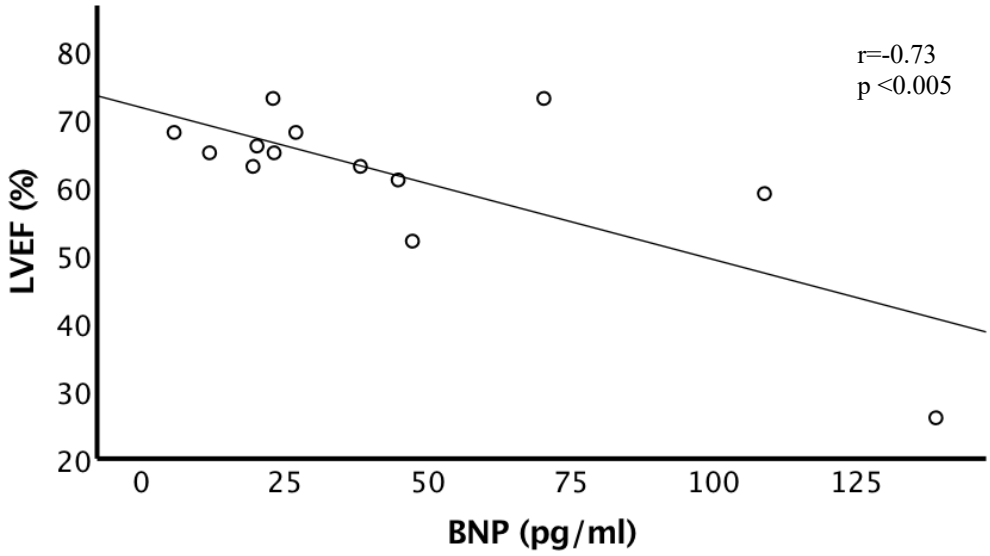

Figure 72 Association between left ventricular ejection fraction and BNP pre-operatively.
Spearman's correlation coefficient.
LVEF – left ventricular ejection fraction, BNP – B-type natriuretic peptide.

	Peak BNP *(n=12)*	**POD2 BNP** *n=(13)*	**POD3 BNP** *n=(12)*	**2mnth BNP** *n=(10)*
POD2 LVEF *(n=12)*	r= -0.15 p= 0.63	r=-0.35 p= 0.26	r= -0.55 p= 0.08	
2mnth LVEF *(n=10)*				r= -0.53 p= 0.15

Table 46 Associations between BNP and LVEF.
Spearman's correlation coefficient.
LVEF – left ventricular ejection fraction, POD – post-operative day, 2mnth – two month post-operatively, n = number. • denotes significance.

9.4.2 NT-proBNP

Associations were sought between NT-proBNP, ΔNT-proBNP and CMR markers of both LV and RV function and volumes.

9.4.2.1 NT-proBNP and Right Ventricle Function and Volumes

The associations for NT-proBNP and RV function differ from those shown for BNP described above. Pre-operative RVEF and RVEDV did not demonstrate association

with pre-operative NT-proBNP (Spearman's test r<0.51, p>0.08 for both parameters, data not shown). A strong association was however evident between pre-operative NT-proBNP and pre-operative RVESV (Spearman's test, r=0.75, p=0.003)

No post-operative NT-proBNP or ΔNT-proBNP value demonstrated association with post-operative RVEF or Δ RVEF (Tables 47 and 48). No associations were shown between POD2 RV volumes and POD2 NT-proBNP values (Spearman's test, r<0.25 p>0.52 for all parameters, data not shown). RVEDV at two-months demonstrated a strong association with two-months NT-proBNP (Pearson's r=0.70, p=0.03) with no association between RVESV and NT-proBNP at two-months (Pearson's r=0.34, p=0.32).

	Peak NT *n=(13)*	**POD2 NT** *n=(13)*	**POD3 NT** *n=(12)*	**2mnth NT** *n=(10)*
POD2 RVEF *(n=12)*	r= -0.13 p= 0.67	r= -0.17 p= 0.60	r= -0.31 p= 0.36	
2mnth RVEF *(n=10)*				r=-0.40 p=0.26

Table 47 Associations between absolute right ventricular function and NT-proBNP post-operatively.
Spearman's correlation coefficient.
RVEF – right ventricular ejection fraction, POD – post-operative day, 2mnth – two months post-operatively, NT- NT-proBNP.

	ΔPeak NT *n=(13)*	**ΔPOD2 NT** *n=(13)*	**ΔPOD3 NT** *n=(12)*	**Δ2mnth NT** *n=(10)*
ΔPOD2 RVEF *(n=12)*	r= 0.05 p= 0.87	r=0.10 p=0.75	r=0.31 p=0.35	
Δ2mnth RVEF *(n=10)*				r=0.35 p=0.33

Table 48 Associations between delta right ventricular ejection fraction and delta NT-proBNP
Spearman's correlation coefficient.
RVEF – right ventricular ejection fraction, POD – post-operative day, 2mnth – two months post-operatively, NT- NT-proBNP, ΔPOD2 - (POD2-pre-op), ΔPOD3 - (POD3-pre-op), Δ2mnth - (2month-pre-op).

9.4.2.2 NT-proBNP and Left Ventricle Function and Volumes

As with BNP and LVEF, higher pre-operative NT-proBNP values were strongly associated with lower pre-operative LVEF values (Spearman's test, r=-0.82, p<0.001), higher LVEDV values (Spearman's test, r=0.86, p <0.001) and higher LVESV values (Spearman's test, r=0.87, p <0.001).

There was no association between LV parameters and NT-proBNP post-operatively at either POD2 or two-months (Table 49). No associations were shown between any post-operative NT-proBNP measurement and either LVEDV or LVESV post-operatively (Spearman's test, r=0.52 p>0.07 for all parameters, data not shown).

	Peak NT *n=(13)*	**POD2 NT** *n=(13)*	**POD3 NT** *n=(12)*	**2mnth NT** *n=(10)*
POD2 LVEF *(n=12)*	r= -0.43 p= 0.14	r= -0.35 p= 0.26	r= -0.55 p= 0.08	
2mnth LVEF *(n=10)*				r= -0.53 p= 0.15

Table 49 Association between NT-proBNP and left ventricular ejection fraction.
Spearman's correlation coefficient.
NT- NT-proBNP, LVEF – left ventricular ejection fraction, POD – post-operative day, 2mnth – two month post-operatively,

9.4.3 CRP

CRP on POD2 showed a strong association with POD2 RVEF (Spearman's test, r=0.60, p=0.04, Figure 73). No association was shown between CRP at two-months and RVEF at two-months (Spearman's test, r=0.39, p=0.31). CRP did not show association with RV volumes or LV function or volume at any time point (Spearman's test, r<0.36, p>0.33 for all parameters, data not shown).

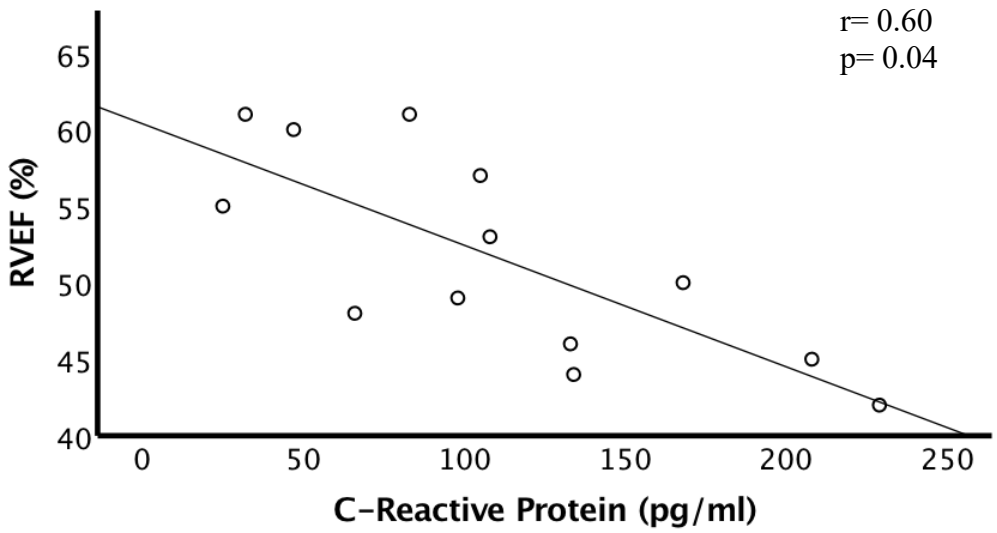

Figure 73 Association between right ventricular ejection fraction and C-reactive protein at post-operative day two.
Spearman's correlation coefficient.
RVEF – right ventricular ejection fraction.

9.5 Association of Biomarkers and CMR Measures of Inflammation

9.5.1 BNP

Associations were sought between T1 and ECV values at the RVIP and septum and BNP, and ΔT1 and ΔECV values at the RVIP and septum and ΔBNP.

9.5.1.1 BNP and Right Ventricular Insertion Point T1

Pre-operative BNP did not demonstrate association with pre-operative T1 measured at the RVIP (Spearman's test, r=0.45, p=0.15). Neither T1 nor ΔT1 at the RVIP on POD2 demonstrated any association with BNP measured post-operatively (Tables 50 and 51). Interestingly, a negative relationship was demonstrated with higher T1 and ΔT1 values and lower BNP and ΔBNP results in the early post-operative period which did not reach significance (Tables 50 and 51). No association was demonstrated between T1, ΔT1, BNP and ΔBNP at two-months post-operatively (Tables 50 and 51).

	Peak BNP *(n=12)*	POD2 BNP *n=(13)*	POD3 BNP *n=(12)*	2mnth BNP *n=(10)*
POD2 RVIP T1 *(n=12)*	r= -0.10 p= 0.75	r= -0.36 p= 0.25	r= -0.13 p= 0.70	
2mnth VIP T1 *(n=10)*				r= -0.04 p= 0.91

Table 50 Association between absolute T1 values at right ventricular insertion point and absolute BNP post-operatively.
Spearman's correlation coefficient.
POD-post-operative day, 2mnth – two-months post-operatively, VIP – ventricular insertion point, n – number.

	Δ Peak BNP *(n=12)*	ΔPOD2 BNP *n=(13)*	ΔPOD3 BNP *n=(12)*	Δ2mnth BNP *(n=10)*
ΔPOD2 VIP T1 *(n=12)*	r= -0.25 p= 0.44	r= -0.34 p= 0.29	r= -0.26 p= 0.43	
Δ2mnth VIP T1 *(n=10)*				r= 0.24 p= 0.51

Table 51 Association between delta T1 values at right ventricular insertion point and delta BNP post-operatively.
Spearman's correlation coefficient.
POD-post-operative day, 2mnth – two-months post-operatively, VIP – ventricular insertion point, n – number, ∆12hr -(12hours-pre-op), ∆POD2 - (POD2-pre-op), ∆POD3 - (POD3-pre-op), ∆2mnth-(2month-pre-op).

9.5.1.2 BNP and Septal T1

Higher pre-operative BNP levels were associated with higher T1 values measured in the septum pre-operatively (Spearman's test, r=0.69, p<0.01). Despite associations pre-operatively, these were not demonstrated in the immediate post-operative period with no association between T1, ΔT1, BNP and ΔBNP at either 12 hours, or POD2 or POD3 (Tables 52 and 53).

BNP and T1, both measured at 2 months post-operatively, did demonstrate a strong positive association with higher BNP values associated with higher T1 vales at the septum (Table 52 and Figure 74). These associations were not demonstrated with ΔT1 and ΔBNP (Table 53).

	Peak BNP *(n=12)*	POD2 BNP *n=(13)*	POD3 BNP *n=(12)*	2mnth BNP *n=(10)*
POD2 Septum T1 *(n=12)*	r= 0.11 p= 0.73	r= -0.04 p= 0.91	r= -0.18 p= 0.64	
2mnth Septum T1 *(n=10)*				**r= 0.81** **p <0.01***

Table 52 Association between absolute T1 values at and the septum and absolute BNP post-operatively.
Spearman's correlation coefficient. * - denotes significance
POD-post-operative day, 2mnth – two-months post-operatively.

	Δ Peak BNP *(n=12)*	ΔPOD2 BNP *n=(13)*	ΔPOD3 BNP *n=(12)*	Δ2mnth BNP *(n=10)*
ΔPOD2 Septum T1 *(n=12)*	r=-0.13 p=0.68	r=0.04 p=0.89	r=0.06 p=0.85	
Δ2mnth Septum T1 *(n=10)*				r= 0.16 p= 0.63

Table 53 Association between delta T1 values at the septum and delta BNP post-operatively.
Spearman's correlation coefficient.
POD-post-operative day, 2mnth – two-months post-operatively, n – number, ∆12hr -(12hours-pre-op), ∆POD2 - (POD2-pre-op), ∆POD3 - (POD3-pre-op), ∆2mnth- (2month-pre-op).

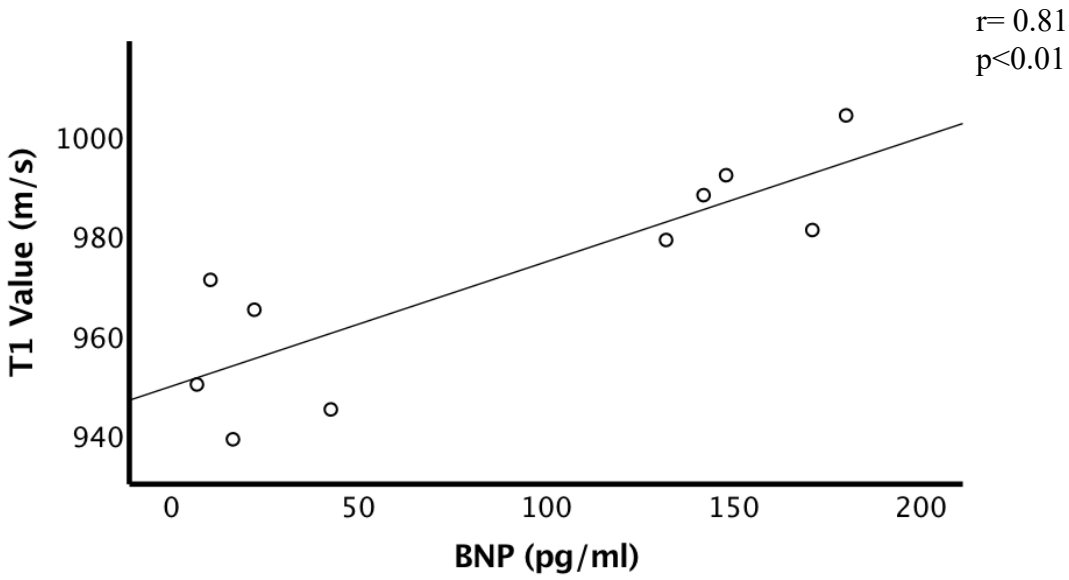

Figure 74 Association between absolute T1 in the septum and absolute BNP at two-months post-operatively.
Spearman's correlation coefficient.
BNP – B-type naturetic peptide.

9.5.1.3 BNP and Right Ventricular Insertion Point Extra-Cellular Volume

In the early post-operative period, there was trend of lower ECV values associated with higher BNP values with a strong negative association between ECV and BNP both measured on POD2 (Table 54 and Figure 75), the inverse relationship of which may be expected. POD2 ECV and Peak BNP and POD3 BNP demonstrated a similar trend but this did not reach significance (Table 54). No association was shown between ΔECV and ΔBNP in the immediate post-operative period (Tables 54 and 55). In the later post-operative period, higher BNP and ΔBNP were associated with higher ECV and ΔECV at two-months; however this did not reach significance (Tables 54 and 55).

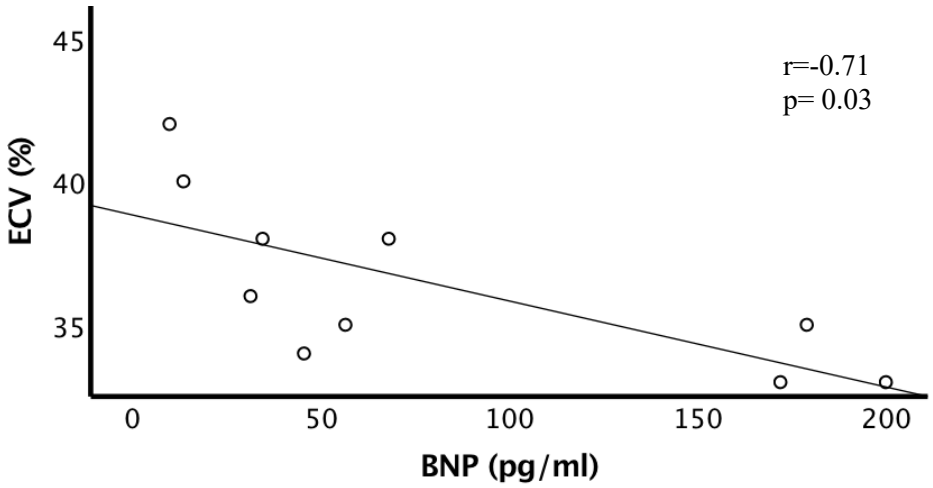

Figure 75 Association between extracellular volume in the right ventricular insertion point and BNP measured on post-operative day two.
Spearman's correlation coefficient.
ECV – extracellular volume, BNP – B-type naturetic peptide.

	Right Ventricular Insertion Point			
	Peak BNP *(n=12)*	**POD2 BNP** *n=(13)*	**POD3 BNP** *n=(12)*	**2mnth BNP** *n=(10)*
POD2 VIP ECV *(n=9)*	r=-0.60 p=0.08	**r=-0.71 p=0.03***	r=-0.48 p=0.23	
2mnth VIP ECV *(n=9)*				r= 0.35 p= 0.35

Table 54 Associations between absolute extracellular volume in the right ventricular insertion point and BNP post-operatively.
Spearman's correlation coefficient. * denotes significance.
POD-post-operative day, 2mnth – two-months post-operatively, VIP – ventricular insertion point, ECV – extracellular volume.

	Right Ventricular Insertion Point			
	ΔPeak BNP *(n=12)*	**ΔPOD2 BNP** *n=(13)*	**ΔPOD3 BNP** *n=(12)*	**Δ2mnth BNP** *n=(10)*
ΔPOD2 VIP ECV *(n=9)*	r= -0.35 p= 0.36	r=-0.38 p=0.32	r=-0.54 p=0.17	
Δ2mnth VIP ECV *(n=9)*				r= 0.60 p= 0.08

Table 55 Association between delta extra-cellular volume at the right ventricular insertion point delta BNP values post-operatively.
Spearman's correlation coefficient.
POD-post-operative day, 2mnth – two-months post-operatively, VIP – ventricular insertion point, ECV – extracellular volume., Δ12hr - (12hours-pre-op), ΔPOD2 - (POD2-pre-op), ΔPOD3 - (POD3-pre-op), Δ2mnth- (2month-pre-op).

9.5.1.4 BNP and Septal Extracellular Volume

As with RVIP ECV, lower septal ECV values were associated with higher BNP values in the immediate post-operative period but these associations did not reach significance (Table 56). A positive relationship was demonstrated with higher ΔECV values at the septum associated with higher ΔBNP values on POD2 (Table 57). At two months post-operatively, higher ECV values at the septum were associated with higher BNP values but again this did not reach significance (Table 56). ΔECV and ΔBNP did not demonstrate any association at two-months (Table 57).

	Septum			
	Peak BNP *(n=12)*	**POD2 BNP** *n=(13)*	**POD3 BNP** *n=(12)*	**2mnth BNP** *n=(10)*
POD2 Septum ECV *(n=9)*	r= -0.60 p= 0.10	r= -0.57 p= 0.11	r= -0.60 p= 0.08	
2mnth Septum ECV *(n=9)*				r= 0.64 p= 0.06

Table 56 Associations between absolute extracellular volume in septum and BNP post-operatively.
Spearman's correlation coefficient.
POD-post-operative day, 2mnth – two-months post-operatively, n – number, ECV – extracellular volume.

	Septum			
	ΔPeak BNP *(n=12)*	**ΔPOD2 BNP** *n=(13)*	**ΔPOD3 BNP** *n=(12)*	**Δ2mnth BNP** *n=(10)*
ΔPOD2 Septum ECV *(n=9)*	r= 0.30 p= 0.40	**r= 0.66** **p= 0.04***	r= 0.18 p= 0.65	
Δ2mnth Septum ECV *(n=9)*				r= 0.33 p= 0.35

Table 57 Association between delta extra-cellular volume at the septum and delta BNP values post-operatively.
Spearman's correlation coefficient. * denotes significance.
POD-post-operative day, 2mnth – two-months post-operatively, Δ12hr -(12hours-pre-op), ΔPOD2 - (POD2-pre-op), ΔPOD3 - (POD3-pre-op), Δ2mnth - (2month-pre-op), n – number, ECV – extracellular volume.

9.5.2 NT-proBNP

Associations were sought between T1 and ECV values at the RVIP and septum and NT-proBNP, and ΔT1 and ΔECV values at the RVIP and septum and ΔNT-proBNP.

9.5.2.1 NT-proBNP and Right Ventricular Insertion Point T1

No association was demonstrated between T1 and NT-proBNP or ΔT1 and ΔNT-proBNP in the early post-operative period (Tables 58 and 59). Neither T1 and NT-proBNP or ΔT1 and ΔNT-proBNP demonstrated any association at two-months post-operatively (Tables 58 and 59).

	Right Ventricular Insertion Point			
	Peak NT *n=(13)*	**POD2 NT** *n=(13)*	**POD3 NT** *n=(12)*	**2mnth NT** *n=(10)*
POD2 VIP T1 *(n=12)*	r= 0.21 p= 0.51	r= 0.03 p= 0.94	r= -0.01 p= 0.98	
2mnth VIPT1 *(n=10)*				r= 0.11 p= 0.76

Table 58 Associations between absolute right ventricular point T1 and NT-proBNP post-operatively.
Spearman's correlation coefficient.
NT- NT-proBNP, POD2 – post-operative day two, POD3 – post-operative day three, VIP – ventricular insertion point, n – number.

	Right Ventricular Insertion Point			
	ΔPeak NT *n=(13)*	**ΔPOD2 NT** *n=(13)*	**ΔPOD3 NT** *n=(12)*	**Δ2mnth NT** *n=(10)*
ΔPOD2 VIP T1 *(n=12)*	r= -0.04 p= 0.90	r= -0.11 p= 0.75	r= -0.24 p= 0.48	
Δ2mnth VIPT1 *(n=10)*				r= -0.08 p= 0.83

Table 59 Association between delta T1 in the right ventricular insertion point and delta NT-proBNP post-operatively.
Spearman's correlation coefficient.
NT- NT-proBNP, POD2 – post-operative day two, POD3 – post-operative day three, 2mnth – two-months post-operatively, VIP – ventricular insertion point, n – number, ΔPOD2 - (POD2-pre-op), ΔPOD2 - (POD3-pre-op), Δ2mnth- (2month-pre-op).

9.5.2.2 NT-proBNP and Septal T1

No association was shown in the early post-operative period with septal T1, ΔT1 and NT-proBNP and ΔNT-proBNP (Tables 60 and 61). A strong association was demonstrated between higher septal T1 and higher NT-proBNP values both measured at two-months post-operatively (Table 60). No association was shown between ΔT1 and ΔNT-proBNP at two-months (Table 61).

	Septum			
	Peak NT *n=(13)*	**POD2 NT** *n=(13)*	**POD3 NT** *n=(12)*	**2mnth NT** *n=(10)*
POD2 Septum T1 *(n=12)*	r= -0.05 p= 0.86	r= -0.05 p= 0.87	r= -0.31 p= 0.36	
2mnth Septum T1 *(n=10)*				**r= 0.86** **p <0.01***

Table 60 Associations between absolute septal T1 and absolute NT-proBNP post-operatively.
Spearman's correlation coefficient.
*** –** denotes significance.
NT- NT-proBNP, POD2 – post-operative day two, POD3 – post-operative day three, 2mnth – two months post-operatively, n – number.

	Septum			
	ΔPeak NT *n=(13)*	**ΔPOD2 NT** *n=(13)*	**ΔPOD3 NT** *n=(12)*	**Δ2mnth NT** *n=(10)*
ΔPOD2 Septum T1 *(n=12)*	r= 0.15 p= 0.65	r= 0.13 p= 0.68	r= 0.06 p= 0.87	
Δ2mnth Septum T1 *(n=10)*				r= 0.14 p= 0.70

Table 61 Association between delta T1 in the septum and delta NT-proBNP post-operatively. Spearman's correlation coefficient.
NT- NT-proBNP, POD2 – post-operative day two, POD3 – post-operative day three, 2mnth – two-months post-operatively, n – number, ΔPOD2 - (POD2-pre-op), ΔPOD2 - (POD3-pre-op), Δ2mnth-(2month-pre-op).

9.5.2.3 NT-proBNP and Extracellular Volume

There was no association demonstrated between RVIP ECV, ΔECV, NT-proBNP and ΔNT-proBNP at any study time point (Spearman's test, $r<-0.50$, $p>0.17$ for all parameters, data not shown). Again there was no association between septal ECV, ΔECV, NT-proBNP and ΔNT-proBNP at any study time point (Spearman's test, $r<0.62$, $p>0.08$ for all parameters, data not shown).

9.5.3 CRP, T1 and Extracellular Volume

Despite CRP being a marker of systemic inflammation, it did not demonstrate associations with CMR evidence of myocardial inflammation in this study (Spearman's $r<0.42$, $p>0.23$ for all parameters, data not shown).

9.6 Discussion

9.6.1 Change in BNP and NT-proBNP

These findings are consistent with other studies that have previously demonstrated a rise in BNP and NT-proBNP following lung resection surgery[74 81 386-388]. In healthy patients, BNP and NT-proBNP convey a similar message despite different normal value ranges. Both BNP and NT-proBNP are released in a 1:1 ratio, however, NT-proBNP levels are higher in the circulation than BNP due to the reduced clearance rate of NT-proBNP. In the presence of acute disease both biomarkers can display different trends due to their kinetics. BNP and NT-proBNP are used routinely in clinical practice, but levels may also be affected by multiple patient factors including age, gender, and renal function and studies

comparing them directly are scarce[62 389]. All patients in this study had an eGFR>60 throughout, therefore biomarker results displayed in this study were unlikely to have been affected by renal function. Given this study design included the same cohort of thirteen patients across eight study time points, patient age and gender would not be responsible for the difference in biomarkers demonstrated.

The ideal biomarker in the pre-operative or early peri-operative period would enable early identification of high-risk patients and predict those at increased risk of post-operative complications to facilitate early intervention and ameliorate post-operative complations[390]. Pre-operative BNP and NT-proBNP have both been shown to predict those patients at risk of post-operative cardiac complications, including AF, and long-term mortality in non-cardiac surgery[67 391-394]. Several national guidelines have suggested NT-proBNP should be used for pre-operative risk stratification. The ESC 2014 peri-operative guideline suggested NT-proBNP or BNP may be considered for risk stratification in patients defined as “high-risk”, however, “high-risk” was not defined in the guideline nor a threshold value suggested for BNP or NT-proBNP to aid defining “high-risk” patients[72]. The 2017 Canadian Cardiovascular Society (CCS) peri-operative guidelines recommended measuring NT-proBNP in patients with a baseline risk greater than five per cent with a NT-proBNP threshold value of 300pg/ml or greater to define those patients at greater risk[395]. In 2020 a subset of the Vascular Events in Non-cardiac Surgery Patients Cohort Evaluation (VISION) study reported the findings of pre-operative NT-proBNP measurement as a predictor of MINS and vascular death in comparison to the Revised Cardiac Risk Index (RCRI) within 30 days of non-cardiac surgery, with over 10,000 patients included in the cohort study[396]. The study found pre-operative NT-proBNP concentrations were independently associated with vascular death or MINS within 30 days of surgery[396]. In the study NT-proBNP values of less than 200pg/ml had a risk of death or MI of three percent or less, whereas those patients with an NT-proBNP greater than 200pg/ml but less than 1500pg/ml had a risk of almost eight percent.[396] The Prospective Comparison of ARNI with ACEI to Determine Impact on Global Mortality and Morbidity in Heart Failure (PARADIGM-HF) trial demonstrated an increase in BNP levels in patients receiving sacubitril/valsartan for management of their HF with no increase in NT-proBNP levels. As a result of

this trial, NT-proBNP measurement is the preferred naturetic peptide for monitoring those with HF. This may account for the lack of similar studies analysing the use of BNP perioperatively[396 397].

Studies that have made direct comparisons between BNP and NT-proBNP were initially performed in patients with congestive cardiac failure[61 64 390 398-401]. In the Val-HeFT study, a large multi-centre trial, a direct comparison of NT-proBNP and BNP was studied in relation to disease severity and clinical outcome in patients with chronic heart failure. NT-proBNP was shown to perform better than BNP when predicting patient outcomes in this population[390].

Although both BNP and NT-proBNP have been associated with outcomes following thoracic surgery, no studies have made direct comparisons of BNP and NT-proBNP in the early post-operative period[74 386 388 393 396 402-405]. In this study, I compared post-operative BNP and NT-proBNP values to determine the time to peak rise of both biomarkers. By identifying the biomarker that peaks the earliest in the peri-operative period, it may be possible to use this biomarker to identify those patients that have sustained an early myocardial injury. BNP demonstrated a peak rise early at 12 hours postoperatively, whereas NT-proBNP peaked later in the post-operative period at 72 hours. Both biomarkers may offer value in the pre- and post-operative period with pre-operative NT-proBNP value being able to predict those who may be at risk of complications whereas the markedly earlier rise in BNP at 12 hours suggests BNP could be better at identifying those who have sustained a myocardial injury early in the post-operative period.

9.6.2 Change in Troponin

Troponin rises are common following non-cardiac surgery (as described in Chapter two) with studies demonstrating a troponin rise within the first 24 hours after thoracic surgery with incidences of troponin rise reported between 7-49.7%[96 406 407]. Conversely, no rise in troponin was documented at any time point in any patient in this study, though this may relate to the Troponin assay used. Troponin I was measured using the Triage SOB panel using POC testing with a TnI range of 50ng/l to $3x10^4$ng/l with an upper limit of normal (99^{th} percentile) of 50ng/l. In the studies describing troponin rise following surgery, different

troponin assays and analysing techniques were used. In the study by McCall et al a high sensitivity troponin T (hsTnT) in a laboratory setting with an upper normal range (99th percentile) of <14ng/l was used[81]. The study demonstrated a rise in troponin at POD2 with a median concentration of 12.3ng/l (3.7, 21.9)[81]. It seems likely that by using a point of care TnI measurement, instead of a high-sensitivity laboratory measurement, minor changes in TnI may not have been demonstrated.

9.6.4 BNP and NT-proBNP and CMR Associations

Myocardial stretch is the key stimulant for BNP synthesis through activation of the proBNP gene, but catecholamines, angiotensin II, endothelin, hypoxia, inflammation, and fibrosis are also factors known to stimulate BNP release. In this study, higher pre-operative BNP values were associated with lower pre-operative RVEF. In the post-operative period, a similar trend was described at POD2 and POD3; but these did not reach significance. Significant associations were shown by McCall et al who demonstrated a moderate association between post-operative BNP on POD2 and delta RVEF on POD2 following lung resection ($r=-0.49$, $p=0.02$)[74 81]. Despite this study being unable to display significant results, the trends reported are in keeping with the results from a similar cohort of patients. Similarly, poorer pre-operative LV function was associated with higher pre-operative BNP values. This trend did continue in the post-operative period but again these associations did not reach significance.

In this study, NT-proBNP and LVEF displayed similar associations to those described with BNP; however there was lack of association with NT-proBNP and RVEF. Elevated pre-operative NT-proBNP levels have been shown to be an independent predictor of cardiac complications following lung resection surgery with higher levels associated with the development of AF[388 403]. NT-proBNP has shown association with RV dysfunction in PH and PE[408-410]. This is the first study to attempt to demonstrate association between NT-proBNP and RV dysfunction following lung resection.

Alterations in native T1 and ECV have been shown to be associated with elevated BNP in hypertrophic cardiomyopathy and hypertension[411 412]. The Multi-Ethnic Study of Atherosclerosis (MESA) study analysed a subset of 80 patients who

underwent CMR and NT-proBNP biomarker analysis, demonstrating an association between elevated ECV and elevated logNT-proBNP ($p<0.001$) in a cross-sectional patient population[413]. Studies seeking association between NT-proBNP and myocardial T1 in patients with end-stage renal failure and systemic sclerosis have however failed to demonstrate any association[414 415].

In this study, neither BNP or NT-proBNP showed any consistent association with T1 or ECV values measured post-operatively. Of the T1 and ΔT1 values measured across the study time period, absolute T1 in the septum and absolute BNP both measured at two-months post-operatively and absolute T1 in the septum and absolute NT-proBNP (again both at two-months) demonstrated a significant positive association. At two-months post-operatively, both RVIP and septal T1 values were returning to baseline values. Conversely, there was a trend of lower ECV values associated with higher BNP values, the opposite relationship that might be expected, with a strong negative association between absolute RVIP ECV and absolute BNP both measured on POD2. Similar trends were also displayed with absolute RVIP ECV and absolute BNP at peak BNP and POD3 time points and ΔECV and ΔBNP at peak, POD2 and POD3 time points; however these associations did not reach significance. Absolute NT-proBNP and absolute ECV in the RVIP displayed a similar trend to those described with BNP; but these did not reach significance.

It is possible that these associations are demonstrating different pathological processes occurring within the myocardium. As described in Chapter eight, the significant and consistent changes seen in myocardial T1, most notably within the RVIPs, may occur as a result of a localised inflammatory process and given that naturetic peptides are a non-specific marker of global myocardial function rather than discrete areas of inflammation, associations may therefore be absent. The changes in T1 may be reflective of small, discrete areas of inflammatory changes within the myocardium rather than overt, diffuse fibrosis described with pathological processes that result in widespread myocardial involvement. Again as described in chapter eight, the changes in ECV may reflect oedematous areas within the myocardium rather than overt fibrosis. There does not appear to be a biologically plausible explanation for the association between lower ECV values and higher BNP values as shown in this study.

The inconsistent associations between biomarkers and CMR markers of inflammation in this study may also be as a result of multiple comparisons between both T1 and ECV at multiple regions with the myocardium and two separate biomarkers at a range of post-operative time periods. As described in chapter eight, due to poorer post-contrast Image Quality Score, the number of ECV results available are also limited and therefore the number of ECV values are reduced in comparison with T1 lessening the statistical power of the ECV comparisons.

9.6.5 CRP and CMR Associations

The rise in CRP at POD2 before returning to baseline at two-months is to be expected in post-operative patients. CRP is an acute phase reactant protein that increases in the post-operative period as a result of tissue damage and inflammation and is a marker of widespread systemic inflammation rather than specific to myocardial injury. CRP has been shown to peak at POD two to three following a range of surgical procedures, in keeping with the findings of this study[299 416-418].

An increase in CRP has been shown to be predictive of post-operative complications in non-cardiac surgery[417 419-421]. In thoracic surgery, elevated peri-operative CRP levels are associated with poorer long-term survival[422-424]. A study examining both pre and peri-operative CRP values in patients undergoing lung resection for non-small cell cancer demonstrated elevated peri-operative CRP values were associated with higher incidence of complications, length of hospital stay, higher incidences of cancer relapse and overall survival[422]. Elevated peri-operative CRP levels were also associated with increased incidence of post-operative complications including MI, arrythmia, and stroke.[422] The CRP rises following thoracic surgery are multi-factorial and are affected by a range of factors including smoking history, history of COPD, cancer staging and surgical technique (open versus VATS surgery)[421-423]. In this study, only one participant died within one year of surgery therefore no associations were sought between biomarkers and long-term clinical outcomes.

In this current study CRP was associated with RVEF on POD2 but not at two-months. Choi et al demonstrated a pre-operative CRP greater than 3.4mg/l is

associated with a 2.5 fold increase in perioperative major cardiovascular events (PMCE) and is superior to the Revised Cardiac Risk Index (RCRI) as a clinical risk predictor; however NT-proBNP was superior to CRP in predicting clinical outcomes[421]. In PE, studies have sought to examine the role of CRP as a biomarker for predicting RV dysfunction; Abul et al. demonstrated higher CRP levels were associated with RV dysfunction (p=0.02)[425]. Conversely, Choi et al failed to demonstrate an increase in CRP in patients with RV dysfunction on TTE following PE compared with no evidence of RV dysfunction[426].

The alterations in T1 and ECV displayed in this study are unlikely to be as a result of widespread, systemic inflammation. Given CRP reflects generalised systemic inflammation, it is perhaps not surprising that it did not demonstrate association with indicators of discrete areas of myocardial inflammation. This further supports the author's belief that a local cardiac process with discrete areas of inflammatory injury is occurring within the myocardium.

9.7 Strengths and Weaknesses

Biomarker analysis was an a-priori secondary outcome and therefore no power analysis was performed and is therefore at risk of a type two error. Given the small sample size and the large number of associations examined (due to the range of biomarkers and time points available for analysis) the results should be considered more as hypothesis generating observations that require further validation in a larger study.

There was a small amount of missing data, with the majority missing at 2-months. The statistically significant comparisons were however made in the earlier post-operative period between the recovery stage and POD2 (when the biomarker signal Is greatest) therefore the missing data is unlikely to have impacted on the reported findings.

In this study, BNP and NT-proBNP samples could be obtained from an arterial cannula (if present) or by venepuncture. It is possible that the values reported in this study may differ depending if they were obtained from arterial or venous blood. Information regarding the site was not obtained at the time of each individual blood sample collection and therefore no comparisons could be made

within this study regarding the impact of arterial or venous sampling of cardiac biomarkers. It is recognised that there may be differences in blood results dependant on the site of sampling but there are no studies in the literature comparing arterial versus venous sampling of BNP or NT-proBNP[427].

A strength of this study was the ability to measure biomarkers at multiple time points and determine the earliest rise; however, I did not measure BNP beyond 72 hours. It has been shown in one study that those patients who develop post-operative complications have BNP levels that peak at POD3 and remain elevated until POD7 and as a result it is possible by not measuring BNP at seven days post-operatively I may have missed association with post-operative complications[392].

As discussed earlier in this chapter, the use of a high sensitivity troponin assay may have demonstrated smaller changes in troponin that were not observed with the use of a POC assay. In future studies, using a high sensitivity troponin assay should be considered.

BNP showed superiority in this study as the biomarker of choice following lung resection given its ability to detect an early rise following surgery and therefore potential predict early those at risk of post-operative complications. However given that peri-operative myocardial injury following non-cardiac surgery appears to be multi-factorial and the lack of association between BNP and T1 and ECV in this study, newer biomarkers may have to be explored. The study highlights the need for biomarkers that specifically examine the inflammatory pathways within the myocardium. As discussed in Chapter 2, examination of microRNA release following non-cardiac surgery has been described and it is possible microRNAs may provide further information specific to the inflammatory hypothesis that is missing in this current study (discussed in Chapter 10)[194].

9.8 Conclusion

Naturetic peptides, BNP and NT-proBNP rise following lung resection surgery; BNP shows the most consistent change with a rise throughout the peri-operative period. The rise in BNP following lung resection surgery has shown association with decreased RV function. In this study, no single biomarker was able to demonstrate consistent association with myocardial inflammation. Further work

is required to identify potential biomarkers that may be able to demonstrate association with myocardial inflammation in patients after lung resection surgery and therefore identify those patients who have sustained myocardial injury and may therefore be at increased risk of poorer functional outcomes. By identifying these patients early, it may be possible to facilitate early intervention and ameliorate post-operative complications.

Chapter 10 Major Findings, Conclusions and Future Work

10.1 Introduction

This thesis describes the RV response to lung resection and explores a potential intrinsic myocardial inflammatory response as a contributing mechanism to the well described post-operative RV dysfunction. Various potential mechanisms have been explored, with considerable focus being on that of an increase in RV afterload; although studies have demonstrated that some indices of afterload (e.g. pulmonary vascular resistance (PVR)) return to baseline from an early acute increase, RV dysfunction persists into the longer post-operative period. Our research group were the first to study pulmonary artery wave intensity analysis (WIA) and pulmonary artery flow, acceleration time (PAAT) and distensibility following lung resection as measures of *pulsatile* afterload. The study demonstrated pulsatile afterload is increased post-operatively and is associated with a reduction in RVEF[171]. The RV dysfunction following lung resection is likely a complex interaction of aetiologies with increased afterload being one such influencing factor. Other potential aetiologies including impaired contractility, myocardial ischaemia and myocardial inflammation are explored.

The literature review in this thesis examines the myocardial inflammatory response following PE and animal models of acute afterload. These models, with transient clamping of the PA, are functionally analogous to the well documented acute increases in PVR seen with one lung ventilation, clamping of the operative PA, and parenchymal resection seen during lung resection surgery. These studies demonstrate a consistent myocardial inflammatory process in response to PA clamping, with associated RV dysfunction. The literature review also demonstrates an improvement in RV dysfunction with the use of anti-inflammatory modulating therapies, further supporting the mechanism of an inflammatory injury in this setting.

10.2 Major Findings

10.2.1 Chapter 6

This chapter describes the patient demographics of the study population, patient reported functional outcomes and CMR derived measures of both LV and RV function. The results show a decline in RVEF in the early post-operative period that remains depressed at two-months, with no change in LV function. The study also reports a decline in patient reported outcomes and quality of life following surgery.

10.2.2 Chapter 7

The feasibility of T1 mapping (both pre-and post-contrast), a CMR technique utilised in a range of pathological processes including MI, PH and heart failure, is described in this chapter. Excellent intra- and inter-observer reproducibility confirm the suitability of measuring both native T1 and ECV of the myocardium following lung resection surgery.

The study protocol was well tolerated in this patient population with 93% of patients participating at POD2 and 79% at two-months post-operatively. Of the CMR T1 maps obtained, 100% of pre-contrast images were assigned an image quality score (IQS) of two or more and were therefore suitable for analysis. Ninety-two percent of the post-contrast images were assigned an IQS of two or more and were suitable for analysis. Of the 75 total pre- and post-contrast maps available for image quality rating, only four percent were assigned an IQS of one (and so were unsuitable for analysis) and were subsequently removed from further T1 and ECV mapping analysis. The three images assigned a score of one were all performed on POD2.

10.2.3 Chapter 8

This is the first study to demonstrate both native T1 and ECV are markedly increased in the right ventricular insertion points (RVIPs) and septum in the post-operative period in a cohort of patients undergoing lung resection surgery. Increases in both T1 and ECV are present in the RVIP and to a lesser extent in the septum with absence of changes within the LV. These changes suggest lung

resection surgery triggers an early inflammatory response within the RV and septum. Relative changes in myocardial T1 measured in the RVIP are associated with relative changes in RVEF suggesting a link between an intrinsic myocardial injury and resultant RV dysfunction.

Increases in myocardial T1 were associated with both pre-operative and post-operative lung function. Higher septal T1 values on POD2 demonstrated strong association with both lower pre-operative DLCO and ppoDLCO% with higher RVIP values on POD2 also displaying strong association with ppoDLCO%. It may be possible to identify and stratify those with poorer lung function who are at higher risker of poor post-operative outcomes and allow for earlier targeted therapies to improve the post-operative course following lung resection. The nature of the surgical insult also impacted on T1 values with a higher number of resected pulmonary segments associated with greater T1 values in RVIP the early post-operative period, suggesting a greater increase in post-operative afterload results in an increased inflammatory response and greater myocardial injury.

Increases in both T1 and ECV in the post-operative period are also associated with poorer patient reported outcomes and patient reported QoL at two-months post-operatively; the Quality of Life Summary Index (reported at two-months) displayed strong association with both RVIP and septal T1 values on POD2. This study therefore suggests longer-term clinical significance of an inflammatory injury that occurs in the peri-operative period. Early identification of patients who have sustained a perioperative injury may aid in the identification of those patients that are at risk of poorer longer-term outcomes following surgery.

10.2.4 Chapter 9

BNP, NT-proBNP and CRP are elevated following lung resection surgery. BNP demonstrates the most consistent change with a rise throughout the peri-operative period, peaking early at 12 hours post-operatively, compared to 72 hours with NT-proBNP. The study highlighted the superiority of BNP over NT-proBNP in the peri-operative period. Studies examining BNP rise following lung resection have identified rises in BNP at POD2 and beyond; however this study provides new information regarding the earlier peak rise of BNP at 12 hours. By measuring BNP earlier in the peri-operative period, it may be possible to identify

those at risk of poorer post-operative outcomes, allowing for earlier targeted intervention.

In this study, there was trend towards higher BNP values being associated with lower RVEF, similar to results described in previous studies examining BNP following lung resection. Neither BNP or NT-proBNP demonstrated consistent associations with either RV function or myocardial inflammation. Lower ECV values in the RVIP and septum demonstrated an association with higher BNP levels in the immediate post-operative period. BNP, NT-proBNP and Troponin are all markers of global cardiac dysfunction whereas the imaging changes in this study are reflective of a localised intracardiac injury, therefore it seems likely that different pathologies are driving the changes in T1 / ECV and BNP / NT-proBNP and may account for the lack of association between natriuretic peptide levels and imaging findings.

CRP is a marker of systemic inflammation therefore it is perhaps unsurprising that this study failed to demonstrate any association between CRP and myocardial inflammation. The lack of association between CRP and CMR indices of myocardial inflammatory injury highlights the mechanisms driving the changes in T1 and ECV are localised cardiac processes rather than a global inflammatory process.

This study highlights the need for biomarkers that specifically examine the inflammatory pathways within the myocardium. Myocardial inflammatory specific biomarkers may allow for accurate identification of those at risk of peri-operative myocardial injury and may provide value in combination with well-establish biomarkers such as BNP. Not only could these biomarkers stratify individual patient risk following surgery, but they could lead to novel therapeutic targets and improved identification of the most suitable therapeutic treatment for a specific patient.

10.2 Conclusion

This thesis reports the feasibility and reproducibility of T1 mapping in a post-operative surgical population. It demonstrates that measuring myocardial inflammation using CMR T1 mapping is a viable and reproducible method in

patients following lung resection surgery. The main finding of this thesis is an increase in T1 and ECV in the myocardium following lung resection surgery. These changes are most notable in the ventricular insertion points, and to a lesser extent the septum, with no changes seen in the LV. The largest changes occur in the immediate post-operative period (POD2), at this time point there was moderate association demonstrated between relative RVEF and relative T1.

This study identified peak natriuretic peptide time points following lung resection; identifying an early spike in BNP at 12 hours post-operatively, compared with a spike at 72 hours for NT-proBNP. By measuring BNP earlier in the peri-operative period, it may be possible to identify those at risk of poorer post-operative outcomes, again allowing for earlier targeted intervention.

This study demonstrated a statistically and clinically significant decrease in quality of life following lung resection surgery. This is the first study to demonstrate a potential link between poorer post-operative functional outcomes and myocardial injury following lung resection surgery. Improved understanding of the likely inflammatory myocardial response should allow for targeted interventions in the pre and post-operative periods with an improvement in patient reported outcomes and quality of life.

10.3 Future Work

Future work building on this thesis needs to further explore the mechanism of RV dysfunction after lung resection and seek to identify specific inflammatory biomarkers and pathways of interest.

10.3.1 Explore Mechanisms

Although this study has demonstrated a likely inflammatory insult immediately following lung resection surgery with associated RV dysfunction, this only provides some insight into the mechanisms of RV dysfunction. The author suggests an intrinsic myocardial injury occurs in the immediate peri-operative period as a result of acute changes in afterload. These changes in afterload impair myocardial contractility and result in RV dysfunction.

Further demonstration of altered contractility following lung resection, specifically using load independent measures of myocardial contractility, is required. Strain and strain rate analysis are considered to be less load dependent than RVEF and therefore may offer a more complete assessment of RV contractility and also allow assessment of regional changes in RV function. Association between CMR strain and T1 and ECV may reveal a link between an inflammatory myocardial injury and altered contractility.

As described previously, collaborators within our research group have measured pulsatile afterload in this patient population using CMR derived pulmonary artery WIA and PAAT. Future work should seek to demonstrate association between these indices of pulsatile afterload and T1 and ECV. Collaboration with Dr Adam Glass from our research group, who has expertise in WIA, is ongoing using data from this current study.

This study demonstrated those with poorer lung function are likely to sustain a more significant myocardial inflammatory injury as a result of pre-existing distorted RV-PA dynamics. Further studies may consider the use of right heart catheterisation (RHC) in a sub-group of patients to allow more comprehensive evaluation of RV-pulmonary vascular haemodynamics in the immediate period following lung resection. The ability to utilise RHC may help to unravel the theories regarding potential underlying mechanisms, in particular the relative contributions of increased afterload and impaired contractility to RV dysfunction.

10.3.2 Further Assessment of the Clinical Impact

This thesis demonstrates an association between CMR evidence of RV dysfunction and patient reported outcomes and quality of life. A larger study combining imaging evidence of RV dysfunction and biomarker analysis in combination with patient reported outcomes would be required to definitively assess these associations.

The primary outcome for a larger study should consider the association between RV dysfunction and clinical impact and patient outcomes. The Standardised Endpoints in Perioperative Medicine Initiative recommends every clinical study

should consider using at least one patient-centred outcome within its range of reported study outcomes[428]. The Initiative recommended days alive and out of hospital at 30 days post-operatively (DAOH30) as a patient-centred outcome[428]. The DAOH30 is a novel scoring tool that encompasses several elements of the peri-operative period and is a composite measure comprising hospital length of stay, additional stays resulting from readmissions, and mortality and has been validated in a range of elective and emergency surgical patient populations[429-432]. The author therefore suggests a larger study should consider the use of patient centred outcomes, such as the DAOH30 as primary endpoint to focus on the impact of longer-term clinical outcomes.

10.3.3 Assessing Alternative Biomarkers as Markers of an Inflammatory Response

Although this study demonstrated cardiac biomarker release following lung resection surgery, the associations between biomarkers and CMR indices of inflammation were inconsistent. BNP and NT-proBNP are markers of global cardiac dysfunction and it is perhaps not surprising therefore that they do not correlate consistently with CMR evidence of discrete, subtle inflammatory changes within the myocardium. Future work should aim to identify biomarkers that demonstrate a discrete inflammatory myocardial injury.

MicroRNAs (miR) are associated with the regulation of inflammation in the cardiovascular system[433]. miRs are short (22 nucleotides long) non-coding RNA transcripts, essential in the role of RNA translation. They bind to specific sequences, most notably in the three prime untranslated regions of the target messenger RNA transcripts, which ultimately lead to protein synthesis inhibition[300]. During disease processes, miRs become dysregulated, leading to differences in gene expression and regulation. A single, individual miR can affect the transcription of a set of genes which can lead to dysregulation and dysfunction of an organ and potentially the development of a disease process. miRs have shown promise as novel biomarkers in a wide variety of pathological disease processes due to their close association with disease pathogenesis and their stability outside of cells, allowing detection from bio-fluids to be easy and reliable[434]. Cellular injury, such as ischaemia, inflammation or infarction, of cells leads to an immediate miR release into the circulation.

MicroRNAs have been explored in a range of pathologies including RV volume and pressure overload, PE and PH (conditions with similarities to lung resection surgery). Reddy et al demonstrated mir-21 (a miR found in the RV free wall) increased 2.5-fold at one month and 4-fold by two months in a murine model of combined moderate-to-severe RV volume overload and mild-to-moderate pressure overload.[435] Mir-21 demonstrated a positive correlation with the development of RV fibrosis and correlated with the degree of diastolic dysfunction. [435] Kessler et al identified 37 miRNAs which were differentially regulated in patients presenting to the emergency department with a confirmed diagnosis of central PE by CTPA.[436] In PH, a range of miRs have been identified and have demonstrated correlation with severity of disease. Sarrion et al showed significant changes in 61 miRs in 12 patients with PH with correlations demonstrated between pulmonary and cardiac function and a range of miRs.[437] In one study analysing miRs in 32 patients with confirmed PH, specific miRs were shown to correlate with severity.[302]

microRNAS may therefore have the potential as a biomarker following lung resection surgery. An initial study should seek to identify a panel of miRs that are specific to RV release, cardiac injury and inflammation and those involved in PH or PE and determine their release following lung resection surgery. Following on from this, studies should aim to quantify the release in a larger group of lung resection patients and seek association with CMR derived indices of inflammation. Additional blood samples taken during this study have been processed and stored for future biomarker analysis. The author is currently seeking funding to explore the role of miRs following lung resection surgery and association between miRs and myocardial inflammatory injury.

10.3.4 Assessing the Inflammatory Myocardial Response in Other Surgical Cohorts

This is the first study to assess myocardial T1 and ECV following surgery. The myocardial injury demonstrated in this study may be a by-product of widespread generalised, systemic inflammation; however, the lack of association with CRP would indicate that systemic inflammation may not be the primary mechanism. Inflammatory injury can however be identified in a range of organs

postoperatively and has been associated with myocardial injury, lung injury, postoperative cognitive dysfunction and acute kidney injury[438] [439] [440] [441].

Alterations in myocardial T1 may be present following other types of major surgery which employ OLV or indeed, it may be that all surgical insults result in a triggered inflammatory response in the myocardium. Insights from other surgical procedures, with similar characteristics to lung resection surgery, may help to ascertain the underlying mechanisms resulting in raised T1 and ECV in the post-operative period. A larger study may seek to compare the myocardial inflammatory response in a range of surgical procedures such as OLV and lung resection, OLV with no resected lung (such as oesophagectomy), two-lung ventilation (such as colorectal surgery), and surgery and anaesthesia requiring no ventilation (such as spinal anaesthesia for lower limb joint arthroplasty).

10.4 Conclusion

In summary, native T1 and ECV are increased following lung resection surgery and may be indictive of a localised myocardial inflammatory response to the acute surgical insult. An acute increase in afterload may trigger a localised, intrinsic cardiac injury which results in altered contractility and resultant RV dysfunction. With greater understanding of the incidence, impact and underlying mechanisms of perioperative RV dysfunction following lung resection surgery, interventions targeted at patients at greatest risk may provide the opportunity to intervene early and provide a personalised, patient-centred approach to perioperative management. Ultimately this could improve patient reported functional outcomes and QoL following lung resection.

Appendices

Appendix 1

The Right Ventricular Inflammation after lung resection study.
CRF 1 – Baseline demographics

Patient ID number in this study:	**T1** |__|__|

1. Sex: □□male □□female

2. Age: |__|__|__| years

3. Date of birth: |__|__| |__|__| |__|__|__|__| d d m m y y y y

4. Height: |__|__|__| cm

5. Weight: |__|__|.|__| kg

6. Ever smoked?: □□yes □□no

6.2 If yes, □□Current smoker* □□Past-smoker*

6.3 If yes, No. of pack years smoked*: |__|__| years

**See footnote for definitions*

6.4. If current smoker, No. of cigarettes per day: |__|__|

6.5. If past smoker, When stopped: |__|__| |__|__|__|__| [mm/yyyy]

7. Ever drink alcohol?: □□yes □□no

7.1 Currently Drinking?: □□yes □□no

7.2 If yes, Units per week: |__|__|__|

8. Chronic co-morbidity: □□yes □□no

8.2 If yes, *tick all that apply*

□ Smoking addiction
□ History of cancer*
□□COPD*
□□Arterial hypertension*
□□Heart disease*
□□Diabetes mellitus*
□□Peripheral vascular disease

*

□□Obesity*
□□Alcoholism*

**See footnote for definitions*

9. Pulmonary function test results:

9.1 Oxygen saturation on air: |__|__|__| %

9.2 FEV1: Pre-bronchodilator |__|.|__|__| L |__|__|__| % predicted

9.3 FEV1: Post-bronchodilator (if applicable) □N/A

|__|.|__|__| L |__|__|__| % predicted

9.4 FVC: |__|.|__|__| L |__|__|__| % predicted

9.5 FEV1/FVC: |__|__| %

9.6 DLCO: |__|__|.|__|__| mmol $kPa^{-1}min^{-1}$ |__|__|__| % predicted

10. Baseline laboratory values:

10.1 Hb: |__|__|__| g/L

10.2. Albumin: |__|__|__|__|__| *g/L*

10.3. Creatinine: |__|__|__| µmol/L

10.4 eGFR: |__|__|__| ml/min

10.5 CRP: |__|__|__| *mg/L*

11. Preoperative neo-adjuvant therapy:

11.1 Preoperative chemo-therapy?□ □□yes □□no

11.2 Preoperative radio-therapy?□ □□yes □□no

12. Medication History:

For coding:□ □□Beta blockers
□□Ace inhibitor
□□Angiotensin receptor antagonist
□□Calcium channel antagonist
□□Inhaled bronchodilator
□□Inhaled steroid
□□Oral steroid

□□Antiplatelet
□□Statin

Please record all medications (including those above and those purchased over the counter):

Medication	***Dose***	***Frequency***

Explanatory notes:
6. Smoking History
Past Smoker (stopped > 1 month prior to operation
Current Smoker should be selected if the patient stopped smoking <1 month prior to the surgical procedure.

Pack Years:
One 'Pack Year' is 20 cigarettes smoked/day for one year

$$\frac{\text{No. of cigarettes/day x number of years}}{20} = \text{No. of pack years}$$

Loos tobacco: ounces per week x 2/7 x number of years = pack years

Info taken from: "Pack year" smoking histories: what about patients who use loose tobacco? doi: 10.1136/tc.2004.009977

8.2 Chronic co-morbidity:

[These co-morbidities are being collected to allow calculation of the Thoracoscore (Ref: http://www.sfar.org/scores2/thoracoscore2.php)].

History of cancer	Includes cancers treated many years previously. But does not include non-melanoma skin cancer or premalignant conditions such as cervical dysplasia or Barrett's disease.
COPD	FEV1/FVC ration <0.7 after bronchodilator therapy
Arterial hypertension	Treated, or higher than 140/90 on more than one occasion
Heart disease	Either ischaemic heart disease (documentation of angina, myocardial infarction (MI), CABG, PCI) or congestive cardiac failure (documentation of symptomatic cardiac failure, asymptomatic low ejection fraction does not count), or symptomatic valvular heart disease.
Diabetes mellitus	Presence and/or history of diabetes mellitus, regardless of duration of disease or need for anti-diabetic agents diagnosed prior to surgical intervention.
Peripheral vascular Disease	Claudication either with exertion or rest; carotid occlusion or > 50% stenosis; previous or planned surgery on abdominal aorta, limb arteries or carotids; documented abdominal (below the diaphragm) aortic aneurysm with or without repair; positive non-invasive or invasive testing documented ankle brachial index ≤ 0.9, angiography, ultrasound, MRI or CT imaging of > 50% stenosis in any peripheral artery.

.

Obesity	Body mass index ≥ 30.
Alcoholism	Current alcohol intake > 14 units/week for Women and >21 units/week for men. Previous treatment for alcohol dependence.

Appendix 2

Right side of heart function after lung resection.
CRF 2 – Self-report of functional status / quality of life

Patient ID number in this study: **T1** |__|__|

Pre-op ❑ **2 months** ❑ **1 year** ❑

We would like to ask you some questions about how your health / symptoms effect your day to day life. Please read the instructions and tick the appropriate box. Though, some of the scoring systems overlap it is important that you answer each one individually. This should take no longer than 10 minutes.

Thank you for your time!

World Health Organization Performance status:

Please tick the ONE box that best describes you:

Fully active, able to carry on all pre-disease performance without restriction	❑
Restricted in physically strenuous activity but ambulatory (able to walk) and able to carry out work of a light or sedentary nature, e.g., light house work, office work	❑
Ambulatory (able to walk) and capable of all self-care but unable to carry out any work activities. Up and about more than 50% of waking hours	❑
Capable of only limited self-care, confined to bed or chair more than 50% of waking hours	❑
Completely disabled. Cannot carry on any self-care. Totally confined to bed or chair	❑

MRC Breathlessness Scale:

Please tick the ONE box that best describes you:

No breathlessness except with strenuous exercise	❑
Breathless when walking up an incline or hurrying on the level	❑
Walks slower than most people on the level, or stops after 15 minutes of walking on the level	❑
Stops after a few minutes of walking on the level	❑
Breathless with minimal activity such as getting dressed, to breathless to leave the house	❑

New York Heart Association classification:

Please tick the ONE box that best describes you:

No symptoms and no limitation in ordinary physical activity, e.g. shortness of breath when walking, climbing stairs etc.	❑
Mild symptoms (mild shortness of breath and/or angina) and slight limitation during ordinary activity.	❑
Marked limitation in activity due to symptoms, even during less-than-ordinary activity, e.g. walking short distances (20–100 m).	❑
Severe limitations. Experiences symptoms even while *at rest*. Mostly bedbound.	❑

Quality of Life

Under each heading, please tick the ONE box that best describes your health TODAY

MOBILITY

I have no problems in walking about ❑
I have slight problems in walking about ❑
I have moderate problems in walking about ❑
I have severe problems in walking about ❑
I am unable to walk about ❑

SELF-CARE

I have no problems washing or dressing myself ❑
I have slight problems washing or dressing myself ❑
I have moderate problems washing or dressing myself ❑
I have severe problems washing or dressing myself ❑
I am unable to wash or dress myself ❑

USUAL ACTIVITIES *(e.g. work, study, housework, family or leisure activities)*

I have no problems doing my usual activities ❑
I have slight problems doing my usual activities ❑
I have moderate problems doing my usual activities ❑
I have severe problems doing my usual activities ❑
I am unable to do my usual activities ❑

PAIN / DISCOMFORT

I have no pain or discomfort ❑
I have slight pain or discomfort ❑
I have moderate pain or discomfort ❑
I have severe pain or discomfort ❑
I have extreme pain or discomfort ❑

ANXIETY / DEPRESSION

I am not anxious or depressed ❑
I am slightly anxious or depressed ❑
I am moderately anxious or depressed ❑
I am severely anxious or depressed ❑
I am extremely anxious or depressed ❑

- We would like to know how good or bad your health is TODAY.
- This scale is numbered from 0 to 100.
- 100 means the <u>best</u> health you can imagine.
  0 means the <u>worst</u> health you can imagine.
- Mark an X on the scale to indicate how your health is TODAY.
- Now, please write the number you marked on the scale in the box below.

YOUR HEALTH TODAY = ☐

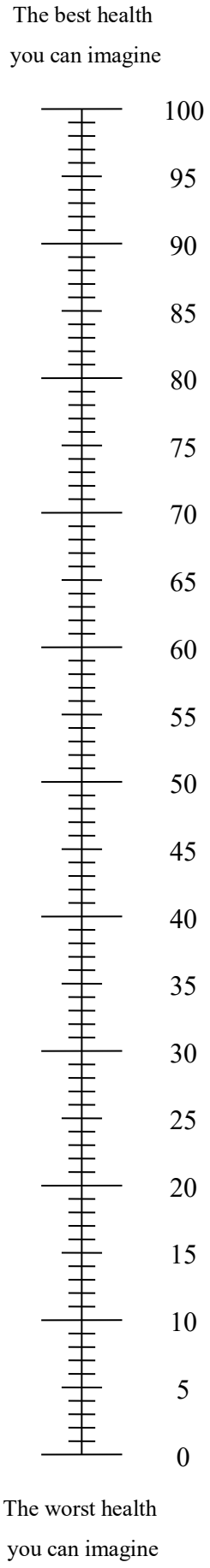

Appendix 3

MRI SAFETY SCREENING FORM

NHS
Golden Jubilee National Hospital

Attach patient label

Weight (kg): _____ Height (cm): _____

NAME: _____ CHI NUMBER: _____

ADDRESS: _____

		YES	NO
1	Have you had an MRI scan before?		
2	Do you have a cardiac pacemaker, pacing wires or defibrillator?		
3	Have you ever had an aneurysm in your head, clipped or treated?		
4	In your lifetime, have you **EVER** had any surgery to your..... (if YES please detail) a) Heart or Chest?		
	b) Head or Brain (e.g. hydrocephalus shunt)		
	c) Eyes? (e.g. retinal tack)		
	d) Ears? (e.g. cochlear implant, stapedectomy)		
	e) Spine? (e.g. spinal fixation, discectomy)		
5	Do you have any metal clips, pins, plates, screws, joint replacements?		
6	Do you have any stents?		
7	Do you have any electronic, mechanical or magnetic implants? (e.g. neuro-stimulator, TENS)		
8	Do you have any other type of implant in your body?		
9	Have you **EVER** had an eye injury where metal could have entered your eyes?		
10	Have you **EVER** had any incidents where bullets, shrapnel or other pieces of metal entered your body?		
11	Have you had any surgery or endoscopy in the last 6 weeks?		
12	Have you **EVER** had any surgery in your lifetime?		
13	Do you have epilepsy or blackouts?		

14	**FEMALE PATIENTS ONLY** a) Is there any possibility that you may be pregnant?		
	b) Do you have breast implants?		
	c) Are you breast feeding?		

15	**Do you have any of the following today?** a) Dentures or dental plate with metal?		
	b) A hearing aid?		
	c) Body piercing or jewellery		
	d) An artificial limb, calliper or corset?		
	e) A nicotine, pain relief or hormone patch?		
	f) A tattoo or permanent eyeliner?		
	g) Coloured contact lenses?		

I confirm that I have been asked the above questions and that the information I have given is correct.

Signature of Patient (X) _____ **Date** _____

I confirm that I have asked the above questions, the patient is safe to be scanned and I have checked that all loose metal has been removed.

Signature of Radiographer _____ **Date** _____

Signature of Radiologist _____ **Date** _____

Appendix 4

Protocol for T1 Cardiovascular Magnetic Resonance

Localisers
Breath hold tru fisp

Field of View (FOV) 400mm
3 Perpendicular groups of 3 slices (tra/sag/cor)

Re-localise at centre

2 chamber, 4 chamber and short axis localisers separately

Black Blood Sequence
In all 3 planes non breath hold

FOV 340-360, 75% phase FOV
Approximately 36-40 slices in transverse plane
24-30 slices in sagittal plane
18-24 slices in coronal plane

256 x 113 resolution
Triggered TR 600-800 dependent on r-r interval
2 trigger pulse (3 if patient's r-r interval is very short >600)

Function
Retro trufisp
Use iPat if patient is unable to hold breath

FOV 340-380
Slice thickness 6mm with 4mm gap
Resolution 256x90% (198) Voxel size 1.5x1.3x6mm
7/8phase partial Fourier
18 segments, 35 calculated phases

Tissue Characterisation
T1 with optimized spatial resolution
Positioning: 2 SA Slices 8mm – positioning orthogonal to wall, trigger delays, 4CH and long axis through inferior and posterior RV insertion segments
RR Timing: diastolic imagine or systolic resting delay
Gd-enhanced post-contrast T1 maps

Flow

Through plane superior to aortic valve and superior to pulmonary valve
Right pulmonary artery and left pulmonary artery

FOV 320-380

Slice thickness 5mm
Resolution 256x100% iPat2
Venc as appropriate (use 150 for normal flow)

Slice Positioning for Function

Vertical Long Axis
Horizontal Long Axis
Left Ventricular Outflow Tract
Left Ventricular Outflow Tract Orthogonal
Short Axis slice above Aortic Valve perpendicular to 2 left ventricular outflow tract views, through plane flow map through this slice
Short Axis Stack
Main Pulmonary Artery
Right pulmonary artery/ left pulmonary artery
Right Ventricular Outflow Tract
Right Ventricular Outflow Tract orthogonal
Short Axis slice above Pulmonary Valve perpendicular to 2 right ventricular outflow tract views, through plane flow map through this slice
RV 3-chamber (inflow-outflow) view

List of References

1. Harvey W. Exercitatio anatomica de motu cordis et sanguinis in animalibus. With an English translation and annotations by CHAUNCEY D. LEAKE. *Exercitatio anatomica de motu cordis et sanguinis in animalibus With an English translation and annotations by CHAUNCEY D LEAKE* 1928:(Tercentennial ed.) vii+74 +184 pp. 8 pl.-(Tercentennial ed.) vii+74 +84 pp. 8 pl.
2. Greyson CR. The right ventricle and pulmonary circulation: basic concepts. *Rev Esp Cardiol* 2010;63(1):81-95.
3. Watts JA, Marchick MR, Kline JA. Right ventricular heart failure from pulmonary embolism: key distinctions from chronic pulmonary hypertension. *J Card Fail* 2010;16(3):250-9. doi: 10.1016/j.cardfail.2009.11.008 [published Online First: 2010/01/15]
4. Repessé X, Charron C, Vieillard-Baron A. Acute respiratory distress syndrome: the heart side of the moon. *Curr Opin Crit Care* 2016;22(1):38-44. doi: 10.1097/MCC.0000000000000267
5. Mehta SR, Eikelboom JW, Natarajan MK, et al. Impact of right ventricular involvement on mortality and morbidity in patients with inferior myocardial infarction. *J Am Coll Cardiol* 2001;37(1):37-43.
6. Davlouros PA, Niwa K, Webb G, et al. The right ventricle in congenital heart disease. *Heart* 2006;92:I27-I38. doi: 10.1136/hrt.2005.077438
7. Haddad F, Couture P, Tousignant C, et al. The right ventricle in cardiac surgery, a perioperative perspective: II. Pathophysiology, clinical importance, and management. *Anesth Analg* 2009;108(2):422-33. doi: 10.1213/ane.0b013e31818d8b92
8. Argiriou M, Kolokotron SM, Sakellaridis T, et al. Right heart failure post left ventricular assist device implantation. *J Thorac Dis* 2014;6 Suppl 1:S52-9. doi: 10.3978/j.issn.2072-1439.2013.10.26
9. Kasai T, Bradley TD. Obstructive Sleep Apnea and Heart Failure Pathophysiologic and Therapeutic Implications. *Journal of the American College of Cardiology* 2011;57(2):119-27. doi: 10.1016/j.jacc.2010.08.627
10. D'Alto M, Scognamiglio G, Dimopoulos K, et al. Right Heart and Pulmonary Vessels Structure and Function. *Echocardiography-a Journal of Cardiovascular Ultrasound and Allied Techniques* 2015;32:3-10. doi: 10.1111/echo.12227
11. Haddad F, Hunt SA, Rosenthal DN, et al. Right ventricular function in cardiovascular disease, part I: Anatomy, physiology, aging, and functional assessment of the right ventricle. *Circulation* 2008;117(11):1436-48. doi: 10.1161/CIRCULATIONAHA.107.653576
12. Farb A, Burke AP, Virmani R. ANATOMY AND PATHOLOGY OF THE RIGHT VENTRICLE INCLUDING ACQUIRED TRICUSPID AND PULMONIC VALVE DISEASE. *Cardiology Clinics* 1992;10(1):1-22.
13. Ho SY, Nihoyannopoulos P. Anatomy, echocardiography, and normal right ventricular dimensions. *Heart* 2006;92:I2-I13. doi: 10.1136/hrt.2005.077875
14. Farrerbrown G. VASCULAR PATTERN OF MYOCARDIUM OF RIGHT VENTRICLE OF HUMAN HEART. *British Heart Journal* 1968;30(5):679-+.
15. Dell'Italia LJ. Anatomy and Physiology of the Right Ventricle. *Cardiology Clinics* 2012;30(2):167-+. doi: 10.1016/j.cc1.2012.03.009

16. Murphy E, Shelley B. The right ventricle - structural and functional importance for anaesthesia and intensive care. . *BJA Education* 2018;18(8):239-45.
17. Ventetuolo CE, Klinger JR. Management of acute right ventricular failure in the intensive care unit. *Ann Am Thorac Soc* 2014;11(5):811-22. doi: 10.1513/AnnalsATS.201312-446FR
18. Kubba S, Davila CD, Forfia PR. Methods for Evaluating Right Ventricular Function and Ventricular-Arterial Coupling. *Progress in Cardiovascular Diseases* 2016;59(1):42-51. doi: 10.1016/j.pcad.2016.06.001
19. Suga H, Sagawa K, Kostiuk DP. CONTROLS OF VENTRICULAR CONTRACTILITY ASSESSED BY PRESSURE-VOLUME RATIO, EMAX. *Cardiovascular Research* 1976;10(5):582-92. doi: 10.1093/cvr/10.5.582
20. Sayer G, Semigran M. Acute and Chronic Right Ventricular Failure. In: Eisen H, ed. Heart Failure. London: Springer, 2017:65-84.
21. Redington AN. Right ventricular function. *Cardiology Clinics* 2002;20(3):341-49. doi: 10.1016/s0733-8651(02)00005-x
22. Santamore WP, Gray L. Significant left ventricular contributions to right ventricular systolic function. Mechanism and clinical implications. *Chest* 1995;107(4):1134-45.
23. Naeije R, Badagliacca R. The overloaded right heart and ventricular interdependence. *Cardiovascular Research* 2017;113(12):1474-85. doi: 10.1093/cvr/cvx160
24. Bleeker GB, Steendijk P, Holman ER, et al. Acquired right ventricular dysfunction. *Heart* 2006;92 Suppl 1:i14-8. doi: 10.1136/hrt.2005.081547
25. Moore W. The Knife Man: Blood, Body Snatching, and the Birth of Modern Surgery: Crown Publishing Group 2006.
26. Sanz J, Garcia-Alvarez A, Fernandez-Friera L, et al. Right ventriculo-arterial coupling in pulmonary hypertension: a magnetic resonance study. *Heart* 2012;98(3):238-43. doi: 10.1136/heartjnl-2011-300462
27. Sheehan F, Redington A. The right ventricle: anatomy, physiology and clinical imaging. *Heart* 2008;94(11):1510-15. doi: 10.1136/hrt.2007.132779
28. McCabe C, White PA, Rana BS, et al. Right Ventricle Functional Assessment Have New Techniques Supplanted the Old Faithful Conductance Catheter? *Cardiology in Review* 2014;22(5):233-40. doi: 10.1097/crd.0000000000000020
29. Marik P. Handbook of Evidence-based Medicine. New York: Springer 2011:182.
30. Gidwani UK, Goel S. The Pulmonary Artery Catheter in 2015 The Swan and the Phoenix. *Cardiology in Review* 2016;24(1):1-13. doi: 10.1097/crd.0000000000000082
31. Visser LC. Right Ventricular Function Imaging Techniques. *Veterinary Clinics of North America-Small Animal Practice* 2017;47(5):989-+. doi: 10.1016/j.cvsm.2017.04.004
32. Surkova E, Muraru D, Iliceto S, et al. The use of multimodality cardiovascular imaging to assess right ventricular size and function. *International Journal of Cardiology* 2016;214:54-69. doi: 10.1016/j.ijcard.2016.03.074
33. Le Tourneau T, Piriou N, Donal E, et al. Imaging and modern assessment of the right ventricle. *Minerva Cardioangiol* 2011;59(4):349-73.
34. Greil GF, Beerbaum P, Razavi R, et al. Imaging the right ventricle: non-invasive imaging. *Heart* 2008;94(6):803-8. doi: 10.1136/hrt.2005.079111
35. Rudski LG, Lai WW, Afilalo J, et al. Guidelines for the Echocardiographic Assessment of the Right Heart in Adults: A Report from the American

Society of Echocardiography Endorsed by the European Association of Echocardiography, a registered branch of the European Society of Cardiology, and the Canadian Society of Echocardiography. *Journal of the American Society of Echocardiography* 2010;23(7):685-713. doi: 10.1016/j.echo.2010.05.010
36. Wharton G, Steeds R, Allen J, et al. A minimum dataset for a standard adult transthoracic echocardiogram: a guideline protocol from the British Society of Echocardiography. *Echo Research and Practice* 2015;2(1):G9-G24. doi: 10.1530/erp-14-0079
37. Recommendations for Cardiac Chamber Quantification by Echocardiography in Adults: An Update from the American Society of Echocardiography and the European Association of Cardiovascular Imaging (vol 16, pg 233, 2015). *European Heart Journal-Cardiovascular Imaging* 2016;17(9):969-69. doi: 10.1093/ehjci/jew124
38. Abouzeid CM, Shah T, Johri A, et al. Multimodality Imaging of the Right Ventricle. *Current treatment options in cardiovascular medicine* 2017;19(11):82-82. doi: 10.1007/s11936-017-0584-9
39. Kossaify A. Echocardiographic Assessment of the Right Ventricle, from the Conventional Approach to Speckle Tracking and Three-Dimensional Imaging, and Insights into the "Right Way" to Explore the Forgotten Chamber. *Clinical Medicine Insights-Cardiology* 2015;9:65-75. doi: 10.4137/cmc.s27462
40. Nagata Y, Wu VC-C, Kado Y, et al. Prognostic Value of Right Ventricular Ejection Fraction Assessed by Transthoracic 3D Echocardiography. *Circulation-Cardiovascular Imaging* 2017;10(2) doi: 10.1161/circimaging.116.005384
41. Dandel M, Lehmkuhl H, Knosalla C, et al. Strain and strain rate imaging by echocardiography - basic concepts and clinical applicability. *Current cardiology reviews* 2009;5(2):133-48. doi: 10.2174/157340309788166642
42. Blessberger H, Binder T. NON-invasive imaging: Two dimensional speckle tracking echocardiography: basic principles. *Heart* 2010;96(9):716-22. doi: 10.1136/hrt.2007.141002
43. Ho CY, Solomon SD. A clinician's guide to tissue Doppler imaging. *Circulation* 2006;113(10):e396-8. doi: 10.1161/CIRCULATIONAHA.105.579268
44. Silverton N, Meineri M. Speckle Tracking Strain of the Right Ventricle: An Emerging Tool for Intraoperative Echocardiography. *Anesth Analg* 2017;125(5):1475-78. doi: 10.1213/ANE.0000000000001910
45. Blessberger H, Binder T. Two dimensional speckle tracking echocardiography: clinical applications. *Heart* 2010;96(24):2032-40. doi: 10.1136/hrt.2010.199885
46. Tadic M. Multimodality Evaluation of the Right Ventricle: An Updated Review. *Clinical Cardiology* 2015;38(12):770-76. doi: 10.1002/clc.22443
47. Pennell DJ, Sechtem UP, Higgins CB, et al. Clinical indications for cardiovascular magnetic resonance (CMR): Consensus Pane report. *European Heart Journal* 2004;25(21):1940-65. doi: 10.1016/j.ehj.2004.06.040
48. Hendel RC, Berman DS, Di Carli MF, et al. ACCF/ASNC/ACR/AHA/ASE/SCCT/SCMR/SNM 2009 Appropriate Use Criteria for Cardiac Radionuclide Imaging: A Report of the American College of Cardiology Foundation Appropriate Use Criteria Task Force, the American Society of Nuclear Cardiology, the American College of Radiology, the American Heart Association, the American Society of Echocardiography, the Society of Cardiovascular Computed Tomography, the Society for

Cardiovascular Magnetic Resonance, and the Society of Nuclear Medicine: Endorsed by the American College of Emergency Physicians. *Circulation* 2009;119(22):E561-E87. doi: 10.1161/circulationaha.109.192519
49. Ridgway JP. Cardiovascular magnetic resonance physics for clinicians: part I. *J Cardiovasc Magn Reson* 2010;12:71. doi: 10.1186/1532-429X-12-71 [published Online First: 2010/11/30]
50. Dharmakumar R, Sharif B, Yang H-J. CMR Pulse Sequences. Basic Principles of Cardiovascular MRI: Physics and Imaging Technique,. Switzerland: Springer International Publishing, 2015:25-40.
51. Hundley WG, Bluemke DA, Finn JP, et al. ACCF/ACR/AHA/NASCI/SCMR 2010 Expert Consensus Document on Cardiovascular Magnetic Resonance A Report of the American College of Cardiology Foundation Task Force on Expert Consensus Documents. *Circulation* 2010;121(22):2462-508. doi: 10.1161/CIR.0b013e3181d44a8f
52. Norton P, Nacey N, Caovan D, et al. Cardiac MRI: The Basics University of Virginia2013 [Available from: https://www.med-ed.virginia.edu/courses/rad/cardiacmr/index.html accessed 02/02/19 2019.
53. Kramer CM, Barkhausen J, Flamm SD, et al. Standardized cardiovascular magnetic resonance (CMR) protocols 2013 update. *Journal of Cardiovascular Magnetic Resonance* 2013;15 doi: 10.1186/1532-429x-15-91
54. Carlsson M, Xanthis C, Smart S, et al. Tissue Characterization: T1, T2 and T2* Techniques. In: Syed M, Raman S, Simonetti O, eds. Basic Principles of Cardiovascular MRI. SWITZERLAND: Springer Publishing, 2015:167-77.
55. Taylor AJ, Salerno M, Dharmakumar R, et al. T1 Mapping Basic Techniques and Clinical Applications. *Jacc-Cardiovascular Imaging* 2016;9(1):67-81. doi: 10.1016/j.jcmg.2015.11.005
56. Kim PK, Hong YJ, Im DJ, et al. Myocardial T1 and T2 Mapping: Techniques and Clinical Applications. *Korean Journal of Radiology* 2017;18(1):113-31. doi: 10.3348/kjr.2017.18.1.113
57. Holloway CJ, Suttie J, Dass S, et al. Clinical cardiac magnetic resonance spectroscopy. *Prog Cardiovasc Dis* 2011;54(3):320-7. doi: 10.1016/j.pcad.2011.08.002
58. Hudsmith LE, Neubauer S. Detection of myocardial disorders by magnetic resonance spectroscopy. *Nat Clin Pract Cardiovasc Med* 2008;5 Suppl 2:S49-56. doi: 10.1038/ncpcardio1158
59. Lopez D, Salerano M. Principles of ECG gating for CMR. In: Syed M, Raman S, Simonetti O, eds. Basic Principles of Cardiovascular MRI: Springer, Cham, 2015.
60. Mair J. Biochemistry of B-type natriuretic peptide - where are we now? *Clinical Chemistry and Laboratory Medicine* 2008;46(11):1507-14. doi: 10.1515/cclm.2008.295
61. Weber M, Hamm C. Role of B-type natriuretic peptide (BNP) and NT-proBNP in clinical routine. *Heart* 2006;92(6):843-49. doi: 10.1136/hrt.2005.071233
62. Redfield MM, Rodeheffer RJ, Jacobsen SJ, et al. Plasma brain natriuretic peptide concentration: Impact of age and gender. *Journal of the American College of Cardiology* 2002;40(5):976-82. doi: 10.1016/s0735-1097(02)02059-4
63. Dworzynski K, Roberts E, Ludman A, et al. GUIDELINES Diagnosing and managing acute heart failure in adults: summary of NICE guidance. *Bmj-British Medical Journal* 2014;349 doi: 10.1136/bmj.g5695

64. Santaguida PL, Don-Wauchope AC, Oremus M, et al. BNP and NT-proBNP as prognostic markers in persons with acute decompensated heart failure: a systematic review. *Heart Failure Reviews* 2014;19(4):453-70. doi: 10.1007/s10741-014-9442-y
65. Coutance G, Le Page O, Lo T, et al. Prognostic value of brain natriuretic peptide in acute pulmonary embolism. *Critical Care* 2008;12(4) doi: 10.1186/cc6996
66. Dernellis J, Panaretou M. Assessment of cardiac risk before non-cardiac surgery: brain natriuretic peptide in 1590 patients. *Heart* 2006;92(11):1645-50. doi: 10.1136/hrt.2005.085530
67. Payne CJ, Gibson SC, Bryce G, et al. B-type natriuretic peptide predicts long-term survival after major non-cardiac surgery. *British Journal of Anaesthesia* 2011;107(2):144-49. doi: 10.1093/bja/aer119
68. Feringa HHH, Schouten O, Dunkelgrun M, et al. Plasma N-terminal pro-B-type natriuretic peptide as long-term prognostic marker after major vascular surgery. *Heart* 2007;93(2):226-31. doi: 10.1136/hrt.2006.093716
69. Nojiri T, Inoue M, Yamamoto K, et al. B-type natriuretic Peptide as a predictor of postoperative cardiopulmonary complications in elderly patients undergoing pulmonary resection for lung cancer. *Ann Thorac Surg* 2011;92(3):1051-5. doi: 10.1016/j.athoracsur.2011.03.085
70. Ryding ADS, Kumar S, Worthington AM, et al. Prognostic Value of Brain Natriuretic Peptide in Noncardiac Surgery A Meta-analysis. *Anesthesiology* 2009;111(2):311-19. doi: 10.1097/ALN.0b013e3181aaeb11
71. Karthikeyan G, Moncur RA, Levine O, et al. Is a Pre-Operative Brain Natriuretic Peptide or N-Terminal Pro-B-Type Natriuretic Peptide Measurement an Independent Predictor of Adverse Cardiovascular Outcomes Within 30 Days of Noncardiac Surgery? A Systematic Review and Meta-Analysis of Observational Studies. *Journal of the American College of Cardiology* 2009;54(17):1599-606. doi: 10.1016/j.jacc.2009.06.028
72. Kristensen SD, Knuuti J, Saraste A, et al. 2014 ESC/ESA Guidelines on non-cardiac surgery: cardiovascular assessment and management The Joint Task Force on non-cardiac surgery: cardiovascular assessment and management of the European Society of Cardiology (ESC) and the European Society of Anaesthesiology (ESA). *European Heart Journal* 2014;35(35):2383-431. doi: 10.1093/eurheartj/ehu282
73. Fleisher LA, Fleischmann KE, Auerbach AD, et al. 2014 ACC/AHA Guideline on Perioperative Cardiovascular Evaluation and Management of Patients Undergoing Noncardiac Surgery: Executive Summary A Report of the American College of Cardiology/American Heart Association Task Force on Practice Guidelines. *Circulation* 2014;130(24):2215-45. doi: 10.1161/cir.0000000000000105
74. Young DJ, McCall PJ, Kirk A, et al. B-type natriuretic peptide predicts deterioration in functional capacity following lung resection. *Interactive cardiovascular and thoracic surgery* 2019 doi: 10.1093/icvts/ivz016
75. Agewall S, Giannitsis E, Jernberg T, et al. Troponin elevation in coronary vs. non-coronary disease. *European Heart Journal* 2011;32(4):404-11B. doi: 10.1093/eurheartj/ehq456
76. Lega JC, Lacasse Y, Lakhal L, et al. Natriuretic peptides and troponins in pulmonary embolism: a meta-analysis. *Thorax* 2009;64(10):869-75. doi: 10.1136/thx.2008.110965
77. Bajaj A, Saleeb M, Rathor P, et al. Prognostic value of troponins in acute nonmassive pulmonary embolism: A meta-analysis. *Heart & Lung* 2015;44(4):327-34. doi: 10.1016/j.hrtlng.2015.03.007

78. Becattini C, Vedovati MC, Agnelli G. Prognostic value of troponins in acute pulmonary embolism - A meta-analysis. *Circulation* 2007;116(4):427-33. doi: 10.1161/circulationaha.106.680421
79. Zhao BC, Liu WF, Deng QW, et al. Meta-analysis of preoperative high-sensitivity cardiac troponin measurement in non-cardiac surgical patients at risk of cardiovascular complications. *British Journal of Surgery* 2020;107(2):E81-+. doi: 10.1002/bjs.11305
80. Levy M, Heels-Ansdell D, Hiralal R, et al. Prognostic Value of Troponin and Creatine Kinase Muscle and Brain Isoenzyme Measurement after Noncardiac Surgery A Systematic Review and Meta-analysis. *Anesthesiology* 2011;114(4):796-806. doi: 10.1097/ALN.0b013e31820ad503
81. McCall PJ, Arthur A, Glass A, et al. The right ventricular response to lung resection. *The Journal of thoracic and cardiovascular surgery* 2019 doi: 10.1016/j.jtcvs.2019.01.067
82. Cancer Research UK. Lung Cancer Incidence Statistics: Cancer Research UK; 2016 [Available from: https://www.cancerresearchuk.org/health-professional/cancer-statistics/statistics-by-cancer-type/lung-cancer/incidence accessed 31/10/2018 2018.
83. Information Services Division Scotland. Cancer Statistics : Lung Cancer and Mesothelioma: Information Services Division Scotland; 2017 [Available from: https://www.isdscotland.org/Health-Topics/Cancer/Cancer-Statistics/Lung-Cancer-and-Mesothelioma/ accessed 31/10/2018 2018.
84. Foundation BL. Lung Cancer Statistics British Lung Foundation2012 [Available from: https://statistics.blf.org.uk/lung-cancer accessed 31/10/18 2018.
85. British Lung Foundation. Lung Cancer Statistics: British Lung Foundation; 2012 [Available from: https://statistics.blf.org.uk/lung-cancer accessed 31/10/2018 2018.
86. National Institute for Health and Care Excellence. NICE Guideline NG122. Lung Cancer: diagnosis and management.: NICE; 2019 [Available from: https://www.nice.org.uk/guidance/ng122 accessed 10/01/2020 2020.
87. Royal College of Physicians. National Lung Cancer Audit: Annual Report 2017.: Royal College of Physicians; 2017 [Available from: https://www.rcplondon.ac.uk/projects/outputs/nlca-annual-report-2017 accessed 31/10/2018 2018.
88. Lim E, Baldwin D, Beckles M, et al. Guidelines on the radical management of patients with lung cancer. *Thorax* 2010;65 Suppl 3:iii1-27. doi: 10.1136/thx.2010.145938
89. Society for Cardiothoracic Surgery in Great Britain and Northern Ireland. Lung Cancer Clinical Outcomes Project 2016: Lung Cancer Clinical Outcomes Project; 2016 [Available from: https://scts.org/lccop/ accessed 26/11/2018 2018.
90. RCP. Lung Cancer Clinical Outcomes Publication 2018 National Lung Cancer Audit2021 [Available from: https://nlca.rcp.ac.uk/content/misc/LCCOP%202021(2018).pdf2022.
91. The Society for Cardiothoracic Surgery in Great Britain and Northern Ireland. Third National Thoracic Surgery Activity and Outcomes Report: The Society for Cardiothoracic Surgery in Great Britain and Northern Ireland; 2018 [Available from: https://scts.org/wp-content/uploads/2019/06/Third-thoracic-blue-book-FINAL.pdf accessed 10/01/2020 2020.
92. Paul S, Altorki NK, Sheng S, et al. Thoracoscopic lobectomy is associated with lower morbidity than open lobectomy: A propensity-matched analysis

from the STS database. *Journal of Thoracic and Cardiovascular Surgery* 2010;139(2):366-78. doi: 10.1016/j.jtcvs.2009.08.026
93. Whitson BA, Groth SS, Duval SJ, et al. Surgery for Early-Stage Non-Small Cell Lung Cancer: A Systematic Review of the Video-Assisted Thoracoscopic Surgery Versus Thoracotomy Approaches to Lobectomy. *Annals of Thoracic Surgery* 2008;86(6):2008-18. doi: 10.1016/j.athoracsur.2008.07.009
94. Cao C, Manganas C, Ang S, et al. VIDEO-ASSISTED THORACIC SURGERY VERSUS OPEN THORACOTOMY FOR NON-SMALL CELL LUNG CANCER - A META-ANALYSIS OF PROPENSITY SCORE MATCHED PATIENTS. *Journal of Thoracic Oncology* 2013;8:S824-S24.
95. In Hospital Clinical Efficacy, Safety, and Oncological Outcomes for VIOLET. 2019 World Conference on Lung Cancer; 2019; Barcelona.
96. Lim E, Li Choy L, Flaks L, et al. Detected troponin elevation is associated with high early mortality after lung resection for cancer. *J Cardiothorac Surg* 2006;1:37. doi: 10.1186/1749-8090-1-37 [published Online First: 2006/10/23]
97. Ginsberg RJ, Rubinstein LV. Randomized trial of lobectomy versus limited resection for T1 N0 non-small cell lung cancer. *Annals of Thoracic Surgery* 1995;60(3):615-21. doi: 10.1016/0003-4975(95)00537-u
98. Takizawa T, Haga M, Yagi N, et al. Pulmonary function after segmentectomy for small peripheral carcinoma of the lung. *Journal of Thoracic and Cardiovascular Surgery* 1999;118(3):536-41. doi: 10.1016/s0022-5223(99)70193-5
99. Harada H, Okada M, Sakamoto T, et al. Functional advantage after radical segmentectomy versus lobectomy for lung cancer. *Annals of Thoracic Surgery* 2005;80(6):2041-45. doi: 10.1016/j.athoracsur.2005.06.010
100. Saito H, Nakagawa T, Ito M, et al. Pulmonary Function After Lobectomy Versus Segmentectomy in Patients with Stage I Non-Small Cell Lung Cancer. *World Journal of Surgery* 2014;38(8):2025-31. doi: 10.1007/s00268-014-2521-3
101. Zhang ZR, Feng HX, Zhao H, et al. Sublobar resection is associated with better perioperative outcomes in elderly patients with clinical stage I non-small cell lung cancer: a multicenter retrospective cohort study. *Journal of Thoracic Disease* 2019;11(5):1838-+. doi: 10.21037/jtd.2019.05.20
102. Busch E, Verazin G, Antkowiak JG, et al. PULMONARY COMPLICATIONS IN PATIENTS UNDERGOING THORACOTOMY FOR LUNG-CARCINOMA. *Chest* 1994;105(3):760-66. doi: 10.1378/chest.105.3.760
103. Stephan F, Boucheseiche S, Hollande J, et al. Pulmonary complications following lung resection - A comprehensive analysis of incidence and possible risk factors. *Chest* 2000;118(5):1263-70. doi: 10.1378/chest.118.5.1263
104. Nagasaki F, Flehinger BJ, Martini N. COMPLICATIONS OF SURGERY IN THE TREATMENT OF CARCINOMA OF THE LUNG. *Chest* 1982;82(1):25-29. doi: 10.1378/chest.82.1.25
105. Korst RJ, Humphrey CB. Complete lobar collapse following pulmonary lobectomy - Its incidence, predisposing factors, and clinical ramifications. *Chest* 1997;111(5):1285-89. doi: 10.1378/chest.111.5.1285
106. Salati M, Refai M, Pompili C, et al. Major morbidity after lung resection: a comparison between the European Society of Thoracic Surgeons Database system and the Thoracic Morbidity and Mortality system. *Journal of Thoracic Disease* 2013;5(3):217-22. doi: 10.3978/j.issn.2072-1439.2013.05.03

107. Patel RL, Townsend ER, Fountain SW. ELECTIVE PNEUMONECTOMY - FACTORS ASSOCIATED WITH MORBIDITY AND OPERATIVE MORTALITY. *Annals of Thoracic Surgery* 1992;54(1):84-88. doi: 10.1016/0003-4975(92)91145-y
108. Dyszkiewicz W, Skrzypczak M. Atrial fibrillation after surgery of the lung: clinical analysis of risk factors. *European Journal of Cardio-Thoracic Surgery* 1998;13(6):625-27. doi: 10.1016/s1010-7940(98)00084-0
109. Vaporciyan AA, Correa AM, Rice DC, et al. Risk factors associated with atrial fibrillation after noncardiac thoracic surgery: Analysis of 2588 patients. *Journal of Thoracic and Cardiovascular Surgery* 2004;127(3):779-86. doi: 10.1016/j.jtcvs.2003.07.011
110. Garner M, Routledge T, King JE, et al. New-onset atrial fibrillation after anatomic lung resection: predictive factors, treatment and follow-up in a UK thoracic centre. *Interactive Cardiovascular and Thoracic Surgery* 2017;24(2):260-64. doi: 10.1093/icvts/ivw348
111. Bagheri R, Yousefi Y, Rezai R, et al. Atrial fibrillation after lung surgery: incidence, underlying factors, and predictors. *Kardiochirurgia I Torakochirurgia Polska-Polish Journal of Thoracic and Cardiovascular Surgery* 2019;16(2):53-56. doi: 10.5114/kitp.2019.86355
112. Amar D, Zhang H, Roistacher N. The incidence and outcome of ventricular arrhythmias after noncardiac thoracic surgery. *Anesthesia and Analgesia* 2002;95(3):537-43. doi: 10.1097/00000539-200209000-00006
113. De Decker K, Jorens PG, Van Schil P. Cardiac complications after noncardiac thoracic surgery: An evidence-based current review. *Annals of Thoracic Surgery* 2003;75(4):1340-48. doi: 10.1016/s0003-4975(02)04824-5
114. Sarna L, Evangelista L, Tashkin D, et al. Impact of respiratory symptoms and pulmonary function on quality of life of long-term survivors of non-small cell lung cancer. *Chest* 2004;125(2):439-45. doi: 10.1378/chest.125.2.439
115. Moller A, Sartipy U. Long-term health-related quality of life following surgery for lung cancer. *European Journal of Cardio-Thoracic Surgery* 2012;41(2):362-67. doi: 10.1016/j.ejcts.2011.05.055
116. Shapiro M, Swanson SJ, Wright CD, et al. Predictors of Major Morbidity and Mortality After Pneumonectomy Utilizing The Society for Thoracic Surgeons General Thoracic Surgery Database. *Annals of Thoracic Surgery* 2010;90(3):927-34. doi: 10.1016/j.athoracsur.2010.05.041
117. Kozower BD, Sheng S, O'Brien SM, et al. STS Database Risk Models: Predictors of Mortality and Major Morbidity for Lung Cancer Resection. *Annals of Thoracic Surgery* 2010;90(3):875-81. doi: 10.1016/j.athoracsur.2010.03.115
118. Zhang R, Lee SM, Wigfield C, et al. Lung Function Predicts Pulmonary Complications Regardless of the Surgical Approach. *Annals of Thoracic Surgery* 2015;99(5):1761-67. doi: 10.1016/j.athoracsur.2015.01.030
119. Ferguson MK, Vigneswaran WT. Diffusing capacity predicts morbidity after lung resection in patients without obstructive lung disease. *Annals of Thoracic Surgery* 2008;85(4):1158-65. doi: 10.1016/j.athoracsur.2007.12.071
120. Ferguson MK, Watson S, Johnson E, et al. Predicted postoperative lung function is associated with all-cause long-term mortality after major lung resection for cancer. *European Journal of Cardio-Thoracic Surgery* 2014;45(4):660-64. doi: 10.1093/ejcts/ezt462
121. Ferguson MK, Celauro AD, Vigneswaran WT. Validation of a modified scoring system for cardiovascular risk associated with major lung resection.

European Journal of Cardio-Thoracic Surgery 2012;41(3):598-601. doi: 10.1093/ejcts/ezr081
122. Brunelli A, Ferguson MK, Salati M, et al. Thoracic Revised Cardiac Risk Index Is Associated With Prognosis After Resection for Stage I Lung Cancer. *Annals of Thoracic Surgery* 2015;100(1):195-200. doi: 10.1016/j.athoracsur.2015.03.103
123. Thomas DC, Blasberg JD, Arnold BN, et al. Validating the Thoracic Revised Cardiac Risk Index Following Lung Resection. *Annals of Thoracic Surgery* 2017;104(2):389-94. doi: 10.1016/j.athoracsur.2017.02.006
124. Brunelli A, Varela G, Salati M, et al. Recalibration of the Revised Cardiac Risk Index in Lung Resection Candidates. *Annals of Thoracic Surgery* 2010;90(1):199-203. doi: 10.1016/j.athoracsur.2010.03.042
125. Brunelli A, Cassivi SD, Fibla J, et al. External Validation of the Recalibrated Thoracic Revised Cardiac Risk Index for Predicting the Risk of Major Cardiac Complications After Lung Resection. *Annals of Thoracic Surgery* 2011;92(2):445-48. doi: 10.1016/j.athoracsur.2011.03.095
126. Ferguson MK, Saha-Chaudhuri P, Mitchell JD, et al. Prediction of Major Cardiovascular Events After Lung Resection Using a Modified Scoring System. *Annals of Thoracic Surgery* 2014;97(4):1135-41. doi: 10.1016/j.athoracsur.2013.12.032
127. Wotton R, Marshall A, Kerr A, et al. Does the revised cardiac risk index predict cardiac complications following elective lung resection? *Journal of Cardiothoracic Surgery* 2013;8 doi: 10.1186/1749-8090-8-220
128. Falcoz PE, Conti M, Brouchet L, et al. The Thoracic Surgery Scoring System (Thoracoscore): Risk model for in-hospital death in 15,183 patients requiring thoracic surgery. *Journal of Thoracic and Cardiovascular Surgery* 2007;133(2):325-32. doi: 10.1016/j.jtcvs.2006.09.020
129. Sharkey A, Ariyaratnam P, Anikin V, et al. Thoracoscore and European Society Objective Score Fail to Predict Mortality in the UK. *World journal of oncology* 2015;6(1):270-75. doi: 10.14740/wjon897w
130. Kaul TK, Fields BL. Postoperative acute refractory right ventricular failure: incidence, pathogenesis, management and prognosis. *Cardiovasc Surg* 2000;8(1):1-9.
131. Kholdani CA, Fares WH. Management of Right Heart Failure in the Intensive Care Unit. *Clin Chest Med* 2015;36(3):511-20. doi: 10.1016/j.ccm.2015.05.015 [published Online First: 2015/06/27]
132. Wardi G, Blanchard D, Dittrich T, et al. Right ventricle dysfunction and echocardiographic parameters in the first 24 h following resuscitation in the post-cardiac arrest patient: A retrospective cohort study. *Resuscitation* 2016;103:71-74. doi: 10.1016/j.resuscitation.2016.03.009
133. Zapol WM, Snider MT. Pulmonary hypertension in severe acute respiratory failure. *N Engl J Med* 1977;296(9):476-80. doi: 10.1056/NEJM197703032960903
134. Vieillard-Baron A, Jardin F. Why protect the right ventricle in patients with acute respiratory distress syndrome? *Curr Opin Crit Care* 2003;9(1):15-21.
135. Gao Y, Du X, Qin W, et al. Assessment of the right ventricular function in patients with chronic obstructive pulmonary disease using MRI. *Acta Radiol* 2011;52(7):711-5. doi: 10.1258/ar.2011.100449
136. Boissier F, Katsahian S, Razazi K, et al. Prevalence and prognosis of cor pulmonale during protective ventilation for acute respiratory distress syndrome. *Intensive Care Med* 2013;39(10):1725-33. doi: 10.1007/s00134-013-2941-9 [published Online First: 2013/05/15]

137. Coz Yataco A, Aguinaga Meza M, Buch KP, et al. Hospital and intensive care unit management of decompensated pulmonary hypertension and right ventricular failure. *Heart Fail Rev* 2016;21(3):323-46. doi: 10.1007/s10741-015-9514-7
138. Zochios V, Parhar K, Tunnicliffe W, et al. The Right Ventricle in ARDS. *Chest* 2017;152(1):181-93. doi: 10.1016/j.chest.2017.02.019
139. Noordegraaf AV, Westerhof BE, Westerhof N. The Relationship Between the Right Ventricle and its Load in Pulmonary Hypertension. *Journal of the American College of Cardiology* 2017;69(2):236-43. doi: 10.1016/j.jacc.2016.10.047
140. Marongiu I, Spinelli E, Mauri T. Cardio-respiratory physiology during one-lung ventilation: complex interactions in need of advanced monitoring. *Annals of Translational Medicine* 2020;8(8) doi: 10.21037/atm.2020.03.179
141. Rana M, Yusuff H, Zochios V. The Right Ventricle During Selective Lung Ventilation for Thoracic Surgery. *J Cardiothorac Vasc Anesth* 2019;33(7):2007-16. doi: 10.1053/j.jvca.2018.11.030 [published Online First: 20181122]
142. Reed CE, Dorman BH, Spinale FG, et al. ASSESSMENT OF RIGHT-VENTRICULAR CONTRACTILE PERFORMANCE AFTER PULMONARY RESECTION. *Annals of Thoracic Surgery* 1993;56(3):426-32. doi: 10.1016/0003-4975(93)90874-h
143. Rams JJ, Harrison RW, Fry WA, et al. OPERATIVE PULMONARY ARTERY PRESSURE MEASUREMENTS AS A GUIDE TO POSTOPERATIVE MANAGEMENT AND PROGNOSIS FOLLOWING PNEUMONECTOMY. *Diseases of the Chest* 1962;41(1):85-90. doi: 10.1378/chest.41.1.85
144. Miyazawa M, Haniuda M, Nishimura H, et al. Longterm effects of pulmonary resection on cardiopulmonary function. *Journal of the American College of Surgeons* 1999;189(1):26-33. doi: 10.1016/s1072-7515(99)00071-x
145. Reed CE, Spinale FG, Crawford FA. EFFECT OF PULMONARY RESECTION ON RIGHT VENTRICULAR-FUNCTION. *Annals of Thoracic Surgery* 1992;53(4):578-82. doi: 10.1016/0003-4975(92)90314-t
146. Nishimura H, Haniuda M, Morimoto M, et al. CARDIOPULMONARY FUNCTION AFTER PULMONARY LOBECTOMY IN PATIENTS WITH LUNG-CANCER. *Annals of Thoracic Surgery* 1993;55(6):1477-84. doi: 10.1016/0003-4975(93)91091-z
147. Okada M, Ota T, Matsuda H, et al. RIGHT-VENTRICULAR DYSFUNCTION AFTER MAJOR PULMONARY RESECTION. *Journal of Thoracic and Cardiovascular Surgery* 1994;108(3):503-11.
148. Reed CE, Dorman BH, Spinale FG. Mechanisms of right ventricular dysfunction after pulmonary resection. *Annals of Thoracic Surgery* 1996;62(1):225-31. doi: 10.1016/0003-4975(96)00258-5
149. Backlund M, Laasonen L, Lepantalo M, et al. Effect of oxygen on pulmonary hemodynamics and incidence of atrial fibrillation after noncardiac thoracotomy. *Journal of Cardiothoracic and Vascular Anesthesia* 1998;12(4):422-28. doi: 10.1016/s1053-0770(98)90196-3
150. Mikami I, Koizumi K, Tanaka S. Changes in right ventricular performance in elderly patients who underwent lobectomy using video-assisted thoracic surgery for primary lung cancer. *The Japanese journal of thoracic and cardiovascular surgery : official publication of the Japanese Association for Thoracic Surgery = Nihon Kyobu Geka Gakkai zasshi* 2001;49(3):153-9.
151. Mageed NA, El-Ghonaimy YAF, Elgamal MAF, et al. Acute effects of lobectomy on right ventricular ejection fraction and mixed venous oxygen

saturation. *Annals of Saudi Medicine* 2005;25(6):481-85. doi: 10.5144/0256-4947.2005.481
152. Elrakhawy HM, Alassal MA, Shaalan AM, et al. Impact of Major Pulmonary Resections on Right Ventricular Function: Early Postoperative Changes. *Heart Surgery Forum* 2018;21(1):E9-E17. doi: 10.1532/hsf.1864
153. Boldt J, Muller M, Uphus D, et al. Cardiorespiratory changes in patients undergoing pulmonary resection using different anesthetic management techniques. *Journal of Cardiothoracic and Vascular Anesthesia* 1996;10(7):854-59. doi: 10.1016/s1053-0770(96)80045-0
154. Gidwani UK, Mohanty B, Chatterjee K. The Pulmonary Artery Catheter A Critical Reappraisal. *Cardiology Clinics* 2013;31(4):545-+. doi: 10.1016/j.ccl.2013.07.008
155. Hoeper MM, Lee SH, Voswinckel R, et al. Complications of right heart catheterization procedures in patients with pulmonary hypertension in experienced centers. *J Am Coll Cardiol* 2006;48(12):2546-52. doi: 10.1016/j.jacc.2006.07.061 [published Online First: 20061128]
156. Harvey S, Harrison DA, Singer M, et al. Assessment of the clinical effectiveness of pulmonary artery catheters in management of patients in intensive care (PAC-Man): a randomised controlled trial. *Lancet* 2005;366(9484):472-7. doi: 10.1016/S0140-6736(05)67061-4
157. Urban P, Scheidegger D, Gabathuler J, et al. THERMODILUTION DETERMINATION OF RIGHT VENTRICULAR VOLUME AND EJECTION FRACTION - A COMPARISON WITH BIPLANE ANGIOGRAPHY. *Critical Care Medicine* 1987;15(7):652-55. doi: 10.1097/00003246-198707000-00005
158. De Simone R, Wolf I, Mottl-Link S, et al. Intraoperative assessment of right ventricular volume and function. *European Journal of Cardio-Thoracic Surgery* 2005;27(6):988-93. doi: 10.1016/j.ejcts.2005.01.022
159. Hein M, Roehl AB, Baumert JH, et al. Continuous right ventricular volumetry by fast-response thermodilution during right ventricular ischemia: Head-to-head comparison with conductance catheter measurements. *Critical Care Medicine* 2009;37(11):2962-67. doi: 10.1097/CCM.0b013e3181b027a5
160. Leibowitz AB. Pulmonary artery catheter determined right ventricular ejection fraction and right ventricular end-diastolic volume: Another case of "The Emperor Has No Clothes". *Critical Care Medicine* 2009;37(11):2992-92. doi: 10.1097/CCM.0b013e3181b01839
161. Amar D, Roistacher N, Burt M, et al. CLINICAL AND ECHOCARDIOGRAPHIC CORRELATES OF SYMPTOMATIC TACHYDYSRHYTHMIAS AFTER NONCARDIAC THORACIC-SURGERY. *Chest* 1995;108(2):349-54. doi: 10.1378/chest.108.2.349
162. Amar D, Burt ME, Roistacher N, et al. Value of perioperative Doppler echocardiography in patients undergoing major lung resection. *Annals of Thoracic Surgery* 1996;61(2):516-20. doi: 10.1016/0003-4975(95)00939-6
163. Venuta F, Sciomer S, Andreetti C, et al. Long-term Doppler echocardiographic evaluation of the right heart after major lung resections. *European Journal of Cardio-Thoracic Surgery* 2007;32(5):787-90. doi: 10.1016/j.ejcts.2007.07.033
164. Foroulis CN, Kotoulas CS, Kakouros S, et al. Study on the late effect of pneumonectomy on right heart pressures using Doppler echocardiography. *European Journal of Cardio-Thoracic Surgery* 2004;26(3):508-14. doi: 10.1016/j.ejcts.2004.05.036
165. Colkesen Y, Acil T, Findikcioglu A, et al. Tissue Doppler evaluation of the effects of major lung resection on cardiac functions. *Turk Kardiyoloji*

Dernegi arsivi : Turk Kardiyoloji Derneginin yayin organidir 2009;37(5):317-20.
166. Kumbasar U, Kavukcu HS, Ozdemir N, et al. Tissue Doppler evaluation of the right ventricle in major pulmonary resections. *Turkish Journal of Medical Sciences* 2013;43(6):971-75. doi: 10.3906/sag-1210-1
167. Wang Z, Yuan J, Chu W, et al. Evaluation of left and right ventricular myocardial function after lung resection using speckle tracking echocardiography. *Medicine* 2016;95(31) doi: 10.1097/md.0000000000004290
168. Smulders SA, Holverda S, Vonk-Noordegraaf A, et al. Cardiac function and position more than 5 years after pneumonectomy. *Annals of Thoracic Surgery* 2007;83(6):1986-92. doi: 10.1016/j.athoracsur.2007.01.036
169. Sanz J, García-Alvarez A, Fernández-Friera L, et al. Right ventriculo-arterial coupling in pulmonary hypertension: a magnetic resonance study. *Heart* 2012;98(3):238-43. doi: 10.1136/heartjnl-2011-300462 [published Online First: 20110913]
170. Konstam MA, Kiernan MS, Bernstein D, et al. Evaluation and Management of Right-Sided Heart Failure: A Scientific Statement From the American Heart Association. *Circulation* 2018;137(20):e578-e622. doi: doi:10.1161/CIR.0000000000000560
171. Glass A, McCall P, Arthur A, et al. Pulmonary artery wave reflection and right ventricular function after lung resection. *Br J Anaesth* 2022 doi: 10.1016/j.bja.2022.07.052 [published Online First: 20220914]
172. Tadic M, Pieske-Kraigher E, Cuspidi C, et al. Right ventricular strain in heart failure: Clinical perspective. *Arch Cardiovasc Dis* 2017;110(10):562-71. doi: 10.1016/j.acvd.2017.05.002 [published Online First: 20170629]
173. Prihadi EA, van der Bijl P, Dietz M, et al. Prognostic Implications of Right Ventricular Free Wall Longitudinal Strain in Patients With Significant Functional Tricuspid Regurgitation. *Circ Cardiovasc Imaging* 2019;12(3):e008666. doi: 10.1161/CIRCIMAGING.118.008666
174. McCall P, Soosay A, Kinsella J, et al. The utility of transthoracic echocardiographic measures of right ventricular systolic function in a lung resection cohort. *Echo Research and Practice* 2019;6(1):7-15. doi: 10.1530/erp-18-0067
175. DRISCOLL AC, HOBIKA JH, ETSTEN BE, et al. Clinically unrecognized myocardial infarction following surgery. *N Engl J Med* 1961;264:633-9. doi: 10.1056/NEJM196103302641302
176. Khan J, Alonso-Coello P, Devereaux PJ. Myocardial injury after noncardiac surgery. *Curr Opin Cardiol* 2014;29(4):307-11. doi: 10.1097/HCO.0000000000000069
177. Botto F, Alonso-Coello P, Chan MT, et al. Myocardial injury after noncardiac surgery: a large, international, prospective cohort study establishing diagnostic criteria, characteristics, predictors, and 30-day outcomes. *Anesthesiology* 2014;120(3):564-78. doi: 10.1097/ALN.0000000000000113
178. Nathoe HM, van Klei WA, Beattie WS. Perioperative troponin elevation: always myocardial injury, but not always myocardial infarction. *Anesth Analg* 2014;119(5):1014-6. doi: 10.1213/ANE.0000000000000422
179. Yano T, Yokoyama H, Fukuyama Y, et al. The current status of postoperative complications and risk factors after a pulmonary resection for primary lung cancer - A multivariate analysis. *European Journal of Cardio-Thoracic Surgery* 1997;11(3):445-49. doi: 10.1016/s1010-7940(96)01097-4

180. Ploeg AJ, Kappetein AP, van Tongeren RB, et al. Factors associated with perioperative complications and long-term results after pulmonary resection for primary carcinoma of the lung. *European Journal of Cardio-Thoracic Surgery* 2003;23(1):26-29. doi: 10.1016/s1010-7940(02)00655-3
181. González-Tallada A, Borrell-Vega J, Coronado C, et al. Myocardial Injury After Noncardiac Surgery: Incidence, Predictive Factors, and Outcome in High-Risk Patients Undergoing Thoracic Surgery: An Observational Study. *J Cardiothorac Vasc Anesth* 2020;34(2):426-32. doi: 10.1053/j.jvca.2019.08.014 [published Online First: 20190816]
182. Spence J, LeManach Y, Chan MTV, et al. Association between complications and death within 30 days after noncardiac surgery. *CMAJ* 2019;191(30):E830-E37. doi: 10.1503/cmaj.190221
183. Devereaux PJ, Biccard BM, Sigamani A, et al. Association of Postoperative High-Sensitivity Troponin Levels With Myocardial Injury and 30-Day Mortality Among Patients Undergoing Noncardiac Surgery. *JAMA* 2017;317(16):1642-51. doi: 10.1001/jama.2017.4360
184. Shelley B, Glass A, Keast T, et al. Perioperative cardiovascular pathophysiology in patients undergoing lung resection surgery: a narrative review. *Br J Anaesth* 2023;130(1):e66-e79. doi: 10.1016/j.bja.2022.06.035 [published Online First: 20220813]
185. Allen MS, Darling GE, Pechet TT, et al. Morbidity and mortality of major pulmonary resections in patients with early-stage lung cancer: initial results of the randomized, prospective ACOSOG Z0030 trial. *Ann Thorac Surg* 2006;81(3):1013-9; discussion 19-20. doi: 10.1016/j.athoracsur.2005.06.066
186. Ackland GL, Abbott TEF, Jones TF, et al. Early elevation in plasma high-sensitivity troponin T and morbidity after elective noncardiac surgery: prospective multicentre observational cohort study. *British Journal of Anaesthesia* 2020;124(5):535-43. doi: 10.1016/j.bja.2020.02.003
187. Sheth T, Chan M, Butler C, et al. Prognostic capabilities of coronary computed tomographic angiography before non-cardiac surgery: prospective cohort study. *BMJ* 2015;350:h1907. doi: 10.1136/bmj.h1907 [published Online First: 20150422]
188. Devereaux PJ, Yang H, Yusuf S, et al. Effects of extended-release metoprolol succinate in patients undergoing non-cardiac surgery (POISE trial): a randomised controlled trial. *Lancet* 2008;371(9627):1839-47. doi: 10.1016/S0140-6736(08)60601-7 [published Online First: 20080512]
189. Thygesen K, Alpert JS, Jaffe AS, et al. Fourth Universal Definition of Myocardial Infarction (2018). *Circulation* 2018;138(20):e618-e51. doi: 10.1161/CIR.0000000000000617
190. Devereaux PJ, Szczeklik W. Myocardial injury after non-cardiac surgery: diagnosis and management. *European heart journal* 2019 doi: 10.1093/eurheartj/ehz301
191. Ackland GL, Abbott TEF, Cain D, et al. Preoperative systemic inflammation and perioperative myocardial injury: prospective observational multicentre cohort study of patients undergoing non-cardiac surgery. *British journal of anaesthesia* 2019;122(2):180-87. doi: 10.1016/j.bja.2018.09.002 [published Online First: 2018/10/02]
192. Kapellos TS, Bonaguro L, Gemünd I, et al. Human Monocyte Subsets and Phenotypes in Major Chronic Inflammatory Diseases. *Frontiers in Immunology* 2019;10(2035) doi: 10.3389/fimmu.2019.02035
193. Alivernini S, MacDonald L, Elmesmari A, et al. Distinct synovial tissue macrophage subsets regulate inflammation and remission in rheumatoid

arthritis. *Nature Medicine* 2020;26(8):1295-306. doi: 10.1038/s41591-020-0939-8
194. May SM, Abbott TEF, Del Arroyo AG, et al. MicroRNA signatures of perioperative myocardial injury after elective noncardiac surgery: a prospective observational mechanistic cohort study. *Br J Anaesth* 2020;125(5):661-71. doi: 10.1016/j.bja.2020.05.066 [published Online First: 20200724]
195. Oerlemans MI, Mosterd A, Dekker MS, et al. Early assessment of acute coronary syndromes in the emergency department: the potential diagnostic value of circulating microRNAs. *EMBO Mol Med* 2012;4(11):1176-85. doi: 10.1002/emmm.201201749 [published Online First: 20121001]
196. Taganov KD, Boldin MP, Chang KJ, et al. NF-kappaB-dependent induction of microRNA miR-146, an inhibitor targeted to signaling proteins of innate immune responses. *Proc Natl Acad Sci U S A* 2006;103(33):12481-6. doi: 10.1073/pnas.0605298103 [published Online First: 20060802]
197. Frangogiannis NG. The inflammatory response in myocardial injury, repair, and remodelling. *Nat Rev Cardiol* 2014;11(5):255-65. doi: 10.1038/nrcardio.2014.28 [published Online First: 20140325]
198. Watts JA, Zagorski J, Gellar MA, et al. Cardiac inflammation contributes to right ventricular dysfunction following experimental pulmonary embolism in rats. *J Mol Cell Cardiol* 2006;41(2):296-307. doi: 10.1016/j.yjmcc.2006.05.011 [published Online First: 2006/06/30]
199. Watts JA, Gellar MA, Obraztsova M, et al. Role of inflammation in right ventricular damage and repair following experimental pulmonary embolism in rats. *Int J Exp Pathol* 2008;89(5):389-99. doi: 10.1111/j.1365-2613.2008.00610.x
200. Zagorski J, Sanapareddy N, Gellar MA, et al. Transcriptional profile of right ventricular tissue during acute pulmonary embolism in rats. *Physiol Genomics* 2008;34(1):101-11. doi: 10.1152/physiolgenomics.00261.2007 [published Online First: 2008/04/22]
201. Wang Q, Ma J, Jiang Z, et al. Prognostic value of neutrophil-to-lymphocyte ratio and platelet-to-lymphocyte ratio in acute pulmonary embolism: a systematic review and meta-analysis. *Int Angiol* 2018;37(1):4-11. doi: 10.23736/S0392-9590.17.03848-2 [published Online First: 2017/05/24]
202. Zhou J, Liu K, Feng C, et al. Therapeutic effect of SP-8356 on pulmonary embolism-associated cardiac injury is mediated by its ability to suppress apoptosis and inflammation. *J Cell Mol Med* 2021;25(11):5260-68. doi: 10.1111/jcmm.16535 [published Online First: 20210504]
203. Watts JA, Zagorski J, Gellar MA, et al. Cardiac inflammation contributes to right ventricular dysfunction following experimental pulmonary embolism in rats. *Journal of Molecular and Cellular Cardiology* 2006;41(2):296-307. doi: 10.1016/j.yjmcc.2006.05.011
204. Neto-Neves EM, Kiss T, Muhl D, et al. Matrix metalloproteinases as drug targets in acute pulmonary embolism. *Curr Drug Targets* 2013;14(3):344-52.
205. Quarck R, Delcroix M. Is inflammation a potential therapeutic target in chronic thromboembolic pulmonary hypertension? *European Respiratory Journal* 2014;44(4):842-45. doi: 10.1183/09031936.00120014
206. Halici B, Ulasli SS, Gunay E, et al. Assessment of Inflammatory Biomarkers and Oxidative Stress in Pulmonary Thromboembolism: Follow-up Results. *Inflammation* 2014;37(4):1186-90. doi: 10.1007/s10753-014-9844-y

207. Hassoun PM. Inflammation in chronic thromboembolic pulmonary hypertension: accomplice or bystander in altered angiogenesis? *European Respiratory Journal* 2015;46(2):303-06. doi: 10.1183/13993003.00962-2015
208. Quarck R, Wynants M, Verbeken E, et al. Contribution of inflammation and impaired angiogenesis to the pathobiology of chronic thromboembolic pulmonary hypertension. *European Respiratory Journal* 2015;46(2):431-43. doi: 10.1183/09031936.00009914
209. Pelletier C, Lapointe L, Leblanc P. EFFECTS OF LUNG RESECTION ON PULMONARY-FUNCTION AND EXERCISE CAPACITY. *Thorax* 1990;45(7):497-502. doi: 10.1136/thx.45.7.497
210. Jezek V, Ourednik A, Lichtenberg J, et al. CARDIOPULMONARY FUNCTION IN LUNG RESECTION PERFORMED FOR BRONCHOGENIC CANCER IN PATIENTS ABOVE 65 YEARS OF AGE. *Respiration* 1970;27(1):42-+.
211. Kowalewski J, Brocki M, Dryjański T, et al. Right ventricular morphology and function after pulmonary resection. *Eur J Cardiothorac Surg* 1999;15(4):444-8.
212. Jovev S, Tager S, Spirovski Z, et al. Right heart haemodynamics after lung resection; the role of the transthoracic echo-doppler cardiography. *Prilozi* 2006;27(2):201-16.
213. Pedoto A, Amar D. Right heart function in thoracic surgery: role of echocardiography. *Current Opinion in Anesthesiology* 2009;22(1):44-49. doi: 10.1097/ACO.0b013e32831d7b72
214. Simsek Z, Gunay E. Evaluating cardiac functions by tissue Doppler echocardiography in the early postoperative period of major lung resection. *Turk Kardiyoloji Dernegi arsivi : Turk Kardiyoloji Derneginin yayin organidir* 2010;38(1):75-76.
215. Kaplan T, Tanindi A, Ugurlu M, et al. Cardiac and respiratory changes in the medium term after lung resection. *Turk Kardiyoloji Dernegi Arsivi-Archives of the Turkish Society of Cardiology* 2015;43(5):434-42.
216. McCall P, Sonecki P, Kirk A, et al. Speckle-tracked strain assessment of right ventricular function after lung resection. *British Journal of Anaesthesia* 2016;116(6):E932-E33.
217. Teng WH, McCall P, Kinsella J, et al. Eccentricity index assessment of right ventricular function following lung resection. *Scottish Medical Journal* 2018;63(2):70-70.
218. Wood KE. Major pulmonary embolism: review of a pathophysiologic approach to the golden hour of hemodynamically significant pulmonary embolism. *Chest* 2002;121(3):877-905.
219. Cao Y, Li Y, Wu M, et al. RNA-sequencing analysis of gene expression in a rat model of acute right heart failure. *Pulm Circ* 2020;10(1):2045894019879396. doi: 10.1177/2045894019879396 [published Online First: 20200221]
220. Jones AE, Watts JA, Debelak JP, et al. Inhibition of prostaglandin synthesis during polystyrene microsphere-induced pulmonary embolism in the rat. *American Journal of Physiology-Lung Cellular and Molecular Physiology* 2003;284(6):L1072-L81. doi: 10.1152/ajplung.00283.2002
221. Jones AE, Watts JA, Debelak JP, et al. Inhibition of prostaglandin synthesis during polystyrene microsphere-induced pulmonary embolism in the rat. *Am J Physiol Lung Cell Mol Physiol* 2003;284(6):L1072-81. doi: 10.1152/ajplung.00283.2002 [published Online First: 2003/03/14]

222. Zagorski J, Sanapareddy N, Gellar MA, et al. Transcriptional Profile of Right Ventricular Tissue During Acute Pulmonary Embolism and Pulmonary Hypertension in Rats. *Molecular Biology of the Cell* 2006;17
223. Zagorski J, Gellar MA, Obraztsova M, et al. Inhibition of CINC-1 decreases right ventricular damage caused by experimental pulmonary embolism in rats. *Journal of Immunology* 2007;179(11):7820-26. doi: 10.4049/jimmunol.179.11.7820
224. Watts JA, Gellar MA, Obraztsova M, et al. Role of inflammation in right ventricular damage and repair following experimental pulmonary embolism in rats. *International Journal of Experimental Pathology* 2008;89(5):389-99. doi: 10.1111/j.1365-2613.2008.00610.x
225. Watts JA, Gellar MA, Stuart LK, et al. Proinflammatory Events in Right Ventricular Damage During Pulmonary Embolism: Effects of Treatment With Ketorolac in Rats. *Journal of Cardiovascular Pharmacology* 2009;54(3):246-52. doi: 10.1097/FJC.0b013e3181b2b699
226. Stenzl W, Walter G, Rehak P, et al. [Myocardial changes in acute pulmonary artery embolism--an experimental study]. *Fortschr Med* 1984;102(9):221-4.
227. Celsus. De medicina. *De medicina* 1938:Vol. II, lxvii + 291p.-Vol. II, lxvii + 91p.
228. Rather LJ. DISTURBANCE OF FUNCTION (FUNCTIO-LAESA) - LEGENDARY FIFTH CARDINAL SIGN OF INFLAMMATION, ADDED BY GALEN TO 4 CARDINAL SIGNS OF CELSUS. *Bulletin of the New York Academy of Medicine* 1971;47(3):303-&.
229. Yilmaz A, Klingel K, Kandolf R, et al. Imaging in Inflammatory Heart Disease: From the Past to Current Clinical Practice. *Hellenic Journal of Cardiology* 2009;50(6):449-60.
230. Orde MM, Puranik R, Morrow PL, et al. Myocardial pathology in pulmonary thromboembolism. *Heart* 2011;97(20):1695-99. doi: 10.1136/hrt.2011.226209
231. Burkard T, Trendelenburg M, Daikeler T, et al. The heart in systemic lupus erythematosus - A comprehensive approach by cardiovascular magnetic resonance tomography. *Plos One* 2018;13(10) doi: 10.1371/journal.pone.0202105
232. Comarmond C, Cacoub P. Myocarditis in auto-immune or auto-inflammatory diseases. *Autoimmunity Reviews* 2017;16(8):811-16. doi: 10.1016/j.autrev.2017.05.021
233. Iwadate K, Tanno K, Doi M, et al. Two cases of right ventricular ischemic injury due to massive pulmonary embolism. *Forensic Science International* 2001;116(2-3):189-95. doi: 10.1016/s0379-0738(00)00367-4
234. Iwadate K, Doi M, Tanno K, et al. Right ventricular damage due to pulmonary embolism: examination of the number of infiltrating macrophages. *Forensic Sci Int* 2003;134(2-3):147-53.
235. Begieneman MPV, de Goot FRWv, van der Bilt IAC, et al. Pulmonary embolism causes endomyocarditis in the human heart. *Heart* 2008;94(4):450-56. doi: 10.1136/hrt.2007.118638
236. Jimenez D, Nieto R, Corres J, et al. Diclofenac for reversal of right ventricular dysfunction in acute normotensive pulmonary embolism: A pilot study. *Thromb Res* 2018;162:1-6. doi: 10.1016/j.thromres.2017.12.002 [published Online First: 20171205]
237. Zagorski J, Obraztsova M, Gellar MA, et al. Transcriptional changes in right ventricular tissues are enriched in the outflow tract compared with the

apex during chronic pulmonary embolism in rats. *Physiological Genomics* 2009;39(1):61-71. doi: 10.1152/physiolgenomics.00076.2009
238. Fortuna GM, Figueiredo-Lopes L, Dias CAC, Jr., et al. A role for matrix metalloproteinase-9 in the hemodynamic changes following acute pulmonary embolism. *International Journal of Cardiology* 2007;114(1):22-27. doi: 10.1016/j.ijcard.2005.11.109
239. Neto-Neves EM, Dias-Junior CA, Rizzi E, et al. Metalloproteinase inhibition protects against cardiomyocyte injury during experimental acute pulmonary thromboembolism. *Critical Care Medicine* 2011;39(2):349-56. doi: 10.1097/CCM.0b013e3181fa3dfe
240. Uzuelli JA, Dias-Junior CAC, Tanus-Santos JE. Severity dependent increases in circulating cardiac troponin I and MMP-9 concentrations after experimental acute pulmonary thromboembolism. *Clinica Chimica Acta* 2008;388(1-2):184-88. doi: 10.1016/j.cca.2007.11.001
241. Neto-Neves EM, Sousa-Santos O, Ferraz KC, et al. Matrix metalloproteinase inhibition attenuates right ventricular dysfunction and improves responses to dobutamine during acute pulmonary thromboembolism. *Journal of Cellular and Molecular Medicine* 2013;17(12):1588-97. doi: 10.1111/jcmm.12163
242. Wu Z-Y, Li H, Tang Y-J. Effect of simvastatin on the SIRT2/NF-kappa B pathway in rats with acute pulmonary embolism. *Pharmaceutical Biology* 2018;56(1):511-18. doi: 10.1080/13880209.2018.1508239
243. Lu G, Jia Z, Zu Q, et al. Inhibition of the cyclophilin A-CD147 interaction attenuates right ventricular injury and dysfunction after acute pulmonary embolism in rats. *Journal of Biological Chemistry* 2018;293(31):12199-208. doi: 10.1074/jbc.RA118.002845
244. McConnell MV, Solomon SD, Rayan ME, et al. Regional right ventricular dysfunction detected by echocadiography in acute pulmonary embolism. *American Journal of Cardiology* 1996;78(4):469-73. doi: 10.1016/s0002-9149(96)00339-6
245. Nissinen L, Kahari V-M. Matrix metalloproteinases in inflammation. *Biochimica Et Biophysica Acta-General Subjects* 2014;1840(8):2571-80. doi: 10.1016/j.bbagen.2014.03.007
246. Battistini B. Modulation and roles of the endothelins in the pathophysiology of pulmonary embolism. *Can J Physiol Pharmacol* 2003;81(6):555-69. doi: 10.1139/y03-017
247. Tanus-Santos JE, Gordo WM, Udelsmann A, et al. Nonselective endothelin-receptor antagonism attenuates hemodynamic changes after massive pulmonary air embolism in dogs. *Chest* 2000;118(1):175-9. doi: 10.1378/chest.118.1.175
248. Chow AK, Cena J, Schulz R. Acute actions and novel targets of matrix metalloproteinases in the heart and vasculature. *Br J Pharmacol* 2007;152(2):189-205. doi: 10.1038/sj.bjp.0707344 [published Online First: 20070625]
249. Fernandez-Patron C, Zouki C, Whittal R, et al. Matrix metalloproteinases regulate neutrophil-endothelial cell adhesion through generation of endothelin-1[1-32]. *FASEB J* 2001;15(12):2230-40. doi: 10.1096/fj.01-0178com
250. Fernandez-Patron C, Stewart KG, Zhang Y, et al. Vascular matrix metalloproteinase-2-dependent cleavage of calcitonin gene-related peptide promotes vasoconstriction. *Circ Res* 2000;87(8):670-6. doi: 10.1161/01.res.87.8.670

251. Palei ACT, Zaneti RAG, Fortuna GM, et al. Hemodynamic benefits of matrix metalloproteinase-9 inhibition by doxycycline during experimental acute pulmonary embolism. *Angiology* 2005;56(5):611-17. doi: 10.1177/000331970505600513
252. Lopez-Candales A, Edelman K, Candales MD. Right Ventricular Apical Contractility in Acute Pulmonary Embolism: The McConnell Sign Revisited. *Echocardiography-a Journal of Cardiovascular Ultrasound and Allied Techniques* 2010;27(6):614-20. doi: 10.1111/j.1540-8175.2009.01103.x
253. Casazza F, Bongarzoni A, Capozi A, et al. Regional right ventricular dysfunction in acute pulmonary embolism and right ventricular infarction. *European journal of echocardiography : the journal of the Working Group on Echocardiography of the European Society of Cardiology* 2005;6(1):11-4. doi: 10.1016/j.euje.2004.06.002
254. Satoh K, Shimokawa H, Berk BC. Cyclophilin A - Promising New Target in Cardiovascular Therapy. *Circulation Journal* 2010;74(11):2249-56. doi: 10.1253/circj.CJ-10-0904
255. Landskron J, Tasken K. CD147 in regulatory T cells. *Cellular Immunology* 2013;282(1):17-20. doi: 10.1016/j.cellimm.2013.04.008
256. Satoh K, Satoh T, Kikuchi N, et al. Basigin Mediates Pulmonary Hypertension by Promoting Inflammation and Vascular Smooth Muscle Cell Proliferation. *Circulation Research* 2014;115(8):738-+. doi: 10.1161/circresaha.115.304563
257. Seizer P, Gawaz M, May AE. Cyclophilin A and EMMPRIN (CD147) in cardiovascular diseases. *Cardiovascular Research* 2014;102(1):17-23. doi: 10.1093/cvr/cvu035
258. Dewachter C, Belhaj A, Rondelet B, et al. Myocardial inflammation in experimental acute right ventricular failure: Effects of prostacyclin therapy. *Journal of Heart and Lung Transplantation* 2015;34(10):1334-45. doi: 10.1016/j.healun.2015.05.004
259. Caforio ALP, Pankuweit S, Arbustini E, et al. Current state of knowledge on aetiology, diagnosis, management, and therapy of myocarditis: a position statement of the European Society of Cardiology Working Group on Myocardial and Pericardial Diseases. *European Heart Journal* 2013;34(33):2636-+. doi: 10.1093/eurheartj/eht210
260. Nishikawa T, Sekiguchi M, Ishibashi-Ueda H. More than 50 Years after Konno's Development of the Endomyocardial Biopsy. *International heart journal* 2017 doi: 10.1536/ihj.16-316
261. Fowles RE, Mason JW. ENDOMYOCARDIAL BIOPSY. *Annals of Internal Medicine* 1982;97(6):885-94. doi: 10.7326/0003-4819-97-6-885
262. Deckers JW, Hare JM, Baughman KL. COMPLICATIONS OF TRANSVENOUS RIGHT VENTRICULAR ENDOMYOCARDIAL BIOPSY IN ADULT PATIENTS WITH CARDIOMYOPATHY - A 7-YEAR SURVEY OF 546 CONSECUTIVE DIAGNOSTIC PROCEDURES IN A TERTIARY REFERRAL CENTER. *Journal of the American College of Cardiology* 1992;19(1):43-47. doi: 10.1016/0735-1097(92)90049-s
263. Anderson L, Pennell D. The role of endomyocardial biopsy in the management of cardiovascular disease: a Scientific Statement from the American Heart Association, the American College of Cardiology, and the European Society of Cardiology. *European Heart Journal* 2008;29(13):1696-96. doi: 10.1093/eurheartj/ehn189
264. Dominguez F, Kuehl U, Pieske B, et al. Update on Myocarditis and Inflammatory Cardiomyopathy: Reemergence of Endomyocardial Biopsy.

Revista Espanola De Cardiologia 2016;69(2):178-87. doi: 10.1016/j.rec.2015.10.015
265. Bennett MK, Gilotra NA, Harrington C, et al. Evaluation of the Role of Endomyocardial Biopsy in 851 Patients With Unexplained Heart Failure From 2000-2009. *Circulation-Heart Failure* 2013;6(4):676-84. doi: 10.1161/circheartfailure.112.000087
266. Unterberg-Buchwald C, Ritter CO, Reupke V, et al. Targeted endomyocardial biopsy guided by real-time cardiovascular magnetic resonance. *Journal of Cardiovascular Magnetic Resonance* 2017;19 doi: 10.1186/s12968-017-0357-3
267. Behm P, Gastl M, Jahn A, et al. CMR-guidance of passively tracked endomyocardial biopsy in an in vivo porcine model. *International Journal of Cardiovascular Imaging* 2018;34(12):1917-26. doi: 10.1007/s10554-018-1402-5
268. Afonso L, Hari P, Pidlaoan V, et al. Acute myocarditis: can novel echocardiographic techniques assist with diagnosis? *Eur J Echocardiogr* 2010;11(3):E5. doi: 10.1093/ejechocard/jep183 [published Online First: 20091124]
269. Escher F, Kasner M, Kühl U, et al. New echocardiographic findings correlate with intramyocardial inflammation in endomyocardial biopsies of patients with acute myocarditis and inflammatory cardiomyopathy. *Mediators Inflamm* 2013;2013:875420. doi: 10.1155/2013/875420 [published Online First: 20130320]
270. Løgstrup BB, Nielsen JM, Kim WY, et al. Myocardial oedema in acute myocarditis detected by echocardiographic 2D myocardial deformation analysis. *Eur Heart J Cardiovasc Imaging* 2016;17(9):1018-26. doi: 10.1093/ehjci/jev302 [published Online First: 20151120]
271. Selvanayagam J, Nucifora G. Early and late gadolinium enhancement. In: Lombardi M, Plein S, Petersen S, et al., eds. The EACVI Textbook of Cardiovascular Magnetic Resonance: Oxford University Press 2018.
272. Friedrich MG, Strohm O, Schulz-Menger J, et al. Contrast media-enhanced magnetic resonance imaging visualizes myocardial changes in the course of viral myocarditis. *Circulation* 1998;97(18):1802-09. doi: 10.1161/01.cir.97.18.1802
273. Greulich S, Ferreira VM, Dall'Armellina E, et al. Myocardial Inflammation-Are We There Yet? *Current Cardiovascular Imaging Reports* 2015;8(3) doi: 10.1007/s12410-015-9320-6
274. Friedrich MG, Sechtem U, Schulz-Menger J, et al. Cardiovascular Magnetic Resonance in Myocarditis: A JACC White Paper. *Journal of the American College of Cardiology* 2009;53(17):1475-87. doi: 10.1016/j.jacc.2009.02.007
275. Hamdy A, Kitagawa K, Ishida M, et al. Native Myocardial T1 Mapping, Are We There Yet? *International Heart Journal* 2016;57(4):400-07.
276. Rieker O, Mohrs O, Oberholzer K, et al. Cardiac MRI in suspected myocarditis. *Rofo-Fortschritte Auf Dem Gebiet Der Rontgenstrahlen Und Der Bildgebenden Verfahren* 2002;174(12):1530-36. doi: 10.1055/s-2002-35999
277. Laissy JP, Hyafil F, Feldman LJ, et al. Differentiating acute myocardial infarction from myocarditis: Diagnostic value of early- and delayed-perfusion cardiac MR imaging. *Radiology* 2005;237(1):75-82. doi: 10.1148/radiol.2371041322
278. Abdel-Aty H, Boye P, Zagrosek A, et al. Diagnostic performance of cardiovascular magnetic resonance in patients with suspected acute

myocarditis - Comparison of different approaches. *Journal of the American College of Cardiology* 2005;45(11):1815-22. doi: 10.1016/j.jacc.2004.11.069
279. Moon JC, Messroghli DR, Kellman P, et al. Myocardial T1 mapping and extracellular volume quantification: a Society for Cardiovascular Magnetic Resonance (SCMR) and CMR Working Group of the European Society of Cardiology consensus statement. *Journal of Cardiovascular Magnetic Resonance* 2013;15 doi: 10.1186/1532-429x-15-92
280. Piechnik SK, Ferreira VM, Lewandowski AJ, et al. Normal variation of magnetic resonance T1 relaxation times in the human population at 1.5 T using ShMOLLI. *J Cardiovasc Magn Reson* 2013;15:13. doi: 10.1186/1532-429X-15-13 [published Online First: 20130120]
281. Burt JR, Zimmerman SL, Kamel IR, et al. Myocardial T1 mapping: techniques and potential applications. *Radiographics* 2014;34(2):377-95. doi: 10.1148/rg.342125121
282. Dall'Armellina E, Piechnik SK, Ferreira VM, et al. Cardiovascular magnetic resonance by non contrast T1-mapping allows assessment of severity of injury in acute myocardial infarction. *J Cardiovasc Magn Reson* 2012;14:15. doi: 10.1186/1532-429X-14-15 [published Online First: 20120206]
283. Bull S, White SK, Piechnik SK, et al. Human non-contrast T1 values and correlation with histology in diffuse fibrosis. *Heart* 2013;99(13):932-7. doi: 10.1136/heartjnl-2012-303052 [published Online First: 20130124]
284. Ferreira VM, Piechnik SK, Dall'Armellina E, et al. Non-contrast T1-mapping detects acute myocardial edema with high diagnostic accuracy: a comparison to T2-weighted cardiovascular magnetic resonance. *J Cardiovasc Magn Reson* 2012;14:42. doi: 10.1186/1532-429X-14-42 [published Online First: 20120621]
285. Ferreira VM, Piechnik SK, Dall'Armellina E, et al. Native T1-mapping detects the location, extent and patterns of acute myocarditis without the need for gadolinium contrast agents. *J Cardiovasc Magn Reson* 2014;16:36. doi: 10.1186/1532-429X-16-36 [published Online First: 20140523]
286. Ferreira V, Messroghli D. Mapping techniques. The EACVI Textbook of Cardiovascular Magnetic Resonance: Oxford University Press 2018.
287. Ibrahim EH, Frank L, Baruah D, et al. Value CMR: Towards a Comprehensive, Rapid, Cost-Effective Cardiovascular Magnetic Resonance Imaging. *Int J Biomed Imaging* 2021;2021:8851958. doi: 10.1155/2021/8851958 [published Online First: 20210515]
288. Robinson AA, Chow K, Salerno M. Myocardial T1 and ECV Measurement: Underlying Concepts and Technical Considerations. *JACC Cardiovasc Imaging* 2019;12(11 Pt 2):2332-44. doi: 10.1016/j.jcmg.2019.06.031 [published Online First: 20190918]
289. Gottbrecht M, Kramer CM, Salerno M. Native T1 and Extracellular Volume Measurements by Cardiac MRI in Healthy Adults: A Meta-Analysis. *Radiology* 2019;290(2):317-26. doi: 10.1148/radiol.2018180226 [published Online First: 20181113]
290. Haaf P, Garg P, Messroghli DR, et al. Cardiac T1 Mapping and Extracellular Volume (ECV) in clinical practice: a comprehensive review. *Journal of Cardiovascular Magnetic Resonance* 2016;18 doi: 10.1186/s12968-016-0308-4
291. Cao Y, Zeng W, Cui Y, et al. Increased myocardial extracellular volume assessed by cardiovascular magnetic resonance T1 mapping and its determinants in type 2 diabetes mellitus patients with normal myocardial

systolic strain. *Cardiovasc Diabetol* 2018;17(1):7. doi: 10.1186/s12933-017-0651-2 [published Online First: 20180104]
292. Abdel-Aty H, Simonetti O, Friedrich MG. T2-weighted cardiovascular magnetic resonance imaging. *Journal of Magnetic Resonance Imaging* 2007;26(3):452-59. doi: 10.1002/jmri.21028
293. Messroghli DR, Moon JC, Ferreira VM, et al. Clinical recommendations for cardiovascular magnetic resonance mapping of T1, T2, T2* and extracellular volume: A consensus statement by the Society for Cardiovascular Magnetic Resonance (SCMR) endorsed by the European Association for Cardiovascular Imaging (EACVI) (vol 19, 75, 2017). *Journal of Cardiovascular Magnetic Resonance* 2018;20 doi: 10.1186/s12968-017-0408-9
294. Thavendiranathan P, Walls M, Giri S, et al. Improved Detection of Myocardial Involvement in Acute Inflammatory Cardiomyopathies Using T2 Mapping. *Circulation-Cardiovascular Imaging* 2012;5(1):102-10. doi: 10.1161/circimaging.111.967836
295. Hassan A, Simonetti O, Friedrich M. T2-weighted cardiovascular magnetic resonance imaging. *Journal of Magnetic Resonance Imaging* 2007;26(3):452-59.
296. Kircher M, Lapa C. Novel Noninvasive Nuclear Medicine Imaging Techniques for Cardiac Inflammation. *Curr Cardiovasc Imaging Rep* 2017;10(2):6. doi: 10.1007/s12410-017-9400-x [published Online First: 2017/02/10]
297. Nappi C, El Fakhri G. State of the Art in Cardiac Hybrid Technology: PET/MR. *Current cardiovascular imaging reports* 2013;6(4):338-45.
298. Clyne B, Olshaker JS. The C-reactive protein. *J Emerg Med* 1999;17(6):1019-25. doi: 10.1016/s0736-4679(99)00135-3
299. Santonocito C, De Loecker I, Donadello K, et al. C-reactive protein kinetics after major surgery. *Anesth Analg* 2014;119(3):624-29. doi: 10.1213/ANE.0000000000000263
300. Batkai S, Baer C, Thum T. MicroRNAs in right ventricular remodelling. *Cardiovascular Research* 2017;113(12):1433-40. doi: 10.1093/cvr/cvx153
301. Corsten MF, Papageorgiou A, Verhesen W, et al. MicroRNA Profiling Identifies MicroRNA-155 as an Adverse Mediator of Cardiac Injury and Dysfunction During Acute Viral Myocarditis. *Circulation Research* 2012;111(4):415-U155. doi: 10.1161/circresaha.112.267443
302. Wei C, Henderson H, Spradley C, et al. Circulating miRNAs as Potential Marker for Pulmonary Hypertension. *Plos One* 2013;8(5) doi: 10.1371/journal.pone.0064396
303. Xiao J, Jing Z-C, Ellinor PT, et al. MicroRNA-134 as a potential plasma biomarker for the diagnosis of acute pulmonary embolism. *Journal of Translational Medicine* 2011;9 doi: 10.1186/1479-5876-9-159
304. National Cancer Intelligence Network. Major resections by cancer site, in England; 2006 to 2010: http://www.ncin.org.uk/item?rid=2952 [accessed 12/05/2016.
305. Ranu H, Wilde M, Madden B. Pulmonary function tests. *The Ulster medical journal* 2011;80(2):84-90.
306. The Criteria Committee of the New York Heart Association. Nomenclature and Criteria for Diagnosis of Diseases of the Heart and Great Vessels . Boston, Mass: Little, Brown and Co, 1994:253-56.
307. West H, Jin JO. Performance Status in Patients With Cancer Patient performance status (PS) is an important part of cancer care and treatment. *Jama Oncology* 2015;1(7):998-98. doi: 10.1001/jamaoncol.2015.3113

308. EuroQoL. EQ-5D-5L: EuroQoL; 2009 [Available from: https://euroqol.org/eq-5d-instruments/eq-5d-5l-about/ accessed 01/10/2017 2017.
309. Williams N. The MRC breathlessness scale. *Occupational Medicine-Oxford* 2017;67(6):496-97. doi: 10.1093/occmed/kqx086
310. Paladini L, Hodder R, Cecchini I, et al. The MRC dyspnoea scale by telephone interview to monitor health status in elderly COPD patients. *Respiratory Medicine* 2010;104(7):1027-34. doi: 10.1016/j.rmed.2009.12.012
311. EuroQoL. EQ-5D-5L : Interviewer Administered version EuroQoL2019 [Available from: https://euroqol.org/eq-5d-instruments/eq-5d-5l-available-modes-of-administration/interview-administered-version/ accessed 20/01/20 2020.
312. Zeiher BG, Gross TJ, Kern JA, et al. PREDICTING POSTOPERATIVE PULMONARY-FUNCTION IN PATIENTS UNDERGOING LUNG RESECTION. *Chest* 1995;108(1):68-72. doi: 10.1378/chest.108.1.68
313. Papageorgiou G, Grant SW, Takkenberg JJM, et al. Statistical primer: how to deal with missing data in scientific research? *Interact Cardiovasc Thorac Surg* 2018;27(2):153-58. doi: 10.1093/icvts/ivy102
314. Bland JM, Altman DG. Statistical methods for assessing agreement between two methods of clinical measurement. *Lancet* 1986;1(8476):307-10.
315. Reed GF, Lynn F, Meade BD. Use of coefficient of variation in assessing variability of quantitative assays (vol 9, pg 1235, 2003). *Clinical and Diagnostic Laboratory Immunology* 2003;10(6):1162-62. doi: 10.1128/cdli.10.6.1162.2003
316. Koo TK, Li MY. A Guideline of Selecting and Reporting Intraclass Correlation Coefficients for Reliability Research (vol 15, pg 155, 2016). *Journal of Chiropractic Medicine* 2017;16(4):346-46. doi: 10.1016/j.jcm.2017.10.001
317. Kawel N, Nacif M, Zavodni A, et al. T1 mapping of the myocardium: Intra-individual assessment of the effect of field strength, cardiac cycle and variation by myocardial region. *Journal of Cardiovascular Magnetic Resonance* 2012;14 doi: 10.1186/1532-429x-14-27
318. Rauhalammi SMO, Mangion K, Barrientos PH, et al. Native myocardial longitudinal (T-1) relaxation time: Regional, age, and sex associations in the healthy adult heart. *Journal of Magnetic Resonance Imaging* 2016;44(3):541-48. doi: 10.1002/jmri.25217
319. Spruijt OA, Vissers L, Bogaard HJ, et al. Increased native T1-values at the interventricular insertion regions in precapillary pulmonary hypertension. *Int J Cardiovasc Imaging* 2016;32(3):451-9. doi: 10.1007/s10554-015-0787-7 [published Online First: 2015/10/16]
320. Reiter U, Reiter G, Kovacs G, et al. Native myocardial T1 mapping in pulmonary hypertension: correlations with cardiac function and hemodynamics. *Eur Radiol* 2016 doi: 10.1007/s00330-016-4360-0
321. Carrick D, Haig C, Rauhalammi S, et al. Pathophysiology of LV Remodeling in Survivors of STEMI: Inflammation, Remote Myocardium, and Prognosis. *JACC Cardiovasc Imaging* 2015;8(7):779-89. doi: 10.1016/j.jcmg.2015.03.007 [published Online First: 20150617]
322. Schulz-Menger J, Bluemke DA, Bremerich J, et al. Standardized image interpretation and post processing in cardiovascular magnetic resonance: Society for Cardiovascular Magnetic Resonance (SCMR) Board of Trustees Task Force on Standardized Post Processing. *Journal of Cardiovascular Magnetic Resonance* 2013;15 doi: 10.1186/1532-429x-15-35

323. Cerqueira MD, Weissman NJ, Dilsizian V, et al. Standardized myocardial segmentation and nomenclature for tomographic imaging of the heart: A statement for healthcare professionals from the Cardiac Imaging Committee of the Council on Clinical Cardiology of the American Heart Association. *Journal of Nuclear Cardiology* 2002;9(2):240-45. doi: 10.1067/mnc.2002.123122
324. Walters SJ, Brazier JE. Comparison of the minimally important difference for two health state utility measures: EQ-5D and SF-6D. *Quality of Life Research* 2005;14(6):1523-32. doi: 10.1007/s11136-004-7713-0
325. Pickard AS, Neary MP, Cella D. Estimation of minimally important differences in EQ-5D utility and VAS scores in cancer. *Health and Quality of Life Outcomes* 2007;5 doi: 10.1186/1477-7525-5-70
326. Cook CE. Clinimetrics Corner: The Minimal Clinically Important Change Score (MCID): A Necessary Pretense. *The Journal of manual & manipulative therapy* 2008;16(4):E82-3.
327. Mooij CF, de Wit CJ, Graham DA, et al. Reproducibility of MRI measurements of right ventricular size and function in patients with normal and dilated ventricles. *J Magn Reson Imaging* 2008;28(1):67-73. doi: 10.1002/jmri.21407
328. Pattynama PM, Lamb HJ, Van der Velde EA, et al. Reproducibility of MRI-derived measurements of right ventricular volumes and myocardial mass. *Magn Reson Imaging* 1995;13(1):53-63. doi: 10.1016/0730-725x(94)00076-f
329. Al-Wakeel-Marquard N, Ferreira da Silva T, Jeuthe S, et al. Measuring myocardial extracellular volume of the right ventricle in patients with congenital heart disease. *Sci Rep* 2021;11(1):2679. doi: 10.1038/s41598-021-81440-z [published Online First: 20210129]
330. Lee S, Kim P, Im DJ, et al. The image quality and diagnostic accuracy of T1-mapping-based synthetic late gadolinium enhancement imaging: comparison with conventional late gadolinium enhancement imaging in real-life clinical situation. *J Cardiovasc Magn Reson* 2022;24(1):28. doi: 10.1186/s12968-022-00857-1 [published Online First: 20220414]
331. Weingärtner S, Meßner NM, Budjan J, et al. Myocardial T. *J Cardiovasc Magn Reson* 2016;18(1):84. doi: 10.1186/s12968-016-0302-x [published Online First: 20161118]
332. Kellman P, Wilson JR, Xue H, et al. Extracellular volume fraction mapping in the myocardium, part 1: evaluation of an automated method. *J Cardiovasc Magn Reson* 2012;14(1):63. doi: 10.1186/1532-429X-14-63 [published Online First: 20120910]
333. García-Álvarez A, García-Lunar I, Pereda D, et al. Association of myocardial T1-mapping CMR with hemodynamics and RV performance in pulmonary hypertension. *JACC Cardiovasc Imaging* 2015;8(1):76-82. doi: 10.1016/j.jcmg.2014.08.012 [published Online First: 2014/11/01]
334. Habert P, Capron T, Hubert S, et al. Quantification of right ventricular extracellular volume in pulmonary hypertension using cardiac magnetic resonance imaging. *Diagn Interv Imaging* 2020;101(5):311-20. doi: 10.1016/j.diii.2019.12.008 [published Online First: 20200114]
335. Patel RB, Li E, Benefield BC, et al. Diffuse right ventricular fibrosis in heart failure with preserved ejection fraction and pulmonary hypertension. *ESC Heart Fail* 2020;7(1):253-63. doi: 10.1002/ehf2.12565 [published Online First: 20200105]
336. Chen YY, Yun H, Jin H, et al. Association of native T1 times with biventricular function and hemodynamics in precapillary pulmonary

hypertension. *Int J Cardiovasc Imaging* 2017;33(8):1179-89. doi: 10.1007/s10554-017-1095-1 [published Online First: 20170317]
337. Nitsche C, Kammerlander AA, Binder C, et al. Native T1 time of right ventricular insertion points by cardiac magnetic resonance: relation with invasive haemodynamics and outcome in heart failure with preserved ejection fraction. *Eur Heart J Cardiovasc Imaging* 2020;21(6):683-91. doi: 10.1093/ehjci/jez221
338. Secchi F, Alì M, Monti CB, et al. Right and left ventricle native T1 mapping in systolic phase in patients with congenital heart disease. *Acta Radiol* 2021;62(3):334-40. doi: 10.1177/0284185120924563 [published Online First: 20200531]
339. Roller FC, Wiedenroth C, Breithecker A, et al. Native T1 mapping and extracellular volume fraction measurement for assessment of right ventricular insertion point and septal fibrosis in chronic thromboembolic pulmonary hypertension. *European Radiology* 2017;27(5):1980-91. doi: 10.1007/s00330-016-4585-y
340. Roller FC, Kriechbaum S, Breithecker A, et al. Correlation of native T1 mapping with right ventricular function and pulmonary haemodynamics in patients with chronic thromboembolic pulmonary hypertension before and after balloon pulmonary angioplasty. *European Radiology* 2019;29(3):1565-73. doi: 10.1007/s00330-018-5702-x
341. Zhao L, Li S, Ma X, et al. Prognostic Significance of Left Ventricular Fibrosis Assessed by T1 Mapping in Patients with Atrial Fibrillation and Heart Failure. *Sci Rep* 2019;9(1):13374. doi: 10.1038/s41598-019-49793-8 [published Online First: 20190916]
342. Kawel-Boehm N, Dellas Buser T, Greiser A, et al. In-vivo assessment of normal T1 values of the right-ventricular myocardium by cardiac MRI. *Int J Cardiovasc Imaging* 2014;30(2):323-8. doi: 10.1007/s10554-013-0326-3 [published Online First: 2013/11/13]
343. Tello K, Dalmer A, Axmann J, et al. Reserve of Right Ventricular-Arterial Coupling in the Setting of Chronic Overload. *Circ Heart Fail* 2019;12(1):e005512. doi: 10.1161/CIRCHEARTFAILURE.118.005512
344. Kim PK, Hong YJ, Shim HS, et al. Serial T1 mapping of right ventricle in pulmonary hypertension: comparison with histology in an animal study. *J Cardiovasc Magn Reson* 2021;23(1):64. doi: 10.1186/s12968-021-00755-y [published Online First: 20210527]
345. Saunders LC, Johns CS, Stewart NJ, et al. Diagnostic and prognostic significance of cardiovascular magnetic resonance native myocardial T1 mapping in patients with pulmonary hypertension. *J Cardiovasc Magn Reson* 2018;20(1):78. doi: 10.1186/s12968-018-0501-8 [published Online First: 20181203]
346. Wang J, Zhao H, Wang Y, et al. Native T1 and T2 mapping by cardiovascular magnetic resonance imaging in pressure overloaded left and right heart diseases. *J Thorac Dis* 2018;10(5):2968-75. doi: 10.21037/jtd.2018.04.141
347. Wang. Effect of lung resection on exercise capacity and on carbon monoxide diffusing capacity during exercise (vol 129, pg 863, 2006). *Chest* 2006;130(1):308-08.
348. Reiter U, Reiter G, Kovacs G, et al. Native myocardial T1 mapping in pulmonary hypertension: correlations with cardiac function and hemodynamics. *European Radiology* 2017;27(1):157-66. doi: 10.1007/s00330-016-4360-0
349. Asano R, Ogo T, Morita Y, et al. Prognostic value of right ventricular native T1 mapping in pulmonary arterial hypertension. *PLoS One*

2021;16(11):e0260456. doi: 10.1371/journal.pone.0260456 [published Online First: 20211129]
350. Kawel-Boehm N, Hetzel SJ, Ambale-Venkatesh B, et al. Reference ranges ("normal values") for cardiovascular magnetic resonance (CMR) in adults and children: 2020 update. *J Cardiovasc Magn Reson* 2020;22(1):87. doi: 10.1186/s12968-020-00683-3 [published Online First: 20201214]
351. Plymen CM, Sado DM, Taylor AM, et al. Diffuse myocardial fibrosis in the systemic right ventricle of patients late after Mustard or Senning surgery: an equilibrium contrast cardiovascular magnetic resonance study. *Eur Heart J Cardiovasc Imaging* 2013;14(10):963-8. doi: 10.1093/ehjci/jet014 [published Online First: 20130206]
352. Georgiopoulos G, Zampieri M, Molaro S, et al. Cardiac magnetic resonance in patients with ARVC and family members: the potential role of native T1 mapping. *Int J Cardiovasc Imaging* 2021;37(6):2037-47. doi: 10.1007/s10554-021-02166-7 [published Online First: 20210207]
353. Kozak MF, Redington A, Yoo SJ, et al. Diffuse myocardial fibrosis following tetralogy of Fallot repair: a T1 mapping cardiac magnetic resonance study. *Pediatr Radiol* 2014;44(4):403-9. doi: 10.1007/s00247-013-2840-9 [published Online First: 20140114]
354. Chahal H, McClelland RL, Tandri H, et al. Obesity and right ventricular structure and function: the MESA-Right Ventricle Study. *Chest* 2012;141(2):388-95. doi: 10.1378/chest.11-0172 [published Online First: 20110825]
355. Observatory TGH. Body Mass Index (BMI) amongst adults 2022 [Available from: https://www.who.int/data/gho/data/themes/topics/topic-details/GHO/body-mass-index accessed November 2022.
356. Mehta BB, Auger DA, Gonzalez JA, et al. Detection of elevated right ventricular extracellular volume in pulmonary hypertension using Accelerated and Navigator-Gated Look-Locker Imaging for Cardiac T1 Estimation (ANGIE) cardiovascular magnetic resonance. *J Cardiovasc Magn Reson* 2015;17:110. doi: 10.1186/s12968-015-0209-y [published Online First: 20151221]
357. Dong Y, Sun J, Yang D, et al. Right ventricular septomarginal trabeculation hypertrophy is associated with disease severity in patients with pulmonary arterial hypertension. *Int J Cardiovasc Imaging* 2018;34(9):1439-49. doi: 10.1007/s10554-018-1347-8 [published Online First: 20180331]
358. Alabed S, Saunders L, Garg P, et al. Myocardial T1-mapping and extracellular volume in pulmonary arterial hypertension: A systematic review and meta-analysis. *Magn Reson Imaging* 2021;79:66-75. doi: 10.1016/j.mri.2021.03.011 [published Online First: 20210318]
359. Jellis CL, Yingchoncharoen T, Gai N, et al. Correlation between right ventricular T. *Int J Cardiovasc Imaging* 2018;34(1):55-65. doi: 10.1007/s10554-017-1113-3 [published Online First: 20170329]
360. Shiina Y, Inai K, Taniguchi K, et al. Potential Value of Native T1 Mapping in Symptomatic Adults with Congenital Heart Disease: A Preliminary Study of 3.0 Tesla Cardiac Magnetic Resonance Imaging. *Pediatr Cardiol* 2020;41(1):94-100. doi: 10.1007/s00246-019-02227-8 [published Online First: 20191025]
361. Bravo PE, Luo HC, Pozios I, et al. Late gadolinium enhancement confined to the right ventricular insertion points in hypertrophic cardiomyopathy: an intermediate stage phenotype? *Eur Heart J Cardiovasc Imaging* 2016;17(3):293-300. doi: 10.1093/ehjci/jev154 [published Online First: 20150614]

362. Sato T, Tsujino I, Ohira H, et al. Paradoxical interventricular septal motion as a major determinant of late gadolinium enhancement in ventricular insertion points in pulmonary hypertension. *PLoS One* 2013;8(6):e66724. doi: 10.1371/journal.pone.0066724 [published Online First: 20130624]
363. Blyth KG, Groenning BA, Martin TN, et al. Contrast enhanced-cardiovascular magnetic resonance imaging in patients with pulmonary hypertension. *European Heart Journal* 2005;26(19):1993-99. doi: 10.1093/eurheartj/ehi328
364. Jayasekera G. Unravelling the role of the left and right ventricles in pulmonary arterial hypertension: patient and small animal cardiac MRI studies. University of Glasgow, 2020.
365. Kawel-Boehm N, Hetzel SJ, Ambale-Venkatesh B, et al. Correction to: Reference ranges ("normal values") for cardiovascular magnetic resonance (CMR) in adults and children: 2020 update. *J Cardiovasc Magn Reson* 2021;23(1):114. doi: 10.1186/s12968-021-00815-3 [published Online First: 20211018]
366. Dabir D, Child N, Kalra A, et al. Reference values for healthy human myocardium using a T1 mapping methodology: results from the International T1 Multicenter cardiovascular magnetic resonance study. *J Cardiovasc Magn Reson* 2014;16:69. doi: 10.1186/s12968-014-0069-x [published Online First: 20141021]
367. Shehata ML, Lossnitzer D, Skrok J, et al. Myocardial delayed enhancement in pulmonary hypertension: pulmonary hemodynamics, right ventricular function, and remodeling. *AJR Am J Roentgenol* 2011;196(1):87-94. doi: 10.2214/ajr.09.4114
368. McCann GP, Gan CT, Beek AM, et al. Extent of MRI delayed enhancement of myocardial mass is related to right ventricular dysfunction in pulmonary artery hypertension. *AJR Am J Roentgenol* 2007;188(2):349-55. doi: 10.2214/AJR.05.1259
369. Liu CY, Liu YC, Wu C, et al. Evaluation of age-related interstitial myocardial fibrosis with cardiac magnetic resonance contrast-enhanced T1 mapping: MESA (Multi-Ethnic Study of Atherosclerosis). *J Am Coll Cardiol* 2013;62(14):1280-87. doi: 10.1016/j.jacc.2013.05.078 [published Online First: 20130717]
370. Rosmini S, Bulluck H, Captur G, et al. Myocardial native T1 and extracellular volume with healthy ageing and gender. *Eur Heart J Cardiovasc Imaging* 2018;19(6):615-21. doi: 10.1093/ehjci/jey034
371. Olivetti G, Melissari M, Capasso JM, et al. Cardiomyopathy of the aging human heart. Myocyte loss and reactive cellular hypertrophy. *Circ Res* 1991;68(6):1560-8. doi: 10.1161/01.res.68.6.1560
372. Messroghli DR, Radjenovic A, Kozerke S, et al. Modified Look-Locker inversion recovery (MOLLI) for high-resolution T1 mapping of the heart. *Magn Reson Med* 2004;52(1):141-6. doi: 10.1002/mrm.20110
373. Spottiswoode B, Russell JB, Moosa S, et al. Abnormal diastolic and systolic septal motion following pericardiectomy demonstrated by ciné DENSE MRI. *Cardiovasc J Afr* 2008;19(4):208-9.
374. Sato T, Tsujino I, Ohira H, et al. Paradoxical motion of the interventricular septum as a primary mechanism of late gadolinium enhancement at ventricular insertion points. *Int J Cardiol* 2012;158(1):156-7. doi: 10.1016/j.ijcard.2012.04.042 [published Online First: 20120504]
375. Teng WH, McCall PJ, Shelley BG. The Utility of Eccentricity Index as a Measure of the Right Ventricular Function in a Lung Resection Cohort. *J Cardiovasc Echogr* 2019;29(3):103-10. doi: 10.4103/jcecho.jcecho_19_19

376. McCall P. the right ventricular response to lung resection. University of Glasgow, 2018.
377. Luetkens JA, Schlesinger-Irsch U, Kuetting DL, et al. Feature-tracking myocardial strain analysis in acute myocarditis: diagnostic value and association with myocardial oedema. *Eur Radiol* 2017;27(11):4661-71. doi: 10.1007/s00330-017-4854-4 [published Online First: 20170512]
378. Neubauer S, Horn M, Naumann A, et al. Impairment of energy metabolism in intact residual myocardium of rat hearts with chronic myocardial infarction. *J Clin Invest* 1995;95(3):1092-100. doi: 10.1172/JCI117756
379. Kolb TM, Hassoun PM. Right ventricular dysfunction in chronic lung disease. *Cardiol Clin* 2012;30(2):243-56. doi: 10.1016/j.ccl.2012.03.005
380. Yang MX, Luo HB, Liu JK, et al. Prognostic value of non-contrast myocardial T1 mapping in cardiovascular diseases: a systematic review and meta-analysis. *Heart Fail Rev* 2022;27(5):1899-909. doi: 10.1007/s10741-021-10191-w [published Online First: 20220122]
381. Nardi Gemme C, Silva TQAC, Martins LC, et al. Diffuse Myocardial Fibrosis and Cardiomyocyte Diameter Are Associated With Heart Failure Symptoms in Chagas Cardiomyopathy. *Front Cardiovasc Med* 2022;9:880151. doi: 10.3389/fcvm.2022.880151 [published Online First: 20220617]
382. Yang D, Li X, Sun JY, et al. Cardiovascular magnetic resonance evidence of myocardial fibrosis and its clinical significance in adolescent and adult patients with Ebstein's anomaly. *J Cardiovasc Magn Reson* 2018;20(1):69. doi: 10.1186/s12968-018-0488-1 [published Online First: 20180927]
383. Jeuthe S, Wassilew K, O H-Ici D, et al. Myocardial T1 maps reflect histological findings in acute and chronic stages of myocarditis in a rat model. *J Cardiovasc Magn Reson* 2016;18:19. doi: 10.1186/s12968-016-0241-6 [published Online First: 20160416]
384. Zhang L, Yang ZG, Xu H, et al. Histological Validation of Cardiovascular Magnetic Resonance T1 Mapping for Assessing the Evolution of Myocardial Injury in Myocardial Infarction: An Experimental Study. *Korean J Radiol* 2020;21(12):1294-304. doi: 10.3348/kjr.2020.0107 [published Online First: 20200811]
385. Kammerlander AA, Marzluf BA, Zotter-Tufaro C, et al. T1 Mapping by CMR Imaging: From Histological Validation to Clinical Implication. *JACC Cardiovasc Imaging* 2016;9(1):14-23. doi: 10.1016/j.jcmg.2015.11.002 [published Online First: 20151209]
386. Cagini L, Andolfi M, Leli C, et al. B-type natriuretic peptide following thoracic surgery: a predictor of postoperative cardiopulmonary complications. *Eur J Cardiothorac Surg* 2014;46(5):e74-80. doi: 10.1093/ejcts/ezu348
387. Tayama K, Takamori S, Mitsuoka M, et al. Natriuretic peptides after pulmonary resection. *Ann Thorac Surg* 2002;73(5):1582-6.
388. Lee CY, Bae MK, Lee JG, et al. N-Terminal Pro-B-type Natriuretic Peptide Is Useful to Predict Cardiac Complications Following Lung Resection Surgery. *The Korean journal of thoracic and cardiovascular surgery* 2011;44(1):44-50. doi: 10.5090/kjtcs.2011.44.1.44
389. Raymond I, Groenning BA, Hildebrandt PR, et al. The influence of age, sex and other variables on the plasma level of N-terminal pro brain natriuretic peptide in a large sample of the general population. *Heart* 2003;89(7):745-51. doi: 10.1136/heart.89.7.745
390. Masson S, Latini R, Anand IS, et al. Direct comparison of B-Type natriuretic peptide (BNP) and amino-terminal proBNP in a large population of patients with chronic and symptomatic heart failure: The valsartan heart

failure (Val-HeFT) data. *Clinical Chemistry* 2006;52(8):1528-38. doi: 10.1373/clinchem.2006.069575
391. Gibson SC, Payne CJ, Byrne DS, et al. B-type natriuretic peptide predicts cardiac morbidity and mortality after major surgery. *British Journal of Surgery* 2007;94(7):903-09. doi: 10.1002/bjs.5690
392. Nojiri T, Maeda H, Takeuchi Y, et al. Predictive value of B-type natriuretic peptide for postoperative atrial fibrillation following pulmonary resection for lung cancer. *Eur J Cardiothorac Surg* 2010;37(4):787-91. doi: 10.1016/j.ejcts.2009.09.043 [published Online First: 2009/11/06]
393. Nojiri T, Inoue M, Shintani Y, et al. B-type natriuretic peptide-guided risk assessment for postoperative complications in lung cancer surgery. *World J Surg* 2015;39(5):1092-8. doi: 10.1007/s00268-015-2943-6
394. Karthikeyan G, Moncur RA, Levine O, et al. Is a pre-operative brain natriuretic peptide or N-terminal pro-B-type natriuretic peptide measurement an independent predictor of adverse cardiovascular outcomes within 30 days of noncardiac surgery? A systematic review and meta-analysis of observational studies. *J Am Coll Cardiol* 2009;54(17):1599-606. doi: 10.1016/j.jacc.2009.06.028
395. Duceppe E, Parlow J, MacDonald P, et al. Canadian Cardiovascular Society Guidelines on Perioperative Cardiac Risk Assessment and Management for Patients Who Undergo Noncardiac Surgery. *Can J Cardiol* 2017;33(1):17-32. doi: 10.1016/j.cjca.2016.09.008 [published Online First: 20161004]
396. Duceppe E, Patel A, Chan MTV, et al. Preoperative N-Terminal Pro-B-Type Natriuretic Peptide and Cardiovascular Events After Noncardiac Surgery: A Cohort Study. *Ann Intern Med* 2020;172(2):96-104. doi: 10.7326/M19-2501 [published Online First: 20191224]
397. Kavsak PA, Beattie J, Ma J. Effect of Storage Temperature for B-Type Natriuretic Peptide Concentrations for Primary Healthcare Populations. *Clin Chem* 2019;65(6):811-12. doi: 10.1373/clinchem.2018.300749 [published Online First: 20190327]
398. Hammerer-Lercher A, Ludwig W, Falkensammer G, et al. Natriuretic peptides as markers of mild forms of left ventricular dysfunction: effects of assays on diagnostic performance of markers. *Clin Chem* 2004;50(7):1174-83. doi: 10.1373/clinchem.2003.028316 [published Online First: 2004/05/13]
399. O'Donoghue M, Chen A, Baggish AL, et al. The effects of ejection fraction on N-terminal ProBNP and BNP levels in patients with acute CHF: analysis from the ProBNP Investigation of Dyspnea in the Emergency Department (PRIDE) study. *J Card Fail* 2005;11(5 Suppl):S9-14.
400. Costello-Boerrigter LC, Boerrigter G, Redfield MM, et al. Amino-terminal pro-B-type natriuretic peptide and B-type natriuretic peptide in the general community: determinants and detection of left ventricular dysfunction. *J Am Coll Cardiol* 2006;47(2):345-53. doi: 10.1016/j.jacc.2005.09.025 [published Online First: 2006/01/04]
401. Macheret F, Boerrigter G, McKie P, et al. Pro-B-type natriuretic peptide(1-108) circulates in the general community: plasma determinants and detection of left ventricular dysfunction. *J Am Coll Cardiol* 2011;57(12):1386-95. doi: 10.1016/j.jacc.2011.01.005
402. Muley T, Kurz M, Männle C, et al. Comparison of serum cardiac specific biomarker release after non-cardiac thoracic surgery. *Clin Lab* 2011;57(11-12):925-32.

403. Gurgo AM, Ciccone AM, D'Andrilli A, et al. Plasma NT-proBNP levels and the risk of atrial fibrillation after major lung resection. *Minerva Cardioangiol* 2008;56(6):581-5.
404. P M. Perioperative BNP changes and functional capacity following lung resection. In: Arthur A MA, Kirk A, Kinsella J, Shelley B, ed. Journal of Cardiothoracic and Vascular Anaesthesia, 2016:26-27.
405. Cardinale D, Cosentino N, Moltrasio M, et al. Acute kidney injury after lung cancer surgery: Incidence and clinical relevance, predictors, and role of N-terminal pro B-type natriuretic peptide. *Lung Cancer* 2018;123:155-59. doi: 10.1016/j.lungcan.2018.07.009 [published Online First: 20180717]
406. Uchoa RB, Caramelli B. Troponin I as a mortality marker after lung resection surgery - a prospective cohort study. *Bmc Anesthesiology* 2020;20(1) doi: 10.1186/s12871-020-01037-3
407. Morales P, Coronado C, Camio E, et al. Postoperative serum troponin I elevation after thoracotomy versus video-assisted thoracoscopic lung resection. Euroanaesthesia. London, 2016.
408. Choi HS, Kim KH, Yoon HJ, et al. Usefulness of cardiac biomarkers in the prediction of right ventricular dysfunction before echocardiography in acute pulmonary embolism. *J Cardiol* 2012;60(6):508-13. doi: 10.1016/j.jjcc.2012.07.006 [published Online First: 20120817]
409. Dursunoğlu N, Dursunoğlu D, Yıldız A, et al. Evaluation of cardiac biomarkers and right ventricular dysfunction in patients with acute pulmonary embolism. *Anatol J Cardiol* 2016;16(4):276-82. doi: 10.5152/akd.2014.5828 [published Online First: 20141231]
410. Blyth KG, Groenning BA, Mark PB, et al. NT-proBNP can be used to detect right ventricular systolic dysfunction in pulmonary hypertension. *Eur Respir J* 2007;29(4):737-44. doi: 10.1183/09031936.00095606 [published Online First: 20061129]
411. Hussain T, Dragulescu A, Benson L, et al. Quantification and significance of diffuse myocardial fibrosis and diastolic dysfunction in childhood hypertrophic cardiomyopathy. *Pediatr Cardiol* 2015;36(5):970-8. doi: 10.1007/s00246-015-1107-7 [published Online First: 20150121]
412. Treibel TA, Zemrak F, Sado DM, et al. Extracellular volume quantification in isolated hypertension - changes at the detectable limits? *J Cardiovasc Magn Reson* 2015;17(1):74. doi: 10.1186/s12968-015-0176-3 [published Online First: 20150812]
413. Liu CY, Heckbert SR, Lai S, et al. Association of Elevated NT-proBNP With Myocardial Fibrosis in the Multi-Ethnic Study of Atherosclerosis (MESA). *J Am Coll Cardiol* 2017;70(25):3102-09. doi: 10.1016/j.jacc.2017.10.044
414. Rutherford E, Talle MA, Mangion K, et al. Defining myocardial tissue abnormalities in end-stage renal failure with cardiac magnetic resonance imaging using native T1 mapping. *Kidney Int* 2016;90(4):845-52. doi: 10.1016/j.kint.2016.06.014 [published Online First: 20160805]
415. Hromadka M, Baxa J, Seidlerova J, et al. Myocardial Involvement Detected Using Cardiac Magnetic Resonance Imaging in Patients with Systemic Sclerosis: A Prospective Observational Study. *J Clin Med* 2021;10(22) doi: 10.3390/jcm10225364 [published Online First: 20211118]
416. Larsson S, Thelander U, Friberg S. C-reactive protein (CRP) levels after elective orthopedic surgery. *Clin Orthop Relat Res* 1992(275):237-42.
417. Straatman J, Cuesta MA, Tuynman JB, et al. C-reactive protein in predicting major postoperative complications are there differences in open and minimally invasive colorectal surgery? Substudy from a randomized

clinical trial. *Surgical Endoscopy and Other Interventional Techniques* 2018;32(6):2877-85. doi: 10.1007/s00464-017-5996-9
418. Neumaier M, Metak G, Scherer MA. C-reactive protein as a parameter of surgical trauma: CRP response after different types of surgery in 349 hip fractures. *Acta Orthop* 2006;77(5):788-90. doi: 10.1080/17453670610013006
419. Kroell D, Nakhostin D, Stirnimann G, et al. C-Reactive Protein on Postoperative Day 1: a Predictor of Early Intra-abdominal Infections After Bariatric Surgery. *Obesity Surgery* 2018;28(9):2760-66. doi: 10.1007/s11695-018-3240-x
420. Nakamoto S, Hirose M. Prediction of early C-reactive protein levels after non-cardiac surgery under general anesthesia. *Plos One* 2019;14(12) doi: 10.1371/journal.pone.0226032
421. Choi JH, Cho DK, Song YB, et al. Preoperative NT-proBNP and CRP predict perioperative major cardiovascular events in non-cardiac surgery. *Heart* 2010;96(1):56-62. doi: 10.1136/hrt.2009.181388
422. Okada S, Shimomura M, Tsunezuka H, et al. Prognostic Significance of Perioperative C-Reactive Protein in Resected Non-Small Cell Lung Cancer. *Semin Thorac Cardiovasc Surg* 2020;32(4):1046-55. doi: 10.1053/j.semtcvs.2020.03.019 [published Online First: 20200511]
423. Pastorino U, Morelli D, Leuzzi G, et al. Baseline and postoperative C-reactive protein levels predict mortality in operable lung cancer. *Eur J Cancer* 2017;79:90-97. doi: 10.1016/j.ejca.2017.03.020 [published Online First: 20170501]
424. Hara M, Yonei A, Ayabe T, et al. Postoperative serum C-reactive protein levels in non-small cell lung cancer patients. *Ann Thorac Cardiovasc Surg* 2010;16(2):85-90.
425. Abul Y, Karakurt S, Ozben B, et al. C-Reactive Protein in Acute Pulmonary Embolism. *Journal of Investigative Medicine* 2011;59(1):8-14.
426. Choi HS, Kim KH, Yoon HJ, et al. Usefulness of cardiac biomarkers in the prediction of right ventricular dysfunction before echocardiography in acute pulmonary embolism. *Journal of Cardiology* 2012;60(5-6):508-13. doi: 10.1016/j.jjcc.2012.07.006
427. Meng QH. Are Arterial Blood Samples Acceptable for Chemistry Testing in Laboratory Practice? *J Appl Lab Med* 2021;6(5):1380-83. doi: 10.1093/jalm/jfab060
428. Moonesinghe SR, Jackson AIR, Boney O, et al. Systematic review and consensus definitions for the Standardised Endpoints in Perioperative Medicine initiative: patient-centred outcomes. *Br J Anaesth* 2019;123(5):664-70. doi: 10.1016/j.bja.2019.07.020 [published Online First: 20190905]
429. Jørgensen CC, Petersen PB, Kehlet H, et al. Days alive and out of hospital after fast-track total hip and knee arthroplasty: an observational cohort study in 16 137 patients. *Br J Anaesth* 2019;123(5):671-78. doi: 10.1016/j.bja.2019.07.022 [published Online First: 20190829]
430. Jerath A, Austin PC, Wijeysundera DN. Days Alive and Out of Hospital: Validation of a Patient-centered Outcome for Perioperative Medicine. *Anesthesiology* 2019;131(1):84-93. doi: 10.1097/ALN.0000000000002701
431. Jerath A, Austin PC, McCormack D, et al. Impact of postoperative intensive care unit utilization on postoperative outcomes in adults undergoing major elective noncardiac surgery. *J Clin Anesth* 2020;62:109707. doi: 10.1016/j.jclinane.2020.109707 [published Online First: 20200114]

432. Spurling LJ, Moonesinghe SR, Oliver CM. Validation of the days alive and out of hospital outcome measure after emergency laparotomy: a retrospective cohort study. *Br J Anaesth* 2022;128(3):449-56. doi: 10.1016/j.bja.2021.12.006 [published Online First: 20220107]
433. Schober A, Nazari-Jahantigh M, Weber C. MicroRNA-mediated mechanisms of the cellular stress response in atherosclerosis. *Nat Rev Cardiol* 2015;12(6):361-74. doi: 10.1038/nrcardio.2015.38 [published Online First: 2015/04/07]
434. Bartel DP. MicroRNAs: genomics, biogenesis, mechanism, and function. *Cell* 2004;116(2):281-97. doi: 10.1016/s0092-8674(04)00045-5
435. Reddy S, Hu D-Q, Zhao M, et al. miR-21 is associated with fibrosis and right ventricular failure. *Jci Insight* 2017;2(9) doi: 10.1172/jci.insight.91625
436. Kessler T, Erdmann J, Vilne B, et al. Serum microRNA-1233 is a specific biomarker for diagnosing acute pulmonary embolism. *Journal of Translational Medicine* 2016;14 doi: 10.1186/s12967-016-0886-9
437. Sarrion I, Milian L, Juan G, et al. Role of Circulating miRNAs as Biomarkers in Idiopathic Pulmonary Arterial Hypertension: Possible Relevance of miR-23a. *Oxidative Medicine and Cellular Longevity* 2015 doi: 10.1155/2015/792846
438. Sanders RD, Craigova L, Schessler B, et al. Postoperative troponin increases after noncardiac surgery are associated with raised neurofilament light: a prospective observational cohort study. *British Journal of Anaesthesia* 2021;126(4):791-98. doi: 10.1016/j.bja.2020.10.012
439. Lohser J, Slinger P. Lung Injury After One-Lung Ventilation: A Review of the Pathophysiologic Mechanisms Affecting the Ventilated and the Collapsed Lung. *Anesth & Analg* 2015;121(2):302-18. doi: 10.1213/ane.0000000000000808
440. Skvarc DR, Berk M, Byrne LK, et al. Post-Operative Cognitive Dysfunction: An exploration of the inflammatory hypothesis and novel therapies. *Neuroscience & Biobehavioral Reviews* 2018;84:116-33. doi: https://doi.org/10.1016/j.neubiorev.2017.11.011
441. Meersch M, Schmidt C, Zarbock A. Perioperative Acute Kidney Injury: An Under-Recognized Problem. *Anesthesia & Analgesia* 2017;125(4):1223-32. doi: 10.1213/ane.0000000000002369